DEVELOPMENT OF A TSUNAMI FORECAST MODEL FOR NIKOLSKI, ALASKA (DRAFT)

Yong Wei

June, 2012

Abstract

As part of NOAA's tsunami forecast system, this study addresses the development, validation, and stability tests of the tsunami forecast models for Nikolski, Alaska. Three tsunami models are developed in the present study based on the Method of Splitting Tsunami (MOST) for different needs in model assessment of tsunami hazards: (1) a forecast model to provide real-time forecast of tsunami impact along Nikolski's coastline; (2) an intermediate model for improved model accuracy in the later arrivals; (3) a reference model computing tsunami inundation at 10 m grid resolution to provide model reference for the models (1) and (2). The difference between models (1) and (2) lies in the computational domain coverage and grid resolution of their lowest resolution grids, also called A grids. These two models use the same B and C grids, and the C grid computes the tsunami inundation with a grid resolution of 2 arc sec (~ 37 m at latitude 53°N) in *x* axis and 1 arc sec (~ 31 m) in *y* axis. The forecast model finishes 4-hour simulation of the tsunami inundation within minutes. Comparing to the forecast model, the intermediate model has a larger domain coverage and finer grid resolution in the A grid to provide better model accuracy for later arrivals crossing the shallow continental shelf. The downside of the intermediate model is that it takes nearly 8 times longer than the forecast model to finish. Its implementation in tsunami forecast may be justified in the near future along with the arrival of high-performance computing in the forecast system. The reference model uses grids of higher resolution at all grid levels to provide model reference for the forecast model. In particular, the reference model computes the tsunami flooding with a grid resolution of 1/3 arc sec (~ 10 m) in its C grid. All models developed for Nikolski, Alaska are validated using three historical tsunami events: 29 September 2009 Samoa, 11 March 2011 Japan, and 24 June 2011 Amukta Pass. The model validation shows good agreement between model results and observations at the Nikolski tide station. The modeling results obtained from the intermediate model and the reference model are highly consistent. The stability of all models is further examined based on 21 synthetic scenarios generated in the major subduction zones in the Pacific Rim with magnitudes of Mw 9.3, Mw 7.5 and Mw 6.4.

1. Background and Objectives

The National Oceanic and Atmospheric Administration (NOAA) Center for Tsunami, Research (NCTR) at the NOAA Pacific Marine Environmental Laboratory (PMEL) has developed a tsunami forecasting capability for operational use by NOAA's two Tsunami Warning Centers located in Hawaii and Alaska (Titov *et al.*, 2005a). The system is designed to provide basin-wide warning of approaching tsunami waves accurately and quickly. The system, termed Short-term Inundation Forecast of Tsunamis (SIFT), combines real-time tsunami event data with numerical models to produce estimates of tsunami wave arrival times and amplitudes at a coastal community of interest. The SIFT system integrates several key components: deep-ocean observations of tsunamis in real

time, a basin-wide pre-computed propagation database of water level and flow velocities based on potential seismic unit sources, an inversion algorithm to refine the tsunami source based on deep-ocean observations during an event, and high-resolution tsunami forecast models.

The objective of the present work is to develop an operational forecast model to be used in near real-time to protect the community of Nikolski, Alaska, from the potential impact of tsunami waves. A few tsunami events since 1946 have been documented for Nikolski coastline (Table 1), and the most severe event is the 1946 Alaska tsunami that brought up to 12-m tsunami runup and severe tsunami inundation to Nikolski coastline (Lander, 1996). Lack of specific studies on tsunami hazard for Nikolski adds to vulnerability of this community to future tsunami strikes. In this aspect, the tsunami forecast models developed in this study may provide useful modeling tools for both short-term (real-time forecast) and long-term assessment of the tsunami hazards at Nikolski.

2. Forecast Methodology

Titov *et al*. (2005a) provides details of NCTR's forecast methodology. The tsunami forecasts are expedited using a basin-wide database of pre-computed water elevations and flow velocities for unit sources covering worldwide subduction zones (Gica *et al.*, 2008). When the tsunami waves propagate across the ocean and successively reach tsunameters employing the Deep-ocean Assessment and Reporting (DART) technology (Meinig et al., 2005), the recorded sea level is ingested into an inversion algorithm (Percival et al., 2011) to produce an improved estimate of the tsunami source in real time. Based on this tsunami source, a linear combination of the pre-computed "unit" tsunami scenarios stored in the database produces synthetic boundary conditions of water elevation and flow velocities to initiate the forecast model computation. The Method of Splitting Tsunami (MOST) is used to develop the tsunami forecast model to provide real-time tsunami forecasts at selected coastal communities. MOST is a suite of numerical simulation codes capable of simulating three processes of tsunami evolution: generation, transoceanic propagation, and inundation of dry land (Titov and González, 1997). It has been extensively tested against a number of laboratory experiments and benchmarks (Synolakis *et al.*, 2008). Forecast models are constructed to operationally provide an estimate of wave arrival time, wave height, and inundation for populous at-risk coastal communities in real time while a tsunami is propagating across the open ocean. The forecast models are designed and tested to perform under stringent time constraints given that time is generally the single limiting factor in saving lives and property. Tang *et al*. (2009) described the technical aspects of forecast model development and stability testing. The forecast methodology and models have been successfully used for tsunami model forecast during a number of historical tsunami events since 2003 (Titov *et al*., 2005b; Titov, 2009; Tang *et al*., 2008 and 2012; Wei *et al*., 2008 and 2013).

3. Model development

Accurate forecasting of the tsunami impact on a coastal community largely relies on the accuracy of bathymetry and topography used in the numerical model. The forecast model utilizes the high-resolution Digital Elevation Models (DEMs) constructed by the National Geophysical Data Center (NGDC) using available bathymetric, topographic, and shoreline data. The vertical datum of these DEMs is set to Mean High Water (MHW),

and the horizontal datum is the World Geodetic System 1984 (http://ngdc.noaa.gov/mgg/inundation/tsunami/inundation.html).

Implementation of high-resolution grids improves modeling accuracy, but also increases the computational time for real-time forecasts. To obtain rapid and accurate model results, a forecast model consists of a set of three telescoping grids, referred to as A, B, and C grids, with successively increasing spatial resolution with approaching to the population and economic center of the community of interest. The offshore area is covered by the A grid with a lowest resolution typically at a range of 0.5 to 2 arc min (1,000 to 3,700 m). The B grid provides computational results for tsunami wave transition from offshore to nearshore at an intermediate grid resolution of 12 to 18 arc sec (360 to 540 m). In the C grid, the model computes the tsunami inundation at a grid resolution ranging from 1 to 3 arc sec (30 to 90 m). This optimal setup allows the model to finish 4 to 10 hr simulations within 10 min of wall-clock time.

Similarly, a set of three high-resolution, "reference" elevation grids can also be constructed to develop a high-resolution reference model. Typically, a reference model provides inundation computation in its C grid at a grid resolution of 1/3 arc sec (~ 10 m), which may be reduced to 1 arc sec (~ 30 m) when the 1/3-arc-sec DEM is not available. Compared to a forecast model, a reference model generally provides better accuracy of the inundation computation, but is much more computationally intensive.

3.1 Forecast area

Nikolski, Alaska is a small coastal community located off the southwest end of Umnak Island, one of the Fox Islands. According to Census 2010, the total population in Nikolski is 18 (http://censusviewer.com/city/AK/Nikolski), a drop of 21 from 39 in Census 2000. In 2010, there were 23 housing units in the community and 13 were occupied. Nikolski is one of the oldest continuously-occupied communities in the world, dating as far back as 8,500 years ago (http://explorenorth.com/library/communities/alaska/bl-Nikolski.htm). However, the drop of population has had a serious social impact on the community – the school was shutdown due to lack of attendees, which forced the residents, especially the younger generation, to leave Nikolski. The village of Nikolski is located in a biologically prime, diverse, and productive area, a fact that has contributed to the continuous habitation of the general area for thousands of years. Most of the neighboring islands are in the Aleutian National Wildlife Refuge. Nikolski is adjacent to the rich fisheries area of the Bering Sea and Alaska/Aleutian shelf and within a prime king crab area. Although there are no mineral deposits in Umnak Island, the general area in the Bering Sea is known for potential outer continental shelf oil and gas fields. Subsistence activities, such as sheep and cattle raising, and fishing-related employment sustain the community. The small Nikolski community is located on the southeast shore of Nikolski Bay, which connects to the Bering Sea (**Figure 1**). The residential area has an elevation ~ 5.5 m or less above mean sea level (or 5 m above MHW), with a gently rolling plain reaching 160 m in elevation above mean sea level at the north end of the village.

The National Ocean Service (NOS) Nikolski tide station is housed 700 m northwest from the Nikolski residential area (**Figure 1**). The water depth at the gage sensor is 2.36 m (water level difference between the MHW and the Station Datum). This station was

established on 28 June 2006. The local mean tide range is about 0.84 m, and the diurnal range is 1.23 m.

3.2 Potential earthquake sources in the Aleutians

The Alaska-Aleutian coastlines have been severely affected by tsunamis, such as the 1946 Unimak, 1952 Kamchatka, 1957 Andreanov, 1960 Chile, and 1964 Alaska. **Figure 2** shows the rupture areas of significant earthquakes that occurred offshore of the Alaska and Aleutian Subduction Zone during the 1900s. The two seismic gaps, namely Shumagin Gap and Unalaska Gap, in are of major concerns of generating the next catastrophic tsunami.

The Shumagin Gap is a segment of the Alaska-Aleutian arc that has not ruptured in a great earthquake since at least 1899-1903. Accordingly, Davies et al. (1981) considered that it may have a high seismic potential. Previous studies have shown that the rupture zones of Aleutian earthquakes in 1938, 1946, and 1948 did not break the inter-plate boundary beneath the Shumagin Islands (Davies et al., 1981; Johnson, 1999). Davies et al. (1981) and Beavan et al. (1983) suggested that the possibility of the occurrence of a major earthquake within this gap in the next two decades. The 13 May 1993 Shumagin Islands earthquake of Mw 6.8 occurred at an expected location in the seismic gap, but the magnitude was too small to fill the gap (Tanioka et al., 1994). This earthquake did not generate a tsunami large enough to be observed at Sand Point tide station or at the ocean bottom pressure gages at a distance of 100 and 300 km away. Nishenko (1991) suggested that a gap-filling event will have an expected magnitude of M_w 7.4, with conditional probabilities of 27%, 48% and 75% of occurring during the 5-, 10-, and 20-year periods that end in 1994, 1999, and 2009, respectively. However, more recent research of Global Positioning System (GPS) velocities and pre-historical earthquakes found little evidence supporting a large seismic gap exists in the vicinity of Shumagin Islands. The GPS study of Fournier and Freymueller (2007) suggested that the Sumagin segment is only weakly coupled and mostly creeping, which does not support a hypothesis of a gap-filling event. Witter et al. (2014) did further investigation to search for evidence of megathrust storing enough strain over the past thousand years in the Shumagin Islands. They found little relative sea-level change, normal tidal inundation at the shoreline, and no abrupt shifts in land elevation resulted from large pre-historical earthquakes. The study of Witter et al. (2014) suggests that the megathrust fault underlying Simeonof Island has not produced a great earthquake in the past 3,400 years. They imply that ruptures in the Shumagin gap, if they occurred, were M8 or less and far out to sea relative to Simeonof Island in the past few thousand years.

To the west of the 1946 rupture area is the 200-km-long Unalaska seismic gap, which has not generated a large earthquake in a century (House *et al.,* 1981). A review of a historic record from 1770 by Boyd and Jacob (1986) reveals that the Unalaska region may have ruptured in great earthquakes in 1878 and 1902. They suggested that a major seismicity gap exists for events of magnitudes greater than M_w 4.6 in the forearc region near Unalaska Island. The study of the 1957 Aleutian tsunami by Johnson (1999) showed low moment release in the eastern half of the aftershock zone, which further confirmed the existence of the Unalaska Gap.

As discussed earlier, the possibility of a large megathrust earthquake in the Shumagin Islands is small. However, a "worst scenario" described by Davis *et al.* (1981) should not be ignored that an earthquake nucleated in the Shumagin Gap may also rupture the possible Unalaska Gap to the west, the 1938 aftershock zone to the east, or both, with resultant magnitude up to M_w 9.0. Tsunami induced by such an earthquake would be devastating for many communities, not only in Alaska-Aleutian coasts, but also as far as in Hawaii and the U.S. West Coast.

3.2 Historical events and data

Located in the Aleutians, Nikolski's coastline has been affected by historical tsunamis since the 1940s (**Figure 3** and **Table 1**). Lander (1996) reported that Nikolski Bay ran dry in the 1940s (probably 1946). The wave was reported over the bank and near the road; driftwood was washed up on lake ice a quarter of a mile from the Bering Sea coast. It was not clear what the runup height was in Nikolski Bay. Lander (1996) also reported a 12-m wave runup on the Pacific coast side of Umnak Island, and the beach there also showed signs of erosion. The 1946 tsunami is probably the only event in recorded history that had brought inundation to the Nikolski coastline. The NOS Nikolski station recorded three small tsunamis, all generated by distant earthquakes, between 2006 and 2009. The time series at the tide station indicates that the 15 November 2006 Kuril tsunami generated a maximum wave amplitude of 19 cm, while the other two events (29 September 2009 Samoa and 7 October 2009 Vanuatu) only brought waves smaller than 10 cm. The 11 March 2011 Japan tsunami, generated by a Mw 9.0 earthquake 4,000 km away, produced 0.81 m tsunami amplitude at the Nikolski tide station. No tsunami inundation was reported along Nikolski coastline. The 24 June 2011 Fox Islands Mw 7.2 earthquake occurred only 220 km southwest of Nikolski, and generated a small tsunami recorded by tide stations as far as Hilo, Hawaii (6 cm) and Midway (4 cm). Nikolski tide station reported the largest tsunami amplitude at 10 cm for this event.

3.3 Model setup

3.3.1 Model diffusion and dispersion

A tsunami slows down after reaching the continental shelf, and increases in height due to shoaling. The shallow water also intensifies the wave diffusion and dispersion of a progressing tsunami. Although MOST is not a dispersive model, careful model setup makes MOST, to a certain degree, mimic physical diffusion and dispersion through a numerical scheme. Burwell et al. (2007) studied the diffusion and dispersion characterization of the MOST model, and concluded that the nature of the scheme, at all resolvable wave numbers, is diffusive and dispersive for $\beta = (gd)^{1/2}\Delta t/\Delta x \neq 1$, where Δt is the temporal step and Δx is the space step. Diffusive effects are stronger for poorly resolved waves (large space step compared to wave length). As β decreases, diffusive effects are reduced and dispersion continues to increase. Numerical dispersion can be an issue closer to shore, but can be controlled through a proper choice of β, or in other words, the ratio between Δt and Δx. The tsunami propagation database (Gica *et al.*, 2008) was developed at a grid spacing of 4 arc min (about 7.2 km at the equator) and saved at 16-arc-min (about 28.8 km at the equator) resolution. Zhou *et al*. (2012 and 2014) showed that, for tsunami propagation in an ocean basin, MOST with numerical dispersion

produces more comparable results with a dispersive model than a shallow water model without numerical dispersion does. However, the same grid resolution may introduce large model diffusion effects if applied directly to the continental shelf, where the water depth is generally less than 100 m. The telescoped grids employed in MOST are critical for wave transformation over the continental shelf, and for the inundation modeling at the coastline. Proper adjustment of β at each grid level allows better calibration of numerical diffusion and dispersion in the model.

3.3.2 Digital Elevation Model of Nikolski, Alaska

Lim et al. (2010) developed a 1-arc-sec digital elevation model for Nikolski, Alaska. The bathymetry was developed based on NOAA hydrographic survey soundings between 1910 and 1940, NGDC's multibeam swath sonar surveys in 2007, and National Geophysical Data Center (NGDC) Earth TOPOgraphy 1 minute (ETOPO1) Global Relief Model. The topography was based on United States Geological Survey (USGS) 2-arc-sec National Elevation Dataset (NED) DEM, NASA 1 arc sec Shuttle Radar Topography Mission (SRTM), and Advanced Spaceborne Thermal Emission and Reflection Radiometer (ASTER) 1 arc sec topographic DEM. Lim et al. (2010) provided a detailed description of how these datasets were implemented in the DEM development for Nikolski. Most of the land elevation is obtained from NASA SRTM DEM, which is well known to have ±16 m of errors in vertical elevation. The model results computed using SRTM topography should be cautiously implemented, and need to be "flagged" in the forecast system. NGDC's Nikolski DEM is used as the base to develop the model grids in this study. As new digital elevation models become available, forecast models will be updated and report updates will be posted at http://nctr.pmel.noaa.gov/forecast_reports/.

3.3.3 Forecast model and intermediate model

The biggest challenge in tsunami forecasting is the optimization between accuracy and speed of model forecast (Titov et al., 2005a). A tsunami forecast model considers both aspects, and is required to provide an accurate simulation of tsunami impact within minutes following the determination of a tsunami source. Computational time depends on the selection of computational domain, grid resolution and time step, which however also affects the model accuracy because of numerical diffusion and dispersion (Burwell *et al*., 2007). As stated in 3.3.1, the grid resolution of 4 arc min (~ 7,200 m) used in NCTR's propagation database suitably accounts for the wave dispersion in deep water (4,000 to 5,000 m or greater). Finer grids help resolve the dispersion and diffusion of the tsunami waves after they enter shallower water (~ 2,000 m or less), but the computational domain may need to be shrunk to compensate for the time constraint. With the same grid resolution, a large computational domain including the deepwater region slows down the computation and thus delays the dissemination of forecast results. A small domain, on the other hand, offers faster computation but may produce less accurate results. This dilemma becomes more prominent for the Nikolski forecast model. A broad area offshore of Nikolski Bay in the Bering Sea has a water depth smaller than 2,000 m. This requires the A grid of the Nikolski forecast model to extend far offshore in the Bering Sea. Two forecast models are developed in this study to better address this situation. The main difference between these two models lies in the configuration of the A grid by its domain coverage and grid resolution. The A grid of the forecast model is bounded at 170.5°W on

the west and has a grid resolution of 1 arc min (~ 1,850 m). The A grid of the intermediate model is bounded at 177.5°W on the west and has a grid resolution of 30 arc sec (~ 925 m). The two models use the same B and C grids. The forecast model can simulate a 4-hr inundation computation in 10 min. The intermediate model takes about eight times longer (77 min) to finish, and is thus not currently suitable for an effective forecast tool. Nevertheless, the intermediate model can provide model accuracy comparable to a reference model, especially in the later arrivals (see Section 4). This model can be easily converted into a forecast tool when new computing technology cuts down the model simulation time radically (Wei *et al*., 2013).

3.3.4 Development of model grids

Model development for Nikolski began with the creation of bathymetric and topographic grids shown in **Figures 4 to 9**. **Table 2** provides specific details of the reference model and two tsunami forecast models, including grid extents, resolution, time step, and other model input parameters. A complete set of input files for Nikolski models is provided in **Appendix 1**.

Figure 4 shows the coverage of A grid at a grid resolution of 30 arc sec (~ 900 m). As stated in 3.3.3, it is used as the outermost grid (A grid) for the intermediate model, as well as for the reference model. The bathymetry and topography in this grid are obtained from the ETOPO 1 global relief database (Amanta and Eakins, 2009). The southern boundary, bounded at 50°N, is placed south of the Aleutian Trench at a water depth deep enough for smooth and linear transition from the 4 arc min (~ 7,200 m) tsunami propagation database. The modeling results in the next section show this implementation results in high consistency between the forecast model and the reference model. The red box in **Figure 5** shows the coverage of A grid (bounded at 170.5°W on the west) used in the forecast model, which is interpolated to a 1-arc-min resolution to save computational time.

Figure 6 and **Figure 7** show the bathymetry and topography of B grid for all three models. The two grids have the same model extent (**Table 2**), but different grid resolutions: the reference model uses a 3 arc sec (~ 90 m) grid resolution, while the forecast model and the intermediate model use 12 arc sec (~ 360 m). Both grids were obtained from the Nikolski 1 arc sec (~ 30 m) DEM developed by NGDC (Lim et al., 2010). The finer grid in **Figure 6** clearly shows more rugged bathymetric contours offshore. The southern boundary of B grid extends approximately 200 km offshore from the Pacific coast of Umnak Island to a water depth of 2,000 m.

The Nikolski C grids provide tsunami inundation computation for the entire Nikolski residential area, and the vicinity along 10 km coastline centered at Nikolski Village. To satisfy the model computing time requirement, the C grid of the forecast models was developed at a grid resolution of 2 arc sec in x direction (~ 37 m at latitude 53°N) and 1 arc sec in y direction (~ 30 m). As NGDC's Nikolski DEM was derived based on data no finer than 1 arc sec (Lim et al., 2010), the C grid of reference model is developed using a 1 arc sec grid resolution for both x (~ 19 m) and y directions (~ 30 m) (**Figures 8 and 9**), not at a 1/3 arc sec (~ 10 m) implemented in other reference models. As Lim et al. (2010) pointed out, the topography built in Nikolski DEM was mostly derived from the NASA

SRTM data, and some of the land features, especially the mountain lakes, were not correctly reproduced. Most of the lakes were given by the elevation of the water surface with unknown water depth. The Umnak Lake may potentially affect the tsunami flow on land when Nikolski is inundated. The actual water depth of the Umnak Lake is unknown, and is set to 33 m throughout the entire lake. This is a water depth that can theoretically minimize the model instability based on Courant-Friedrichs-Lowy (CFL) condition (Burwell et al., 2007). All Nikolski models developed in this study need to be improved when better topography becomes available.

4. Results and Discussion

4.1 Model validation

Three historical events, 2009 Samoa, 2011 Japan and 2011 Amukta (**Table 3**), are used to validate the models developed for Nikolski. The April 1, 1946 Unimak tsunami is not constrained by near-field or deep-water instrumental observations, therefore is not as certain as DART-constrained events. Therefore, it is not used for model validation here. The computed maximum wave amplitudes have less than 15% difference among all three models (**Table 4**). Results from the forecast model show discrepancies in the later arrivals when compared to the intermediate model and the reference model, while the model results from the latter two models are more consistent in the waveforms.

The 2009 Samoa tsunami was triggered by a complex rupture process that probably had involved one Mw 8.1 earthquake in the outer trench and two major 7.8 interplate underthrusting subevents (Lay et al., 2010). Beavan et al. (2010) suggested that an outer rise earthquake was probably triggered by a thrust fault event, and they both contributed to the tsunami. NOAA's experimental tsunami forecast system constrained a tsunami source using three deep-ocean tsunameters that recorded a distinct signal of the 2009 Samoa tsunami (Zhou et al., 2012). The tsunameter-constrained source indicates that the tsunami source was a combination of an outer-rise event and a thrust-fault event. At the Nikolski tide gauge, the tsunami waves reached a maximum amplitude of 7.7 cm 14.25 hours after the earthquake (4.75 hours after the tsunami arrived at Nikolski tide station). All three models underestimate the maximum wave amplitude, as shown in **Table 3**. We attribute these discrepancies to the fact that the tide gage records contain significant noise that precludes a valid point-to-point comparison between observations and model results (**Figure 10g**). The computed maximum wave amplitude and maximum flow speed in all three models show consistent results, but the intermediate model and reference model predicted slightly larger wave amplitude in the south of Nikolski Bay, especially near the Nikolski Village (**Figure 10a–f**). Although the same B and C grid are used in both the forecast model and the intermediate model, different A grids result in different wave dynamics in Nikolski Bay, as shown by the current speed offshore of Nikolski Village in **Figure 10b** and **10d**.

The 2011 Japan tsunami is the largest event ever recorded at the Nikolski tide gage, where the tsunami waves reached 81 cm above mean sea level. Based on a tsunami source constrained in real time using the two closest tsunameters, accurate model forecasts were obtained for more than 32 coastal communities five hours before the tsunami arrived in Hawaii (Tang et al., 2012; Wei et al., 2013). The hindcast inundation

modeling using the same tsunami source indicated an 85.5% model accuracy in predicting the flooded areas in the near field along the east coastline of Japan (Wei et al., 2013). **Figure 11** shows all models give good estimates of the first four waves, but spike up at the fifth wave that resulting in a 30-40% overestimate of the maximum wave amplitude. While this provides inconsistent timing of the maximum wave, the observed record shows similar amplitude later in the wave train. Since these model results produce conservative assessment and the overall amplitude envelope is well reproduced, we consider them to be a satisfactory performance of the forecast model. The modeling results shown in **Figure 11** also indicate that the maximum tsunami water level in the model domain is close to 2 m near Nikolski Village and about 1.1 m at the tide gauge, but has no major inundation impact on the residents or the coastline. The computed maximum flow speed is 0.5 to 1 m/s in the bay, and may have reached 2 m/s at the shallow area offshore of Nikolski Village. However, it is worth noting that these current speed estimates are not confirmed due to lack of measurements in this area.

The 2011 Amukta Pass tsunami triggered by a Mw 7.3 earthquake was reported by several deep-ocean tsunameters with peak wave amplitude smaller than 2 cm. The real-time inversion using these deep-ocean measurements estimates an average slip of 0.26 m over a 100 km × 100 km rupture area. This source produces model results agreeable with the recorded data (**Figure 12**). All models correctly reproduce the arrival time and the waveform for up to three hours after the arrival. The difference of the predicted maximum wave amplitude is less than 10% among all models. The late arrivals (after five hours) computed using the forecast model decay more rapidly than those computed from intermediate model and the reference model.

The results from the intermediate model and the reference model are highly consistent in wave amplitude, wave period, arrival time, and current speed. However, use of the intermediate model is not the most efficient for forecast purposes due to its long computational time. In comparison to the intermediate model, the forecast model reduces the model simulation time by nearly 10 times, but may introduce an additional computational error upwards of 15%.

4.2 Model stability testing using synthetic scenarios

Model stability testing using synthetic scenarios provides important case studies to test the robustness, durability, and efficiency of the developed models from different perspectives:

1. Synthetic scenarios examine the developed models with extreme tsunami events to test the model stability. These model tests ensure the efficiency and robustness of the forecast model during a tsunami event.

2. Synthetic scenarios also examine the developed models with medium tsunami events to test model stability under smaller wave conditions. These model tests ensure the efficiency and robustness of the forecast model during a moderate event.

3. Synthetic scenarios examine the developed models with negligible tsunami waves to ensure the modeling results are not affected by the numerical errors.

4. The synthetic scenarios are selected in such a way that each potential tsunami source region is tested. These cases test the reliability of the developed models in relation to directionality of the tsunami waves.

Table 5 summarizes all the synthetic scenarios (plotted in **Figure 3**) used in the present model testing. All scenarios are artificially constructed using a combination of the unit sources, shown as red boxes in **Figure 3**. **Table 5** gives the details of unit source combination and the coefficients for a total of 21 scenarios, including 19 Mw 9.3, one Mw 7.5 and one micro scenario of Mw 6.4. All scenarios are tested using the forecast model, the intermediate model, and the reference model for 24-hour model runs. All tests are able to maintain the model stability without spurious values throughout the run.

Among all the Mw 9.3 synthetic scenarios, ACSZ 06-15, ACSZ 16-25, and ACSZ 22-31, in the western Alaska-Aleutian subduction zone may produce the most catastrophic tsunami impact to Nikolski. **Figures 13–15** show all three scenarios cause serious flooding at Nikolski. The tsunami flow penetrates the residential village and reaches the Umnak Lake that rests on high ground at the southwest end of the village. Scenario ACSZ 16-25 probably represents a worst case among all synthetic scenarios tested for Nikolski – it produces tsunami water level up to 16 m (reference model results) above the MHW resulting in inundation of the entire village. The maximum tsunami wave amplitude at the tide gage may reach 11.2 m above MHW (**Table 6**). One phenomenal model result of the ACSZ 16-25 scenario is that it can produce tsunamis devastating Nikolski from the shores of the Pacific Ocean. This tsunami flooding is able to penetrate the Umnak Island through the low lying lakes located in the south of Nikolski, propagating about 3 km inland from the Pacific Ocean side. Model results shown in Figure 14 indicate that tsunamis striking from both the Bering Sea and the Pacific shores will result in severe flooding over the entire Nikolski community. A detailed study of the tsunamis generated in the region of ACSZ 16-25, although beyond the scope of this report, is critical and urgently needed to address the tsunami hazard assessment for Nikolski. Figure **14** shows that for such an extreme event the tsunami flooding may also occur along the entire coastline of Nikolski Bay. The flow speed induced by the ACSZ 16-25 scenario is as large as 13 m/s over the Nikolski Village. The Nikolski Bay may be saturated with strong currents of similar flow speed. The computational results from the intermediate model and the reference model indicate large later arrivals (3 to 4 m) may continue for more than half a day after the tsunami is generated. Scenario ACSZ 06-15 also causes flooding in Nikolski Village, and induces high tsunami waves that may reach the Umnak Lake. The wave amplitude at the tide station, however, is approximately half as much in comparison with that obtained from scenario ACSZ 16-25. In scenarios ACSZ 06-15 and ACSZ 22-31, the time series at the tide gage location computed from the forecast model agrees well with the results obtained in the intermediate model and the reference model for the first 5 waves, but shows discrepancies in both phase and wave period thereafter. These differences start at an earlier time, 1.5 hours after the tsunami is generated, in the scenario ACSZ 16-25. The water level at Nikolski is generally lower than 1.5 m when the tsunami is generated by a Mw 9.3 earthquake in east Alaska, Canada or Cascadia, as shown in **Figures 16 and 17**. However, it is worth noting that in these scenarios the trailing waves decay very slowly, indicating strong wave oscillation in the Nikolski Bay. As a result, the maximum wave amplitude may arrive hours later. For

instance, the maximum water level occurs seven hours after tsunami arrival in scenarios ACSZ 50-59 and ACSZ 56-65 (**Figure 16g and 17g,** respectively). In case of a real event, the tsunami warning along the coastline of Nikolski needs to be sustained for at least a half day due to local wave oscillations.

Radiation of tsunami energy in the ocean basin is affected by the tsunami source alignment, as well as the bathymetry (Titov et al., 2005b; Grilli et al., 2007). The two synthetic Mw 9.3 scenarios in the north of Central-South Subduction Zone, CSSZ 01-10 and CSSZ 37-46, only cause small water level increase along Nikolski's coastline. The time series at the tide gage in the two cases shows that the maximum water level is less than 40 cm. For the scenario of CSSZ 01-10, the discrepancy of the maximum water level between forecast models and reference model is due to a different simulation time specified in the two models. During the model development the reference model is tested only for up to 8 hours after the tsunami arrival, while the maximum waves occur 14 to 15 hours after the tsunami waves first arrive at the tide gage (**Figure 18g**). It is a strong indication of tsunami impact affecting the coastline of Nikolski for hours or days. In comparison to the other two models (intermediate model and the reference model), the forecast model may underestimate the maximum water level when it occurs in the later arrivals (**Figures 18 and 19**).

It is worth noting that, in the cases of CSSZ 89-98 and CSSZ 102-111, the fault orientation makes tsunami energy radiate more effectively towards the Aleutians. The tsunami waves originated by these sources, about 15,000 km away from Nikolski, can still reach up to 2.9 m at the Nikolski tide gage (**Figures 20 and 21**).

Another region that may generate serious tsunami impact to coasts of Nikolski is the Kamchatka-Yap-Mariana-Izu-Bonin source zone. Computational results show that an earthquake of Mw 9.3 in the northern segment of KISZ (KISZ 01-10) can generate tsunami waves up to 3 m at Nikolski tide gage (**Figure 22**). The generated tsunami waves approach Nikolski from both the Bering Sea and the Pacific Ocean along the Aleutian Island chain. The coastal communities in the Aleutians are vulnerable to tsunamis generated in the northern part of Kuril-Kamchatka subduction zone (Wei, 2012). These tsunamis strike Nikolski more severely than those generated in the east of the Alaska-Aleutian Subduction Zone. The sea bottom funnels the tsunami waves towards Nikolski after they cross the Bering Sea from the west. Tsunamis generated from the central segment of the Kuril-Kamchatka Subduction Zone (KISZ 22-31) cause a water level increase of up to 1.5 m at the Nikolski tide gauge (**Figure 23**). The southern segment of the Kuril-Kamchatka Subduction Zone (KISZ 56-65 and KISZ 32-41) may produce tsunami waves as high as 3.2 m in Nikolski, but cause very limited flooding to the community at Nikolski (**Figure 24 and 25**). The peak-to-trough wave heights in both cases are greater than 4 m, indicating strong tsunami energy may still cause damage to the fishing boats, local ecology and coastal structures. Different than those generated in east Aleutian-Alaska Subduction Zone or South America Subduction Zone, the tsunamis generated in the Kuril-Kamchatka Subduction Zone usually bring the maximum water level within three to four hours of tsunami arrival. Although the later waves cannot be ignored, it may be more important to issue an alert for the coastal community at Nikolski

for the first group of large waves if they are generated in the Kuril-Kamchatka source region.

When comparing modeling results between the intermediate model and the reference model, one can observe an excellent agreement in computed wave amplitude, flow speed, and time series at the tide gage for the first eight hours. The main discrepancies between the forecast model and the other two models are mostly in the later waves, where A grid coverage and grid resolution play a major role in the numerical simulation of tsunami propagation along Aleutian Islands.

Excellent agreement is also found between the intermediate model and the reference model for many other synthetic Mw 9.3 scenarios, such as EPSZ 06-15, MOSZ 01-10, NGSZ 03-12, NTZ 30-39, NVSZ 28-37 and RNSZ 12-21 (**Figure 26 to 31**). The model results show that EPSZ 06-10 and MOSZ 01-10 may produce a 1.8-m water level at the Nikolski tide gage (**Table 6**).

The synthetic scenario of magnitude 7.5, NTSZ b36, introduces only up to 3.2 cm wave amplitude along the shoreline of Nikolski, and 1.8 cm at the tide gage (**Figure 32**). Both the intermediate model and the reference model show good model consistency and stability with respect to maximum wave amplitude, flow speed and the time series at the tide gage (**Figure 32**). The Mw 6.4 scenario EPSZ b19 is useful in testing the model stability under the conditions of a negligible wave. From the computed maximum wave amplitude (**Figure 33**), one can see that the water elevation at the oceanfront is only on the order of 10^{-4} m. The computed time series from both models match excellently, meaning the numerical error generated by the models themselves is negligible.

5. Summary and conclusions

Nikolski, Alaska is a coastal community on northern Umnak Island. A tsunami forecast model is presently developed for the community of Nikolski, Alaska. The developed model is being implemented into NOAA's Short-term Inundation Forecast of Tsunamis (SIFT) to provide real-time modeling forecast of tsunami wave characteristics, runup and inundation along Nikolski's coastline. This report provides detailed discussion on development of the forecast model, including the bathymetry and topography, the basic model setup, and the model parameters. Aside from the forecast model, this study also developed an intermediate models for improved model accuracy in the late arrivals. While using the same B and C grids, these two models employ different A grids of grid coverage and grid resolution. Due to the lack of a higher resolution DEM, a reference model is developed with a grid resolution of 1 arc sec (19 m in *x* axis and 31 m in *y* axis) to provide reference results for a performance evaluation of the forecast model. The forecast model computes the tsunami inundation at Nikolski, Alaska in a grid as fine as 2 arc sec (~ 37 m) in *x* axis and 1 arc sec (~ 31 m) in *y* axis. This model can accomplish a four-hour simulation in 12.4 minutes of the clock time. Model validation and tests indicate that the intermediate model and the reference model give highly consistent modeling results. Compared to the other two models, the forecast model shows up to 30% difference in the maximum wave amplitude, and small differences in wave period and phase speed in the later waves. The forecast model is capable of providing real-time forecast of tsunami impact along Nikolski's coastline. The intermediate model can be

considered as an alternative forecast tool of better model accuracy with the use of new computing technology in the near future.

Nikolski tide station has recorded several tsunamis since it was established in 2006. The 2009 Samoa, 2011 Japan and 2011 Amukta Pass tsunamis were used for model validation. The models correctly predicted the arrival time and first few waves. The model accuracies of the maximum wave amplitude at the tide station are 59% (significant background noise), 65%, and 90% for the three events, respectively. The model results of the three events indicated that the 2011 Japan tsunami might have produced a strong tsunami up to 2 m/s offshore of Nikolski. The results from all three models show good agreement in wave amplitude, wave period, arrival time, and current speed.

A total of 21 synthetic scenarios, including 19 synthetic events generated by Mw 9.3, Mw 7.5 and micro-size sources are used to examine the stability of the developed forecast model and reference model for Nikolski. The results obtained from the forecast model, the intermediate model and the reference model show good model robustness for all synthetic scenarios, meaning that the developed models are suitable for simulating tsunami waves from different directions. These synthetic scenarios reveal some common characteristics of tsunami waves in Nikolski.

1. A Mw 9.3 earthquake offshore of the Pacific coast of Umnak Island (ACSZ 16-25) may cause catastrophic tsunami along the coastline of Nikolski. The modeling results show such a tsunami may inundate the entire Nikolski Village from the shores of the Pacific and the Bering Sea with wave amplitude up to 16-m and flow speed up to 13m/s . A more detailed assessment of tsunamis generated in the region of ACSZ 16-25 is critical and urgently needed for Nikolski. Tsunamis caused by an earthquake of the same magnitude in the Aleutians (ACSZ 06-15 and ACSZ 22-31) may cause part of the Nikolski Village to be flooded.

2. Other scenarios are unlikely to cause major flooding at Nikolski Village. Although they are less threatening, the rapid tsunami current offshore may still cause damage along the coastline of Nikolski Bay in terms of fishing activity, ecology system, as well as coastal facilities.

3. Tsunami waves inside Nikolski Bay and near Nikolski Village are featured with long duration of wave oscillation, which may amplify the wave amplitude and result in delaying the arrival of the maximum wave. As such, the tsunami warning should be sustained for at least a half day after the first arrival of the tsunami waves.

4. During a tsunami, Nikolski Village is likely to be the most affected area within the entire Nikolski Bay. All model results indicate that the location of Nikolski may correspond to a node of the resonant tsunami waves at the southeast corner of the Nikolski Bay, and therefore is effective to trap the tsunami energy there.

All model validation and stability tests demonstrate that the developed tsunami forecast models and reference model for Nikolski, Alaska, are robust and accurate for their implementation in SIFT. These models can also be used for long-term tsunami hazard

assessment. However, since the model grids are developed from DEMs with coarse resolution and large error range, they need to be further improved when more accurate DEMs become available.

6. Acknowledgement

Funding for this publication and all work leading to development of a tsunami forecast model for Nikolski, Alaska was provided by the National Oceanic and Atmospheric Administration. This publication was partially funded by the Joint Institute for the Study of the Atmosphere and Ocean (JISAO) under NOAA Cooperative Agreement NO. NA17RJ1232, JISAO Contribution No. ****. This is PMEL Contribution No. ****.

7. References:

Amante, C. and B. W. Eakins (2009). ETOPO1 1 Arc-Minute Global Relief Model: Procedures, Data Sources and Analysis. NOAA Technical Memorandum NESDIS NGDC-24, 19 pp.

Beavan, J.E., E. Hauksson, S.R. McNutt, R. Bilham, and K.H. Jacob (1983): Tilt and seismicity changes in the Shumagin seismic gap. *Science*, *222*, 322–325.

Beavan, J., Wang, X., Holden, C., Wilson, K., Power, K., Prasetya, G., Bevis, M. and Kautoke, R. (2010). Near-simultaneous great earthquakes at Tongan megathrust and outer rise in September 2009, Nature, 466, 959–963.

Boyd, T.M., and K. Jacob (1986): Seismicity of the Unalaska region, Alaska. Bull. Seismol. Soc. Am., 76, 463–481.

Burwell, D., E. Tolkova, and A. Chawla (2007), Diffusion and dispersion characterization of a numerical tsunami model, Ocean Modeling, 19, 10-30.

Davies, J., L. Sykes, L. House, and K. Jacob (1981). Schumagin seismic gap, Alaska Peninsula: history of great earthquakes, tectonic setting, and evidence for high seismic potential. *J. Geophys. Res.*, *86*(B5), 3821–3856.

Fournier, T.J. and J.T. Freymueller (2007). Transition from locked to creeping subduction in the Shumagin region, Alaska. Geophys. Res. Lett., 34, L06303, doi:10.1029/2006GL029073.

Gica, E., M. Spillane, V.V. Titov, C. Chamberlin, and J.C. Newman (2008), Development of the forecast propagation database for NOAA's Short-term Inundation Forecast for Tsunamis (SIFT). NOAA Tech. Memo. OAR PMEL-139, 89 pp.

Grilli, S.T., M. Ioualalen, J. Asavanant, F.Y. Shi, J.T. Kirby, and P. Watts (2007). Source constraint and model simulation of the December 26, 2004, Indian Ocean tsunami, *J. Waterway Port Coastal Ocean Eng.*, 133(6), 414-428.

House, L.S., L.R. Sykes, J.N. Davis, K. H., and Jacob (1981): Identification of a possible seismic gap near Unalaska Island, eastern Aleutians, Alaska. Earthquake prediction—an international review. AGU, Washington D.C., 81–92.

Johnson, J.M. (1999). Heterogeneous coupling along Alaska-Aleutians as inferred from tsunami, seismic, and geodetic inversions. *Adv. Geophys.*, *39*, 1–116.

Lander, J.F. (1996). Tsunamis Affecting Alaska 1737-1996, NGDC Key to Geophysical Record Documentation No. 31, NOAA, NESDIS, NGDC, 195 pp.

Lay, T., Ammon, C.J., Kanamori, H., Rivera, L., Koper, K.D. and Hutko, A.R. (2010). The 2009 Samoa-Tonga great earthquake triggered doublet, Nature, 466, 964-968, doi:10.1038/nature09214.

Lim, E., L.A. Taylor, B.W. Eakins, K.S. Carignan, P.R. Grothe, R.J. Caldwell, and D.Z. Friday (2010). Digital elevation model of Nikolski, Alaska: procedures, data sources and analysis – prepared for the Pacific Marine Environmental Laboratory (PMEL) NOAA Center for Tsunami Research by the NOAA National Geophysical Data Center (NGDC), 24p.

Meinig, C., S.E. Stalin, A.I. Nakamura, F. González, and H.G. Milburn (2005): Technology Developments in Real-Time Tsunami Measuring, Monitoring and Forecasting. In Oceans 2005 MTS/IEEE, 19–23 September 2005, Washington, D.C.

Nishenko, S.P. (1991): Circum-Pacific seismic potential 1989–1999. *Pure Appl. Geophys.*, *135*, 169–259.

Percival, D.B., D.W. Denbo, M.C. Eble, E. Gica, H.O. Mofjeld, M.C. Spillane, L. Tang, and V.V. Titov (2011). Extraction of tsunami source coefficients via inversion of DART® buoy data. *Nat. Hazards*, *58*(1), doi: 10.1007/s11069-010-9688-1, 567–590.

Synolakis, C.E., E.N. Bernard, V.V. Titov, U. Kânoğlu, and F.I. González (2008): Validation and verification of tsunami numerical models. *Pure Appl. Geophys.*, *165*(11–12), 2197–2228.

Tang, L., V. V. Titov, and C. D. Chamberlin (2009), Development, testing, and applications of site-specific tsunami inundation models for real-time forecasting, *J. Geophys. Res.*, 114, C12025, doi:10.1029/2009JC005476.

Tang, L., V.V. Titov, E. Bernard, Y. Wei, C. Chamberlin, J.C. Newman, H. Mofjeld, D. Arcas, M. Eble, C. Moore, B. Uslu, C. Pells, M.C. Spillane, L.M. Wright, and E. Gica (2012): Direct energy estimation of the 2011 Japan tsunami using deep-ocean pressure measurements. J. Geophys. Res., 117, C08008, doi: 10.1029/2011JC007635.

Tang, L., V.V. Titov, Y. Wei, H.O. Mofjeld, M. Spillane, D. Arcas, E.N. Bernard, C. Chamberlin, E. Gica, and J. Newman (2008): Tsunami forecast analysis for the May 2006 Tonga tsunami. *J. Geophys. Res.*, *113*, C12015, doi: 10.1029/2008JC004922.

Tanioka, Y., K. Satake, L. Ruff, and F. González (1994): Fault parameters and tsunami excitation of the May 13, 1993, Shumagin Islands earthquake. *Geophys. Res. Lett.*, *21*(11), 967–970.

Titov, V.V. (2009): Tsunami forecasting. Chapter 12 in *The Sea, Volume 15: Tsunamis*, Harvard University Press, Cambridge, MA and London, England, 371–400.

Titov, V., and F.I. González (1997): Implementation and testing of the Method of Splitting Tsunami (MOST) model. NOAA Tech. Memo. ERL PMEL-112 (PB98-122773), NOAA/Pacific Marine Environmental Laboratory, Seattle, WA, 11 pp.

Titov, V.V., F.I. González, E.N. Bernard, M.C. Eble, H.O. Mofjeld, J.C. Newman, and A.J. Venturato (2005a): Real-time tsunami forecasting: Challenges and solutions. Nat. Hazards, 35(1), Special Issue, U.S. National Tsunami Hazard Mitigation Program, 41–58.

Titov, V.V., A.B. Rabinovich, H.O. Mofjeld, R.E. Thomson, and F.I. González (2005b), The global reach of the 26 December 2004 Sumatra Tsunami. *Science*. doi: 10.1126/science.1114576.

Wei, Y. (2012): A Tsunami Forecast Model for Unalaska, Alaska. NOAA OAR Special Report, PMEL Tsunami Forecast Series: Vol. 10, in press.

Wei, Y., E. Bernard, L. Tang, R. Weiss, V. Titov, C. Moore, M. Spillane, M. Hopkins, and U. Kânoğlu (2008): Real-time experimental forecast of the Peruvian tsunami of August 2007 for U.S. coastlines. *Geophys. Res. Lett.*, *35*, L04609, doi: 10.1029/2007GL032250.

Wei, Y., C. Chamberlin, V.V. Titov, L. Tang, and E.N. Bernard (2013): Modeling of 2011 Japan Tsunami - lessons for near-field forecast, *Pure Appl. Geophys*., 170(6–8), doi: 10.1007/s00024-012-0519-z, 1309–1331.

Witter, R. C., R. W. Briggs, S. E. Engelhart, G. Gelfenbaum, R. D. Koehler, and W. D. Barnhart (2014), Little late Holocenestrain accumulation and release on theAleutian megathrust below theShumagin Islands, Alaska, Geophys. Res.Lett., 41, 2359–2367, doi:10.1002/2014GL059393.

Zhou, H., Y. Wei, L. Wright and V.V. Titov (2014): Waves and currents in Hawaii waters induced by the dispersive 2011 Tohoku tsunami. Pure and Appl. Geophys., in press.

Zhou, H., Y. Wei, and V.V. Titov (2012): Dispersive modeling of the 2009 Samoa tsunami. Geophys. Res. Lett., 39(16), L16603, doi: 1029/2012GL053068.

Figures:

Figure 1. (a) Aerial view of Nikolski, Alaska and the location of the Nikolski tide station. (b) Land view of Nikolski, Alaska and location of the Nikolski tide station.

Figure 2. Potential earthquake sources in the Alaska-Aleutian Subduction Zone, The red boxes are the tsunami unit sources employed in SIFT. The yellow square denotes the approximate location of Nikolski.

Figure 3. Historical tsunami events (● and ●) that have affected Nikolski, Alaska, where ● are events used for model validation in this study, and ● are events not used for model validation. ▲ represents the location of deep-ocean tsunameters. The red boxes are the tsunami propagation unit sources (Gica *et al.*, 2008). Also included are model scenarios used in model validation and stability testing.

Figure 4. A-grid bathymetry and topography for the reference model, where the black boxes indicate the coverage of B grid and C grid.

Figure 5. A-grid bathymetry and topography for the forecast models and the reference model. The red box indicates the coverage of A grid of the forecast model, and the black boxes indicate the coverage of B grid and C grid.

Figure 6. B-grid bathymetry and topography for the reference model, where the black box indicates the coverage of C grid. The red solid circle labels the location of the Nikolski tide station.

Figure 7. B-grid bathymetry and topography for both forecast models, where the black box indicates the coverage of C grid. The red solid circle labels the location of the Nikolski tide station.

Figure 8. C-grid bathymetry and topography for the reference model, where the red solid circle labels the location of the Nikolski tide station.

Figure 9. C-grid bathymetry and topography for both forecast models, where the red solid circle labels the location of the Nikolski tide station.

Figure 10. Modeling results for the 29 September 2009 Samoa tsunami. (a) Maximum wave amplitude in the C grid computed from the forecast model; (b) Maximum flow speed in the C grid computed from the forecast model; (c) Maximum wave amplitude in the C grid computed from the intermediate model; (d) Maximum flow speed in the C grid computed from the intermediate model 2; (e) Maximum wave amplitude in the C grid computed from the reference model; (f) Maximum flow speed in the C grid computed from reference model; (g) Comparison of the time series between observation and model results at the Nikolski tide station.

Figure 11. Modeling results for the 11 March 2011 Japan tsunami. (a) Maximum wave amplitude in the C grid computed from the forecast model; (b) Maximum flow speed in the C-grid computed from the forecast model; (c) Maximum wave amplitude in the C grid computed from the intermediate model; (d) Maximum flow speed in the C grid

grid computed from the intermediate model; (d) Maximum flow speed in the C grid computed from the intermediate model; (e) Maximum wave amplitude in the C grid computed from the reference model; (f) Maximum flow speed in the C grid computed from reference model; (g) Comparison of the time series between observation and model results at the Nikolski tide station.

Figure 12. Modeling results for the 24 June 2011 Amukta Pass event. (a) Maximum wave amplitude in the C grid computed from the forecast model; (b) Maximum flow speed in the C-grid computed from the forecast model; (c) Maximum wave amplitude in the C grid computed from the intermediate model; (d) Maximum flow speed in the C grid computed from the intermediate model; (e) Maximum wave amplitude in the C grid computed from the reference model; (f) Maximum flow speed in the C grid computed from reference model; (g) Comparison of the time series between observation and model results at the Nikolski tide station.

Figure 13. Modeling results for the ACSZ 06-15 scenario. (a) Maximum wave amplitude in the C grid computed from the forecast model; (b) Maximum flow speed in the C grid computed from the forecast model; (c) Maximum wave amplitude in the C grid computed from the intermediate model; (d) Maximum flow speed in the C grid computed from the intermediate model; (e) Maximum wave amplitude in the C grid computed from the reference model; (f) Maximum flow speed in the C-grid computed from reference model; (g) Comparison of the time series between observation and model results at the Nikolski tide station.

Figure 14. Modeling results for the ACSZ 16-25 scenario. (a) Maximum wave amplitude in the C grid computed from the forecast model; (b) Maximum flow speed in the C grid computed from the forecast model; (c) Maximum wave amplitude in the C grid computed from the intermediate model; (d) Maximum flow speed in the C grid computed from the intermediate model; (e) Maximum wave amplitude in the C grid computed from the reference model; (f) Maximum flow speed in the C grid computed from reference model; (g) Comparison of the time series between observation and model results at the Nikolski tide station.

Figure 15. Modeling results for the ACSZ 22-31 scenario. (a) Maximum wave amplitude in the C grid computed from the forecast model; (b) Maximum flow speed in the C grid computed from the forecast model; (c) Maximum wave amplitude in the C grid computed from the intermediate model; (d) Maximum flow speed in the C grid computed from the intermediate model; (e) Maximum wave amplitude in the C grid computed from the reference model; (f) Maximum flow speed in the C-grid computed from reference model; (g) Comparison of the time series between observation and model results at the Nikolski tide station.

Figure 16. Modeling results for the ACSZ 50-59 scenario. (a) Maximum wave amplitude in the C grid computed from the forecast model; (b) Maximum flow speed in the C grid computed from the forecast model; (c) Maximum wave amplitude in the C grid computed from the intermediate model; (d) Maximum flow speed in the C grid computed from the intermediate model; (e) Maximum wave amplitude in the C grid computed from the reference model; (f) Maximum flow speed in the C-grid computed from reference model;

(g) Comparison of the time series between observation and model results at the Nikolski tide station.

Figure 17. Modeling results for the ACSZ 56-65 scenario. (a) Maximum wave amplitude in the C grid computed from the forecast model; (b) Maximum flow speed in the C grid computed from the forecast model; (c) Maximum wave amplitude in the C grid computed from the intermediate model; (d) Maximum flow speed in the C grid computed from the intermediate model; (e) Maximum wave amplitude in the C grid computed from the reference model; (f) Maximum flow speed in the C-grid computed from reference model; (g) Comparison of the time series between observation and model results at the Nikolski tide station.

Figure 18. Modeling results for the CSSZ 01-10 scenario. (a) Maximum wave amplitude in the C grid computed from the forecast model; (b) Maximum flow speed in the C grid computed from the forecast model; (c) Maximum wave amplitude in the C grid computed from the intermediate model; (d) Maximum flow speed in the C grid computed from the intermediate model; (e) Maximum wave amplitude in the C grid computed from the reference model; (f) Maximum flow speed in the C grid computed from reference model; (g) Comparison of the time series between observation and model results at the Nikolski tide station.

Figure 19. Modeling results for the CSSZ 37-46 scenario. (a) Maximum wave amplitude in the C grid computed from the forecast model; (b) Maximum flow speed in the C grid computed from the forecast model; (c) Maximum wave amplitude in the C grid computed from the intermediate model; (d) Maximum flow speed in the C grid computed from the intermediate model; (e) Maximum wave amplitude in the C grid computed from the reference model; (f) Maximum flow speed in the C grid computed from reference model; (g) Comparison of the time series between observation and model results at the Nikolski tide station.

Figure 20. Modeling results for the CSSZ 89-98 scenario. (a) Maximum wave amplitude in the C grid computed from the forecast model; (b) Maximum flow speed in the C grid computed from the forecast model; (c) Maximum wave amplitude in the C grid computed from the intermediate model; (d) Maximum flow speed in the C grid computed from the intermediate model; (e) Maximum wave amplitude in the C grid computed from the reference model; (f) Maximum flow speed in the C grid computed from reference model; (g) Comparison of the time series between observation and model results at the Nikolski tide station.

Figure 21. Modeling results for the CSSZ 102-111 scenario. (a) Maximum wave amplitude in the C grid computed from the forecast model; (b) Maximum flow speed in the C grid computed from the forecast model; (c) Maximum wave amplitude in the C grid computed from the intermediate model; (d) Maximum flow speed in the C grid computed from the intermediate model; (e) Maximum wave amplitude in the C grid computed from the reference model; (f) Maximum flow speed in the C grid computed from reference model; (g) Comparison of the time series between observation and model results at the Nikolski tide station.

Figure 22. Modeling results for the KISZ 01-10 scenario. (a) Maximum wave amplitude in the C grid computed from the forecast model; (b) Maximum flow speed in the C grid computed from the forecast model; (c) Maximum wave amplitude in the C grid computed from the intermediate model; (d) Maximum flow speed in the C grid computed from the intermediate model; (e) Maximum wave amplitude in the C grid computed from the reference model; (f) Maximum flow speed in the C grid computed from reference model; (g) Comparison of the time series between observation and model results at the Nikolski tide station.

Figure 23. Modeling results for the KISZ 22-31 scenario. (a) Maximum wave amplitude in the C grid computed from the forecast model; (b) Maximum flow speed in the C grid computed from the forecast model; (c) Maximum wave amplitude in the C grid computed from the intermediate model; (d) Maximum flow speed in the C grid computed from the intermediate model; (e) Maximum wave amplitude in the C grid computed from the reference model; (f) Maximum flow speed in the C grid computed from reference model; (g) Comparison of the time series between observation and model results at the Nikolski tide station.

Figure 24. Modeling results for the KISZ 32-41 scenario. (a) Maximum wave amplitude in the C grid computed from the forecast model; (b) Maximum flow speed in the C grid computed from the forecast model; (c) Maximum wave amplitude in the C grid computed from the intermediate model; (d) Maximum flow speed in the C grid computed from the intermediate model; (e) Maximum wave amplitude in the C grid computed from the reference model; (f) Maximum flow speed in the C grid computed from reference model; (g) Comparison of the time series between observation and model results at the Nikolski tide station.

Figure 25. Modeling results for the KISZ 56-65 scenario. (a) Maximum wave amplitude in the C grid computed from the forecast model; (b) Maximum flow speed in the C grid computed from the forecast model; (c) Maximum wave amplitude in the C grid computed from the intermediate model; (d) Maximum flow speed in the C grid computed from the intermediate model; (e) Maximum wave amplitude in the C grid computed from the reference model; (f) Maximum flow speed in the C grid computed from reference model; (g) Comparison of the time series between observation and model results at the Nikolski tide station.

Figure 26. Modeling results for the EPSZ 06-15 scenario. (a) Maximum wave amplitude in the C grid computed from the forecast model; (b) Maximum flow speed in the C grid computed from the forecast model; (c) Maximum wave amplitude in the C grid computed from the intermediate model; (d) Maximum flow speed in the C grid computed from the intermediate model; (e) Maximum wave amplitude in the C grid computed from the reference model; (f) Maximum flow speed in the C grid computed from reference model; (g) Comparison of the time series between observation and model results at the Nikolski tide station.

Figure 27. Modeling results for the MOSZ 01-10 scenario. (a) Maximum wave amplitude in the C grid computed from the forecast model; (b) Maximum flow speed in the C grid computed from the forecast model; (c) Maximum wave amplitude in the C grid computed

from the intermediate model; (d) Maximum flow speed in the C grid computed from the intermediate model; (e) Maximum wave amplitude in the C grid computed from the reference model; (f) Maximum flow speed in the C grid computed from reference model; (g) Comparison of the time series between observation and model results at the Nikolski tide station.

Figure 28. Modeling results for the NGSZ 03-12 scenario. (a) Maximum wave amplitude in the C grid computed from the forecast model; (b) Maximum flow speed in the C grid computed from the forecast model; (c) Maximum wave amplitude in the C grid computed from the intermediate model; (d) Maximum flow speed in the C grid computed from the intermediate model; (e) Maximum wave amplitude in the C grid computed from the reference model; (f) Maximum flow speed in the C grid computed from reference model; (g) Comparison of the time series between observation and model results at the Nikolski tide station.

Figure 29. Modeling results for the NTSZ 30-39 scenario. (a) Maximum wave amplitude in the C grid computed from the forecast model; (b) Maximum flow speed in the C grid computed from the forecast model; (c) Maximum wave amplitude in the C grid computed from the intermediate model; (d) Maximum flow speed in the C grid computed from the intermediate model; (e) Maximum wave amplitude in the C grid computed from the reference model; (f) Maximum flow speed in the C grid computed from reference model; (g) Comparison of the time series between observation and model results at the Nikolski tide station.

Figure 30. Modeling results for the NVSZ 28-37 scenario. (a) Maximum wave amplitude in the C grid computed from the forecast model; (b) Maximum flow speed in the C grid computed from the forecast model; (c) Maximum wave amplitude in the C grid computed from the intermediate model; (d) Maximum flow speed in the C grid computed from the intermediate model; (e) Maximum wave amplitude in the C grid computed from the reference model; (f) Maximum flow speed in the C grid computed from reference model; (g) Comparison of the time series between observation and model results at the Nikolski tide station.

Figure 31. Modeling results for the RNSZ 12-21 scenario. (a) Maximum wave amplitude in the C grid computed from the forecast model; (b) Maximum flow speed in the C grid computed from the forecast model; (c) Maximum wave amplitude in the C grid computed from the intermediate model; (d) Maximum flow speed in the C grid computed from the intermediate model; (e) Maximum wave amplitude in the C grid computed from the reference model; (f) Maximum flow speed in the C grid computed from reference model; (g) Comparison of the time series between observation and model results at the Nikolski tide station.

Figure 32. Modeling results for the NTSZ B36 scenario. (a) Maximum wave amplitude in the C grid computed from the forecast model; (b) Maximum flow speed in the C grid computed from the forecast model; (c) Maximum wave amplitude in the C grid computed from the intermediate model; (d) Maximum flow speed in the C grid computed from the intermediate model; (e) Maximum wave amplitude in the C grid computed from the reference model; (f) Maximum flow speed in the C grid computed from reference model;

(g) Comparison of the time series between observation and model results at the Nikolski tide station.

Figure 33. Modeling results for the EPSZ B19 scenario. (a) Maximum wave amplitude in the C grid computed from the forecast model; (b) Maximum flow speed in the C grid computed from the forecast model; (c) Maximum wave amplitude in the C grid computed from the intermediate model; (d) Maximum flow speed in the C grid computed from the intermediate model; (e) Maximum wave amplitude in the C grid computed from the reference model; (f) Maximum flow speed in the C grid computed from reference model. (g) Comparison of the time series between observation and model results at the Nikolski tide station.

(a)


4/3/2009 12:00:00 am
Figure 1
Bering Sea
N52.9452°
Model warning point
Depth = 2.3 m
Gage sensor depth = 2.36 m
W168.872°
52.941111N, 168.87W
W168.865°
W168.858°
Tide gage housing
Nikolski, AK
Nikolski
N52.938°
© 2012 Google
Image © 2012 DigitalGlobe
287 m
Google earth
Imagery Date: 4/3/2009 2009
lat 52.941342° lon -168.86378° elev 2 m
Eye alt 1.24 km

(b)


Tide gage housing
Welcome To
NIKOLSKI
Class of 2004

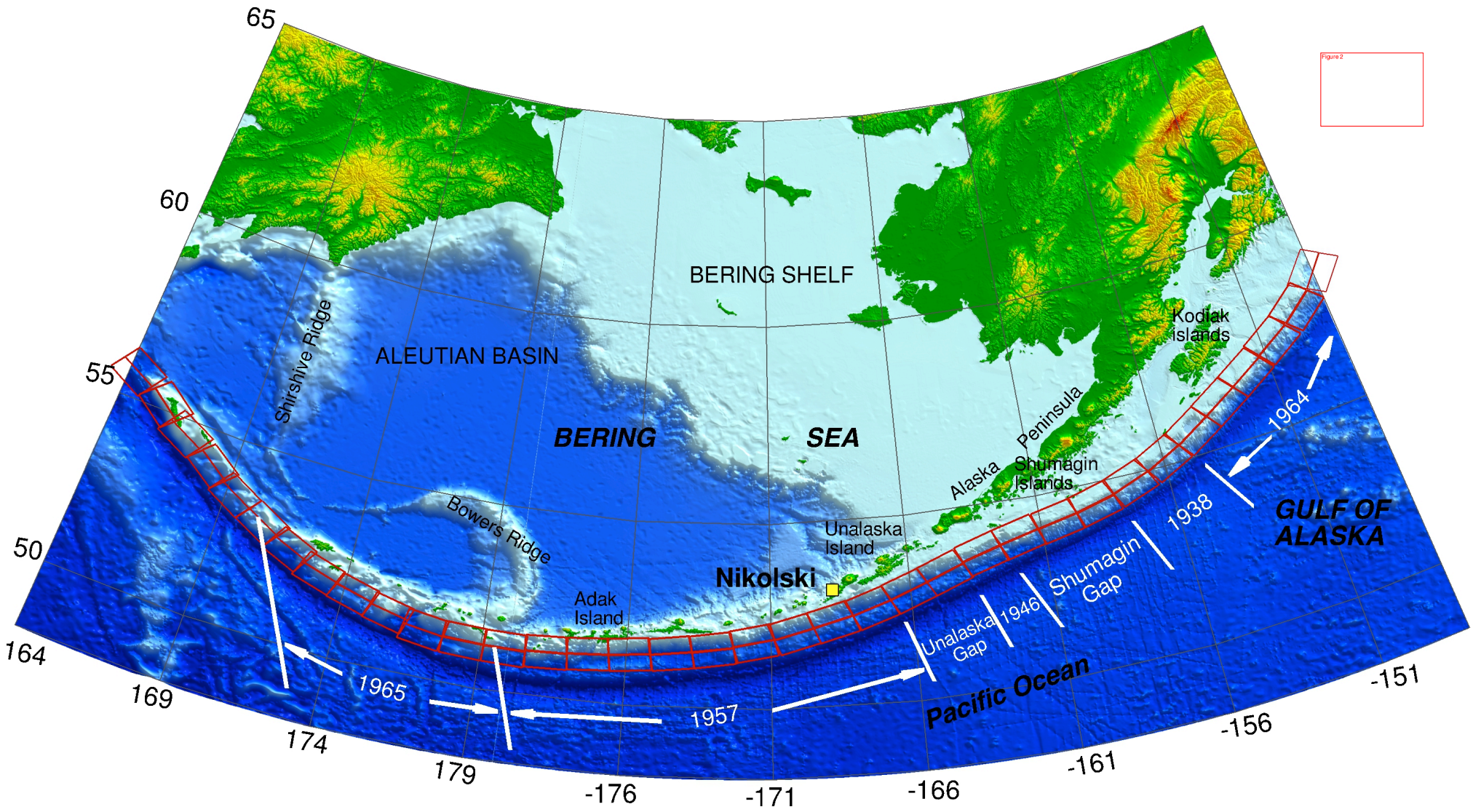
65
60
55
50
164
169
174
179
-176
-171
-166
-161
-156
-151
BERING SHELF
ALEUTIAN BASIN
Shirshive Ridge
BERING
SEA
Bowers Ridge
Adak
Island
Unalaska
Island
Nikolski
Alaska
Peninsula
Shumagin
Islands
Kodiak
islands
1965
1957
Unalaska
Gap
1946
Shumagin
Gap
1938
1964
GULF OF
ALASKA
Pacific Ocean

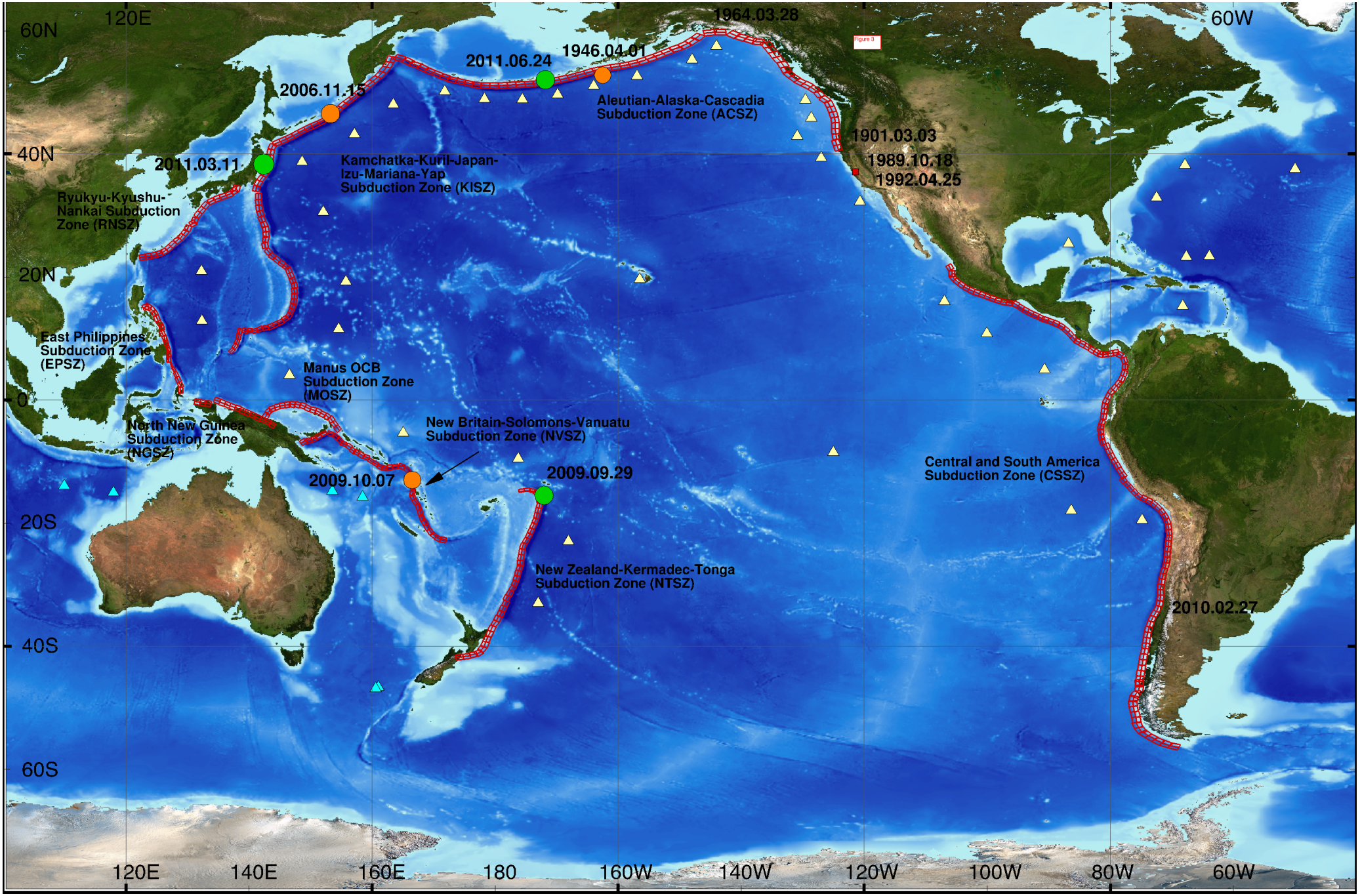
60N
120E
60W
40N
20N
0
20S
40S
60S
120E
140E
160E
180
160W
140W
120W
100W
80W
60W
1964.03.28
1946.04.01
2011.06.24
2006.11.15
2011.03.11
1901.03.03
1989.10.18
1992.04.25
2009.10.07
2009.09.29
2010.02.27
Aleutian-Alaska-Cascadia Subduction Zone (ACSZ)
Kamchatka-Kuril-Japan-Izu-Mariana-Yap Subduction Zone (KISZ)
Ryukyu-Kyushu-Nankai Subduction Zone (RNSZ)
East Philippines Subduction Zone (EPSZ)
Manus OCB Subduction Zone (MOSZ)
North New Guinea Subduction Zone (NGSZ)
New Britain-Solomons-Vanuatu Subduction Zone (NVSZ)
New Zealand-Kermadec-Tonga Subduction Zone (NTSZ)
Central and South America Subduction Zone (CSSZ)

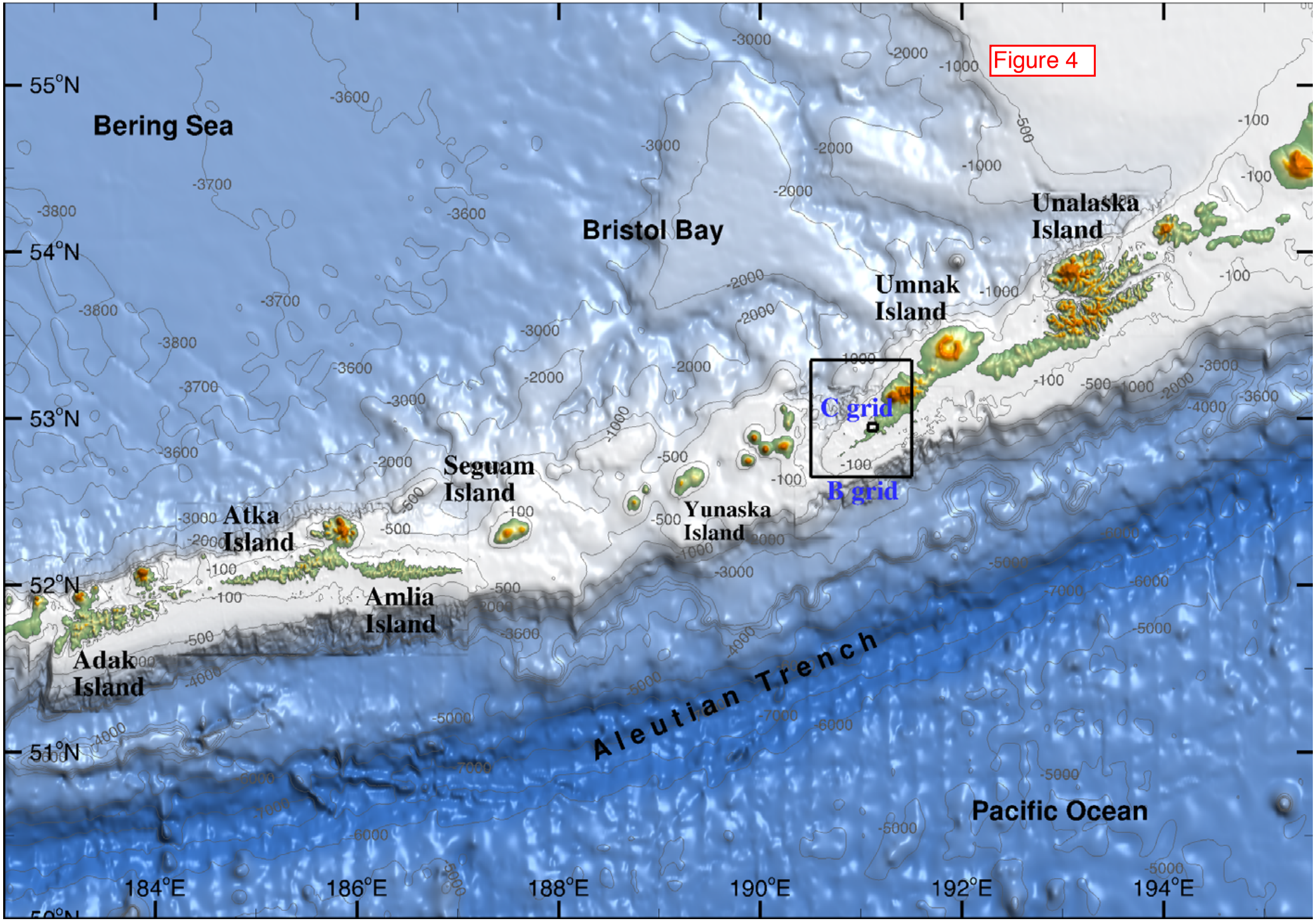
Figure 4
Bering Sea
Bristol Bay
Unalaska Island
Umnak Island
C grid
B grid
Seguam Island
Atka Island
Amlia Island
Yunaska Island
Adak Island
Aleutian Trench
Pacific Ocean
55°N
54°N
53°N
52°N
51°N
184°E
186°E
188°E
190°E
192°E
194°E

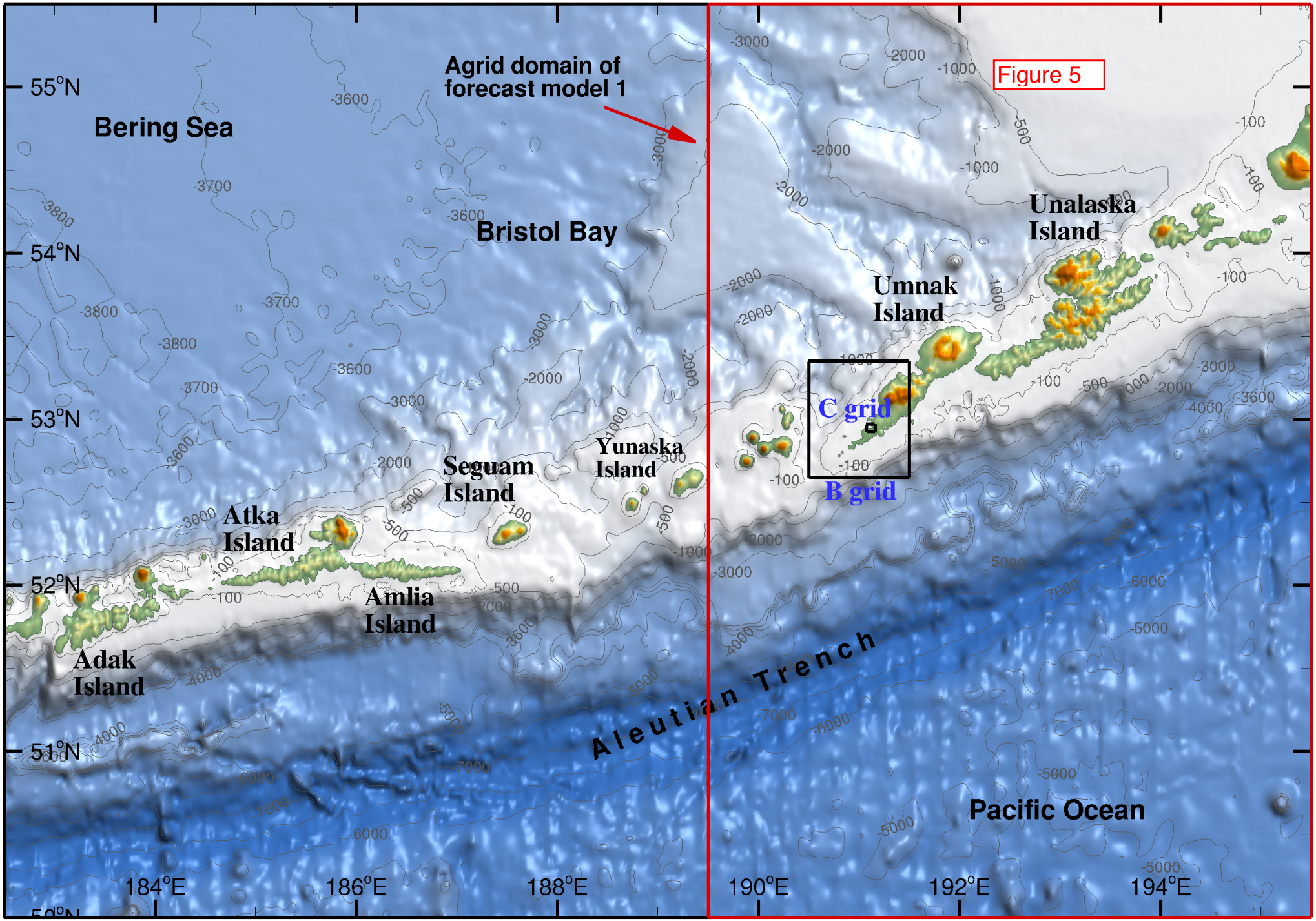
Figure 5
Agrid domain of forecast model 1
Bering Sea
Bristol Bay
Unalaska Island
Umnak Island
C grid
B grid
Seguam Island
Yunaska Island
Atka Island
Amlia Island
Adak Island
Aleutian Trench
Pacific Ocean
55°N
54°N
53°N
52°N
51°N
184°E
186°E
188°E
190°E
192°E
194°E

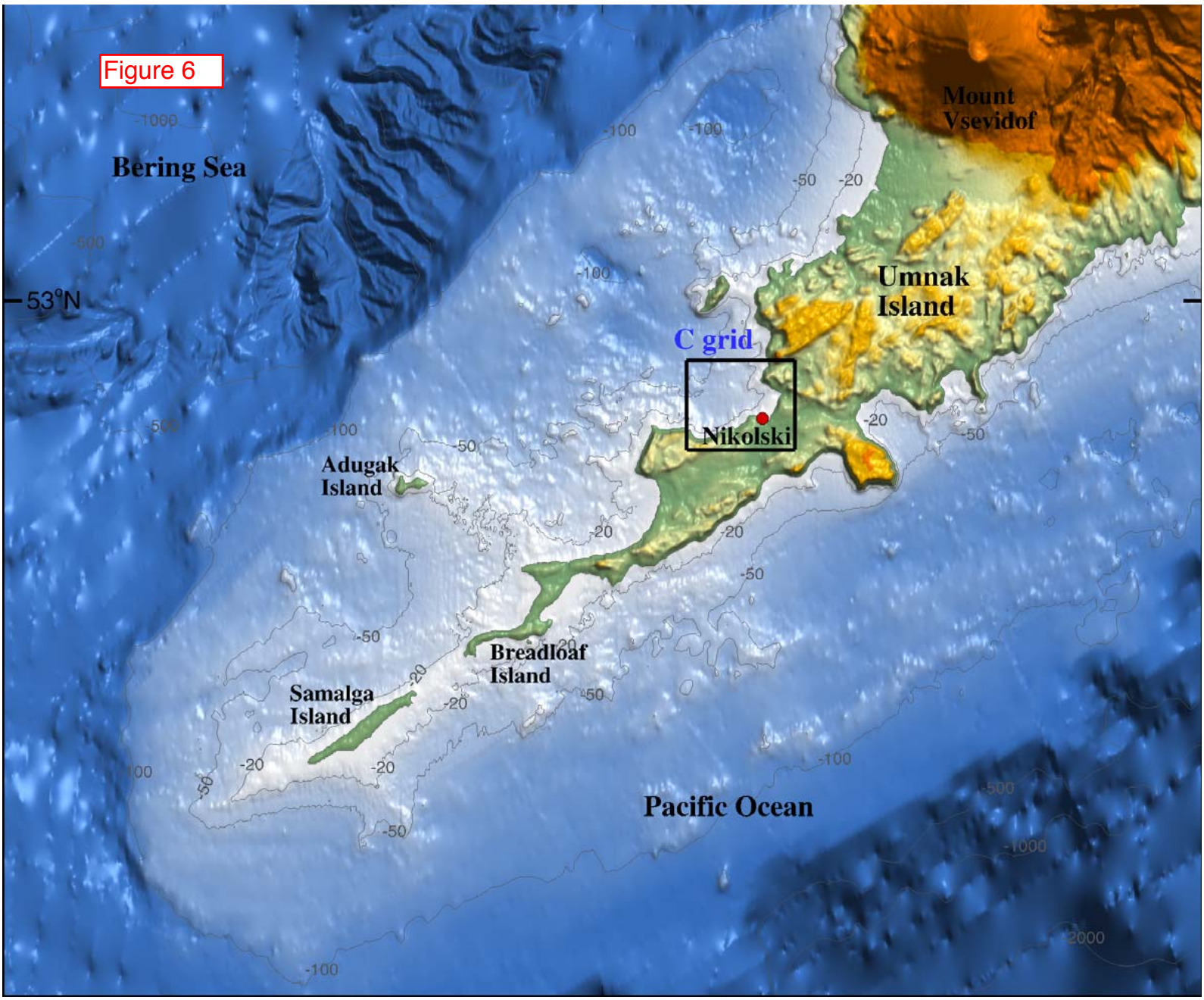
Figure 6
Bering Sea
Mount Vsevidof
Umnak Island
C grid
Nikolski
Adugak Island
Breadloaf Island
Samalga Island
Pacific Ocean
53°N
-1000
-500
-100
-50
-20
-2000

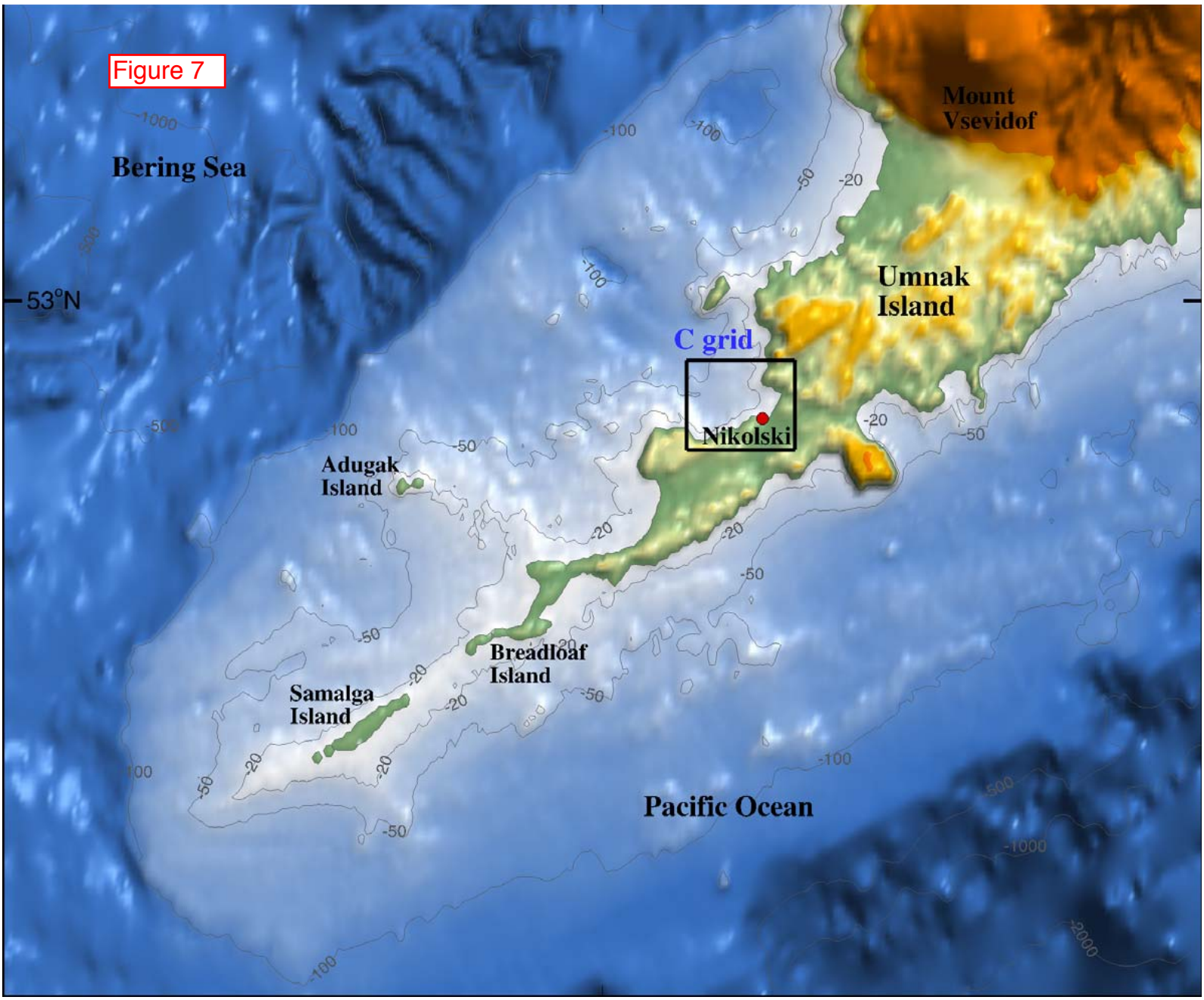
Figure 7
Bering Sea
Mount
Vsevidof
Umnak
Island
C grid
Nikolski
Adugak
Island
Breadloaf
Island
Samalga
Island
Pacific Ocean
53°N
-1000
-500
-100
-50
-20

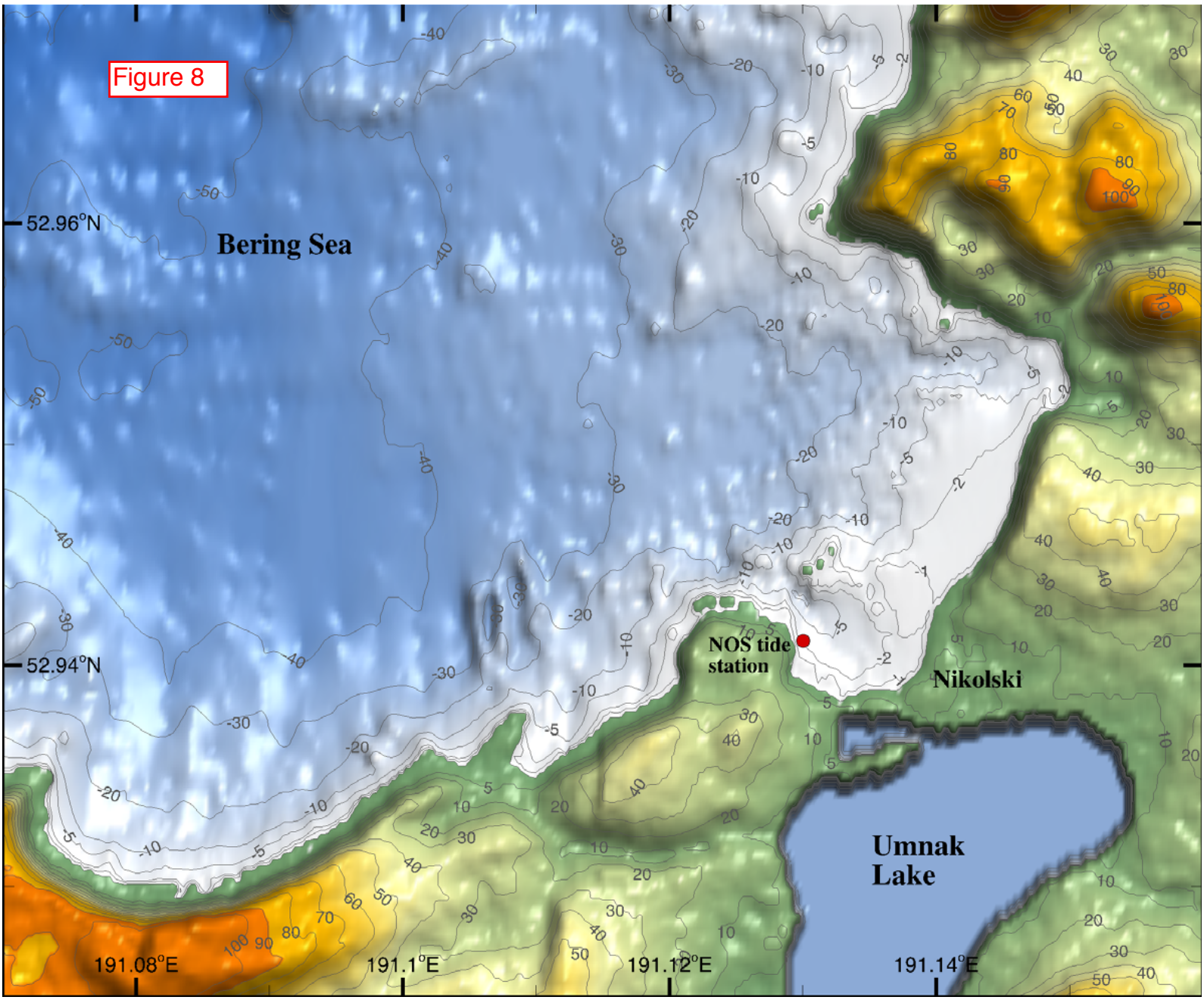
Figure 8
52.96°N
52.94°N
Bering Sea
NOS tide station
Nikolski
Umnak Lake
191.08°E
191.1°E
191.12°E
191.14°E

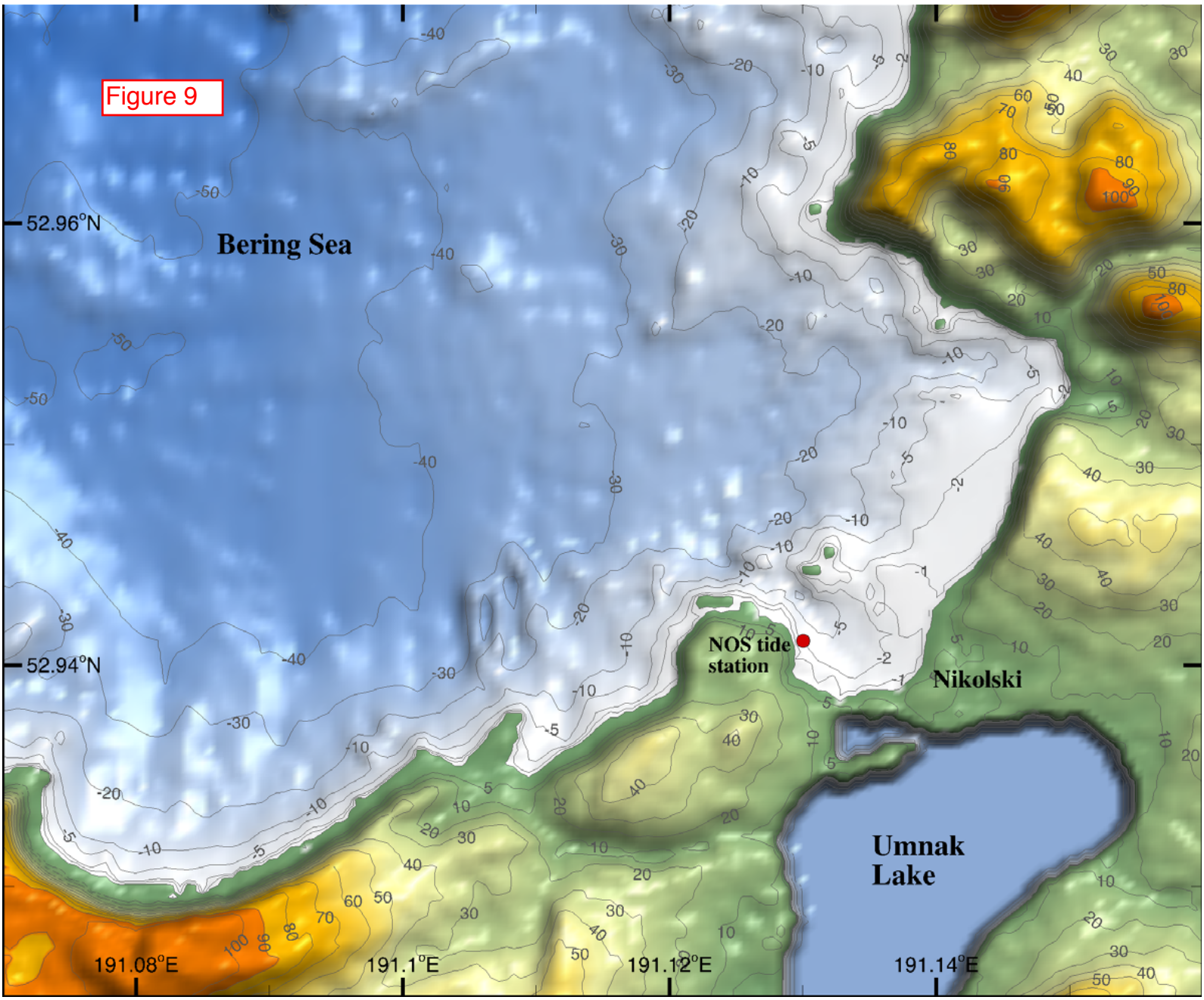
Figure 9
52.96°N
52.94°N
Bering Sea
NOS tide station
Nikolski
Umnak Lake
191.08°E
191.1°E
191.12°E
191.14°E

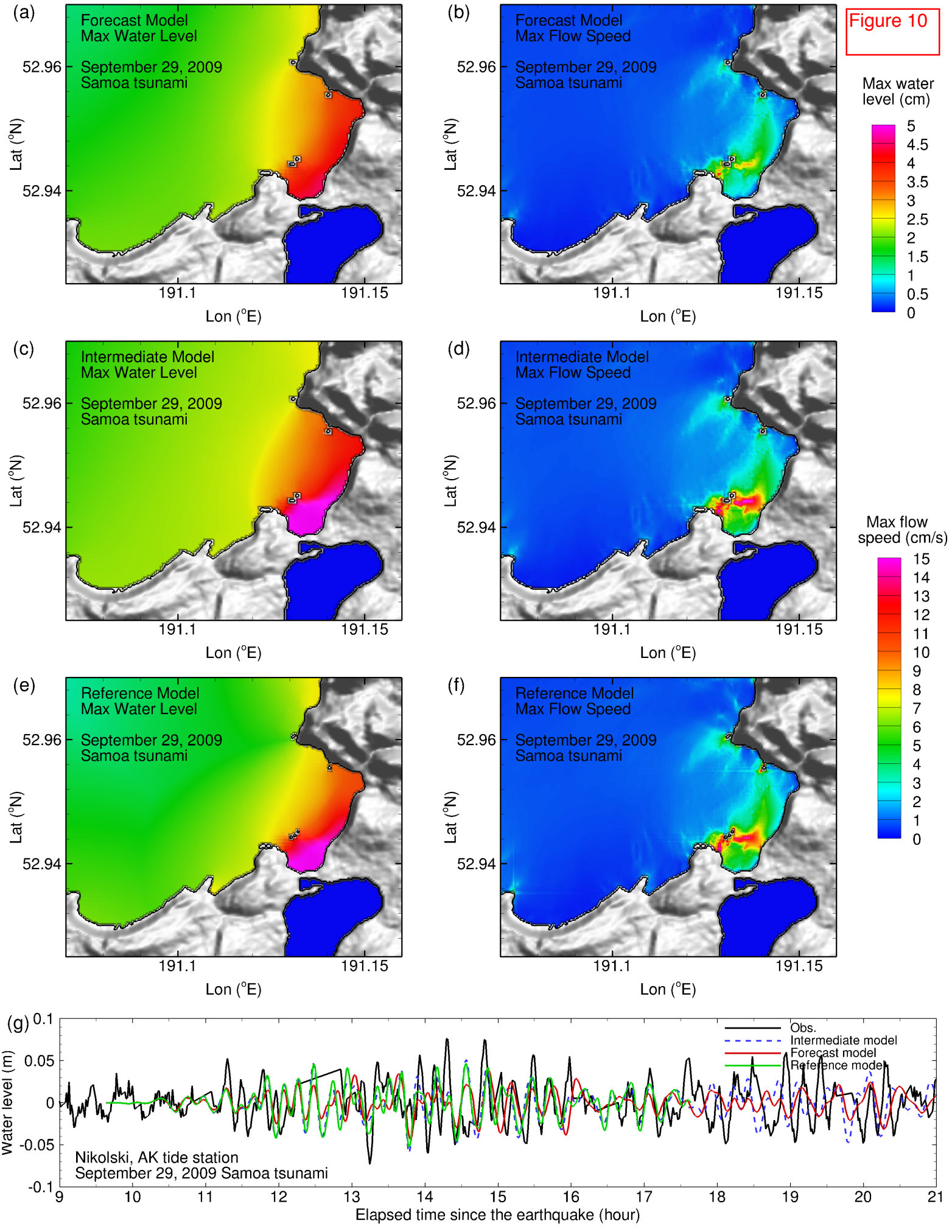
Figure 10
(a)
Forecast Model
Max Water Level
September 29, 2009
Samoa tsunami
(b)
Forecast Model
Max Flow Speed
September 29, 2009
Samoa tsunami
Max water level (cm)
5
4.5
4
3.5
3
2.5
2
1.5
1
0.5
0
(c)
Intermediate Model
Max Water Level
September 29, 2009
Samoa tsunami
(d)
Intermediate Model
Max Flow Speed
September 29, 2009
Samoa tsunami
Max flow speed (cm/s)
15
14
13
12
11
10
9
8
7
6
5
4
3
2
1
0
(e)
Reference Model
Max Water Level
September 29, 2009
Samoa tsunami
(f)
Reference Model
Max Flow Speed
September 29, 2009
Samoa tsunami
Lat (°N)
52.96
52.94
Lon (°E)
191.1
191.15
(g)
Water level (m)
0.1
0.05
0
-0.05
-0.1
Obs.
Intermediate model
Forecast model
Reference model
Nikolski, AK tide station
September 29, 2009 Samoa tsunami
9
10
11
12
13
14
15
16
17
18
19
20
21
Elapsed time since the earthquake (hour)

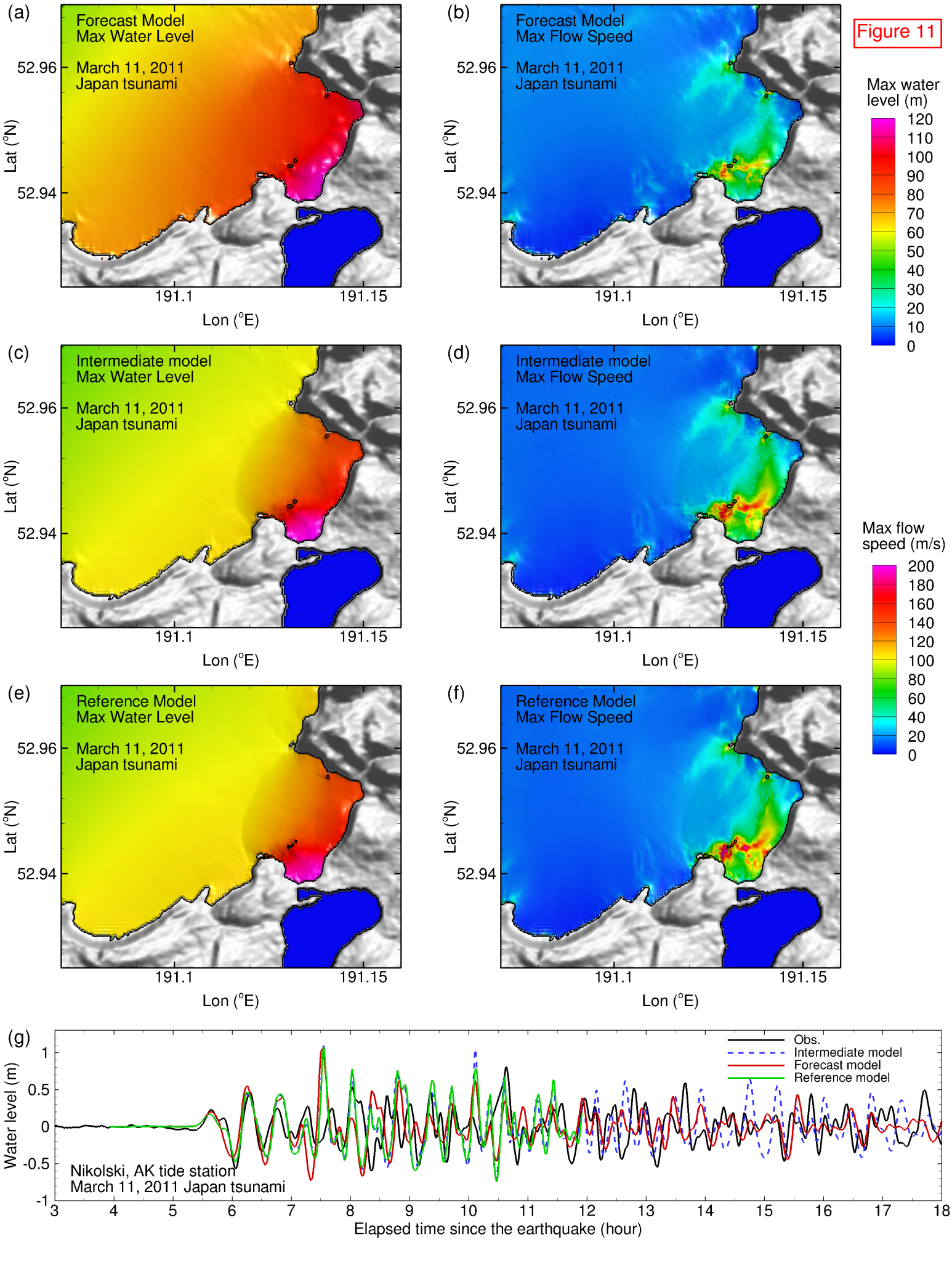
(a)
Forecast Model
Max Water Level
March 11, 2011
Japan tsunami
(b)
Forecast Model
Max Flow Speed
March 11, 2011
Japan tsunami
Figure 11
Max water level (m)
120
110
100
90
80
70
60
50
40
30
20
10
0
(c)
Intermediate model
Max Water Level
March 11, 2011
Japan tsunami
(d)
Intermediate model
Max Flow Speed
March 11, 2011
Japan tsunami
Max flow speed (m/s)
200
180
160
140
120
100
80
60
40
20
0
(e)
Reference Model
Max Water Level
March 11, 2011
Japan tsunami
(f)
Reference Model
Max Flow Speed
March 11, 2011
Japan tsunami
Lat (°N)
52.96
52.94
191.1
191.15
Lon (°E)
(g)
Obs.
Intermediate model
Forecast model
Reference model
Water level (m)
1
0.5
0
-0.5
-1
Nikolski, AK tide station
March 11, 2011 Japan tsunami
3
4
5
6
7
8
9
10
11
12
13
14
15
16
17
18
Elapsed time since the earthquake (hour)

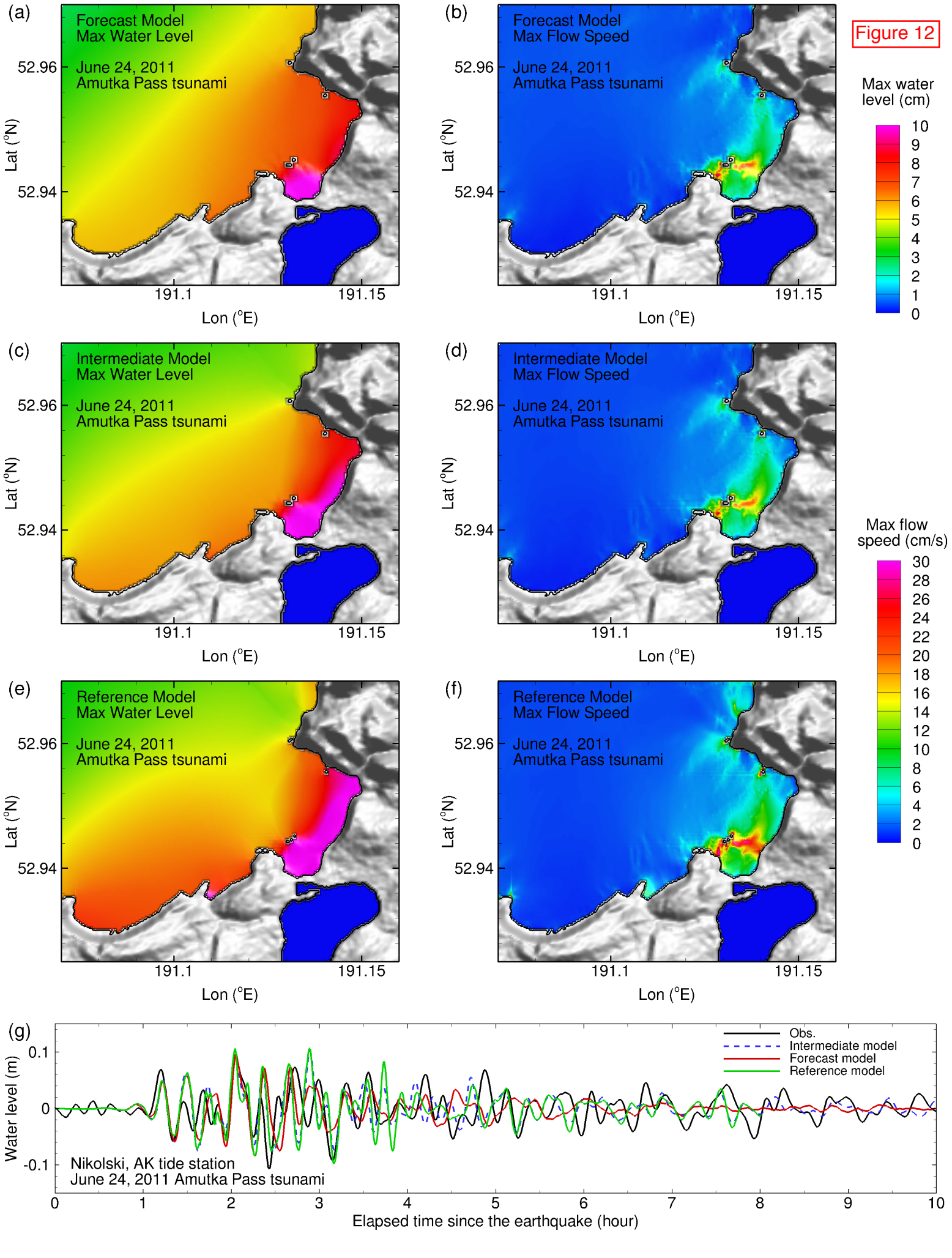
(a)
Forecast Model
Max Water Level
June 24, 2011
Amutka Pass tsunami
(b)
Forecast Model
Max Flow Speed
June 24, 2011
Amutka Pass tsunami
Figure 12
Max water level (cm)
10
9
8
7
6
5
4
3
2
1
0
(c)
Intermediate Model
Max Water Level
June 24, 2011
Amutka Pass tsunami
(d)
Intermediate Model
Max Flow Speed
June 24, 2011
Amutka Pass tsunami
Max flow speed (cm/s)
30
28
26
24
22
20
18
16
14
12
10
8
6
4
2
0
(e)
Reference Model
Max Water Level
June 24, 2011
Amutka Pass tsunami
(f)
Reference Model
Max Flow Speed
June 24, 2011
Amutka Pass tsunami
52.96
52.94
Lat (°N)
191.1
191.15
Lon (°E)
(g)
Water level (m)
0.1
0
-0.1
Nikolski, AK tide station
June 24, 2011 Amutka Pass tsunami
Obs.
Intermediate model
Forecast model
Reference model
0
1
2
3
4
5
6
7
8
9
10
Elapsed time since the earthquake (hour)

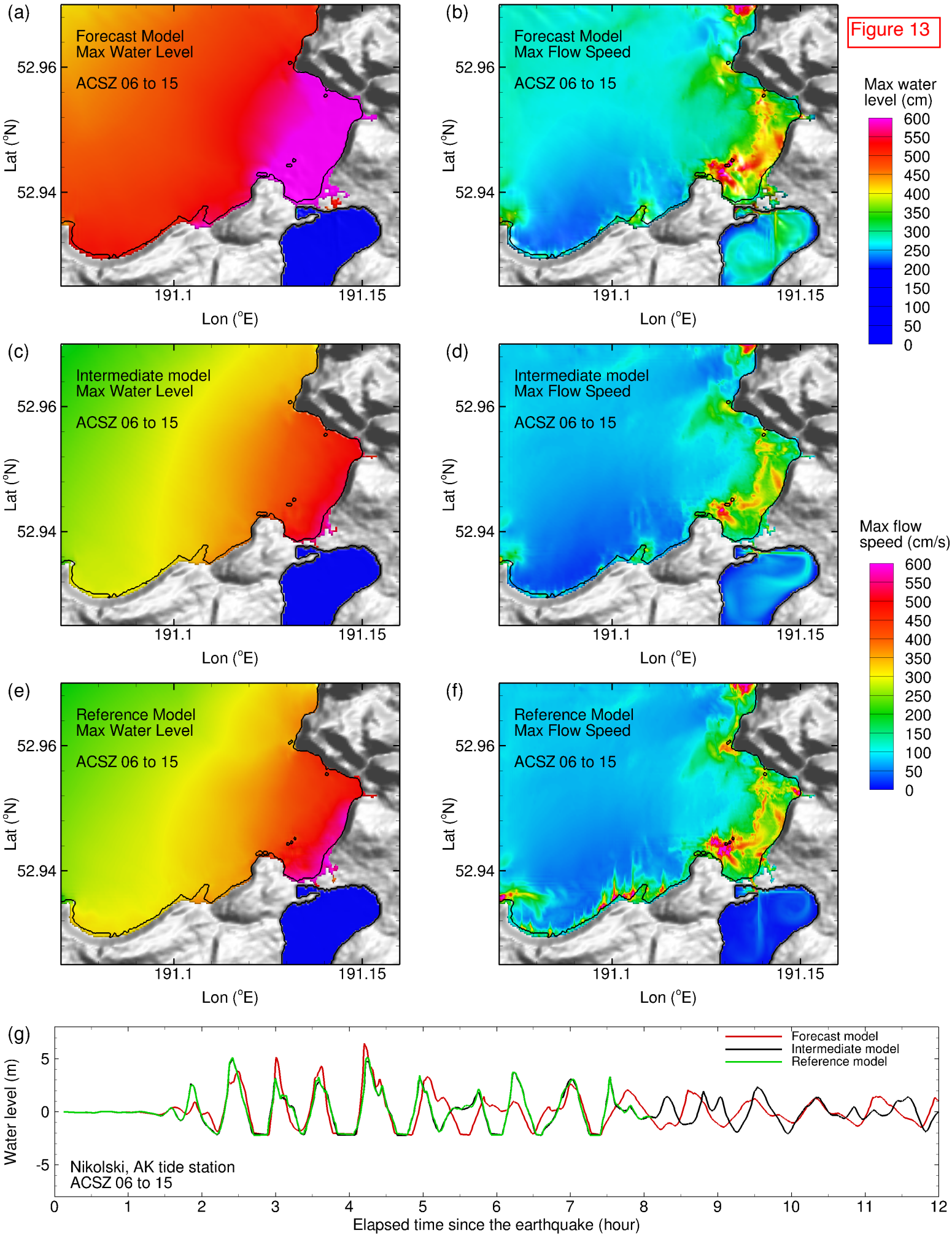
Figure 13
(a)
Forecast Model
Max Water Level
ACSZ 06 to 15
(b)
Forecast Model
Max Flow Speed
ACSZ 06 to 15
(c)
Intermediate model
Max Water Level
ACSZ 06 to 15
(d)
Intermediate model
Max Flow Speed
ACSZ 06 to 15
(e)
Reference Model
Max Water Level
ACSZ 06 to 15
(f)
Reference Model
Max Flow Speed
ACSZ 06 to 15
Lat (°N)
52.96
52.94
Lon (°E)
191.1
191.15
Max water level (cm)
600
550
500
450
400
350
300
250
200
150
100
50
0
Max flow speed (cm/s)
600
550
500
450
400
350
300
250
200
150
100
50
0
(g)
Water level (m)
5
0
-5
Nikolski, AK tide station
ACSZ 06 to 15
Forecast model
Intermediate model
Reference model
0
1
2
3
4
5
6
7
8
9
10
11
12
Elapsed time since the earthquake (hour)

Figure 14

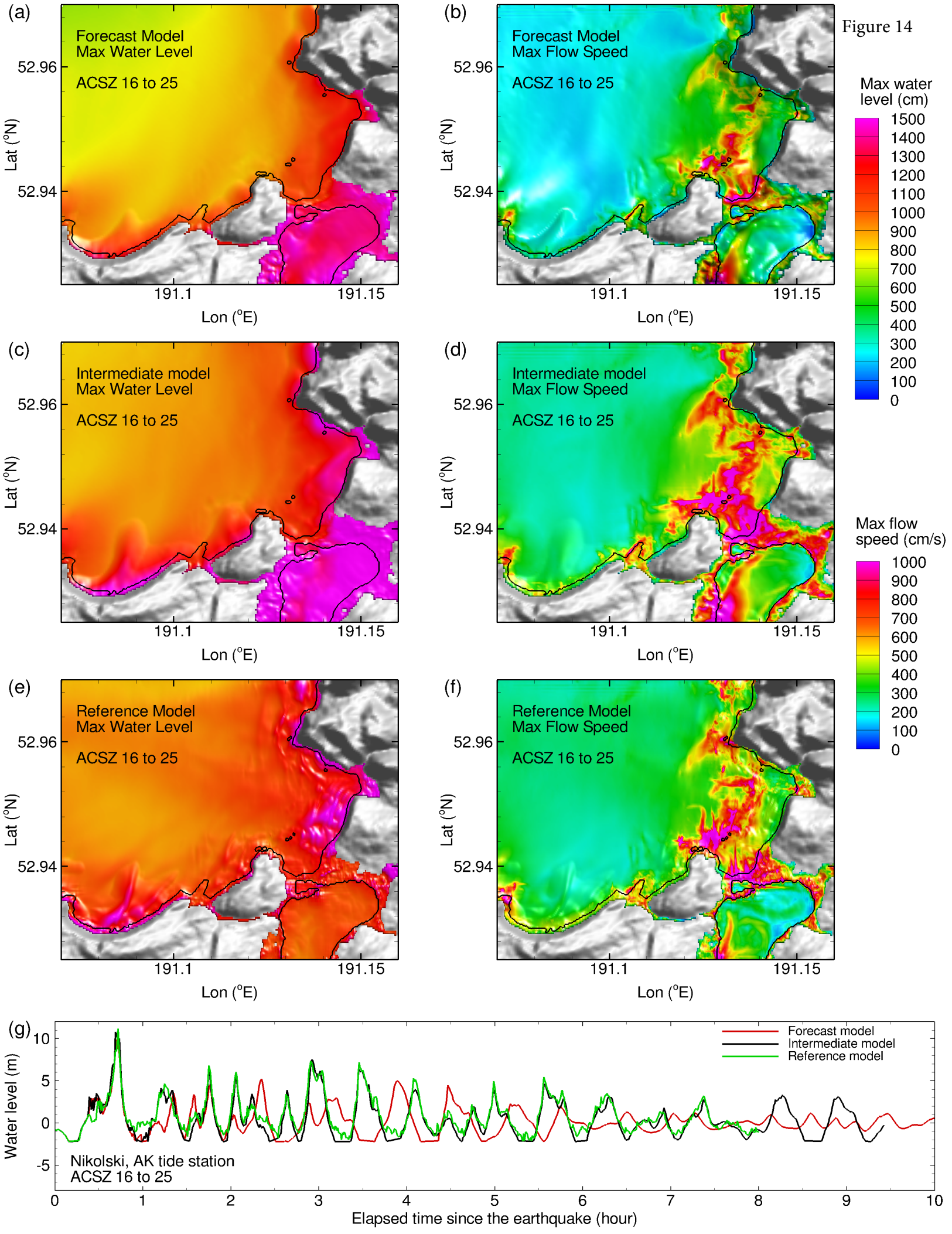
(a)
Forecast Model
Max Water Level
ACSZ 16 to 25
(b)
Forecast Model
Max Flow Speed
ACSZ 16 to 25
(c)
Intermediate model
Max Water Level
ACSZ 16 to 25
(d)
Intermediate model
Max Flow Speed
ACSZ 16 to 25
(e)
Reference Model
Max Water Level
ACSZ 16 to 25
(f)
Reference Model
Max Flow Speed
ACSZ 16 to 25
52.96
52.94
191.1
191.15
Lat (°N)
Lon (°E)
Max water level (cm)
1500
1400
1300
1200
1100
1000
900
800
700
600
500
400
300
200
100
0
Max flow speed (cm/s)
1000
900
800
700
600
500
400
300
200
100
0
(g)
Water level (m)
10
5
0
-5
Nikolski, AK tide station
ACSZ 16 to 25
Forecast model
Intermediate model
Reference model
0
1
2
3
4
5
6
7
8
9
10
Elapsed time since the earthquake (hour)

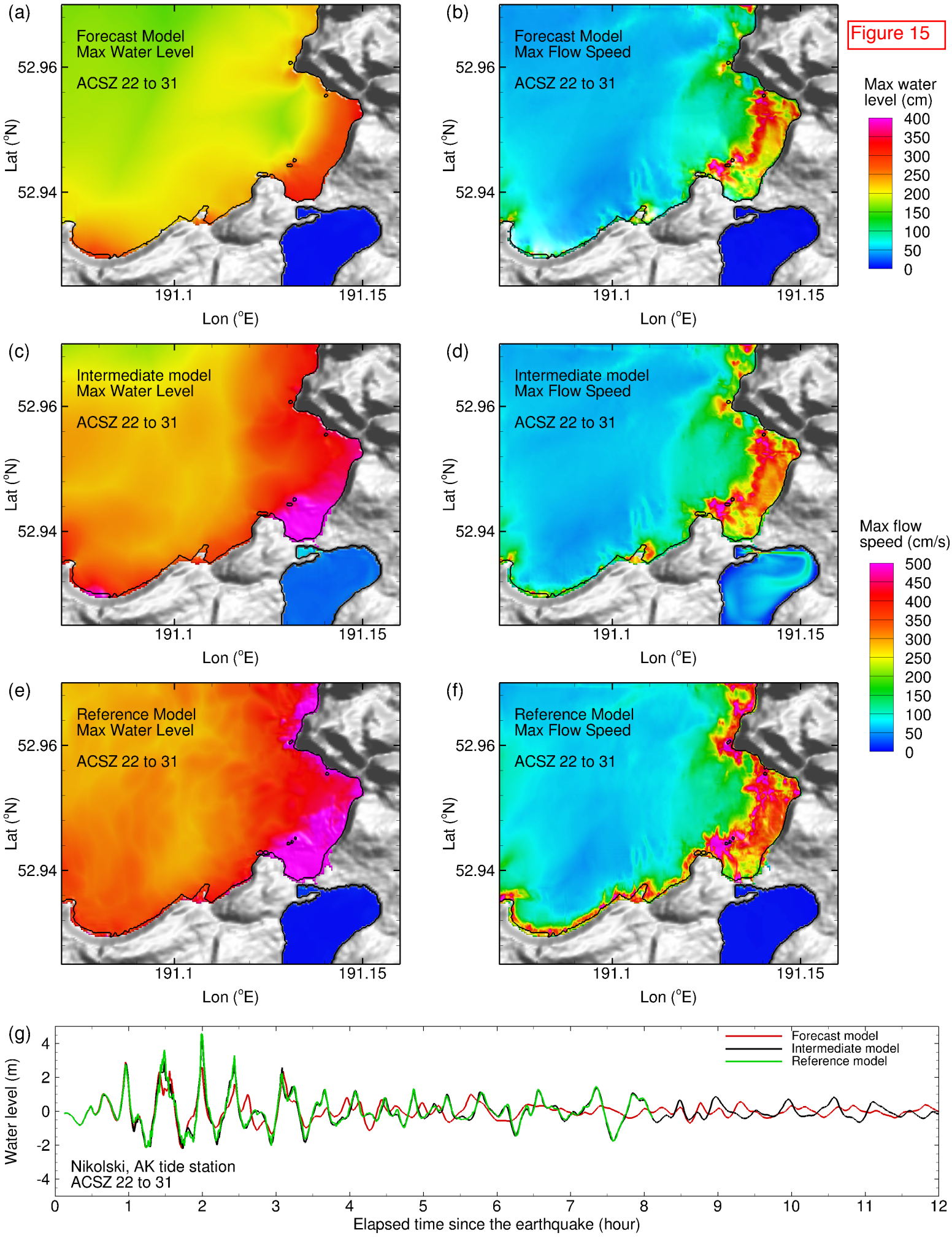
Figure 15
(a)
Forecast Model
Max Water Level
ACSZ 22 to 31
(b)
Forecast Model
Max Flow Speed
ACSZ 22 to 31
Max water level (cm)
400
350
300
250
200
150
100
50
0
(c)
Intermediate model
Max Water Level
ACSZ 22 to 31
(d)
Intermediate model
Max Flow Speed
ACSZ 22 to 31
Max flow speed (cm/s)
500
450
400
350
300
250
200
150
100
50
0
(e)
Reference Model
Max Water Level
ACSZ 22 to 31
(f)
Reference Model
Max Flow Speed
ACSZ 22 to 31
Lat (°N)
52.96
52.94
Lon (°E)
191.1
191.15
(g)
Water level (m)
Forecast model
Intermediate model
Reference model
Nikolski, AK tide station
ACSZ 22 to 31
Elapsed time since the earthquake (hour)

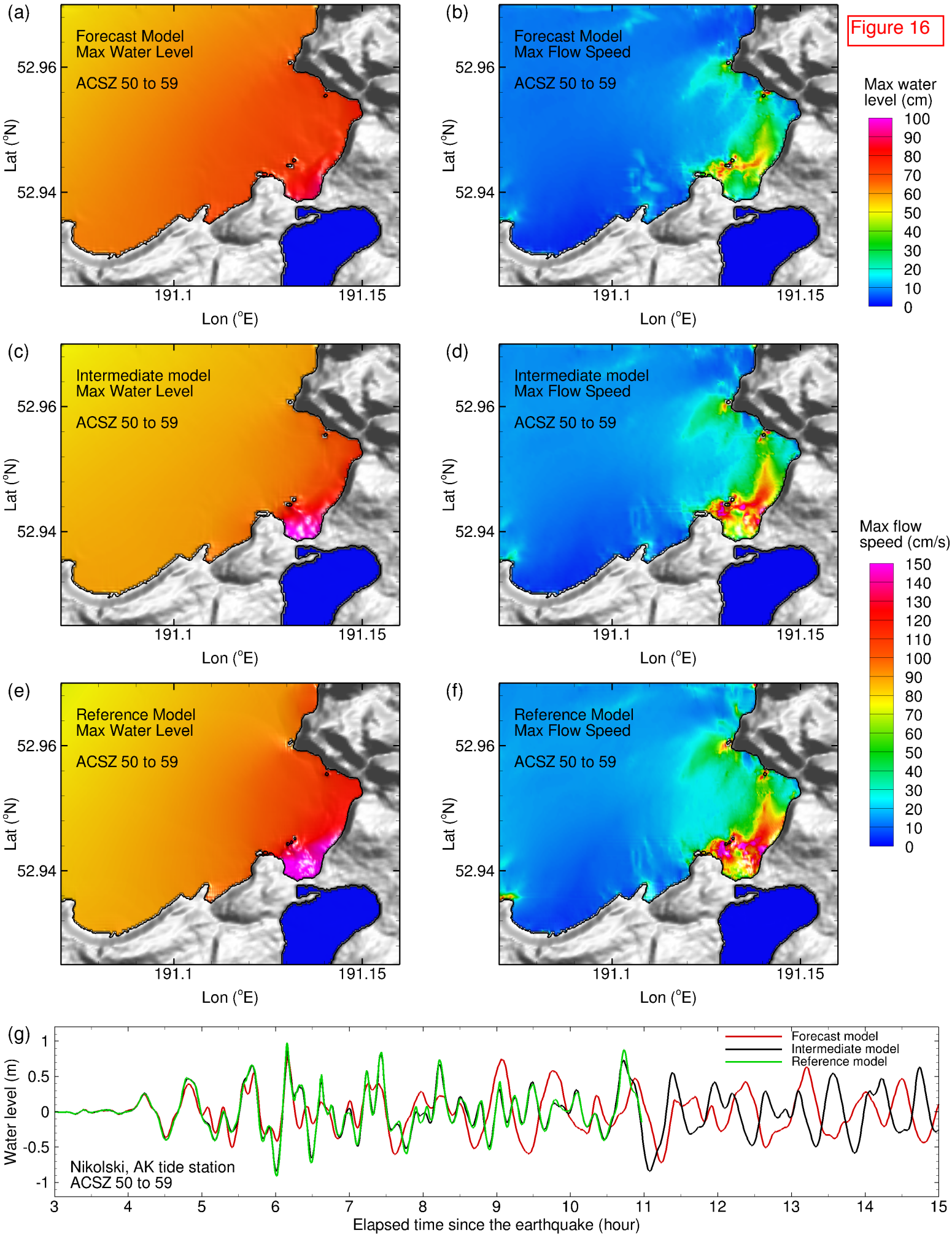
Figure 16
(a)
Forecast Model
Max Water Level
ACSZ 50 to 59
(b)
Forecast Model
Max Flow Speed
ACSZ 50 to 59
Max water level (cm)
100
90
80
70
60
50
40
30
20
10
0
(c)
Intermediate model
Max Water Level
ACSZ 50 to 59
(d)
Intermediate model
Max Flow Speed
ACSZ 50 to 59
Max flow speed (cm/s)
150
140
130
120
110
100
90
80
70
60
50
40
30
20
10
0
(e)
Reference Model
Max Water Level
ACSZ 50 to 59
(f)
Reference Model
Max Flow Speed
ACSZ 50 to 59
52.96
52.94
Lat (°N)
191.1
191.15
Lon (°E)
(g)
Forecast model
Intermediate model
Reference model
Water level (m)
1
0.5
0
-0.5
-1
Nikolski, AK tide station
ACSZ 50 to 59
3
4
5
6
7
8
9
10
11
12
13
14
15
Elapsed time since the earthquake (hour)

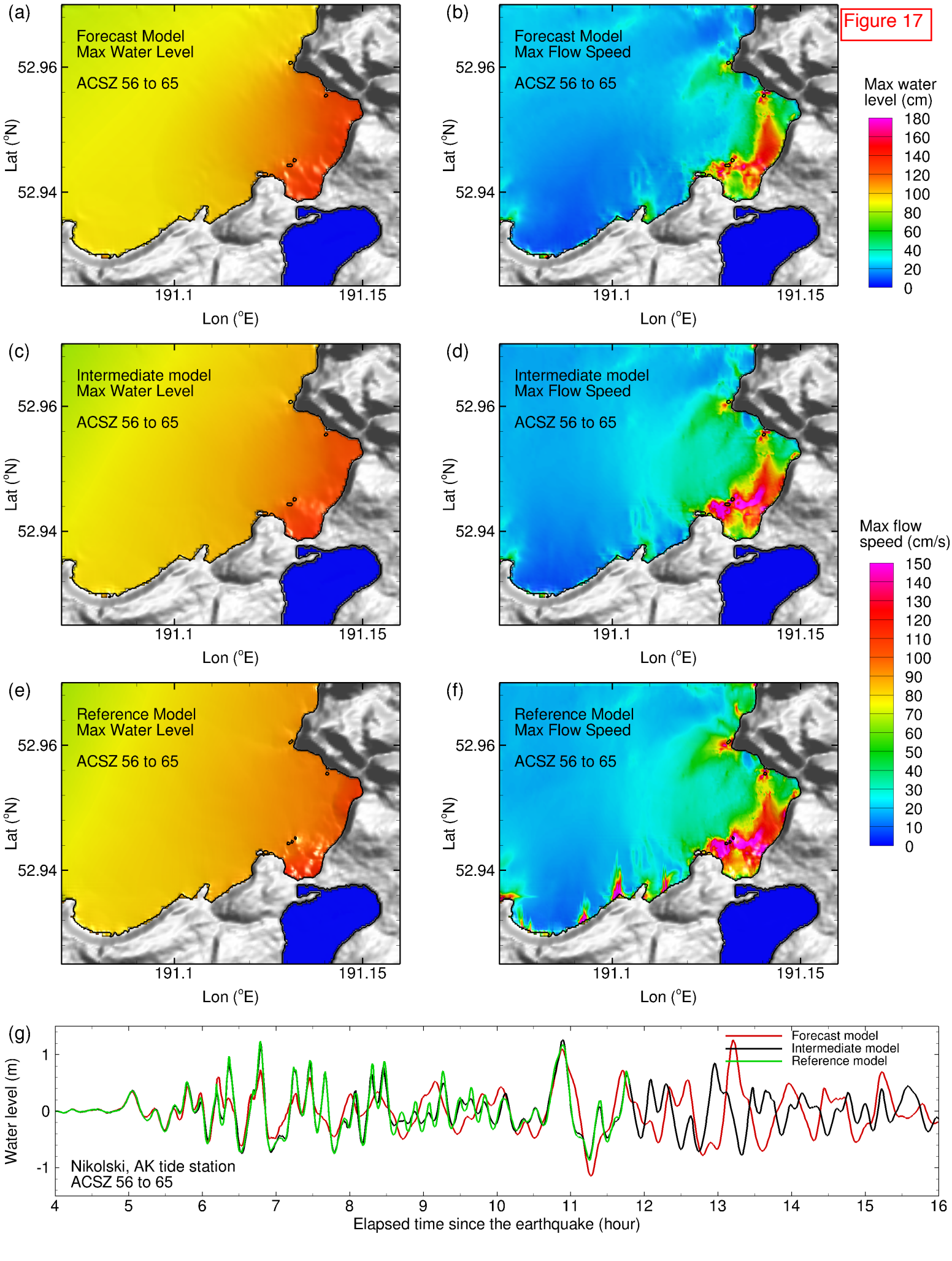
Figure 17
(a)
Forecast Model
Max Water Level
ACSZ 56 to 65
(b)
Forecast Model
Max Flow Speed
ACSZ 56 to 65
Max water level (cm)
180
160
140
120
100
80
60
40
20
0
(c)
Intermediate model
Max Water Level
ACSZ 56 to 65
(d)
Intermediate model
Max Flow Speed
ACSZ 56 to 65
Max flow speed (cm/s)
150
140
130
120
110
100
90
80
70
60
50
40
30
20
10
0
(e)
Reference Model
Max Water Level
ACSZ 56 to 65
(f)
Reference Model
Max Flow Speed
ACSZ 56 to 65
Lat (°N)
52.96
52.94
Lon (°E)
191.1
191.15
(g)
Water level (m)
1
0
-1
Nikolski, AK tide station
ACSZ 56 to 65
Forecast model
Intermediate model
Reference model
4
5
6
7
8
9
10
11
12
13
14
15
16
Elapsed time since the earthquake (hour)

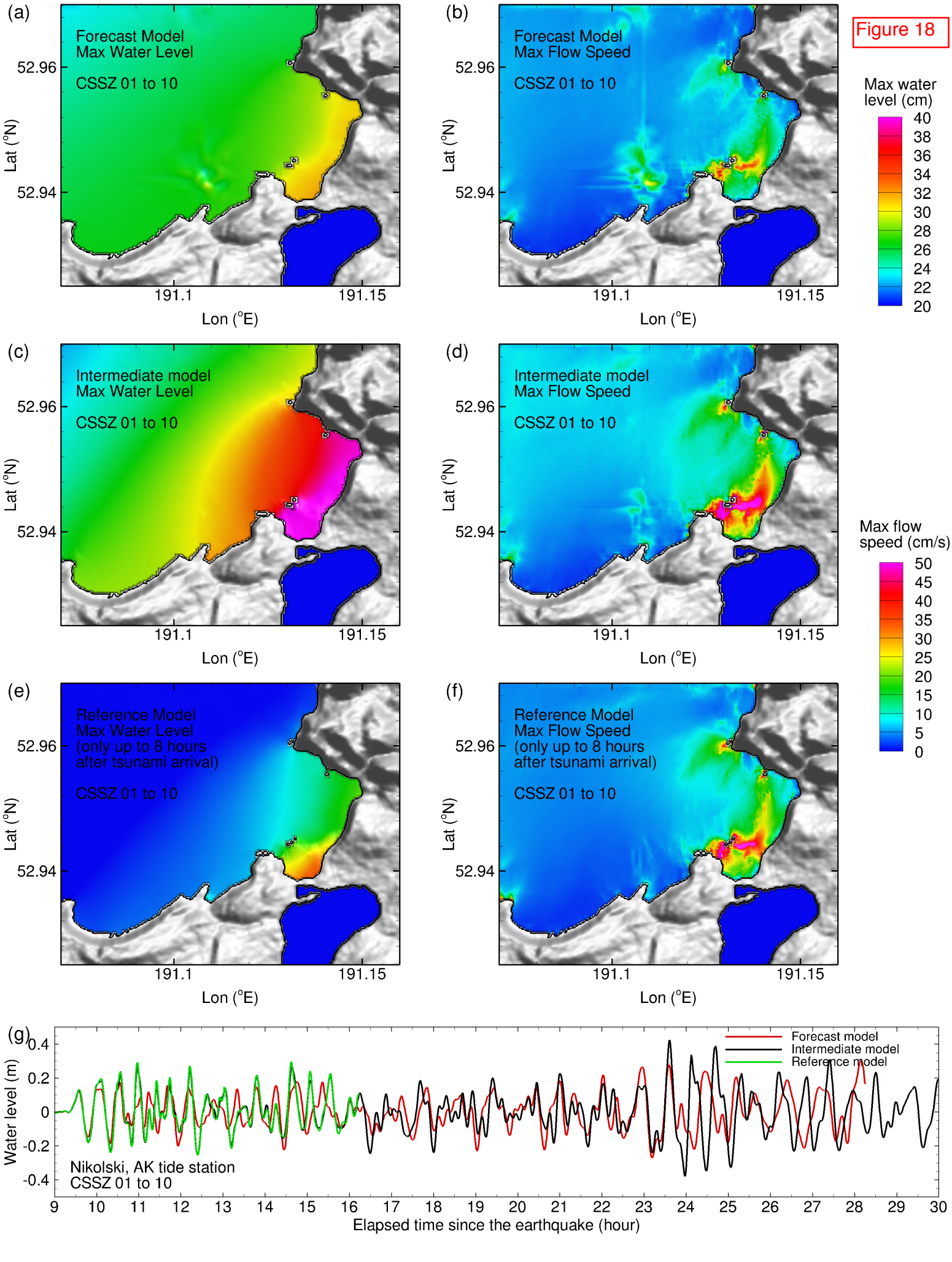
Figure 18
(a)
Forecast Model
Max Water Level
CSSZ 01 to 10
(b)
Forecast Model
Max Flow Speed
CSSZ 01 to 10
Max water level (cm)
40
38
36
34
32
30
28
26
24
22
20
(c)
Intermediate model
Max Water Level
CSSZ 01 to 10
(d)
Intermediate model
Max Flow Speed
CSSZ 01 to 10
Max flow speed (cm/s)
50
45
40
35
30
25
20
15
10
5
0
(e)
Reference Model
Max Water Level
(only up to 8 hours
after tsunami arrival)
CSSZ 01 to 10
(f)
Reference Model
Max Flow Speed
(only up to 8 hours
after tsunami arrival)
CSSZ 01 to 10
Lat (°N)
52.96
52.94
Lon (°E)
191.1
191.15
(g)
Water level (m)
0.4
0.2
0
-0.2
-0.4
Forecast model
Intermediate model
Reference model
Nikolski, AK tide station
CSSZ 01 to 10
9
10
11
12
13
14
15
16
17
18
19
20
21
22
23
24
25
26
27
28
29
30
Elapsed time since the earthquake (hour)

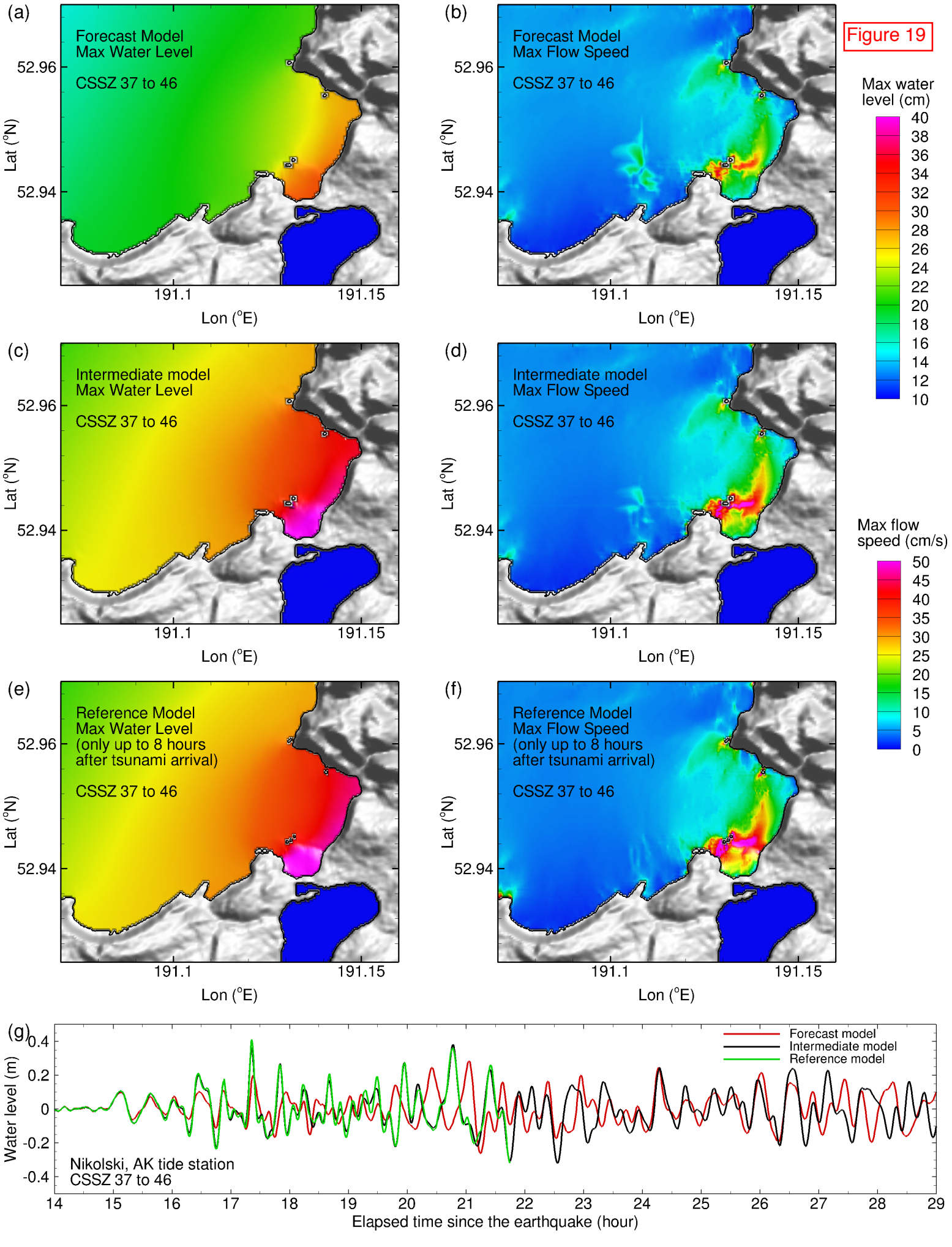
Figure 19
(a)
Forecast Model
Max Water Level
CSSZ 37 to 46
(b)
Forecast Model
Max Flow Speed
CSSZ 37 to 46
Max water level (cm)
40
38
36
34
32
30
28
26
24
22
20
18
16
14
12
10
(c)
Intermediate model
Max Water Level
CSSZ 37 to 46
(d)
Intermediate model
Max Flow Speed
CSSZ 37 to 46
Max flow speed (cm/s)
50
45
40
35
30
25
20
15
10
5
0
(e)
Reference Model
Max Water Level
(only up to 8 hours
after tsunami arrival)
CSSZ 37 to 46
(f)
Reference Model
Max Flow Speed
(only up to 8 hours
after tsunami arrival)
CSSZ 37 to 46
Lat (°N)
52.96
52.94
Lon (°E)
191.1
191.15
(g)
Forecast model
Intermediate model
Reference model
Water level (m)
0.4
0.2
0
-0.2
-0.4
Nikolski, AK tide station
CSSZ 37 to 46
14
15
16
17
18
19
20
21
22
23
24
25
26
27
28
29
Elapsed time since the earthquake (hour)

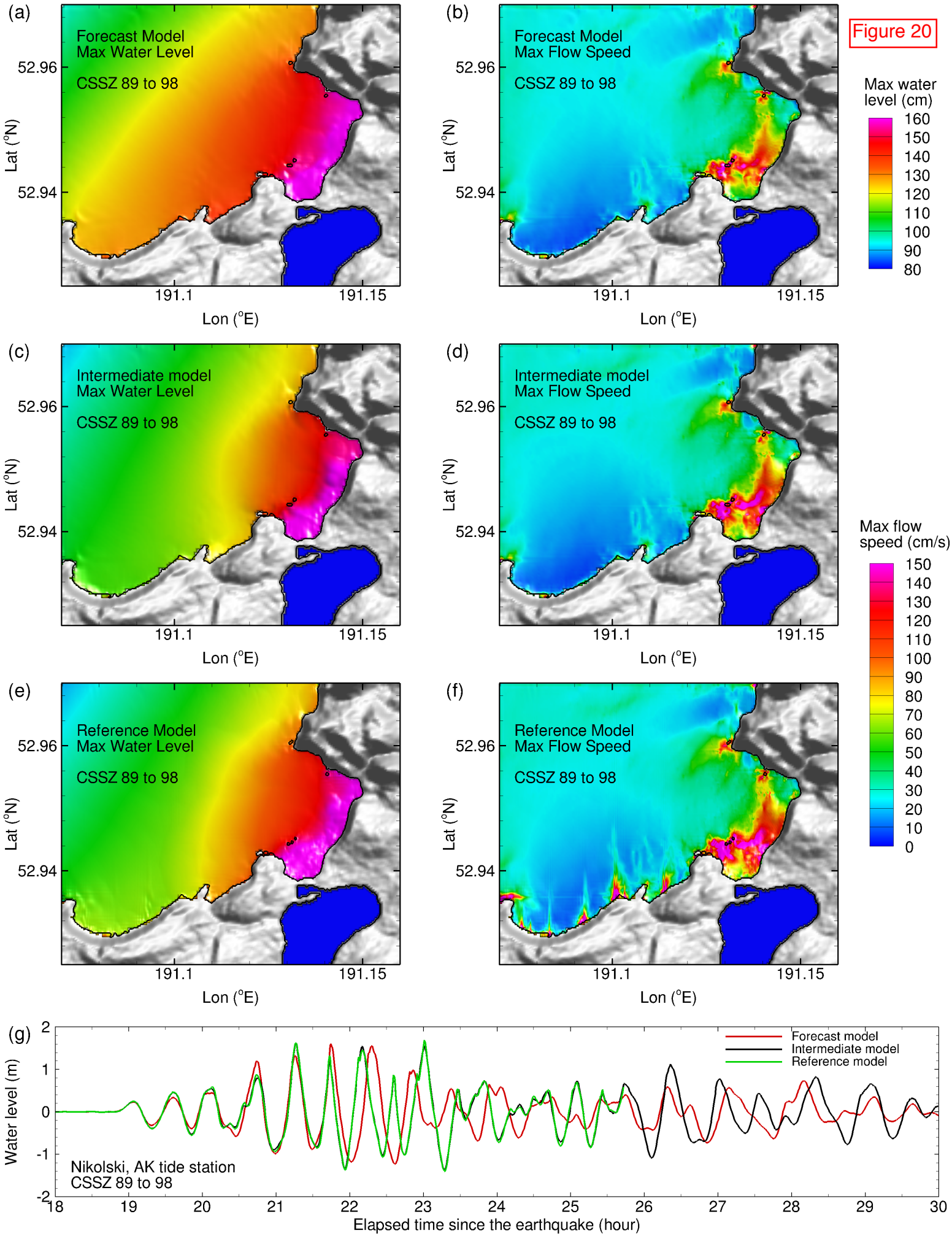
Figure 20
(a)
Forecast Model
Max Water Level
CSSZ 89 to 98
(b)
Forecast Model
Max Flow Speed
CSSZ 89 to 98
Max water level (cm)
160
150
140
130
120
110
100
90
80
(c)
Intermediate model
Max Water Level
CSSZ 89 to 98
(d)
Intermediate model
Max Flow Speed
CSSZ 89 to 98
Max flow speed (cm/s)
150
140
130
120
110
100
90
80
70
60
50
40
30
20
10
0
(e)
Reference Model
Max Water Level
CSSZ 89 to 98
(f)
Reference Model
Max Flow Speed
CSSZ 89 to 98
Lat (°N)
52.96
52.94
Lon (°E)
191.1
191.15
(g)
Water level (m)
2
1
0
-1
-2
Nikolski, AK tide station
CSSZ 89 to 98
Forecast model
Intermediate model
Reference model
18
19
20
21
22
23
24
25
26
27
28
29
30
Elapsed time since the earthquake (hour)

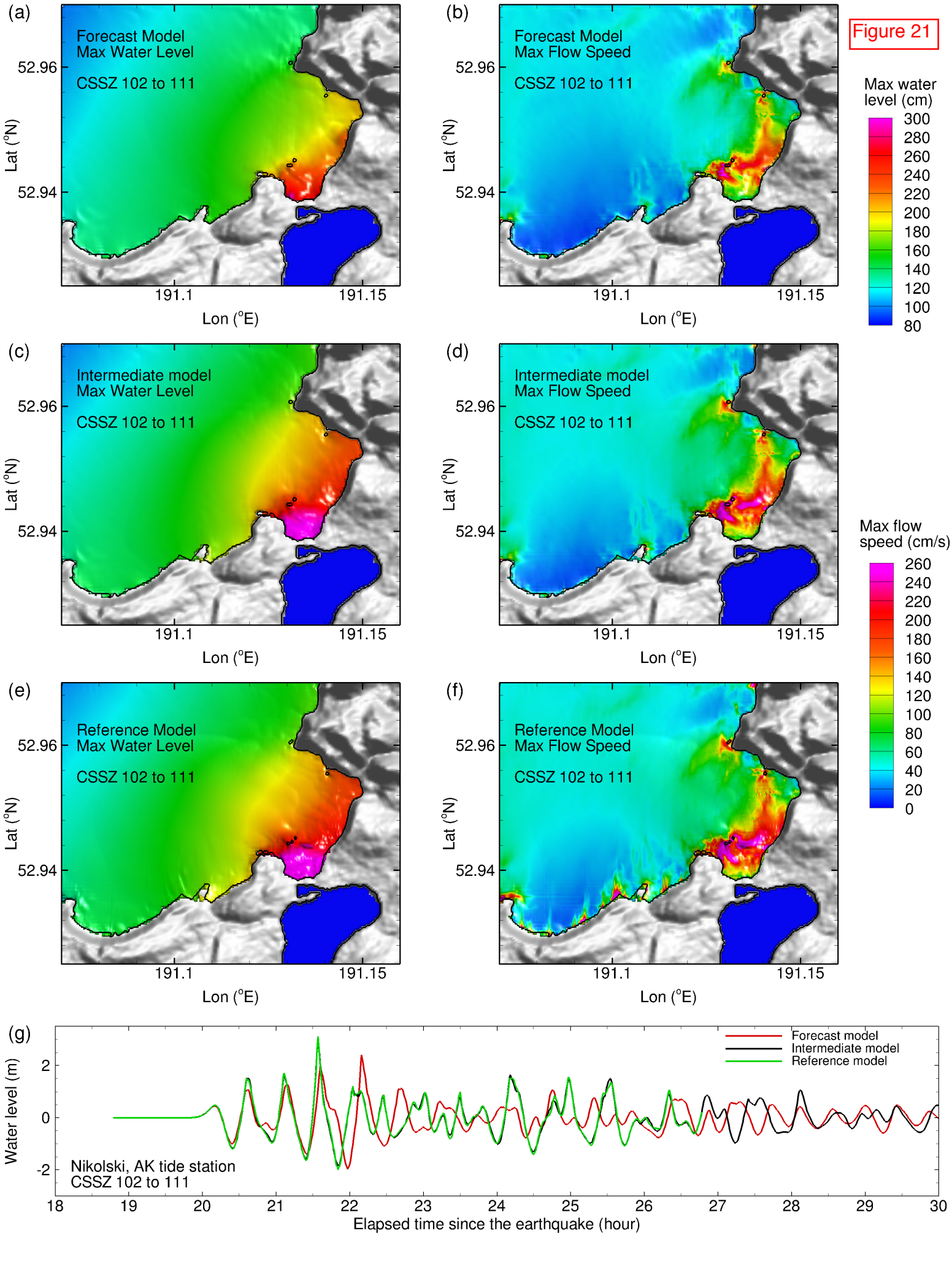
(a)
Forecast Model
Max Water Level
CSSZ 102 to 111
(b)
Forecast Model
Max Flow Speed
CSSZ 102 to 111
Figure 21
Max water level (cm)
300
280
260
240
220
200
180
160
140
120
100
80
(c)
Intermediate model
Max Water Level
CSSZ 102 to 111
(d)
Intermediate model
Max Flow Speed
CSSZ 102 to 111
Max flow speed (cm/s)
260
240
220
200
180
160
140
120
100
80
60
40
20
0
(e)
Reference Model
Max Water Level
CSSZ 102 to 111
(f)
Reference Model
Max Flow Speed
CSSZ 102 to 111
52.96
52.94
Lat (°N)
191.1
191.15
Lon (°E)
(g)
Forecast model
Intermediate model
Reference model
Water level (m)
2
0
-2
Nikolski, AK tide station
CSSZ 102 to 111
18
19
20
21
22
23
24
25
26
27
28
29
30
Elapsed time since the earthquake (hour)

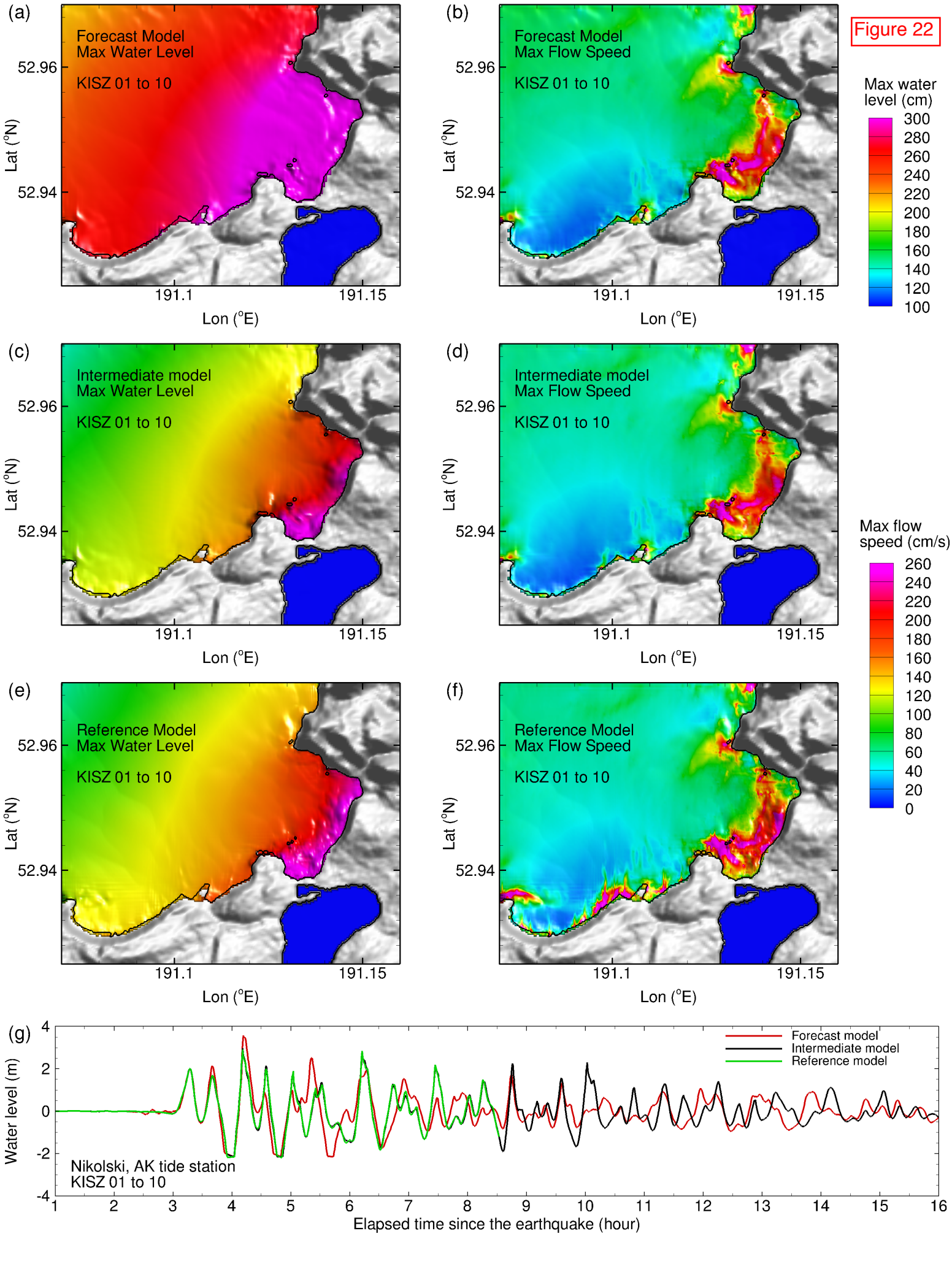
Figure 22
(a)
Forecast Model
Max Water Level
KISZ 01 to 10
(b)
Forecast Model
Max Flow Speed
KISZ 01 to 10
Max water level (cm)
300
280
260
240
220
200
180
160
140
120
100
(c)
Intermediate model
Max Water Level
KISZ 01 to 10
(d)
Intermediate model
Max Flow Speed
KISZ 01 to 10
Max flow speed (cm/s)
260
240
220
200
180
160
140
120
100
80
60
40
20
0
(e)
Reference Model
Max Water Level
KISZ 01 to 10
(f)
Reference Model
Max Flow Speed
KISZ 01 to 10
Lat (°N)
52.96
52.94
Lon (°E)
191.1
191.15
(g)
Water level (m)
4
2
0
-2
-4
Nikolski, AK tide station
KISZ 01 to 10
Forecast model
Intermediate model
Reference model
1
2
3
4
5
6
7
8
9
10
11
12
13
14
15
16
Elapsed time since the earthquake (hour)

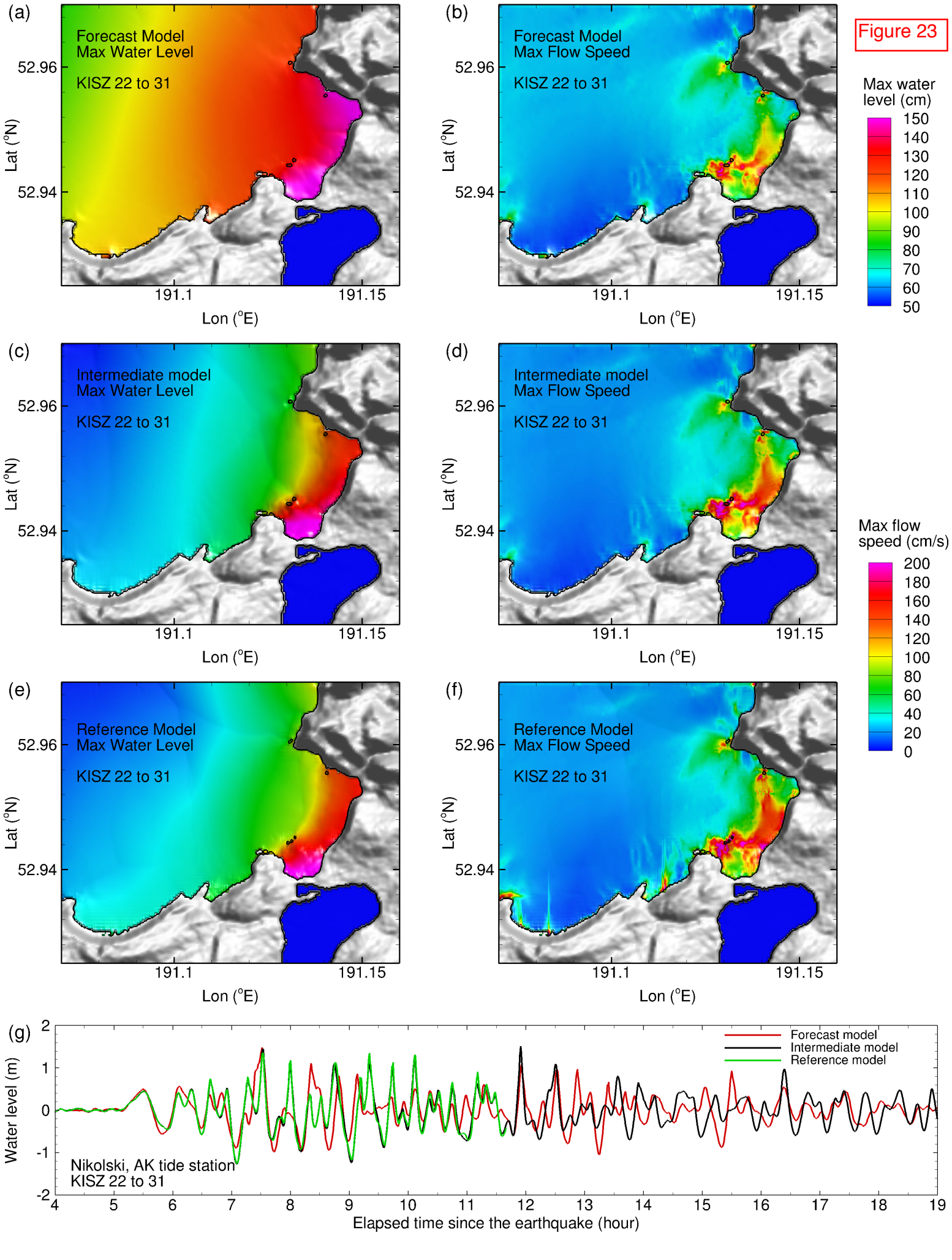
Figure 23
(a)
Forecast Model
Max Water Level
KISZ 22 to 31
(b)
Forecast Model
Max Flow Speed
KISZ 22 to 31
Max water level (cm)
150
140
130
120
110
100
90
80
70
60
50
(c)
Intermediate model
Max Water Level
KISZ 22 to 31
(d)
Intermediate model
Max Flow Speed
KISZ 22 to 31
Max flow speed (cm/s)
200
180
160
140
120
100
80
60
40
20
0
(e)
Reference Model
Max Water Level
KISZ 22 to 31
(f)
Reference Model
Max Flow Speed
KISZ 22 to 31
52.96
52.94
Lat (°N)
191.1
191.15
Lon (°E)
(g)
Forecast model
Intermediate model
Reference model
Water level (m)
Nikolski, AK tide station
KISZ 22 to 31
Elapsed time since the earthquake (hour)

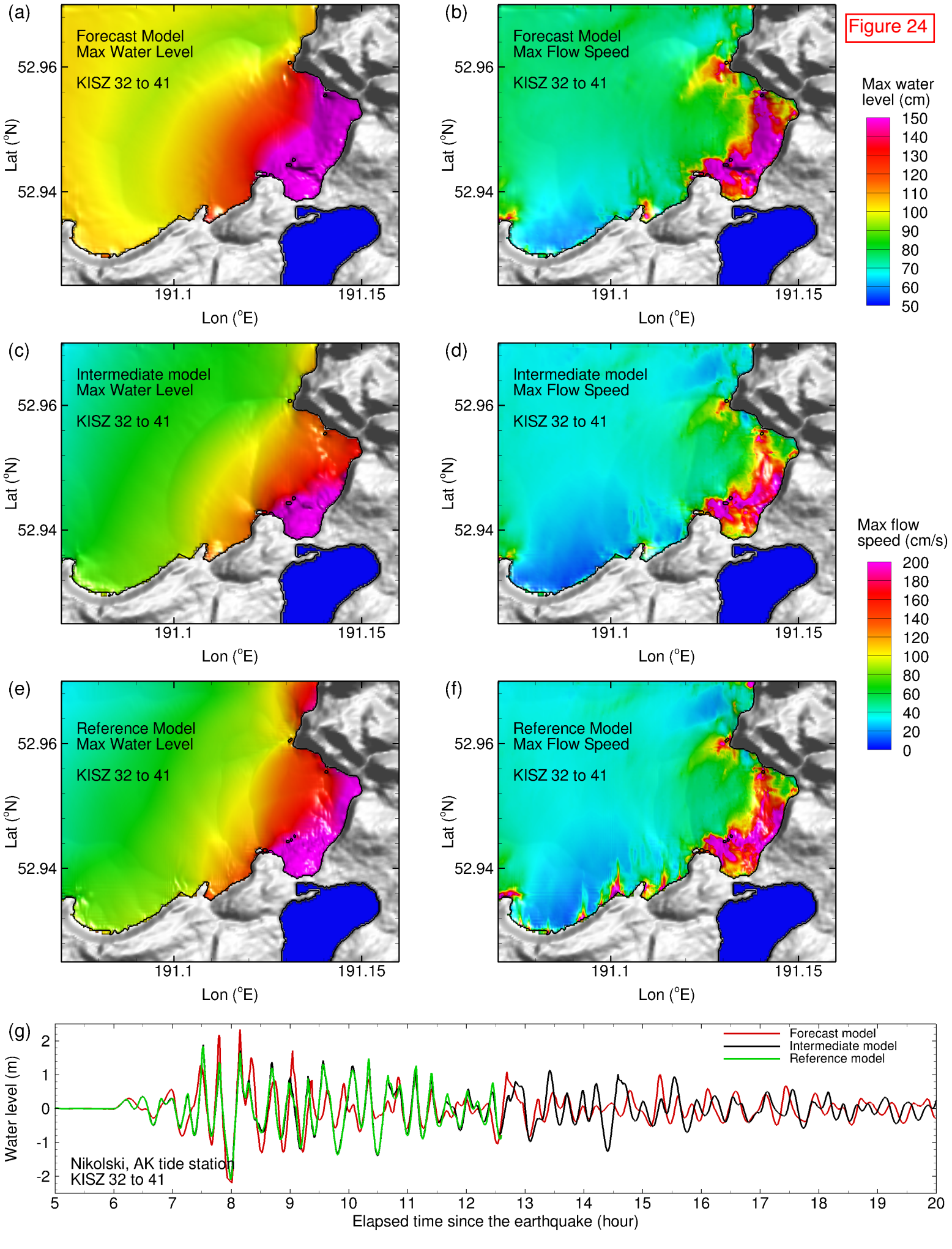
Figure 24
(a)
Forecast Model
Max Water Level
KISZ 32 to 41
(b)
Forecast Model
Max Flow Speed
KISZ 32 to 41
Max water level (cm)
150
140
130
120
110
100
90
80
70
60
50
(c)
Intermediate model
Max Water Level
KISZ 32 to 41
(d)
Intermediate model
Max Flow Speed
KISZ 32 to 41
Max flow speed (cm/s)
200
180
160
140
120
100
80
60
40
20
0
(e)
Reference Model
Max Water Level
KISZ 32 to 41
(f)
Reference Model
Max Flow Speed
KISZ 32 to 41
Lat (°N)
52.96
52.94
Lon (°E)
191.1
191.15
(g)
Water level (m)
2
1
0
-1
-2
Nikolski, AK tide station
KISZ 32 to 41
Forecast model
Intermediate model
Reference model
5
6
7
8
9
10
11
12
13
14
15
16
17
18
19
20
Elapsed time since the earthquake (hour)

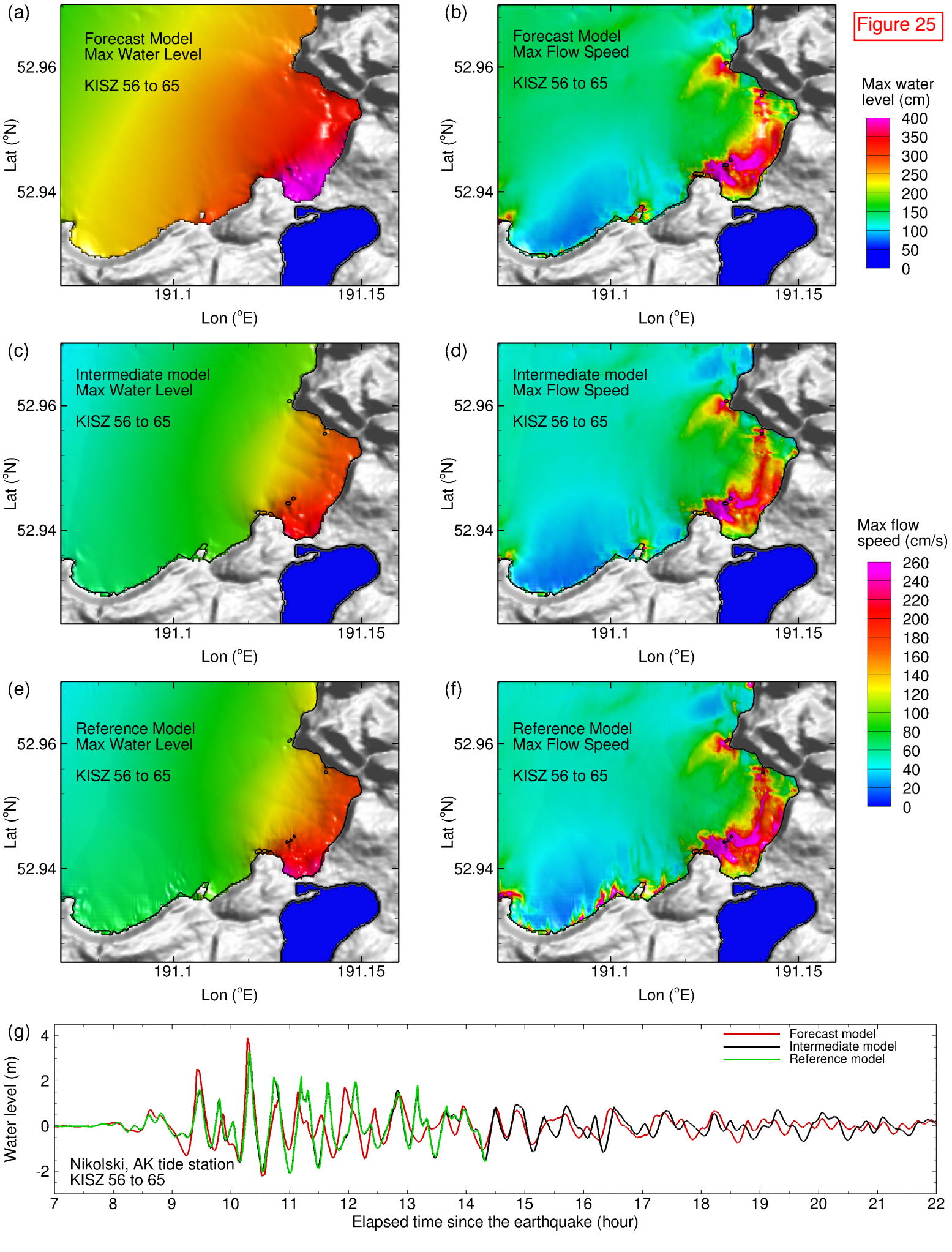
Figure 25
(a)
Forecast Model
Max Water Level
KISZ 56 to 65
(b)
Forecast Model
Max Flow Speed
KISZ 56 to 65
Max water level (cm)
400
350
300
250
200
150
100
50
0
(c)
Intermediate model
Max Water Level
KISZ 56 to 65
(d)
Intermediate model
Max Flow Speed
KISZ 56 to 65
Max flow speed (cm/s)
260
240
220
200
180
160
140
120
100
80
60
40
20
0
(e)
Reference Model
Max Water Level
KISZ 56 to 65
(f)
Reference Model
Max Flow Speed
KISZ 56 to 65
Lat (°N)
52.96
52.94
Lon (°E)
191.1
191.15
(g)
Water level (m)
4
2
0
-2
Nikolski, AK tide station
KISZ 56 to 65
Forecast model
Intermediate model
Reference model
7
8
9
10
11
12
13
14
15
16
17
18
19
20
21
22
Elapsed time since the earthquake (hour)

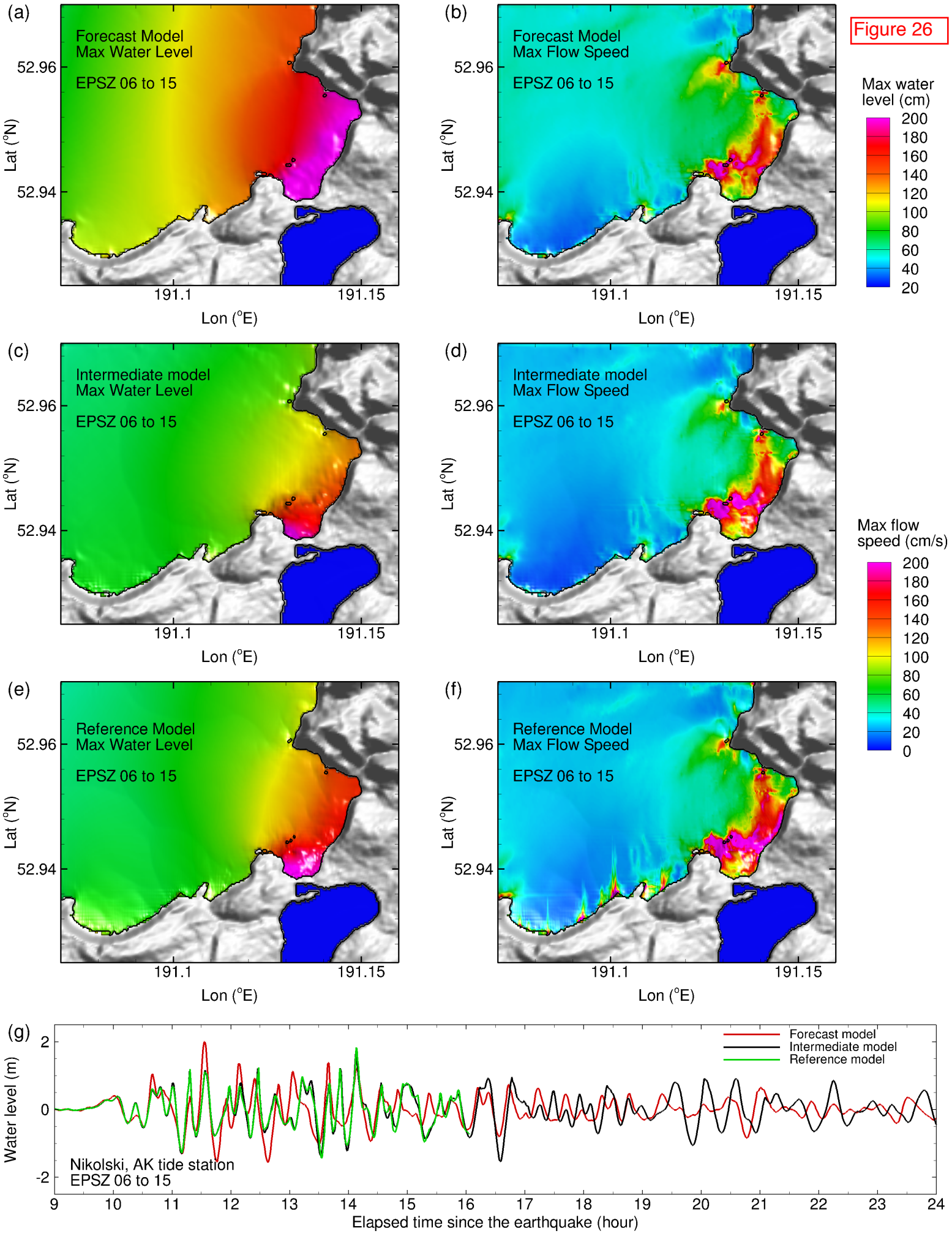
Figure 26
(a)
Forecast Model
Max Water Level
EPSZ 06 to 15
(b)
Forecast Model
Max Flow Speed
EPSZ 06 to 15
Max water level (cm)
200
180
160
140
120
100
80
60
40
20
(c)
Intermediate model
Max Water Level
EPSZ 06 to 15
(d)
Intermediate model
Max Flow Speed
EPSZ 06 to 15
Max flow speed (cm/s)
200
180
160
140
120
100
80
60
40
20
0
(e)
Reference Model
Max Water Level
EPSZ 06 to 15
(f)
Reference Model
Max Flow Speed
EPSZ 06 to 15
52.96
52.94
Lat (°N)
191.1
191.15
Lon (°E)
(g)
Forecast model
Intermediate model
Reference model
Water level (m)
2
0
-2
Nikolski, AK tide station
EPSZ 06 to 15
9
10
11
12
13
14
15
16
17
18
19
20
21
22
23
24
Elapsed time since the earthquake (hour)

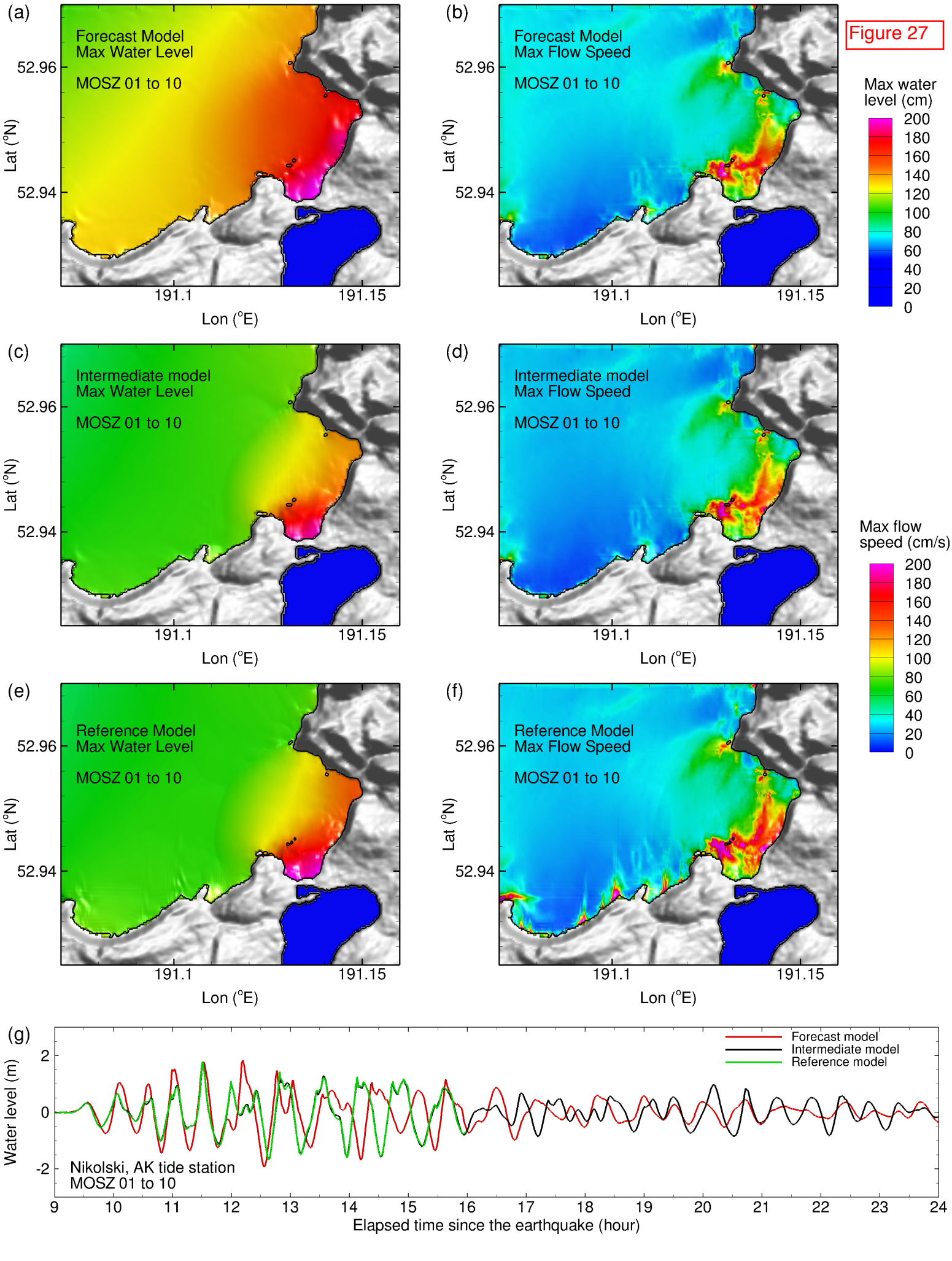
Figure 27
(a)
Forecast Model
Max Water Level
MOSZ 01 to 10
(b)
Forecast Model
Max Flow Speed
MOSZ 01 to 10
Max water level (cm)
200
180
160
140
120
100
80
60
40
20
0
(c)
Intermediate model
Max Water Level
MOSZ 01 to 10
(d)
Intermediate model
Max Flow Speed
MOSZ 01 to 10
Max flow speed (cm/s)
200
180
160
140
120
100
80
60
40
20
0
(e)
Reference Model
Max Water Level
MOSZ 01 to 10
(f)
Reference Model
Max Flow Speed
MOSZ 01 to 10
Lat (°N)
52.96
52.94
Lon (°E)
191.1
191.15
(g)
Forecast model
Intermediate model
Reference model
Water level (m)
2
0
-2
Nikolski, AK tide station
MOSZ 01 to 10
9
10
11
12
13
14
15
16
17
18
19
20
21
22
23
24
Elapsed time since the earthquake (hour)

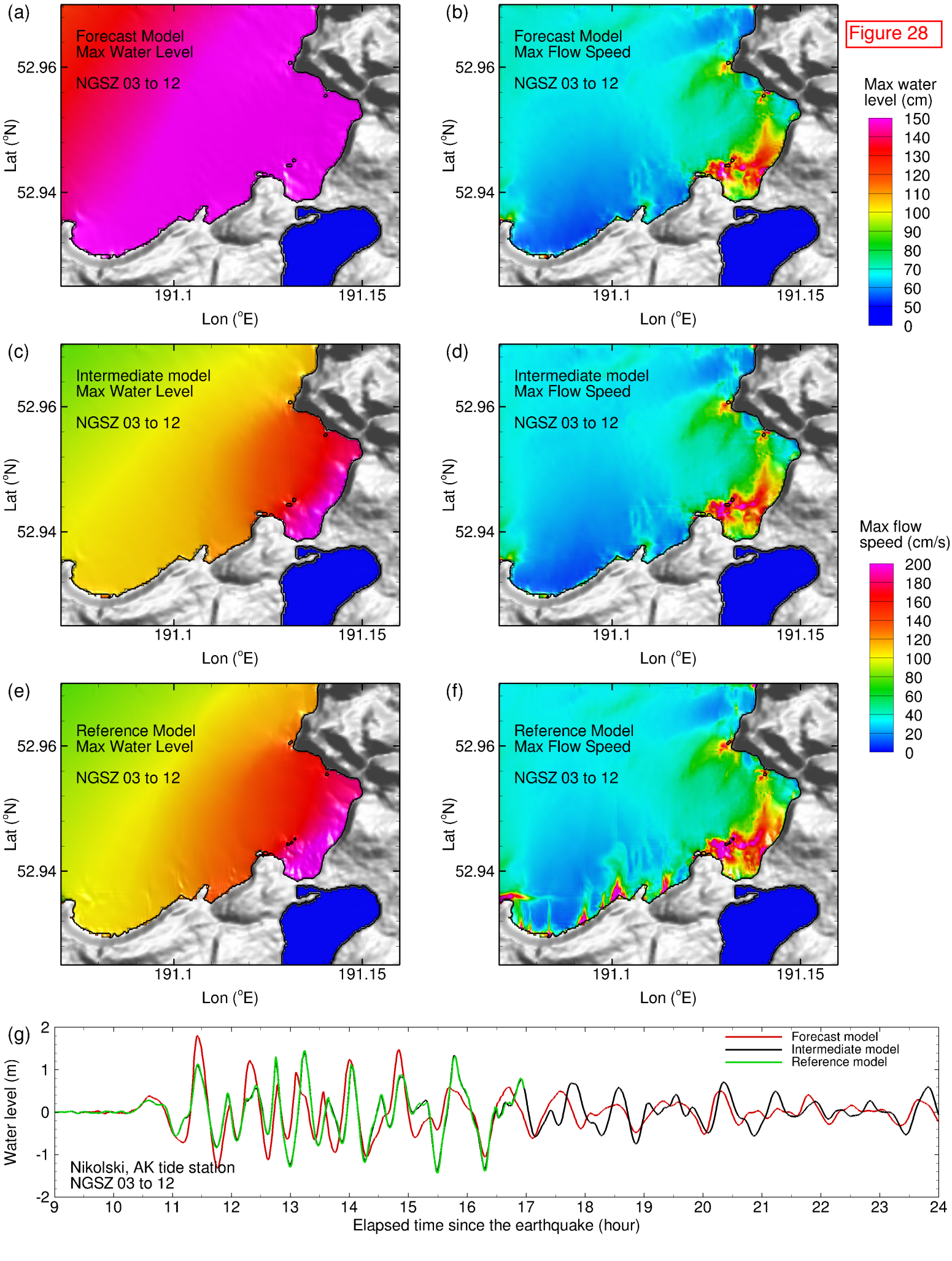
Figure 28
(a)
Forecast Model
Max Water Level
NGSZ 03 to 12
(b)
Forecast Model
Max Flow Speed
NGSZ 03 to 12
Max water level (cm)
150
140
130
120
110
100
90
80
70
60
50
0
(c)
Intermediate model
Max Water Level
NGSZ 03 to 12
(d)
Intermediate model
Max Flow Speed
NGSZ 03 to 12
Max flow speed (cm/s)
200
180
160
140
120
100
80
60
40
20
0
(e)
Reference Model
Max Water Level
NGSZ 03 to 12
(f)
Reference Model
Max Flow Speed
NGSZ 03 to 12
52.96
52.94
Lat (°N)
191.1
191.15
Lon (°E)
(g)
Forecast model
Intermediate model
Reference model
Water level (m)
2
1
0
-1
-2
Nikolski, AK tide station
NGSZ 03 to 12
9
10
11
12
13
14
15
16
17
18
19
20
21
22
23
24
Elapsed time since the earthquake (hour)

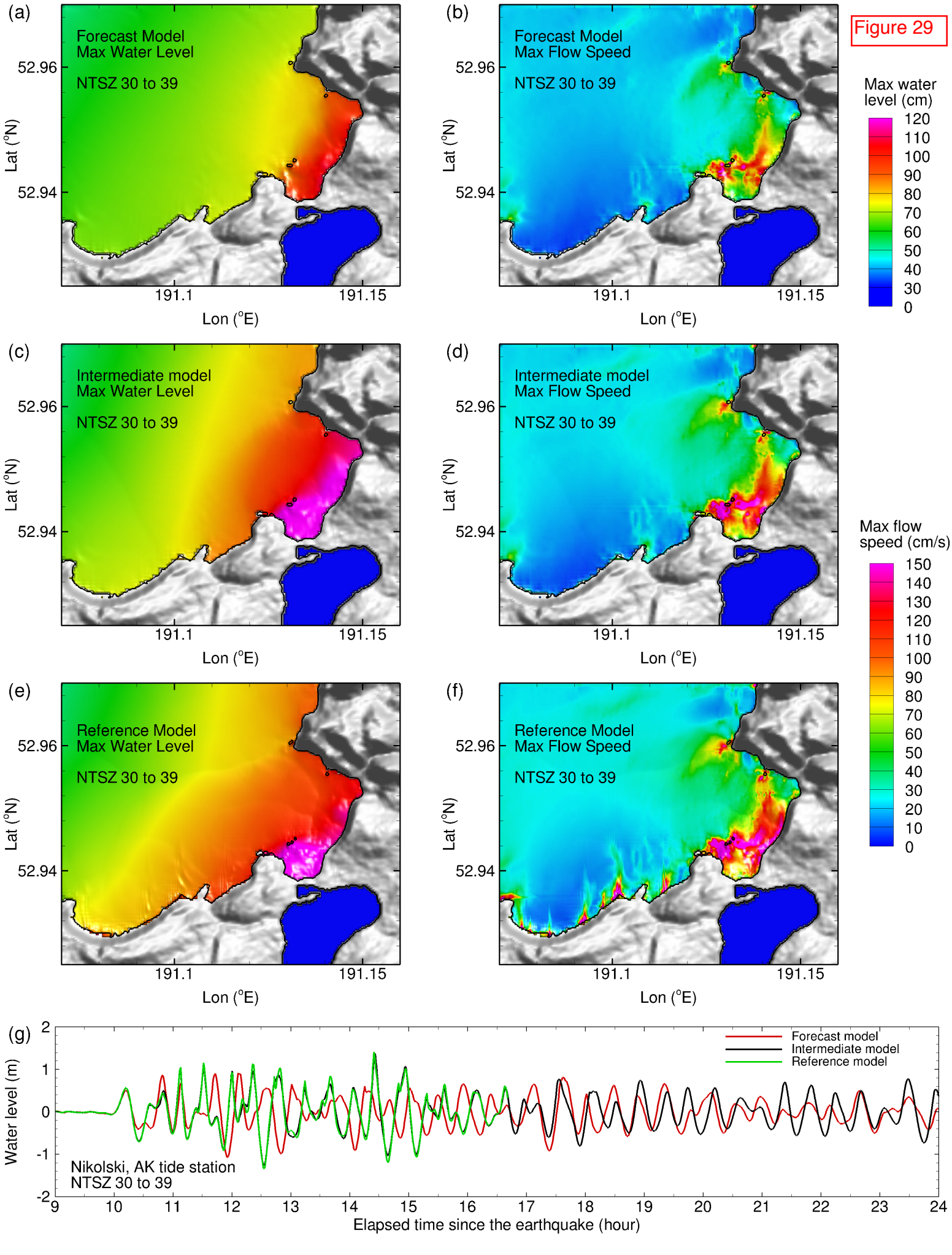
(a)
Forecast Model
Max Water Level
NTSZ 30 to 39
(b)
Forecast Model
Max Flow Speed
NTSZ 30 to 39
Figure 29
Max water level (cm)
120
110
100
90
80
70
60
50
40
30
0
(c)
Intermediate model
Max Water Level
NTSZ 30 to 39
(d)
Intermediate model
Max Flow Speed
NTSZ 30 to 39
Max flow speed (cm/s)
150
140
130
120
110
100
90
80
70
60
50
40
30
20
10
0
(e)
Reference Model
Max Water Level
NTSZ 30 to 39
(f)
Reference Model
Max Flow Speed
NTSZ 30 to 39
Lat (°N)
52.96
52.94
Lon (°E)
191.1
191.15
(g)
Water level (m)
2
1
0
-1
-2
Nikolski, AK tide station
NTSZ 30 to 39
Forecast model
Intermediate model
Reference model
9
10
11
12
13
14
15
16
17
18
19
20
21
22
23
24
Elapsed time since the earthquake (hour)

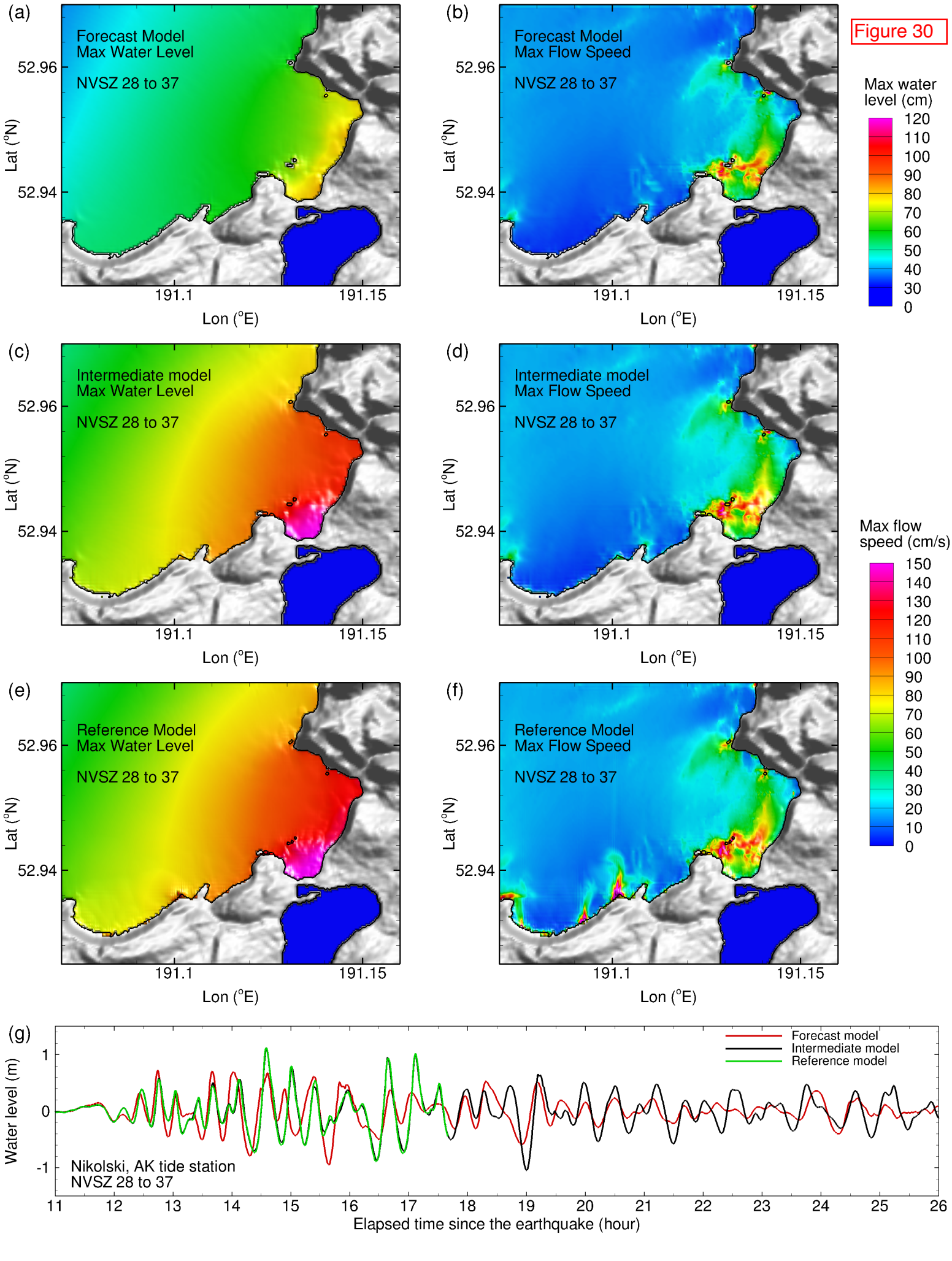
Figure 30
(a)
Forecast Model
Max Water Level
NVSZ 28 to 37
(b)
Forecast Model
Max Flow Speed
NVSZ 28 to 37
Max water level (cm)
120
110
100
90
80
70
60
50
40
30
0
(c)
Intermediate model
Max Water Level
NVSZ 28 to 37
(d)
Intermediate model
Max Flow Speed
NVSZ 28 to 37
Max flow speed (cm/s)
150
140
130
120
110
100
90
80
70
60
50
40
30
20
10
0
(e)
Reference Model
Max Water Level
NVSZ 28 to 37
(f)
Reference Model
Max Flow Speed
NVSZ 28 to 37
52.96
52.94
Lat (°N)
191.1
191.15
Lon (°E)
(g)
Forecast model
Intermediate model
Reference model
Water level (m)
1
0
-1
Nikolski, AK tide station
NVSZ 28 to 37
11
12
13
14
15
16
17
18
19
20
21
22
23
24
25
26
Elapsed time since the earthquake (hour)

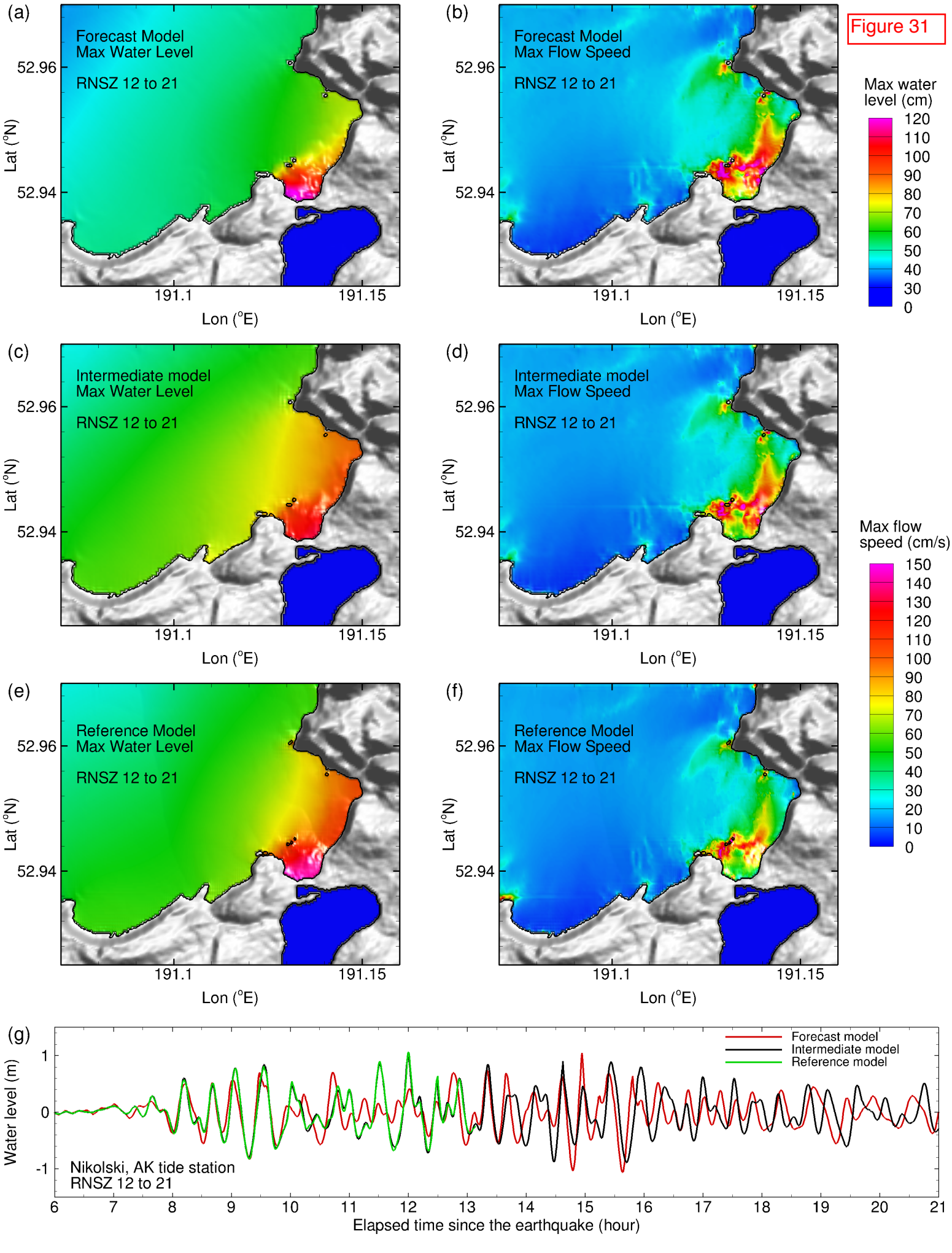
Figure 31
(a)
Forecast Model
Max Water Level
RNSZ 12 to 21
(b)
Forecast Model
Max Flow Speed
RNSZ 12 to 21
Max water level (cm)
120
110
100
90
80
70
60
50
40
30
0
(c)
Intermediate model
Max Water Level
RNSZ 12 to 21
(d)
Intermediate model
Max Flow Speed
RNSZ 12 to 21
Max flow speed (cm/s)
150
140
130
120
110
100
90
80
70
60
50
40
30
20
10
0
(e)
Reference Model
Max Water Level
RNSZ 12 to 21
(f)
Reference Model
Max Flow Speed
RNSZ 12 to 21
52.96
52.94
Lat (°N)
191.1
191.15
Lon (°E)
(g)
Forecast model
Intermediate model
Reference model
Water level (m)
1
0
-1
Nikolski, AK tide station
RNSZ 12 to 21
6
7
8
9
10
11
12
13
14
15
16
17
18
19
20
21
Elapsed time since the earthquake (hour)

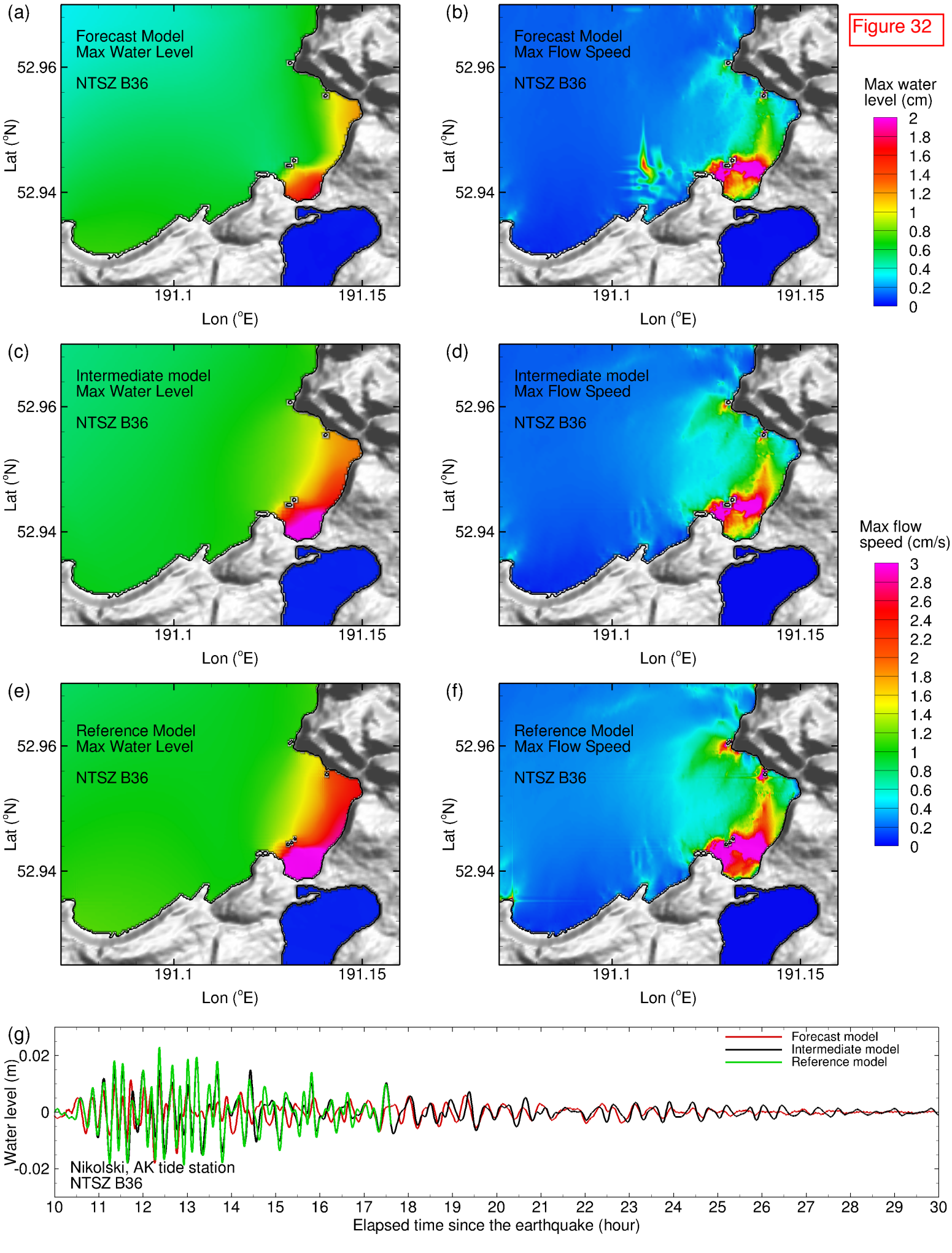
Figure 32
(a)
Forecast Model
Max Water Level
NTSZ B36
(b)
Forecast Model
Max Flow Speed
NTSZ B36
Max water level (cm)
2
1.8
1.6
1.4
1.2
1
0.8
0.6
0.4
0.2
0
(c)
Intermediate model
Max Water Level
NTSZ B36
(d)
Intermediate model
Max Flow Speed
NTSZ B36
Max flow speed (cm/s)
3
2.8
2.6
2.4
2.2
2
1.8
1.6
1.4
1.2
1
0.8
0.6
0.4
0.2
0
(e)
Reference Model
Max Water Level
NTSZ B36
(f)
Reference Model
Max Flow Speed
NTSZ B36
Lat (°N)
52.96
52.94
Lon (°E)
191.1
191.15
(g)
Forecast model
Intermediate model
Reference model
Water level (m)
0.02
0
-0.02
Nikolski, AK tide station
NTSZ B36
10
11
12
13
14
15
16
17
18
19
20
21
22
23
24
25
26
27
28
29
30
Elapsed time since the earthquake (hour)

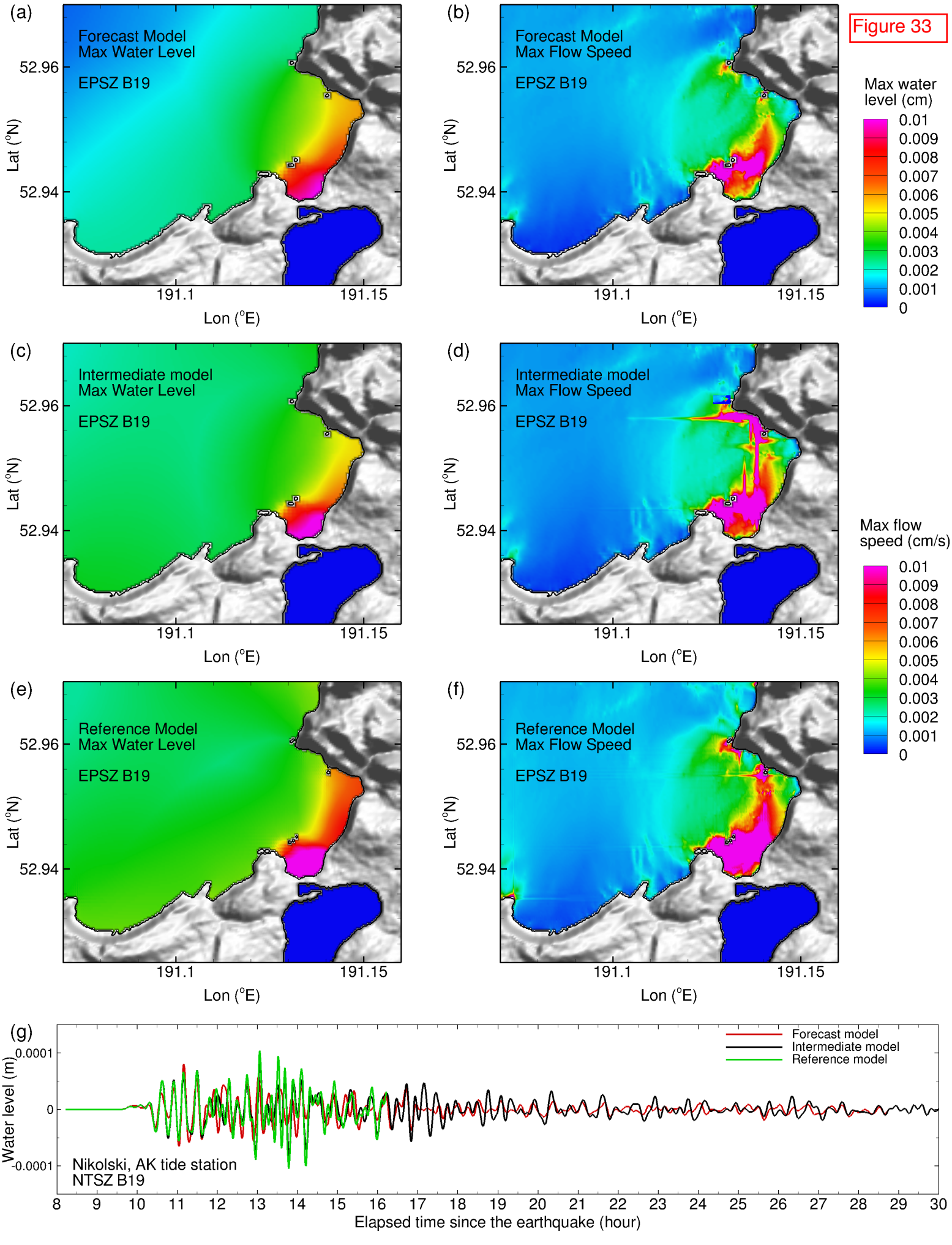
Figure 33
(a)
Forecast Model
Max Water Level
EPSZ B19
(b)
Forecast Model
Max Flow Speed
EPSZ B19
Max water level (cm)
0.01
0.009
0.008
0.007
0.006
0.005
0.004
0.003
0.002
0.001
0
(c)
Intermediate model
Max Water Level
EPSZ B19
(d)
Intermediate model
Max Flow Speed
EPSZ B19
Max flow speed (cm/s)
(e)
Reference Model
Max Water Level
EPSZ B19
(f)
Reference Model
Max Flow Speed
EPSZ B19
52.96
52.94
Lat (°N)
191.1
191.15
Lon (°E)
(g)
Forecast model
Intermediate model
Reference model
Water level (m)
0.0001
0
-0.0001
Nikolski, AK tide station
NTSZ B19
8 9 10 11 12 13 14 15 16 17 18 19 20 21 22 23 24 25 26 27 28 29 30
Elapsed time since the earthquake (hour)

Tables:

Table 1. Historical tsunami events that have affected Nikolski, Alaska.

Tables 2. Model parameters.

Table 3. Tsunami sources of historical events that were recorded at Nikolski tide station and used for model validation.

Table 4. Computed maximum wave amplitude at Nikolski tide station for historical events. The percentage in the parentheses is the model error of the maximum wave amplitude at the Nikolski tide gage, where the error = $(\eta_{model} - \eta_{obs}) / \eta_{obs} \times 100\%$. η_{model} is the computed maximum wave amplitude, and η_{obs} is the observed maximum wave amplitude.

Tables 5. Synthetic tsunami events in the Pacific.

Table 6. Computed maximum wave amplitude at Nikolski tide station for synthetic scenarios. The percentage in the parentheses is the error of the maximum wave amplitude at the Nikolski tide gage computed by $(\eta_{fm} - \eta_{rm}) / \eta_{rm} \times 100\%$. η_{fm} is the computed maximum wave amplitude using the forecast models, and η_{rm} is the computed maximum wave amplitude using the reference model.

Table 1. Historical tsunami events that have affected Nikolski, Alaska.

Event	Date, Time (UTC), Epicenter	Magnitude	Earthquake source area	Max water elev. at Nikolski, AK
1946 Unimak	01 April 12:28:56 53.32ºN 163.19ºW	8.1 – 8.5	Unimak Island, Alaska	12.2 m
2006 Kuril	15 Nov. 11:14:13.5 46.592ºN 153.266ºE	8.3	Kuril Islands	0.19 m
2009 Samoa	29 Sep 17:48:10.9 15.489ºS, 172.095ºW	8.0	American Somoa	0.077 m
2009 Vanuatu	7 Oct. 22:03:14.4 13.006ºS 166.51ºE	7.6	Vanuatu Islands	0.08 m
2011 Japan	11 Mar 05:46:24.1 38.297ºN 142.373ºE	9.0	Tohoku Island, Japan	0.81 m
2011 Amukta Pass	24 Jun 03:09:39.4 52.05ºN 171.836ºW	7.2	Amukta Pass, Alaska	0.09 m

Table 2: MOST parameters.

		Reference Model				Forecast and Intermediate Models				
Grid	Region	Coverage Lat. [ºN] Lon. [ºW]	Cell Size [“]	nx x ny	Time Step [sec]	Coverage Lat. [ºN] Lon. [ºW]		Cell Size [“]	nx x ny	Time Step [sec]
A	Central Aleutian	50.0 – 55.5 177.5 – 164.5	30”	1561 × 661	1.8	Forecast Model	50.0 – 55.5 170.5 – 164.5	60”	361 × 331	3.6
						Interme diate Model	50.0 – 55.5 177.5 – 164.5	30”	1561 × 661	1.8
B	Fox Islands	52.65 -53.15 169.5 – 168.5	3”	1201 × 601	0.3	52.65 -53.15 169.5 – 168.5		12”	301 × 151	1.2
C	Nikolski	52.925 -52.97 168.93 – 168.84	1”	325 × 163	0.3	52.925 -52.97 168.93 – 168.84		2”×1”	163 × 163	1.2
Minimum offshore depth [m]		1.0				1.0				
Water depth for dry land [m]		0.1				0.1				
Friction coefficient [n^2]		0.0009				0.0009				
CPU time for 4-hr simulation		~ 6.4 hours				~ 9.8 minutes for the forecast model, and ~ 77 minutes for the intermediate model				
Reference point at tide gage		168.87W, 52.941111N (I = 109, J = 105) in forecast model C grid; I = 217, J = 105 in reference model C grid)								

Computations were performed on a single Intel Xeon processor at 3.6 GHz, Dell PowerEdge 1850.

Table 3. Tsunami sources of historical events that were recorded at Nikolski tide station and used for model validation.

Earthquake / Seismic				Model		
Event	**USGS Date Time (UTC) Epicenter**	**CMT Date Time (UTC) Centroid**	**Magnitude Mw**	**Tsunami Magnitude[1]**	**Subduction Zone**	**Tsunami Source**
2009 Samoa	29 Sep 17:48:10 15.509ºS 172.034ºW	29 Sep 17:48:26.8 15.13ºS 171.97ºW	[5]8.1	8.1	New Zealand-Kermadec-Tonga (NTSZ)	[6]3.96 × a34+3.96 × b34 (forecast) 4.7xa34+6.5xb34+1.5*c34+0.4*a35+4.5*b35+ 3.6*c35+0.4*b36+0.6*c36 (revised with outer rise)
2011 Japan	11 Mar 05:46:24 38.297ºN 142.372ºE	11 Mar 05:47:32.8 37.52ºN 142.05ºE	[5]9.1	8.8	Kamchatka-Kuril-Japan-Izu-Mariana-Yap (KISZ)	[6]4.66 × b24 + 12.23 × b25 + 26.31 × a26 + 21.27 × b26 + 22.75 × a27 + 4.98 × b27
2011 Amukta Pass	24 Jun 03:09:40 52.008ºN 171.859ºW	11 Mar 03:09:51.1 51.06ºN 171.7ºW	[5]7.3	7.3	Alaska-Aleutian-Cascadia (ACSZ)	[6]0.27 x a19 + 0.25 x b19

[1] Preliminary source – derived from source and deep-ocean observations
[1] López and Okal (2006)
[3] United States Geological Survey (USGS)
[4] Kanamori and Ciper (1974)
[5] Centroid Moment Tensor
[6] Tsunami source was obtained in real time and applied to the forecast

Table 4. Computed maximum wave amplitude at Nikolski tide station for historical events. The percentage in the parentheses is the model error of the maximum wave amplitude at the Nikolski tide gage, where the error = $(\eta_{model} - \eta_{obs}) / \eta_{obs} \times 100\%$. η_{model} is the computed maximum wave amplitude, and η_{obs} is the observed maximum wave amplitude.

Historical Event	Obs. (cm)	Forecast model (cm)	Intermediate model (cm)	Reference model (cm)
2009 Samoa	7.7	3.9 (- 49.4%)	5.1 (- 33.8%)	4.7 (- 39.0%)
2011 Japan	80.9	113.5 (+ 40.3%)	109.5 (+ 35.4%)	107.4 (+ 32.8%)
2011 Amukta Pass	9.2	9.7 (+ 5.4%)	10.2 (+ 10.9%)	10.7 (+ 16.3%)

Table 5. Synthetic tsunami events in the Pacific.

Sce No.	Scenario Name	Source Zone	Tsunami Source	α (m)
		Mega-tsunami scenario		
1	KISZ 1-10	Kamchatka-Yap-Mariana-Izu-Bonin	A1-A10, B1-B10	25
2	KISZ 22-31	Kamchatka-Yap-Mariana-Izu-Bonin	A22-A31, B22-B31	25
3	KISZ 32-41	Kamchatka-Yap-Mariana-Izu-Bonin	A32-A41, B32-B41	25
4	KISZ 56-65	Kamchatka-Yap-Mariana-Izu-Bonin	A56-65, B56-65	25
5	ACSZ 6-15	Aleutian-Alaska-Cascadia	A6-A15, B6-B15	25
6	ACSZ 16-25	Aleutian-Alaska-Cascadia	A16-A25, B16-B25	25
7	ACSZ 22-31	Aleutian-Alaska-Cascadia	A22-A31, B22-B31	25
8	ACSZ 50-59	Aleutian-Alaska-Cascadia	A50-A59, B50-B59	25
9	ACSZ 56-65	Aleutian-Alaska-Cascadia	A56-A65, B56-B65	25
10	CSSZ 1-10	Central and South America	A1-A10, B1-B10	25
11	CSSZ 37-46	Central and South America	A37-A46, B37-B46	25
12	CSSZ 89-98	Central and South America	A89-A98, B89-B98	25
13	CSSZ 102 – 111	Central and South America	A102-A111, B102-B111	25
14	NTSZ 30-39	New Zealand-Kermadec-Tonga	A30-A39, B30-B39	25
15	NVSZ 28-37	New Britain-Solomons-Vanuatu	A28-A37, B28-B37	25
16	MOSZ 1-10	ManusOCB	A1-A10, B1-B10	25
17	NGSZ 3-12	North New Guinea	A3-A12, B3-B12	25
18	EPSZ 6-15	East Philippines	A6-A15, B6-B15	25
19	RNSZ 12-21	Ryukus-Kyushu-Nankai	A12-A21, B12-B21	25
		Mw 7.5 Tsunami scenario		
20	NTSZ B36	New Zealand-Kermadec-Tonga	B36	1
		Micro-tsunami scenario (select one)		
21	EPSZ B19	East Philippines	B19	0.01

Table 6. Computed maximum wave amplitude at Nikolski tide station for synthetic scenarios. The percentage in the parentheses is the error of the maximum wave amplitude at the Nikolski tide gage computed by $(\eta_{fm} - \eta_{rm}) / \eta_{rm} \times 100\%$. η_{fm} is the computed maximum wave amplitude using the forecast models, and η_{rm} is the computed maximum wave amplitude using the reference model.

Synthetic events	Forecast model (m)	Intermediate model (m)	Reference model (m)
KISZ 01 to 10	3.57 (+ 23.1%)	2.97 (+ %2.4)	2.90
KISZ 22 to 31	1.48 (max at 12 hours, + 8.0%)	1.51 (max at 12 hours, + 10.2%)	1.37 (max of first 11 hours)
KISZ 32 to 41	2.33 (+ 26.6%)	1.89 (+ 2.7%)	1.84
KISZ 56 to 65	3.92 (+ 18.1%)	3.21 (- 3.3%)	3.32
ACSZ 06 to 15	6.45 (+ 26.2%)	5.00 (- 2.2%)	5.11
ACSZ 16 to 25	9.88 (- 11.4%)	10.80 (- 3.1%)	11.15
ACSZ 22 to 31	2.90 (- 36.8%)	4.30 (- 6.3%)	4.59
ACSZ 50 to 59	0.78 (- 20.4%)	0.92 (- 6.1%)	0.98
ACSZ 56 to 65	1.26 (+ 1.6%)	1.26 (+ 1.6%)	1.24
CSSZ 01 to 10	0.30 (max at 23.5 hours, + 0%)	0.43 (max at 23.5 hours, + 43.3%)	0.30 (max of first 8 hours)
CSSZ 37 to 46	0.28 (- 31.7%)	0.38 (- 7.3%)	0.41
CSSZ 89 to 98	1.61 (- 4.7%)	1.59 (- 5.9%)	1.69
CSSZ 102 to 111	2.40 (- 22.8%)	2.89 (- 7.1%)	3.11
NTSZ 30 to 39	0.91 (- 35.5%)	1.38 (- 2.1%)	1.41
NVSZ 28 to 37	0.73 (- 34.8%)	1.12 (+ 0.0%)	1.12
MOSZ 01 to 10	1.83 (+ 2.2%)	1.76 (- 1.7%)	1.79
NGSZ 03 to 12	1.81 (+ 24.0%)	1.41 (- 3.4%)	1.46
EPSZ 06 to 15	2.01 (+ 9.2%)	1.77 (- 3.8%)	1.84
RNSZ 12 to 21	1.05 (- 1.9%)	0.99 (- 7.5%)	1.07
NTSZ B36	0.012 (- 47.8%)	0.018 (- 21.7%)	0.023

Appendix A.

Development of the Nikolski, Alaska, tsunami forecast model occurred prior to parameters changes that were made to reflect modification to the MOST model code. As a result, the input file for running the forecast model, the intermediate model and the high-resolution reference inundation model in MOST have been updated accordingly. Appendix A1, A2 and A3 provide the updated files for Nikolski, Alaska.

A1. Forecast model .in file:

```
0.005    Minimum amplitude of input offshore wave (m)
1.0  Input minimum depth for offshore (m)
0.1  Input "dry land" depth for inundation (m)
0.0009   Input friction coefficient (n**2)
1    let a and b run up
300.0    blowup limit
1    input time step (sec)
24000    input amount of steps
3    Compute "A" arrays every n-th time step, n=
1    COmpute "B" arrays every n-th time step, n=
30   Input number of steps between snapshots
0    ...Starting from
1    ...saveing grid every n-th node, n=
nikolski1_run2d/niko1_Agrid_1min.most
nikolski1_run2d/niko_Bgrid_12s.most
nikolski1_run2d/niko_Cgrid_x2s_y1s.most
./
./
1 1 1 1  NetCDF output for A, B, C, SIFT
1    Timeseries locations:
3 109 105nikolski1191.13   52.941111depth m: 2.3  NK1
  Nikolski, AK
```

A2. Intermediate model .in file:

```
0.005    Minimum amplitude of input offshore wave (m)
1.0  Input minimum depth for offshore (m)
0.1  Input "dry land" depth for inundation (m)
0.0009   Input friction coefficient (n**2)
1    let a and b run up
300.0    blowup limit
1    input time step (sec)
28800    input amount of steps
2    Compute "A" arrays every n-th time step, n=
1    COmpute "B" arrays every n-th time step, n=
30   Input number of steps between snapshots
0    ...Starting from
1    ...saveing grid every n-th node, n=
nikolski2_run2d/niko2_Agrid_30s.most
nikolski2_run2d/niko_Bgrid_12s.most
nikolski2_run2d/niko_Cgrid_x2s_y1s.most
./
./
1 1 1 1  NetCDF output for A, B, C, SIFT
1    Timeseries locations:
3 109 105nikolski2191.13   52.941111depth m: 2.3  NK2
  Nikolski, AK
```

A3. Reference model .in file:

```
0.005 Minimum amplitude of input offshore wave (m)
1.0  Input minimum depth for offshore (m)
0.1   Input "dry land" depth for inundation (m)
0.0009 Input friction coefficient (n**2)
1     let a and b run up
300.0 blowup limit
0.3   input time step (sec)
96000 input amount of steps
6     Compute "A" arrays every n-th time step, n=
1     COmpute "B" arrays every n-th time step, n=
120    Input number of steps between snapshots
0   ...Starting from
1     ...saveing grid every n-th node, n=
nikolski_run2d/niko_rim_Agrid.most
nikolski_run2d/niko_rim_Bgrid.most
nikolski_run2d/niko_rim_Cgrid.most
./
./
1 1 1 1
1    Timeseries locations:
3 217 105nikolski2191.13   52.941111depth m: 2.3  NK
  Nikolski, AK
```

Appendix B. Propagation database:

Pacific Ocean Unit Sources

These propagation source details reflect the database as of February 2013, and there may have been updates in the earthquake source parameters after this date.

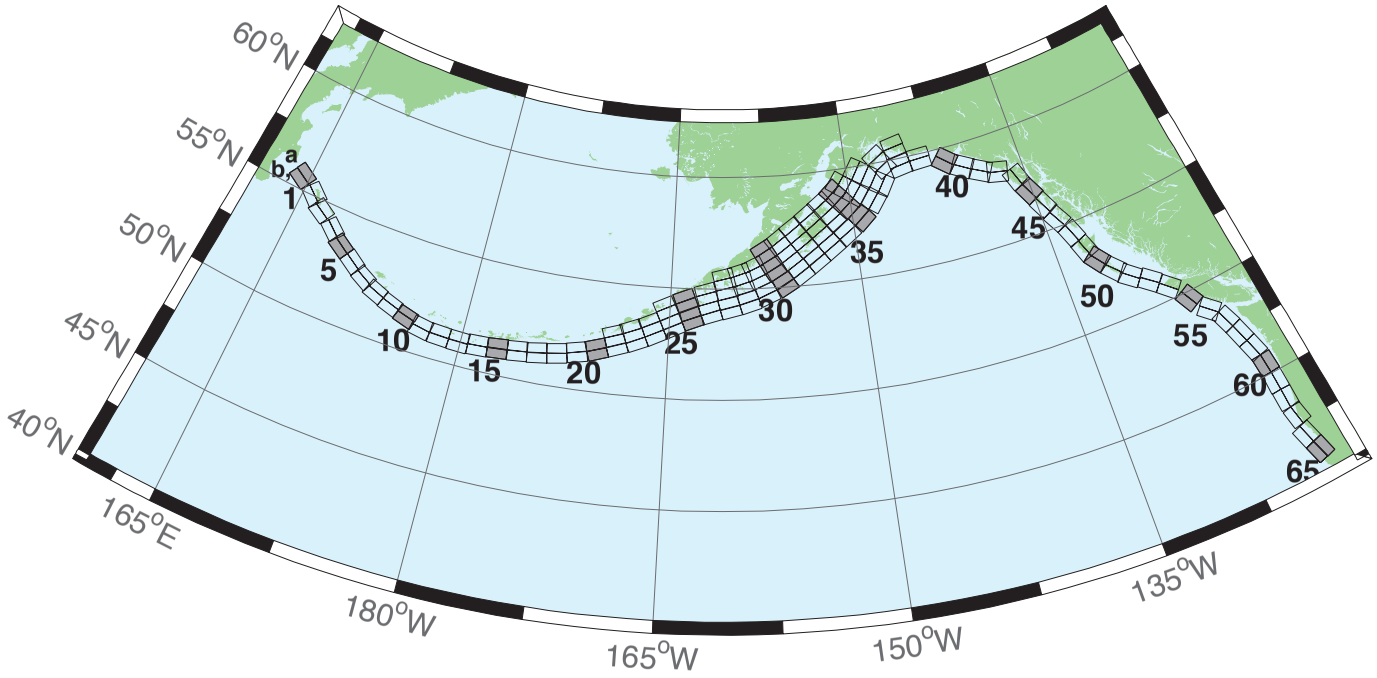

Figure B.1: Aleutian–Alaska–Cascadia Subduction Zone unit sources.

Table B.1: Earthquake parameters for Aleutian–Alaska–Cascadia Subduction Zone unit sources.

Segment	Description	Longitude(°E)	Latitude(°N)	Strike(°)	Dip(°)	Depth (km)
acsz–1a	Aleutian–Alaska–Cascadia	164.7994	55.9606	299	17	19.61
acsz–1b	Aleutian–Alaska–Cascadia	164.4310	55.5849	299	17	5
acsz–2a	Aleutian–Alaska–Cascadia	166.3418	55.4016	310.2	17	19.61
acsz–2b	Aleutian–Alaska–Cascadia	165.8578	55.0734	310.2	17	5
acsz–3a	Aleutian–Alaska–Cascadia	167.2939	54.8919	300.2	23.36	24.82
acsz–3b	Aleutian–Alaska–Cascadia	166.9362	54.5356	300.2	23.36	5
acsz–4a	Aleutian–Alaska–Cascadia	168.7131	54.2852	310.2	38.51	25.33
acsz–4b	Aleutian–Alaska–Cascadia	168.3269	54.0168	310.2	24	5
acsz–5a	Aleutian–Alaska–Cascadia	169.7447	53.7808	302.8	37.02	23.54
acsz–5b	Aleutian–Alaska–Cascadia	169.4185	53.4793	302.8	21.77	5
acsz–6a	Aleutian–Alaska–Cascadia	171.0144	53.3054	303.2	35.31	22.92
acsz–6b	Aleutian–Alaska–Cascadia	170.6813	52.9986	303.2	21	5
acsz–7a	Aleutian–Alaska–Cascadia	172.1500	52.8528	298.2	35.56	20.16
acsz–7b	Aleutian–Alaska–Cascadia	171.8665	52.5307	298.2	17.65	5
acsz–8a	Aleutian–Alaska–Cascadia	173.2726	52.4579	290.8	37.92	20.35
acsz–8b	Aleutian–Alaska–Cascadia	173.0681	52.1266	290.8	17.88	5
acsz–9a	Aleutian–Alaska–Cascadia	174.5866	52.1434	289	39.09	21.05
acsz–9b	Aleutian–Alaska–Cascadia	174.4027	51.8138	289	18.73	5
acsz–10a	Aleutian–Alaska–Cascadia	175.8784	51.8526	286.1	40.51	20.87
acsz–10b	Aleutian–Alaska–Cascadia	175.7265	51.5245	286.1	18.51	5
acsz–11a	Aleutian–Alaska–Cascadia	177.1140	51.6488	280	15	17.94
acsz–11b	Aleutian–Alaska–Cascadia	176.9937	51.2215	280	15	5
acsz–12a	Aleutian–Alaska–Cascadia	178.4500	51.5690	273	15	17.94
acsz–12b	Aleutian–Alaska–Cascadia	178.4130	51.1200	273	15	5
acsz–13a	Aleutian–Alaska–Cascadia	179.8550	51.5340	271	15	17.94
acsz–13b	Aleutian–Alaska–Cascadia	179.8420	51.0850	271	15	5
acsz–14a	Aleutian–Alaska–Cascadia	181.2340	51.5780	267	15	17.94
acsz–14b	Aleutian–Alaska–Cascadia	181.2720	51.1290	267	15	5
acsz–15a	Aleutian–Alaska–Cascadia	182.6380	51.6470	265	15	17.94
acsz–15b	Aleutian–Alaska–Cascadia	182.7000	51.2000	265	15	5
acsz–16a	Aleutian–Alaska–Cascadia	184.0550	51.7250	264	15	17.94
acsz–16b	Aleutian–Alaska–Cascadia	184.1280	51.2780	264	15	5
acsz–17a	Aleutian–Alaska–Cascadia	185.4560	51.8170	262	15	17.94
acsz–17b	Aleutian–Alaska–Cascadia	185.5560	51.3720	262	15	5
acsz–18a	Aleutian–Alaska–Cascadia	186.8680	51.9410	261	15	17.94
acsz–18b	Aleutian–Alaska–Cascadia	186.9810	51.4970	261	15	5
acsz–19a	Aleutian–Alaska–Cascadia	188.2430	52.1280	257	15	17.94
acsz–19b	Aleutian–Alaska–Cascadia	188.4060	51.6900	257	15	5
acsz–20a	Aleutian–Alaska–Cascadia	189.5810	52.3550	251	15	17.94
acsz–20b	Aleutian–Alaska–Cascadia	189.8180	51.9300	251	15	5
acsz–21a	Aleutian–Alaska–Cascadia	190.9570	52.6470	251	15	17.94
acsz–21b	Aleutian–Alaska–Cascadia	191.1960	52.2220	251	15	5
acsz–21z	Aleutian–Alaska–Cascadia	190.7399	53.0443	250.8	15	30.88
acsz–22a	Aleutian–Alaska–Cascadia	192.2940	52.9430	247	15	17.94
acsz–22b	Aleutian–Alaska–Cascadia	192.5820	52.5300	247	15	5
acsz–22z	Aleutian–Alaska–Cascadia	192.0074	53.3347	247.8	15	30.88
acsz–23a	Aleutian–Alaska–Cascadia	193.6270	53.3070	245	15	17.94
acsz–23b	Aleutian–Alaska–Cascadia	193.9410	52.9000	245	15	5
acsz–23z	Aleutian–Alaska–Cascadia	193.2991	53.6768	244.6	15	30.88
acsz–24a	Aleutian–Alaska–Cascadia	194.9740	53.6870	245	15	17.94
acsz–24b	Aleutian–Alaska–Cascadia	195.2910	53.2800	245	15	5
acsz–24y	Aleutian–Alaska–Cascadia	194.3645	54.4604	244.4	15	43.82
acsz–24z	Aleutian–Alaska–Cascadia	194.6793	54.0674	244.6	15	30.88

Continued on next page

Table B.1 – continued

Segment	Description	Longitude(°E)	Latitude(°N)	Strike(°)	Dip(°)	Depth (km)
acsz–25a	Aleutian–Alaska–Cascadia	196.4340	54.0760	250	15	17.94
acsz–25b	Aleutian–Alaska–Cascadia	196.6930	53.6543	250	15	5
acsz–25y	Aleutian–Alaska–Cascadia	195.9009	54.8572	247.9	15	43.82
acsz–25z	Aleutian–Alaska–Cascadia	196.1761	54.4536	248.1	15	30.88
acsz–26a	Aleutian–Alaska–Cascadia	197.8970	54.3600	253	15	17.94
acsz–26b	Aleutian–Alaska–Cascadia	198.1200	53.9300	253	15	5
acsz–26y	Aleutian–Alaska–Cascadia	197.5498	55.1934	253.1	15	43.82
acsz–26z	Aleutian–Alaska–Cascadia	197.7620	54.7770	253.3	15	30.88
acsz–27a	Aleutian–Alaska–Cascadia	199.4340	54.5960	256	15	17.94
acsz–27b	Aleutian–Alaska–Cascadia	199.6200	54.1600	256	15	5
acsz–27x	Aleutian–Alaska–Cascadia	198.9736	55.8631	256.5	15	56.24
acsz–27y	Aleutian–Alaska–Cascadia	199.1454	55.4401	256.6	15	43.82
acsz–27z	Aleutian–Alaska–Cascadia	199.3135	55.0170	256.8	15	30.88
acsz–28a	Aleutian–Alaska–Cascadia	200.8820	54.8300	253	15	17.94
acsz–28b	Aleutian–Alaska–Cascadia	201.1080	54.4000	253	15	5
acsz–28x	Aleutian–Alaska–Cascadia	200.1929	56.0559	252.5	15	56.24
acsz–28y	Aleutian–Alaska–Cascadia	200.4167	55.6406	252.7	15	43.82
acsz–28z	Aleutian–Alaska–Cascadia	200.6360	55.2249	252.9	15	30.88
acsz–29a	Aleutian–Alaska–Cascadia	202.2610	55.1330	247	15	17.94
acsz–29b	Aleutian–Alaska–Cascadia	202.5650	54.7200	247	15	5
acsz–29x	Aleutian–Alaska–Cascadia	201.2606	56.2861	245.7	15	56.24
acsz–29y	Aleutian–Alaska–Cascadia	201.5733	55.8888	246	15	43.82
acsz–29z	Aleutian–Alaska–Cascadia	201.8797	55.4908	246.2	15	30.88
acsz–30a	Aleutian–Alaska–Cascadia	203.6040	55.5090	240	15	17.94
acsz–30b	Aleutian–Alaska–Cascadia	203.9970	55.1200	240	15	5
acsz–30w	Aleutian–Alaska–Cascadia	201.9901	56.9855	239.5	15	69.12
acsz–30x	Aleutian–Alaska–Cascadia	202.3851	56.6094	239.8	15	56.24
acsz–30y	Aleutian–Alaska–Cascadia	202.7724	56.2320	240.2	15	43.82
acsz–30z	Aleutian–Alaska–Cascadia	203.1521	55.8534	240.5	15	30.88
acsz–31a	Aleutian–Alaska–Cascadia	204.8950	55.9700	236	15	17.94
acsz–31b	Aleutian–Alaska–Cascadia	205.3400	55.5980	236	15	5
acsz–31w	Aleutian–Alaska–Cascadia	203.0825	57.3740	234.5	15	69.12
acsz–31x	Aleutian–Alaska–Cascadia	203.5408	57.0182	234.9	15	56.24
acsz–31y	Aleutian–Alaska–Cascadia	203.9904	56.6607	235.3	15	43.82
acsz–31z	Aleutian–Alaska–Cascadia	204.4315	56.3016	235.7	15	30.88
acsz–32a	Aleutian–Alaska–Cascadia	206.2080	56.4730	236	15	17.94
acsz–32b	Aleutian–Alaska–Cascadia	206.6580	56.1000	236	15	5
acsz–32w	Aleutian–Alaska–Cascadia	204.4129	57.8908	234.3	15	69.12
acsz–32x	Aleutian–Alaska–Cascadia	204.8802	57.5358	234.7	15	56.24
acsz–32y	Aleutian–Alaska–Cascadia	205.3385	57.1792	235.1	15	43.82
acsz–32z	Aleutian–Alaska–Cascadia	205.7880	56.8210	235.5	15	30.88
acsz–33a	Aleutian–Alaska–Cascadia	207.5370	56.9750	236	15	17.94
acsz–33b	Aleutian–Alaska–Cascadia	207.9930	56.6030	236	15	5
acsz–33w	Aleutian–Alaska–Cascadia	205.7126	58.3917	234.2	15	69.12
acsz–33x	Aleutian–Alaska–Cascadia	206.1873	58.0371	234.6	15	56.24
acsz–33y	Aleutian–Alaska–Cascadia	206.6527	57.6808	235	15	43.82
acsz–33z	Aleutian–Alaska–Cascadia	207.1091	57.3227	235.4	15	30.88
acsz–34a	Aleutian–Alaska–Cascadia	208.9371	57.5124	236	15	17.94
acsz–34b	Aleutian–Alaska–Cascadia	209.4000	57.1400	236	15	5
acsz–34w	Aleutian–Alaska–Cascadia	206.9772	58.8804	233.5	15	69.12
acsz–34x	Aleutian–Alaska–Cascadia	207.4677	58.5291	233.9	15	56.24
acsz–34y	Aleutian–Alaska–Cascadia	207.9485	58.1760	234.3	15	43.82
acsz–34z	Aleutian–Alaska–Cascadia	208.4198	57.8213	234.7	15	30.88
acsz–35a	Aleutian–Alaska–Cascadia	210.2597	58.0441	230	15	17.94
acsz–35b	Aleutian–Alaska–Cascadia	210.8000	57.7000	230	15	5

Continued on next page

Table B.1 – continued

Segment	Description	Longitude(°E)	Latitude(°N)	Strike(°)	Dip(°)	Depth (km)
acsz–35w	Aleutian–Alaska–Cascadia	208.0204	59.3199	228.8	15	69.12
acsz–35x	Aleutian–Alaska–Cascadia	208.5715	58.9906	229.3	15	56.24
acsz–35y	Aleutian–Alaska–Cascadia	209.1122	58.6590	229.7	15	43.82
acsz–35z	Aleutian–Alaska–Cascadia	209.6425	58.3252	230.2	15	30.88
acsz–36a	Aleutian–Alaska–Cascadia	211.3249	58.6565	218	15	17.94
acsz–36b	Aleutian–Alaska–Cascadia	212.0000	58.3800	218	15	5
acsz–36w	Aleutian–Alaska–Cascadia	208.5003	59.5894	215.6	15	69.12
acsz–36x	Aleutian–Alaska–Cascadia	209.1909	59.3342	216.2	15	56.24
acsz–36y	Aleutian–Alaska–Cascadia	209.8711	59.0753	216.8	15	43.82
acsz–36z	Aleutian–Alaska–Cascadia	210.5412	58.8129	217.3	15	30.88
acsz–37a	Aleutian–Alaska–Cascadia	212.2505	59.2720	213.7	15	17.94
acsz–37b	Aleutian–Alaska–Cascadia	212.9519	59.0312	213.7	15	5
acsz–37x	Aleutian–Alaska–Cascadia	210.1726	60.0644	213	15	56.24
acsz–37y	Aleutian–Alaska–Cascadia	210.8955	59.8251	213.7	15	43.82
acsz–37z	Aleutian–Alaska–Cascadia	211.6079	59.5820	214.3	15	30.88
acsz–38a	Aleutian–Alaska–Cascadia	214.6555	60.1351	260.1	0	15
acsz–38b	Aleutian–Alaska–Cascadia	214.8088	59.6927	260.1	0	15
acsz–38y	Aleutian–Alaska–Cascadia	214.3737	60.9838	259	0	15
acsz–38z	Aleutian–Alaska–Cascadia	214.5362	60.5429	259	0	15
acsz–39a	Aleutian–Alaska–Cascadia	216.5607	60.2480	267	0	15
acsz–39b	Aleutian–Alaska–Cascadia	216.6068	59.7994	267	0	15
acsz–40a	Aleutian–Alaska–Cascadia	219.3069	59.7574	310.9	0	15
acsz–40b	Aleutian–Alaska–Cascadia	218.7288	59.4180	310.9	0	15
acsz–41a	Aleutian–Alaska–Cascadia	220.4832	59.3390	300.7	0	15
acsz–41b	Aleutian–Alaska–Cascadia	220.0382	58.9529	300.7	0	15
acsz–42a	Aleutian–Alaska–Cascadia	221.8835	58.9310	298.9	0	15
acsz–42b	Aleutian–Alaska–Cascadia	221.4671	58.5379	298.9	0	15
acsz–43a	Aleutian–Alaska–Cascadia	222.9711	58.6934	282.3	0	15
acsz–43b	Aleutian–Alaska–Cascadia	222.7887	58.2546	282.3	0	15
acsz–44a	Aleutian–Alaska–Cascadia	224.9379	57.9054	340.9	12	11.09
acsz–44b	Aleutian–Alaska–Cascadia	224.1596	57.7617	340.9	7	5
acsz–45a	Aleutian–Alaska–Cascadia	225.4994	57.1634	334.1	12	11.09
acsz–45b	Aleutian–Alaska–Cascadia	224.7740	56.9718	334.1	7	5
acsz–46a	Aleutian–Alaska–Cascadia	226.1459	56.3552	334.1	12	11.09
acsz–46b	Aleutian–Alaska–Cascadia	225.4358	56.1636	334.1	7	5
acsz–47a	Aleutian–Alaska–Cascadia	226.7731	55.5830	332.3	12	11.09
acsz–47b	Aleutian–Alaska–Cascadia	226.0887	55.3785	332.3	7	5
acsz–48a	Aleutian–Alaska–Cascadia	227.4799	54.6763	339.4	12	11.09
acsz–48b	Aleutian–Alaska–Cascadia	226.7713	54.5217	339.4	7	5
acsz–49a	Aleutian–Alaska–Cascadia	227.9482	53.8155	341.2	12	11.09
acsz–49b	Aleutian–Alaska–Cascadia	227.2462	53.6737	341.2	7	5
acsz–50a	Aleutian–Alaska–Cascadia	228.3970	53.2509	324.5	12	11.09
acsz–50b	Aleutian–Alaska–Cascadia	227.8027	52.9958	324.5	7	5
acsz–51a	Aleutian–Alaska–Cascadia	229.1844	52.6297	318.4	12	11.09
acsz–51b	Aleutian–Alaska–Cascadia	228.6470	52.3378	318.4	7	5
acsz–52a	Aleutian–Alaska–Cascadia	230.0306	52.0768	310.9	12	11.09
acsz–52b	Aleutian–Alaska–Cascadia	229.5665	51.7445	310.9	7	5
acsz–53a	Aleutian–Alaska–Cascadia	231.1735	51.5258	310.9	12	11.09
acsz–53b	Aleutian–Alaska–Cascadia	230.7150	51.1935	310.9	7	5
acsz–54a	Aleutian–Alaska–Cascadia	232.2453	50.8809	314.1	12	11.09
acsz–54b	Aleutian–Alaska–Cascadia	231.7639	50.5655	314.1	7	5
acsz–55a	Aleutian–Alaska–Cascadia	233.3066	49.9032	333.7	12	11.09
acsz–55b	Aleutian–Alaska–Cascadia	232.6975	49.7086	333.7	7	5
acsz–56a	Aleutian–Alaska–Cascadia	234.0588	49.1702	315	11	12.82
acsz–56b	Aleutian–Alaska–Cascadia	233.5849	48.8584	315	9	5

Continued on next page

Table B.1 – continued

Segment	Description	Longitude(°E)	Latitude(°N)	Strike(°)	Dip(°)	Depth (km)
acsz–57a	Aleutian–Alaska–Cascadia	234.9041	48.2596	341	11	12.82
acsz–57b	Aleutian–Alaska–Cascadia	234.2797	48.1161	341	9	5
acsz–58a	Aleutian–Alaska–Cascadia	235.3021	47.3812	344	11	12.82
acsz–58b	Aleutian–Alaska–Cascadia	234.6776	47.2597	344	9	5
acsz–59a	Aleutian–Alaska–Cascadia	235.6432	46.5082	345	11	12.82
acsz–59b	Aleutian–Alaska–Cascadia	235.0257	46.3941	345	9	5
acsz–60a	Aleutian–Alaska–Cascadia	235.8640	45.5429	356	11	12.82
acsz–60b	Aleutian–Alaska–Cascadia	235.2363	45.5121	356	9	5
acsz–61a	Aleutian–Alaska–Cascadia	235.9106	44.6227	359	11	12.82
acsz–61b	Aleutian–Alaska–Cascadia	235.2913	44.6150	359	9	5
acsz–62a	Aleutian–Alaska–Cascadia	235.9229	43.7245	359	11	12.82
acsz–62b	Aleutian–Alaska–Cascadia	235.3130	43.7168	359	9	5
acsz–63a	Aleutian–Alaska–Cascadia	236.0220	42.9020	350	11	12.82
acsz–63b	Aleutian–Alaska–Cascadia	235.4300	42.8254	350	9	5
acsz–64a	Aleutian–Alaska–Cascadia	235.9638	41.9818	345	11	12.82
acsz–64b	Aleutian–Alaska–Cascadia	235.3919	41.8677	345	9	5
acsz–65a	Aleutian–Alaska–Cascadia	236.2643	41.1141	345	11	12.82
acsz–65b	Aleutian–Alaska–Cascadia	235.7000	41.0000	345	9	5
acsz–238a	Aleutian–Alaska–Cascadia	213.2878	59.8406	236.8	15	17.94
acsz–238y	Aleutian–Alaska–Cascadia	212.3424	60.5664	236.8	15	43.82
acsz–238z	Aleutian–Alaska–Cascadia	212.8119	60.2035	236.8	15	30.88

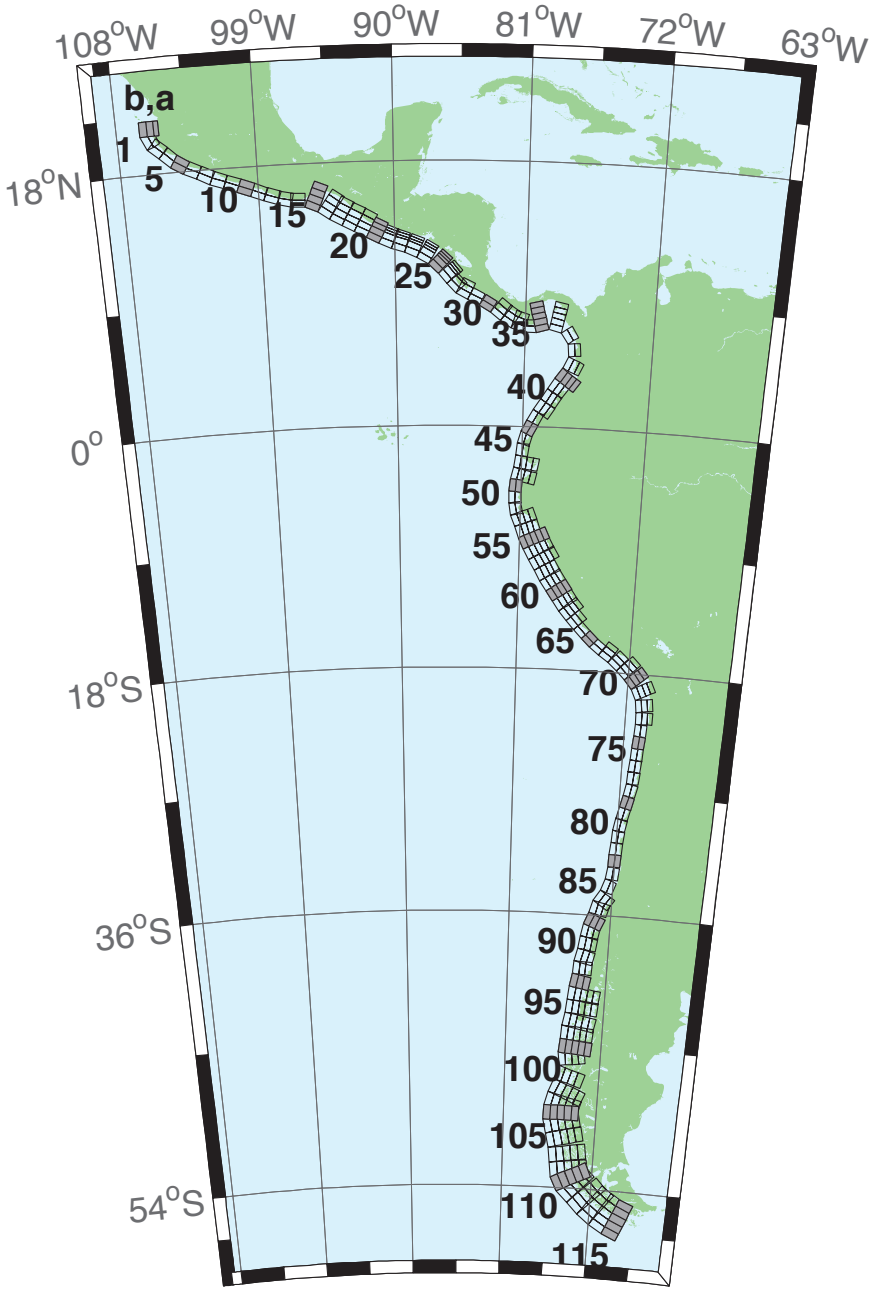

Figure B.2: Central and South America Subduction Zone unit sources.

Table B.2: Earthquake parameters for Central and South America Subduction Zone unit sources.

Segment	Description	Longitude(°E)	Latitude(°N)	Strike(°)	Dip(°)	Depth (km)
cssz–1a	Central and South America	254.4573	20.8170	359	19	15.4
cssz–1b	Central and South America	254.0035	20.8094	359	12	5
cssz–1z	Central and South America	254.7664	20.8222	359	50	31.67
cssz–2a	Central and South America	254.5765	20.2806	336.8	19	15.4
cssz–2b	Central and South America	254.1607	20.1130	336.8	12	5
cssz–3a	Central and South America	254.8789	19.8923	310.6	18.31	15.27
cssz–3b	Central and South America	254.5841	19.5685	310.6	11.85	5
cssz–4a	Central and South America	255.6167	19.2649	313.4	17.62	15.12
cssz–4b	Central and South America	255.3056	18.9537	313.4	11.68	5
cssz–5a	Central and South America	256.2240	18.8148	302.7	16.92	15
cssz–5b	Central and South America	255.9790	18.4532	302.7	11.54	5
cssz–6a	Central and South America	256.9425	18.4383	295.1	16.23	14.87
cssz–6b	Central and South America	256.7495	18.0479	295.1	11.38	5
cssz–7a	Central and South America	257.8137	18.0339	296.9	15.54	14.74
cssz–7b	Central and South America	257.6079	17.6480	296.9	11.23	5
cssz–8a	Central and South America	258.5779	17.7151	290.4	14.85	14.61
cssz–8b	Central and South America	258.4191	17.3082	290.4	11.08	5
cssz–9a	Central and South America	259.4578	17.4024	290.5	14.15	14.47
cssz–9b	Central and South America	259.2983	16.9944	290.5	10.92	5
cssz–10a	Central and South America	260.3385	17.0861	290.8	13.46	14.34
cssz–10b	Central and South America	260.1768	16.6776	290.8	10.77	5
cssz–11a	Central and South America	261.2255	16.7554	291.8	12.77	14.21
cssz–11b	Central and South America	261.0556	16.3487	291.8	10.62	5
cssz–12a	Central and South America	262.0561	16.4603	288.9	12.08	14.08
cssz–12b	Central and South America	261.9082	16.0447	288.9	10.46	5
cssz–13a	Central and South America	262.8638	16.2381	283.2	11.38	13.95
cssz–13b	Central and South America	262.7593	15.8094	283.2	10.31	5
cssz–14a	Central and South America	263.6066	16.1435	272.1	10.69	13.81
cssz–14b	Central and South America	263.5901	15.7024	272.1	10.15	5
cssz–15a	Central and South America	264.8259	15.8829	293	10	13.68
cssz–15b	Central and South America	264.6462	15.4758	293	10	5
cssz–15y	Central and South America	265.1865	16.6971	293	10	31.05
cssz–15z	Central and South America	265.0060	16.2900	293	10	22.36
cssz–16a	Central and South America	265.7928	15.3507	304.9	15	15.82
cssz–16b	Central and South America	265.5353	14.9951	304.9	12.5	5
cssz–16y	Central and South America	266.3092	16.0619	304.9	15	41.7
cssz–16z	Central and South America	266.0508	15.7063	304.9	15	28.76
cssz–17a	Central and South America	266.4947	14.9019	299.5	20	17.94
cssz–17b	Central and South America	266.2797	14.5346	299.5	15	5
cssz–17y	Central and South America	266.9259	15.6365	299.5	20	52.14
cssz–17z	Central and South America	266.7101	15.2692	299.5	20	35.04
cssz–18a	Central and South America	267.2827	14.4768	298	21.5	17.94
cssz–18b	Central and South America	267.0802	14.1078	298	15	5
cssz–18y	Central and South America	267.6888	15.2148	298	21.5	54.59
cssz–18z	Central and South America	267.4856	14.8458	298	21.5	36.27
cssz–19a	Central and South America	268.0919	14.0560	297.6	23	17.94
cssz–19b	Central and South America	267.8943	13.6897	297.6	15	5
cssz–19y	Central and South America	268.4880	14.7886	297.6	23	57.01
cssz–19z	Central and South America	268.2898	14.4223	297.6	23	37.48
cssz–20a	Central and South America	268.8929	13.6558	296.2	24	17.94
cssz–20b	Central and South America	268.7064	13.2877	296.2	15	5
cssz–20y	Central and South America	269.1796	14.2206	296.2	45.5	73.94
cssz–20z	Central and South America	269.0362	13.9382	296.2	45.5	38.28

Continued on next page

Table B.2 – continued

Segment	Description	Longitude(°E)	Latitude(°N)	Strike(°)	Dip(°)	Depth (km)
cssz–21a	Central and South America	269.6797	13.3031	292.6	25	17.94
cssz–21b	Central and South America	269.5187	12.9274	292.6	15	5
cssz–21x	Central and South America	269.8797	13.7690	292.6	68	131.8
cssz–21y	Central and South America	269.8130	13.6137	292.6	68	85.43
cssz–21z	Central and South America	269.7463	13.4584	292.6	68	39.07
cssz–22a	Central and South America	270.4823	13.0079	288.6	25	17.94
cssz–22b	Central and South America	270.3492	12.6221	288.6	15	5
cssz–22x	Central and South America	270.6476	13.4864	288.6	68	131.8
cssz–22y	Central and South America	270.5925	13.3269	288.6	68	85.43
cssz–22z	Central and South America	270.5374	13.1674	288.6	68	39.07
cssz–23a	Central and South America	271.3961	12.6734	292.4	25	17.94
cssz–23b	Central and South America	271.2369	12.2972	292.4	15	5
cssz–23x	Central and South America	271.5938	13.1399	292.4	68	131.8
cssz–23y	Central and South America	271.5279	12.9844	292.4	68	85.43
cssz–23z	Central and South America	271.4620	12.8289	292.4	68	39.07
cssz–24a	Central and South America	272.3203	12.2251	300.2	25	17.94
cssz–24b	Central and South America	272.1107	11.8734	300.2	15	5
cssz–24x	Central and South America	272.5917	12.6799	300.2	67	131.1
cssz–24y	Central and South America	272.5012	12.5283	300.2	67	85.1
cssz–24z	Central and South America	272.4107	12.3767	300.2	67	39.07
cssz–25a	Central and South America	273.2075	11.5684	313.8	25	17.94
cssz–25b	Central and South America	272.9200	11.2746	313.8	15	5
cssz–25x	Central and South America	273.5950	11.9641	313.8	66	130.4
cssz–25y	Central and South America	273.4658	11.8322	313.8	66	84.75
cssz–25z	Central and South America	273.3366	11.7003	313.8	66	39.07
cssz–26a	Central and South America	273.8943	10.8402	320.4	25	17.94
cssz–26b	Central and South America	273.5750	10.5808	320.4	15	5
cssz–26x	Central and South America	274.3246	11.1894	320.4	66	130.4
cssz–26y	Central and South America	274.1811	11.0730	320.4	66	84.75
cssz–26z	Central and South America	274.0377	10.9566	320.4	66	39.07
cssz–27a	Central and South America	274.4569	10.2177	316.1	25	17.94
cssz–27b	Central and South America	274.1590	9.9354	316.1	15	5
cssz–27z	Central and South America	274.5907	10.3444	316.1	66	39.07
cssz–28a	Central and South America	274.9586	9.8695	297.1	22	14.54
cssz–28b	Central and South America	274.7661	9.4988	297.1	11	5
cssz–28z	Central and South America	275.1118	10.1643	297.1	42.5	33.27
cssz–29a	Central and South America	275.7686	9.4789	296.6	19	11.09
cssz–29b	Central and South America	275.5759	9.0992	296.6	7	5
cssz–30a	Central and South America	276.6346	8.9973	302.2	19	9.36
cssz–30b	Central and South America	276.4053	8.6381	302.2	5	5
cssz–31a	Central and South America	277.4554	8.4152	309.1	19	7.62
cssz–31b	Central and South America	277.1851	8.0854	309.1	3	5
cssz–31z	Central and South America	277.7260	8.7450	309.1	19	23.9
cssz–32a	Central and South America	278.1112	7.9425	303	18.67	8.49
cssz–32b	Central and South America	277.8775	7.5855	303	4	5
cssz–32z	Central and South America	278.3407	8.2927	303	21.67	24.49
cssz–33a	Central and South America	278.7082	7.6620	287.6	18.33	10.23
cssz–33b	Central and South America	278.5785	7.2555	287.6	6	5
cssz–33z	Central and South America	278.8328	8.0522	287.6	24.33	25.95
cssz–34a	Central and South America	279.3184	7.5592	269.5	18	17.94
cssz–34b	Central and South America	279.3223	7.1320	269.5	15	5
cssz–35a	Central and South America	280.0039	7.6543	255.9	17.67	14.54
cssz–35b	Central and South America	280.1090	7.2392	255.9	11	5
cssz–35x	Central and South America	279.7156	8.7898	255.9	29.67	79.22
cssz–35y	Central and South America	279.8118	8.4113	255.9	29.67	54.47

Continued on next page

Table B.2 – continued

Segment	Description	Longitude(°E)	Latitude(°N)	Strike(°)	Dip(°)	Depth (km)
cssz–35z	Central and South America	279.9079	8.0328	255.9	29.67	29.72
cssz–36a	Central and South America	281.2882	7.6778	282.5	17.33	11.09
cssz–36b	Central and South America	281.1948	7.2592	282.5	7	5
cssz–36x	Central and South America	281.5368	8.7896	282.5	32.33	79.47
cssz–36y	Central and South America	281.4539	8.4190	282.5	32.33	52.73
cssz–36z	Central and South America	281.3710	8.0484	282.5	32.33	25.99
cssz–37a	Central and South America	282.5252	6.8289	326.9	17	10.23
cssz–37b	Central and South America	282.1629	6.5944	326.9	6	5
cssz–38a	Central and South America	282.9469	5.5973	355.4	17	10.23
cssz–38b	Central and South America	282.5167	5.5626	355.4	6	5
cssz–39a	Central and South America	282.7236	4.3108	24.13	17	10.23
cssz–39b	Central and South America	282.3305	4.4864	24.13	6	5
cssz–39z	Central and South America	283.0603	4.1604	24.13	35	24.85
cssz–40a	Central and South America	282.1940	3.3863	35.28	17	10.23
cssz–40b	Central and South America	281.8427	3.6344	35.28	6	5
cssz–40y	Central and South America	282.7956	2.9613	35.28	35	53.52
cssz–40z	Central and South America	282.4948	3.1738	35.28	35	24.85
cssz–41a	Central and South America	281.6890	2.6611	34.27	17	10.23
cssz–41b	Central and South America	281.3336	2.9030	34.27	6	5
cssz–41z	Central and South America	281.9933	2.4539	34.27	35	24.85
cssz–42a	Central and South America	281.2266	1.9444	31.29	17	10.23
cssz–42b	Central and South America	280.8593	2.1675	31.29	6	5
cssz–42z	Central and South America	281.5411	1.7533	31.29	35	24.85
cssz–43a	Central and South America	280.7297	1.1593	33.3	17	10.23
cssz–43b	Central and South America	280.3706	1.3951	33.3	6	5
cssz–43z	Central and South America	281.0373	0.9573	33.3	35	24.85
cssz–44a	Central and South America	280.3018	0.4491	28.8	17	10.23
cssz–44b	Central and South America	279.9254	0.6560	28.8	6	5
cssz–45a	Central and South America	279.9083	-0.3259	26.91	10	8.49
cssz–45b	Central and South America	279.5139	-0.1257	26.91	4	5
cssz–46a	Central and South America	279.6461	-0.9975	15.76	10	8.49
cssz–46b	Central and South America	279.2203	-0.8774	15.76	4	5
cssz–47a	Central and South America	279.4972	-1.7407	6.9	10	8.49
cssz–47b	Central and South America	279.0579	-1.6876	6.9	4	5
cssz–48a	Central and South America	279.3695	-2.6622	8.96	10	8.49
cssz–48b	Central and South America	278.9321	-2.5933	8.96	4	5
cssz–48y	Central and South America	280.2444	-2.8000	8.96	10	25.85
cssz–48z	Central and South America	279.8070	-2.7311	8.96	10	17.17
cssz–49a	Central and South America	279.1852	-3.6070	13.15	10	8.49
cssz–49b	Central and South America	278.7536	-3.5064	13.15	4	5
cssz–49y	Central and South America	280.0486	-3.8082	13.15	10	25.85
cssz–49z	Central and South America	279.6169	-3.7076	13.15	10	17.17
cssz–50a	Central and South America	279.0652	-4.3635	4.78	10.33	9.64
cssz–50b	Central and South America	278.6235	-4.3267	4.78	5.33	5
cssz–51a	Central and South America	279.0349	-5.1773	359.4	10.67	10.81
cssz–51b	Central and South America	278.5915	-5.1817	359.4	6.67	5
cssz–52a	Central and South America	279.1047	-5.9196	349.8	11	11.96
cssz–52b	Central and South America	278.6685	-5.9981	349.8	8	5
cssz–53a	Central and South America	279.3044	-6.6242	339.2	10.25	11.74
cssz–53b	Central and South America	278.8884	-6.7811	339.2	7.75	5
cssz–53y	Central and South America	280.1024	-6.3232	339.2	19.25	37.12
cssz–53z	Central and South America	279.7035	-6.4737	339.2	19.25	20.64
cssz–54a	Central and South America	279.6256	-7.4907	340.8	9.5	11.53
cssz–54b	Central and South America	279.2036	-7.6365	340.8	7.5	5
cssz–54y	Central and South America	280.4267	-7.2137	340.8	20.5	37.29

Continued on next page

Table B.2 – continued

Segment	Description	Longitude(°E)	Latitude(°N)	Strike(°)	Dip(°)	Depth (km)
cssz–54z	Central and South America	280.0262	-7.3522	340.8	20.5	19.78
cssz–55a	Central and South America	279.9348	-8.2452	335.4	8.75	11.74
cssz–55b	Central and South America	279.5269	-8.4301	335.4	7.75	5
cssz–55x	Central and South America	281.0837	-7.7238	335.4	21.75	56.4
cssz–55y	Central and South America	280.7009	-7.8976	335.4	21.75	37.88
cssz–55z	Central and South America	280.3180	-8.0714	335.4	21.75	19.35
cssz–56a	Central and South America	280.3172	-8.9958	331.6	8	11.09
cssz–56b	Central and South America	279.9209	-9.2072	331.6	7	5
cssz–56x	Central and South America	281.4212	-8.4063	331.6	23	57.13
cssz–56y	Central and South America	281.0534	-8.6028	331.6	23	37.59
cssz–56z	Central and South America	280.6854	-8.7993	331.6	23	18.05
cssz–57a	Central and South America	280.7492	-9.7356	328.7	8.6	10.75
cssz–57b	Central and South America	280.3640	-9.9663	328.7	6.6	5
cssz–57x	Central and South America	281.8205	-9.0933	328.7	23.4	57.94
cssz–57y	Central and South America	281.4636	-9.3074	328.7	23.4	38.08
cssz–57z	Central and South America	281.1065	-9.5215	328.7	23.4	18.22
cssz–58a	Central and South America	281.2275	-10.5350	330.5	9.2	10.4
cssz–58b	Central and South America	280.8348	-10.7532	330.5	6.2	5
cssz–58y	Central and South America	281.9548	-10.1306	330.5	23.8	38.57
cssz–58z	Central and South America	281.5913	-10.3328	330.5	23.8	18.39
cssz–59a	Central and South America	281.6735	-11.2430	326.2	9.8	10.05
cssz–59b	Central and South America	281.2982	-11.4890	326.2	5.8	5
cssz–59y	Central and South America	282.3675	-10.7876	326.2	24.2	39.06
cssz–59z	Central and South America	282.0206	-11.0153	326.2	24.2	18.56
cssz–60a	Central and South America	282.1864	-11.9946	326.5	10.4	9.71
cssz–60b	Central and South America	281.8096	-12.2384	326.5	5.4	5
cssz–60y	Central and South America	282.8821	-11.5438	326.5	24.6	39.55
cssz–60z	Central and South America	282.5344	-11.7692	326.5	24.6	18.73
cssz–61a	Central and South America	282.6944	-12.7263	325.5	11	9.36
cssz–61b	Central and South America	282.3218	-12.9762	325.5	5	5
cssz–61y	Central and South America	283.3814	-12.2649	325.5	25	40.03
cssz–61z	Central and South America	283.0381	-12.4956	325.5	25	18.9
cssz–62a	Central and South America	283.1980	-13.3556	319	11	9.79
cssz–62b	Central and South America	282.8560	-13.6451	319	5.5	5
cssz–62y	Central and South America	283.8178	-12.8300	319	27	42.03
cssz–62z	Central and South America	283.5081	-13.0928	319	27	19.33
cssz–63a	Central and South America	283.8032	-14.0147	317.9	11	10.23
cssz–63b	Central and South America	283.4661	-14.3106	317.9	6	5
cssz–63z	Central and South America	284.1032	-13.7511	317.9	29	19.77
cssz–64a	Central and South America	284.4144	-14.6482	315.7	13	11.96
cssz–64b	Central and South America	284.0905	-14.9540	315.7	8	5
cssz–65a	Central and South America	285.0493	-15.2554	313.2	15	13.68
cssz–65b	Central and South America	284.7411	-15.5715	313.2	10	5
cssz–66a	Central and South America	285.6954	-15.7816	307.7	14.5	13.68
cssz–66b	Central and South America	285.4190	-16.1258	307.7	10	5
cssz–67a	Central and South America	286.4127	-16.2781	304.3	14	13.68
cssz–67b	Central and South America	286.1566	-16.6381	304.3	10	5
cssz–67z	Central and South America	286.6552	-15.9365	304.3	23	25.78
cssz–68a	Central and South America	287.2481	-16.9016	311.8	14	13.68
cssz–68b	Central and South America	286.9442	-17.2264	311.8	10	5
cssz–68z	Central and South America	287.5291	-16.6007	311.8	26	25.78
cssz–69a	Central and South America	287.9724	-17.5502	314.9	14	13.68
cssz–69b	Central and South America	287.6496	-17.8590	314.9	10	5
cssz–69y	Central and South America	288.5530	-16.9934	314.9	29	50.02
cssz–69z	Central and South America	288.2629	-17.2718	314.9	29	25.78

Continued on next page

Table B.2 – continued

Segment	Description	Longitude(°E)	Latitude(°N)	Strike(°)	Dip(°)	Depth (km)
cssz–70a	Central and South America	288.6731	-18.2747	320.4	14	13.25
cssz–70b	Central and South America	288.3193	-18.5527	320.4	9.5	5
cssz–70y	Central and South America	289.3032	-17.7785	320.4	30	50.35
cssz–70z	Central and South America	288.9884	-18.0266	320.4	30	25.35
cssz–71a	Central and South America	289.3089	-19.1854	333.2	14	12.82
cssz–71b	Central and South America	288.8968	-19.3820	333.2	9	5
cssz–71y	Central and South America	290.0357	-18.8382	333.2	31	50.67
cssz–71z	Central and South America	289.6725	-19.0118	333.2	31	24.92
cssz–72a	Central and South America	289.6857	-20.3117	352.4	14	12.54
cssz–72b	Central and South America	289.2250	-20.3694	352.4	8.67	5
cssz–72z	Central and South America	290.0882	-20.2613	352.4	32	24.63
cssz–73a	Central and South America	289.7731	-21.3061	358.9	14	12.24
cssz–73b	Central and South America	289.3053	-21.3142	358.9	8.33	5
cssz–73z	Central and South America	290.1768	-21.2991	358.9	33	24.34
cssz–74a	Central and South America	289.7610	-22.2671	3.06	14	11.96
cssz–74b	Central and South America	289.2909	-22.2438	3.06	8	5
cssz–75a	Central and South America	289.6982	-23.1903	4.83	14.09	11.96
cssz–75b	Central and South America	289.2261	-23.1536	4.83	8	5
cssz–76a	Central and South America	289.6237	-24.0831	4.67	14.18	11.96
cssz–76b	Central and South America	289.1484	-24.0476	4.67	8	5
cssz–77a	Central and South America	289.5538	-24.9729	4.3	14.27	11.96
cssz–77b	Central and South America	289.0750	-24.9403	4.3	8	5
cssz–78a	Central and South America	289.4904	-25.8621	3.86	14.36	11.96
cssz–78b	Central and South America	289.0081	-25.8328	3.86	8	5
cssz–79a	Central and South America	289.3491	-26.8644	11.34	14.45	11.96
cssz–79b	Central and South America	288.8712	-26.7789	11.34	8	5
cssz–80a	Central and South America	289.1231	-27.7826	14.16	14.54	11.96
cssz–80b	Central and South America	288.6469	-27.6762	14.16	8	5
cssz–81a	Central and South America	288.8943	-28.6409	13.19	14.63	11.96
cssz–81b	Central and South America	288.4124	-28.5417	13.19	8	5
cssz–82a	Central and South America	288.7113	-29.4680	9.68	14.72	11.96
cssz–82b	Central and South America	288.2196	-29.3950	9.68	8	5
cssz–83a	Central and South America	288.5944	-30.2923	5.36	14.81	11.96
cssz–83b	Central and South America	288.0938	-30.2517	5.36	8	5
cssz–84a	Central and South America	288.5223	-31.1639	3.8	14.9	11.96
cssz–84b	Central and South America	288.0163	-31.1351	3.8	8	5
cssz–85a	Central and South America	288.4748	-32.0416	2.55	15	11.96
cssz–85b	Central and South America	287.9635	-32.0223	2.55	8	5
cssz–86a	Central and South America	288.3901	-33.0041	7.01	15	11.96
cssz–86b	Central and South America	287.8768	-32.9512	7.01	8	5
cssz–87a	Central and South America	288.1050	-34.0583	19.4	15	11.96
cssz–87b	Central and South America	287.6115	-33.9142	19.4	8	5
cssz–88a	Central and South America	287.5309	-35.0437	32.81	15	11.96
cssz–88b	Central and South America	287.0862	-34.8086	32.81	8	5
cssz–88z	Central and South America	287.9308	-35.2545	32.81	30	24.9
cssz–89a	Central and South America	287.2380	-35.5993	14.52	16.67	11.96
cssz–89b	Central and South America	286.7261	-35.4914	14.52	8	5
cssz–89z	Central and South America	287.7014	-35.6968	14.52	30	26.3
cssz–90a	Central and South America	286.8442	-36.5645	22.64	18.33	11.96
cssz–90b	Central and South America	286.3548	-36.4004	22.64	8	5
cssz–90z	Central and South America	287.2916	-36.7142	22.64	30	27.68
cssz–91a	Central and South America	286.5925	-37.2488	10.9	20	11.96
cssz–91b	Central and South America	286.0721	-37.1690	10.9	8	5
cssz–91z	Central and South America	287.0726	-37.3224	10.9	30	29.06
cssz–92a	Central and South America	286.4254	-38.0945	8.23	20	11.96

Continued on next page

Table B.2 – continued

Segment	Description	Longitude(°E)	Latitude(°N)	Strike(°)	Dip(°)	Depth (km)
cssz–92b	Central and South America	285.8948	-38.0341	8.23	8	5
cssz–92z	Central and South America	286.9303	-38.1520	8.23	26.67	29.06
cssz–93a	Central and South America	286.2047	-39.0535	13.46	20	11.96
cssz–93b	Central and South America	285.6765	-38.9553	13.46	8	5
cssz–93z	Central and South America	286.7216	-39.1495	13.46	23.33	29.06
cssz–94a	Central and South America	286.0772	-39.7883	3.4	20	11.96
cssz–94b	Central and South America	285.5290	-39.7633	3.4	8	5
cssz–94z	Central and South America	286.6255	-39.8133	3.4	20	29.06
cssz–95a	Central and South America	285.9426	-40.7760	9.84	20	11.96
cssz–95b	Central and South America	285.3937	-40.7039	9.84	8	5
cssz–95z	Central and South America	286.4921	-40.8481	9.84	20	29.06
cssz–96a	Central and South America	285.7839	-41.6303	7.6	20	11.96
cssz–96b	Central and South America	285.2245	-41.5745	7.6	8	5
cssz–96x	Central and South America	287.4652	-41.7977	7.6	20	63.26
cssz–96y	Central and South America	286.9043	-41.7419	7.6	20	46.16
cssz–96z	Central and South America	286.3439	-41.6861	7.6	20	29.06
cssz–97a	Central and South America	285.6695	-42.4882	5.3	20	11.96
cssz–97b	Central and South America	285.0998	-42.4492	5.3	8	5
cssz–97x	Central and South America	287.3809	-42.6052	5.3	20	63.26
cssz–97y	Central and South America	286.8101	-42.5662	5.3	20	46.16
cssz–97z	Central and South America	286.2396	-42.5272	5.3	20	29.06
cssz–98a	Central and South America	285.5035	-43.4553	10.53	20	11.96
cssz–98b	Central and South America	284.9322	-43.3782	10.53	8	5
cssz–98x	Central and South America	287.2218	-43.6866	10.53	20	63.26
cssz–98y	Central and South America	286.6483	-43.6095	10.53	20	46.16
cssz–98z	Central and South America	286.0755	-43.5324	10.53	20	29.06
cssz–99a	Central and South America	285.3700	-44.2595	4.86	20	11.96
cssz–99b	Central and South America	284.7830	-44.2237	4.86	8	5
cssz–99x	Central and South America	287.1332	-44.3669	4.86	20	63.26
cssz–99y	Central and South America	286.5451	-44.3311	4.86	20	46.16
cssz–99z	Central and South America	285.9574	-44.2953	4.86	20	29.06
cssz–100a	Central and South America	285.2713	-45.1664	5.68	20	11.96
cssz–100b	Central and South America	284.6758	-45.1246	5.68	8	5
cssz–100x	Central and South America	287.0603	-45.2918	5.68	20	63.26
cssz–100y	Central and South America	286.4635	-45.2500	5.68	20	46.16
cssz–100z	Central and South America	285.8672	-45.2082	5.68	20	29.06
cssz–101a	Central and South America	285.3080	-45.8607	352.6	20	9.36
cssz–101b	Central and South America	284.7067	-45.9152	352.6	5	5
cssz–101y	Central and South America	286.5089	-45.7517	352.6	20	43.56
cssz–101z	Central and South America	285.9088	-45.8062	352.6	20	26.46
cssz–102a	Central and South America	285.2028	-47.1185	17.72	5	9.36
cssz–102b	Central and South America	284.5772	-46.9823	17.72	5	5
cssz–102y	Central and South America	286.4588	-47.3909	17.72	5	18.07
cssz–102z	Central and South America	285.8300	-47.2547	17.72	5	13.72
cssz–103a	Central and South America	284.7075	-48.0396	23.37	7.5	11.53
cssz–103b	Central and South America	284.0972	-47.8630	23.37	7.5	5
cssz–103x	Central and South America	286.5511	-48.5694	23.37	7.5	31.11
cssz–103y	Central and South America	285.9344	-48.3928	23.37	7.5	24.58
cssz–103z	Central and South America	285.3199	-48.2162	23.37	7.5	18.05
cssz–104a	Central and South America	284.3440	-48.7597	14.87	10	13.68
cssz–104b	Central and South America	283.6962	-48.6462	14.87	10	5
cssz–104x	Central and South America	286.2962	-49.1002	14.87	10	39.73
cssz–104y	Central and South America	285.6440	-48.9867	14.87	10	31.05
cssz–104z	Central and South America	284.9933	-48.8732	14.87	10	22.36
cssz–105a	Central and South America	284.2312	-49.4198	0.25	9.67	13.4

Continued on next page

Table B.2 – continued

Segment	Description	Longitude(°E)	Latitude(°N)	Strike(°)	Dip(°)	Depth (km)
cssz–105b	Central and South America	283.5518	-49.4179	0.25	9.67	5
cssz–105x	Central and South America	286.2718	-49.4255	0.25	9.67	38.59
cssz–105y	Central and South America	285.5908	-49.4236	0.25	9.67	30.2
cssz–105z	Central and South America	284.9114	-49.4217	0.25	9.67	21.8
cssz–106a	Central and South America	284.3730	-50.1117	347.5	9.25	13.04
cssz–106b	Central and South America	283.6974	-50.2077	347.5	9.25	5
cssz–106x	Central and South America	286.3916	-49.8238	347.5	9.25	37.15
cssz–106y	Central and South America	285.7201	-49.9198	347.5	9.25	29.11
cssz–106z	Central and South America	285.0472	-50.0157	347.5	9.25	21.07
cssz–107a	Central and South America	284.7130	-50.9714	346.5	9	12.82
cssz–107b	Central and South America	284.0273	-51.0751	346.5	9	5
cssz–107x	Central and South America	286.7611	-50.6603	346.5	9	36.29
cssz–107y	Central and South America	286.0799	-50.7640	346.5	9	28.47
cssz–107z	Central and South America	285.3972	-50.8677	346.5	9	20.64
cssz–108a	Central and South America	285.0378	-51.9370	352	8.67	12.54
cssz–108b	Central and South America	284.3241	-51.9987	352	8.67	5
cssz–108x	Central and South America	287.1729	-51.7519	352	8.67	35.15
cssz–108y	Central and South America	286.4622	-51.8136	352	8.67	27.61
cssz–108z	Central and South America	285.7505	-51.8753	352	8.67	20.07
cssz–109a	Central and South America	285.2635	-52.8439	353.1	8.33	12.24
cssz–109b	Central and South America	284.5326	-52.8974	353.1	8.33	5
cssz–109x	Central and South America	287.4508	-52.6834	353.1	8.33	33.97
cssz–109y	Central and South America	286.7226	-52.7369	353.1	8.33	26.73
cssz–109z	Central and South America	285.9935	-52.7904	353.1	8.33	19.49
cssz–110a	Central and South America	285.5705	-53.4139	334.2	8	11.96
cssz–110b	Central and South America	284.8972	-53.6076	334.2	8	5
cssz–110x	Central and South America	287.5724	-52.8328	334.2	8	32.83
cssz–110y	Central and South America	286.9081	-53.0265	334.2	8	25.88
cssz–110z	Central and South America	286.2408	-53.2202	334.2	8	18.92
cssz–111a	Central and South America	286.1627	-53.8749	313.8	8	11.96
cssz–111b	Central and South America	285.6382	-54.1958	313.8	8	5
cssz–111x	Central and South America	287.7124	-52.9122	313.8	8	32.83
cssz–111y	Central and South America	287.1997	-53.2331	313.8	8	25.88
cssz–111z	Central and South America	286.6832	-53.5540	313.8	8	18.92
cssz–112a	Central and South America	287.3287	-54.5394	316.4	8	11.96
cssz–112b	Central and South America	286.7715	-54.8462	316.4	8	5
cssz–112x	Central and South America	288.9756	-53.6190	316.4	8	32.83
cssz–112y	Central and South America	288.4307	-53.9258	316.4	8	25.88
cssz–112z	Central and South America	287.8817	-54.2326	316.4	8	18.92
cssz–113a	Central and South America	288.3409	-55.0480	307.6	8	11.96
cssz–113b	Central and South America	287.8647	-55.4002	307.6	8	5
cssz–113x	Central and South America	289.7450	-53.9914	307.6	8	32.83
cssz–113y	Central and South America	289.2810	-54.3436	307.6	8	25.88
cssz–113z	Central and South America	288.8130	-54.6958	307.6	8	18.92
cssz–114a	Central and South America	289.5342	-55.5026	301.5	8	11.96
cssz–114b	Central and South America	289.1221	-55.8819	301.5	8	5
cssz–114x	Central and South America	290.7472	-54.3647	301.5	8	32.83
cssz–114y	Central and South America	290.3467	-54.7440	301.5	8	25.88
cssz–114z	Central and South America	289.9424	-55.1233	301.5	8	18.92
cssz–115a	Central and South America	290.7682	-55.8485	292.7	8	11.96
cssz–115b	Central and South America	290.4608	-56.2588	292.7	8	5
cssz–115x	Central and South America	291.6714	-54.6176	292.7	8	32.83
cssz–115y	Central and South America	291.3734	-55.0279	292.7	8	25.88
cssz–115z	Central and South America	291.0724	-55.4382	292.7	8	18.92

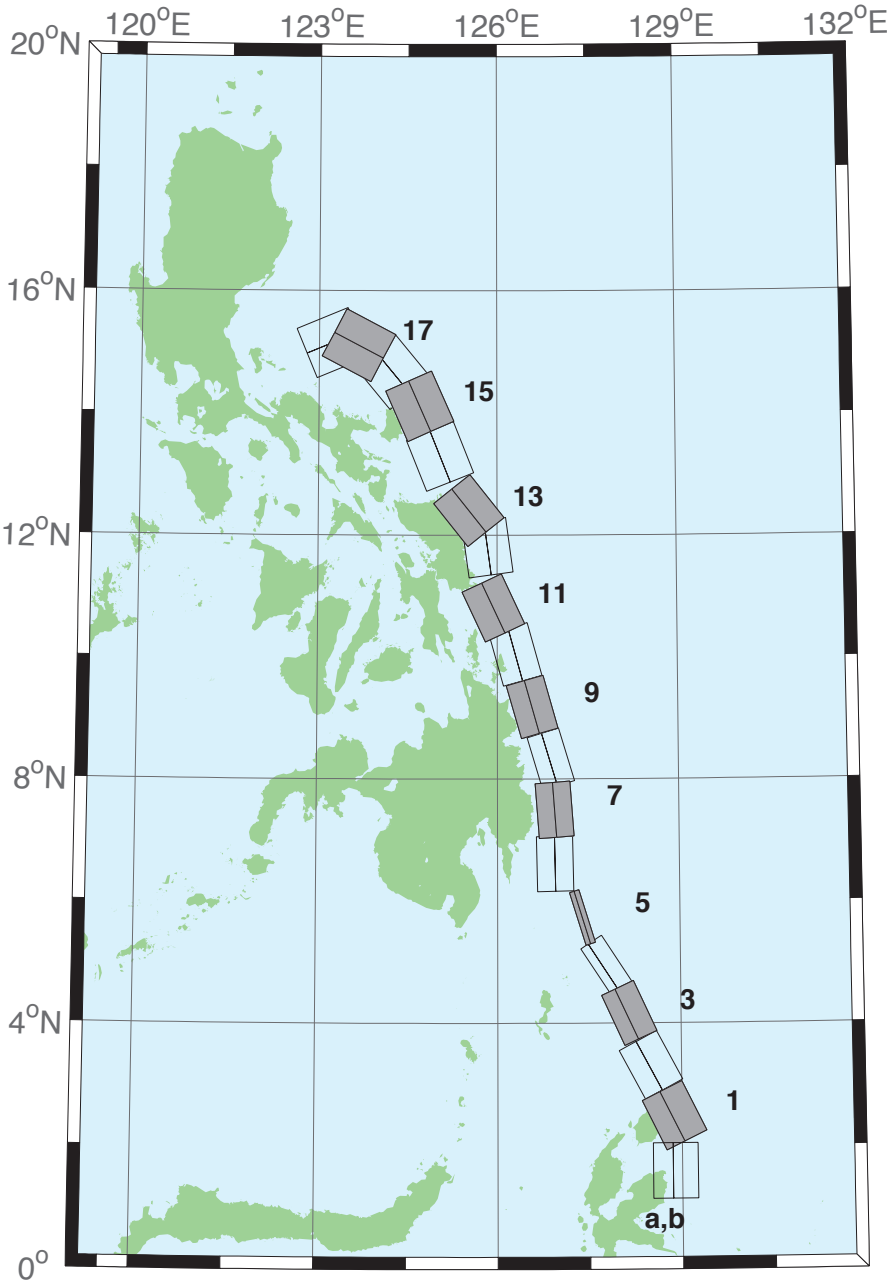

Figure B.3: Eastern Philippines Subduction Zone unit sources.

Table B.3: Earthquake parameters for Eastern Philippines Subduction Zone unit sources.

Segment	Description	Longitude(°E)	Latitude(°N)	Strike(°)	Dip(°)	Depth (km)
epsz–1a	Eastern Philippines	128.5521	2.3289	153.6	44.2	27.62
epsz–1b	Eastern Philippines	128.8408	2.4720	153.6	26.9	5
epsz–2a	Eastern Philippines	128.1943	3.1508	151.9	45.9	32.44
epsz–2b	Eastern Philippines	128.4706	3.2979	151.9	32.8	5.35
epsz–3a	Eastern Philippines	127.8899	4.0428	155.2	57.3	40.22
epsz–3b	Eastern Philippines	128.1108	4.1445	155.2	42.7	6.31
epsz–4a	Eastern Philippines	127.6120	4.8371	146.8	71.4	48.25
epsz–4b	Eastern Philippines	127.7324	4.9155	146.8	54.8	7.39
epsz–5a	Eastern Philippines	127.3173	5.7040	162.9	79.9	57.4
epsz–5b	Eastern Philippines	127.3930	5.7272	162.9	79.4	8.25
epsz–6a	Eastern Philippines	126.6488	6.6027	178.9	48.6	45.09
epsz–6b	Eastern Philippines	126.9478	6.6085	178.9	48.6	7.58
epsz–7a	Eastern Philippines	126.6578	7.4711	175.8	50.7	45.52
epsz–7b	Eastern Philippines	126.9439	7.4921	175.8	50.7	6.83
epsz–8a	Eastern Philippines	126.6227	8.2456	163.3	56.7	45.6
epsz–8b	Eastern Philippines	126.8614	8.3164	163.3	48.9	7.92
epsz–9a	Eastern Philippines	126.2751	9.0961	164.1	47	43.59
epsz–9b	Eastern Philippines	126.5735	9.1801	164.1	44.9	8.3
epsz–10a	Eastern Philippines	125.9798	9.9559	164.5	43.1	42.25
epsz–10b	Eastern Philippines	126.3007	10.0438	164.5	43.1	8.09
epsz–11a	Eastern Philippines	125.6079	10.6557	155	37.8	38.29
epsz–11b	Eastern Philippines	125.9353	10.8059	155	37.8	7.64
epsz–12a	Eastern Philippines	125.4697	11.7452	172.1	36	37.01
epsz–12b	Eastern Philippines	125.8374	11.7949	172.1	36	7.62
epsz–13a	Eastern Philippines	125.2238	12.1670	141.5	32.4	33.87
epsz–13b	Eastern Philippines	125.5278	12.4029	141.5	32.4	7.08
epsz–14a	Eastern Philippines	124.6476	13.1365	158.2	23	25.92
epsz–14b	Eastern Philippines	125.0421	13.2898	158.2	23	6.38
epsz–15a	Eastern Philippines	124.3107	13.9453	156.1	24.1	26.51
epsz–15b	Eastern Philippines	124.6973	14.1113	156.1	24.1	6.09
epsz–16a	Eastern Philippines	123.8998	14.4025	140.3	19.5	21.69
epsz–16b	Eastern Philippines	124.2366	14.6728	140.3	19.5	5
epsz–17a	Eastern Philippines	123.4604	14.7222	117.6	15.3	18.19
epsz–17b	Eastern Philippines	123.6682	15.1062	117.6	15.3	5
epsz–18a	Eastern Philippines	123.3946	14.7462	67.4	15	17.94
epsz–18b	Eastern Philippines	123.2219	15.1467	67.4	15	5
epsz–19a	Eastern Philippines	121.3638	15.7400	189.6	15	17.94
epsz–19b	Eastern Philippines	121.8082	15.6674	189.6	15	5
epsz–20a	Eastern Philippines	121.6833	16.7930	203.3	15	17.94
epsz–20b	Eastern Philippines	122.0994	16.6216	203.3	15	5
epsz–21a	Eastern Philippines	121.8279	17.3742	184.2	15	17.94
epsz–21b	Eastern Philippines	122.2814	17.3425	184.2	15	5

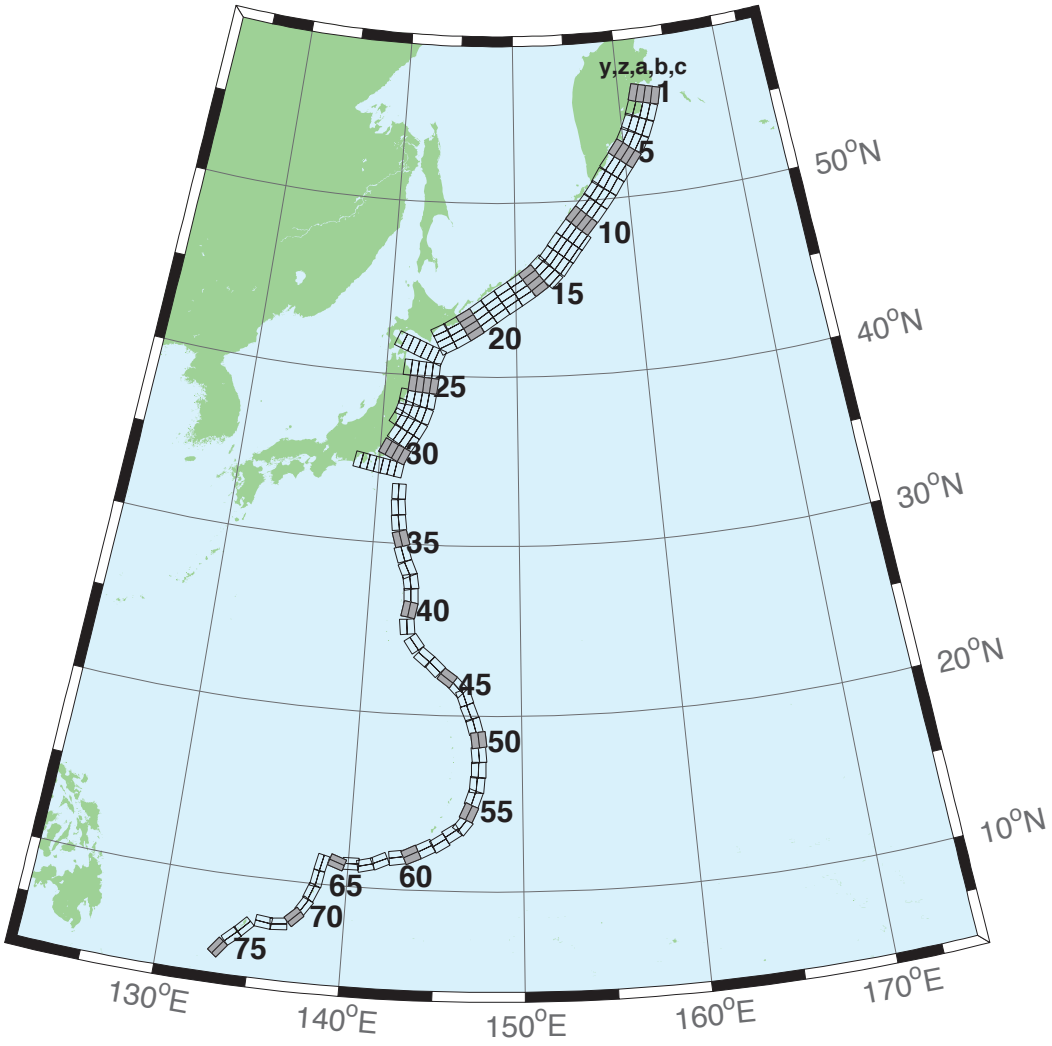

Figure B.4: Kamchatka-Kuril-Japan-Izu-Mariana-Yap Subduction Zone unit sources.

Table B.4: Earthquake parameters for Kamchatka-Kuril-Japan-Izu-Mariana-Yap Subduction Zone unit sources.

Segment	Description	Longitude(°E)	Latitude(°N)	Strike(°)	Dip(°)	Depth (km)
kisz–1a	Kamchatka-Kuril-Japan-Izu-Mariana-Yap	162.4318	55.5017	195	29	26.13
kisz–1b	Kamchatka-Kuril-Japan-Izu-Mariana-Yap	163.1000	55.4000	195	25	5
kisz–1y	Kamchatka-Kuril-Japan-Izu-Mariana-Yap	161.0884	55.7050	195	29	74.61
kisz–1z	Kamchatka-Kuril-Japan-Izu-Mariana-Yap	161.7610	55.6033	195	29	50.37
kisz–2a	Kamchatka-Kuril-Japan-Izu-Mariana-Yap	161.9883	54.6784	200	29	26.13
kisz–2b	Kamchatka-Kuril-Japan-Izu-Mariana-Yap	162.6247	54.5440	200	25	5
kisz–2y	Kamchatka-Kuril-Japan-Izu-Mariana-Yap	160.7072	54.9471	200	29	74.61
kisz–2z	Kamchatka-Kuril-Japan-Izu-Mariana-Yap	161.3488	54.8127	200	29	50.37
kisz–3a	Kamchatka-Kuril-Japan-Izu-Mariana-Yap	161.4385	53.8714	204	29	26.13
kisz–3b	Kamchatka-Kuril-Japan-Izu-Mariana-Yap	162.0449	53.7116	204	25	5
kisz–3y	Kamchatka-Kuril-Japan-Izu-Mariana-Yap	160.2164	54.1910	204	29	74.61
kisz–3z	Kamchatka-Kuril-Japan-Izu-Mariana-Yap	160.8286	54.0312	204	29	50.37
kisz–4a	Kamchatka-Kuril-Japan-Izu-Mariana-Yap	160.7926	53.1087	210	29	26.13
kisz–4b	Kamchatka-Kuril-Japan-Izu-Mariana-Yap	161.3568	52.9123	210	25	5
kisz–4y	Kamchatka-Kuril-Japan-Izu-Mariana-Yap	159.6539	53.5015	210	29	74.61
kisz–4z	Kamchatka-Kuril-Japan-Izu-Mariana-Yap	160.2246	53.3051	210	29	50.37
kisz–5a	Kamchatka-Kuril-Japan-Izu-Mariana-Yap	160.0211	52.4113	218	29	26.13
kisz–5b	Kamchatka-Kuril-Japan-Izu-Mariana-Yap	160.5258	52.1694	218	25	5
kisz–5y	Kamchatka-Kuril-Japan-Izu-Mariana-Yap	159.0005	52.8950	218	29	74.61
kisz–5z	Kamchatka-Kuril-Japan-Izu-Mariana-Yap	159.5122	52.6531	218	29	50.37
kisz–6a	Kamchatka-Kuril-Japan-Izu-Mariana-Yap	159.1272	51.7034	218	29	26.13
kisz–6b	Kamchatka-Kuril-Japan-Izu-Mariana-Yap	159.6241	51.4615	218	25	5
kisz–6y	Kamchatka-Kuril-Japan-Izu-Mariana-Yap	158.1228	52.1871	218	29	74.61
kisz–6z	Kamchatka-Kuril-Japan-Izu-Mariana-Yap	158.6263	51.9452	218	29	50.37
kisz–7a	Kamchatka-Kuril-Japan-Izu-Mariana-Yap	158.2625	50.9549	214	29	26.13
kisz–7b	Kamchatka-Kuril-Japan-Izu-Mariana-Yap	158.7771	50.7352	214	25	5
kisz–7y	Kamchatka-Kuril-Japan-Izu-Mariana-Yap	157.2236	51.3942	214	29	74.61
kisz–7z	Kamchatka-Kuril-Japan-Izu-Mariana-Yap	157.7443	51.1745	214	29	50.37
kisz–8a	Kamchatka-Kuril-Japan-Izu-Mariana-Yap	157.4712	50.2459	218	31	27.7
kisz–8b	Kamchatka-Kuril-Japan-Izu-Mariana-Yap	157.9433	50.0089	218	27	5
kisz–8y	Kamchatka-Kuril-Japan-Izu-Mariana-Yap	156.5176	50.7199	218	31	79.2
kisz–8z	Kamchatka-Kuril-Japan-Izu-Mariana-Yap	156.9956	50.4829	218	31	53.45
kisz–9a	Kamchatka-Kuril-Japan-Izu-Mariana-Yap	156.6114	49.5583	220	31	27.7
kisz–9b	Kamchatka-Kuril-Japan-Izu-Mariana-Yap	157.0638	49.3109	220	27	5
kisz–9y	Kamchatka-Kuril-Japan-Izu-Mariana-Yap	155.6974	50.0533	220	31	79.2
kisz–9z	Kamchatka-Kuril-Japan-Izu-Mariana-Yap	156.1556	49.8058	220	31	53.45
kisz–10a	Kamchatka-Kuril-Japan-Izu-Mariana-Yap	155.7294	48.8804	221	31	27.7
kisz–10b	Kamchatka-Kuril-Japan-Izu-Mariana-Yap	156.1690	48.6278	221	27	5
kisz–10y	Kamchatka-Kuril-Japan-Izu-Mariana-Yap	154.8413	49.3856	221	31	79.2
kisz–10z	Kamchatka-Kuril-Japan-Izu-Mariana-Yap	155.2865	49.1330	221	31	53.45
kisz–11a	Kamchatka-Kuril-Japan-Izu-Mariana-Yap	154.8489	48.1821	219	31	27.7
kisz–11b	Kamchatka-Kuril-Japan-Izu-Mariana-Yap	155.2955	47.9398	219	27	5
kisz–11y	Kamchatka-Kuril-Japan-Izu-Mariana-Yap	153.9472	48.6667	219	31	79.2
kisz–11z	Kamchatka-Kuril-Japan-Izu-Mariana-Yap	154.3991	48.4244	219	31	53.45
kisz–11c	Kamchatka-Kuril-Japan-Izu-Mariana-Yap	156.0358	47.5374	39	57.89	4.602
kisz–12a	Kamchatka-Kuril-Japan-Izu-Mariana-Yap	153.9994	47.4729	217	31	27.7
kisz–12b	Kamchatka-Kuril-Japan-Izu-Mariana-Yap	154.4701	47.2320	217	27	5
kisz–12y	Kamchatka-Kuril-Japan-Izu-Mariana-Yap	153.0856	47.9363	217	31	79.2
kisz–12z	Kamchatka-Kuril-Japan-Izu-Mariana-Yap	153.5435	47.7046	217	31	53.45
kisz–12c	Kamchatka-Kuril-Japan-Izu-Mariana-Yap	155.2208	46.8473	37	57.89	4.602
kisz–13a	Kamchatka-Kuril-Japan-Izu-Mariana-Yap	153.2239	46.7564	218	31	27.7
kisz–13b	Kamchatka-Kuril-Japan-Izu-Mariana-Yap	153.6648	46.5194	218	27	5

Continued on next page

Table B.4 – continued

Segment	Description	Longitude(°E)	Latitude(°N)	Strike(°)	Dip(°)	Depth (km)
kisz–13y	Kamchatka-Kuril-Japan-Izu-Mariana-Yap	152.3343	47.2304	218	31	79.2
kisz–13z	Kamchatka-Kuril-Japan-Izu-Mariana-Yap	152.7801	46.9934	218	31	53.45
kisz–13c	Kamchatka-Kuril-Japan-Izu-Mariana-Yap	154.3957	46.1257	38	57.89	4.602
kisz–14a	Kamchatka-Kuril-Japan-Izu-Mariana-Yap	152.3657	46.1514	225	23	24.54
kisz–14b	Kamchatka-Kuril-Japan-Izu-Mariana-Yap	152.7855	45.8591	225	23	5
kisz–14y	Kamchatka-Kuril-Japan-Izu-Mariana-Yap	151.5172	46.7362	225	23	63.62
kisz–14z	Kamchatka-Kuril-Japan-Izu-Mariana-Yap	151.9426	46.4438	225	23	44.08
kisz–14c	Kamchatka-Kuril-Japan-Izu-Mariana-Yap	153.4468	45.3976	45	57.89	4.602
kisz–15a	Kamchatka-Kuril-Japan-Izu-Mariana-Yap	151.4663	45.5963	233	25	23.73
kisz–15b	Kamchatka-Kuril-Japan-Izu-Mariana-Yap	151.8144	45.2712	233	22	5
kisz–15y	Kamchatka-Kuril-Japan-Izu-Mariana-Yap	150.7619	46.2465	233	25	65.99
kisz–15z	Kamchatka-Kuril-Japan-Izu-Mariana-Yap	151.1151	45.9214	233	25	44.86
kisz–16a	Kamchatka-Kuril-Japan-Izu-Mariana-Yap	150.4572	45.0977	237	25	23.73
kisz–16b	Kamchatka-Kuril-Japan-Izu-Mariana-Yap	150.7694	44.7563	237	22	5
kisz–16y	Kamchatka-Kuril-Japan-Izu-Mariana-Yap	149.8253	45.7804	237	25	65.99
kisz–16z	Kamchatka-Kuril-Japan-Izu-Mariana-Yap	150.1422	45.4390	237	25	44.86
kisz–17a	Kamchatka-Kuril-Japan-Izu-Mariana-Yap	149.3989	44.6084	237	25	23.73
kisz–17b	Kamchatka-Kuril-Japan-Izu-Mariana-Yap	149.7085	44.2670	237	22	5
kisz–17y	Kamchatka-Kuril-Japan-Izu-Mariana-Yap	148.7723	45.2912	237	25	65.99
kisz–17z	Kamchatka-Kuril-Japan-Izu-Mariana-Yap	149.0865	44.9498	237	25	44.86
kisz–18a	Kamchatka-Kuril-Japan-Izu-Mariana-Yap	148.3454	44.0982	235	25	23.73
kisz–18b	Kamchatka-Kuril-Japan-Izu-Mariana-Yap	148.6687	43.7647	235	22	5
kisz–18y	Kamchatka-Kuril-Japan-Izu-Mariana-Yap	147.6915	44.7651	235	25	65.99
kisz–18z	Kamchatka-Kuril-Japan-Izu-Mariana-Yap	148.0194	44.4316	235	25	44.86
kisz–19a	Kamchatka-Kuril-Japan-Izu-Mariana-Yap	147.3262	43.5619	233	25	23.73
kisz–19b	Kamchatka-Kuril-Japan-Izu-Mariana-Yap	147.6625	43.2368	233	22	5
kisz–19y	Kamchatka-Kuril-Japan-Izu-Mariana-Yap	146.6463	44.2121	233	25	65.99
kisz–19z	Kamchatka-Kuril-Japan-Izu-Mariana-Yap	146.9872	43.8870	233	25	44.86
kisz–20a	Kamchatka-Kuril-Japan-Izu-Mariana-Yap	146.3513	43.0633	237	25	23.73
kisz–20b	Kamchatka-Kuril-Japan-Izu-Mariana-Yap	146.6531	42.7219	237	22	5
kisz–20y	Kamchatka-Kuril-Japan-Izu-Mariana-Yap	145.7410	43.7461	237	25	65.99
kisz–20z	Kamchatka-Kuril-Japan-Izu-Mariana-Yap	146.0470	43.4047	237	25	44.86
kisz–21a	Kamchatka-Kuril-Japan-Izu-Mariana-Yap	145.3331	42.5948	239	25	23.73
kisz–21b	Kamchatka-Kuril-Japan-Izu-Mariana-Yap	145.6163	42.2459	239	22	5
kisz–21y	Kamchatka-Kuril-Japan-Izu-Mariana-Yap	144.7603	43.2927	239	25	65.99
kisz–21z	Kamchatka-Kuril-Japan-Izu-Mariana-Yap	145.0475	42.9438	239	25	44.86
kisz–22a	Kamchatka-Kuril-Japan-Izu-Mariana-Yap	144.3041	42.1631	242	25	23.73
kisz–22b	Kamchatka-Kuril-Japan-Izu-Mariana-Yap	144.5605	41.8037	242	22	5
kisz–22y	Kamchatka-Kuril-Japan-Izu-Mariana-Yap	143.7854	42.8819	242	25	65.99
kisz–22z	Kamchatka-Kuril-Japan-Izu-Mariana-Yap	144.0455	42.5225	242	25	44.86
kisz–23a	Kamchatka-Kuril-Japan-Izu-Mariana-Yap	143.2863	41.3335	202	21	21.28
kisz–23b	Kamchatka-Kuril-Japan-Izu-Mariana-Yap	143.8028	41.1764	202	19	5
kisz–23v	Kamchatka-Kuril-Japan-Izu-Mariana-Yap	140.6816	42.1189	202	21	110.9
kisz–23w	Kamchatka-Kuril-Japan-Izu-Mariana-Yap	141.2050	41.9618	202	21	92.95
kisz–23x	Kamchatka-Kuril-Japan-Izu-Mariana-Yap	141.7273	41.8047	202	21	75.04
kisz–23y	Kamchatka-Kuril-Japan-Izu-Mariana-Yap	142.2482	41.6476	202	21	57.12
kisz–23z	Kamchatka-Kuril-Japan-Izu-Mariana-Yap	142.7679	41.4905	202	21	39.2
kisz–24a	Kamchatka-Kuril-Japan-Izu-Mariana-Yap	142.9795	40.3490	185	21	21.28
kisz–24b	Kamchatka-Kuril-Japan-Izu-Mariana-Yap	143.5273	40.3125	185	19	5
kisz–24x	Kamchatka-Kuril-Japan-Izu-Mariana-Yap	141.3339	40.4587	185	21	75.04
kisz–24y	Kamchatka-Kuril-Japan-Izu-Mariana-Yap	141.8827	40.4221	185	21	57.12
kisz–24z	Kamchatka-Kuril-Japan-Izu-Mariana-Yap	142.4312	40.3856	185	21	39.2
kisz–25a	Kamchatka-Kuril-Japan-Izu-Mariana-Yap	142.8839	39.4541	185	21	21.28
kisz–25b	Kamchatka-Kuril-Japan-Izu-Mariana-Yap	143.4246	39.4176	185	19	5
kisz–25y	Kamchatka-Kuril-Japan-Izu-Mariana-Yap	141.8012	39.5272	185	21	57.12

Continued on next page

Table B.4 – continued

Segment	Description	Longitude(°E)	Latitude(°N)	Strike(°)	Dip(°)	Depth (km)
kisz–25z	Kamchatka-Kuril-Japan-Izu-Mariana-Yap	142.3426	39.4907	185	21	39.2
kisz–26a	Kamchatka-Kuril-Japan-Izu-Mariana-Yap	142.7622	38.5837	188	21	21.28
kisz–26b	Kamchatka-Kuril-Japan-Izu-Mariana-Yap	143.2930	38.5254	188	19	5
kisz–26x	Kamchatka-Kuril-Japan-Izu-Mariana-Yap	141.1667	38.7588	188	21	75.04
kisz–26y	Kamchatka-Kuril-Japan-Izu-Mariana-Yap	141.6990	38.7004	188	21	57.12
kisz–26z	Kamchatka-Kuril-Japan-Izu-Mariana-Yap	142.2308	38.6421	188	21	39.2
kisz–27a	Kamchatka-Kuril-Japan-Izu-Mariana-Yap	142.5320	37.7830	198	21	21.28
kisz–27b	Kamchatka-Kuril-Japan-Izu-Mariana-Yap	143.0357	37.6534	198	19	5
kisz–27x	Kamchatka-Kuril-Japan-Izu-Mariana-Yap	141.0142	38.1717	198	21	75.04
kisz–27y	Kamchatka-Kuril-Japan-Izu-Mariana-Yap	141.5210	38.0421	198	21	57.12
kisz–27z	Kamchatka-Kuril-Japan-Izu-Mariana-Yap	142.0269	37.9126	198	21	39.2
kisz–28a	Kamchatka-Kuril-Japan-Izu-Mariana-Yap	142.1315	37.0265	208	21	21.28
kisz–28b	Kamchatka-Kuril-Japan-Izu-Mariana-Yap	142.5941	36.8297	208	19	5
kisz–28x	Kamchatka-Kuril-Japan-Izu-Mariana-Yap	140.7348	37.6171	208	21	75.04
kisz–28y	Kamchatka-Kuril-Japan-Izu-Mariana-Yap	141.2016	37.4202	208	21	57.12
kisz–28z	Kamchatka-Kuril-Japan-Izu-Mariana-Yap	141.6671	37.2234	208	21	39.2
kisz–29a	Kamchatka-Kuril-Japan-Izu-Mariana-Yap	141.5970	36.2640	211	21	21.28
kisz–29b	Kamchatka-Kuril-Japan-Izu-Mariana-Yap	142.0416	36.0481	211	19	5
kisz–29y	Kamchatka-Kuril-Japan-Izu-Mariana-Yap	140.7029	36.6960	211	21	57.12
kisz–29z	Kamchatka-Kuril-Japan-Izu-Mariana-Yap	141.1506	36.4800	211	21	39.2
kisz–30a	Kamchatka-Kuril-Japan-Izu-Mariana-Yap	141.0553	35.4332	205	21	21.28
kisz–30b	Kamchatka-Kuril-Japan-Izu-Mariana-Yap	141.5207	35.2560	205	19	5
kisz–30y	Kamchatka-Kuril-Japan-Izu-Mariana-Yap	140.1204	35.7876	205	21	57.12
kisz–30z	Kamchatka-Kuril-Japan-Izu-Mariana-Yap	140.5883	35.6104	205	21	39.2
kisz–31a	Kamchatka-Kuril-Japan-Izu-Mariana-Yap	140.6956	34.4789	190	22	22.1
kisz–31b	Kamchatka-Kuril-Japan-Izu-Mariana-Yap	141.1927	34.4066	190	20	5
kisz–31v	Kamchatka-Kuril-Japan-Izu-Mariana-Yap	138.2025	34.8405	190	22	115.8
kisz–31w	Kamchatka-Kuril-Japan-Izu-Mariana-Yap	138.7021	34.7682	190	22	97.02
kisz–31x	Kamchatka-Kuril-Japan-Izu-Mariana-Yap	139.2012	34.6958	190	22	78.29
kisz–31y	Kamchatka-Kuril-Japan-Izu-Mariana-Yap	139.6997	34.6235	190	22	59.56
kisz–31z	Kamchatka-Kuril-Japan-Izu-Mariana-Yap	140.1979	34.5512	190	22	40.83
kisz–32a	Kamchatka-Kuril-Japan-Izu-Mariana-Yap	141.0551	33.0921	180	32	23.48
kisz–32b	Kamchatka-Kuril-Japan-Izu-Mariana-Yap	141.5098	33.0921	180	21.69	5
kisz–33a	Kamchatka-Kuril-Japan-Izu-Mariana-Yap	141.0924	32.1047	173.8	27.65	20.67
kisz–33b	Kamchatka-Kuril-Japan-Izu-Mariana-Yap	141.5596	32.1473	173.8	18.27	5
kisz–34a	Kamchatka-Kuril-Japan-Izu-Mariana-Yap	141.1869	31.1851	172.1	25	18.26
kisz–34b	Kamchatka-Kuril-Japan-Izu-Mariana-Yap	141.6585	31.2408	172.1	15.38	5
kisz–35a	Kamchatka-Kuril-Japan-Izu-Mariana-Yap	141.4154	30.1707	163	25	17.12
kisz–35b	Kamchatka-Kuril-Japan-Izu-Mariana-Yap	141.8662	30.2899	163	14.03	5
kisz–36a	Kamchatka-Kuril-Japan-Izu-Mariana-Yap	141.6261	29.2740	161.7	25.73	18.71
kisz–36b	Kamchatka-Kuril-Japan-Izu-Mariana-Yap	142.0670	29.4012	161.7	15.91	5
kisz–37a	Kamchatka-Kuril-Japan-Izu-Mariana-Yap	142.0120	28.3322	154.7	20	14.54
kisz–37b	Kamchatka-Kuril-Japan-Izu-Mariana-Yap	142.4463	28.5124	154.7	11	5
kisz–38a	Kamchatka-Kuril-Japan-Izu-Mariana-Yap	142.2254	27.6946	170.3	20	14.54
kisz–38b	Kamchatka-Kuril-Japan-Izu-Mariana-Yap	142.6955	27.7659	170.3	11	5
kisz–39a	Kamchatka-Kuril-Japan-Izu-Mariana-Yap	142.3085	26.9127	177.2	24.23	17.42
kisz–39b	Kamchatka-Kuril-Japan-Izu-Mariana-Yap	142.7674	26.9325	177.2	14.38	5
kisz–40a	Kamchatka-Kuril-Japan-Izu-Mariana-Yap	142.2673	26.1923	189.4	26.49	22.26
kisz–40b	Kamchatka-Kuril-Japan-Izu-Mariana-Yap	142.7090	26.1264	189.4	20.2	5
kisz–41a	Kamchatka-Kuril-Japan-Izu-Mariana-Yap	142.1595	25.0729	173.7	22.07	19.08
kisz–41b	Kamchatka-Kuril-Japan-Izu-Mariana-Yap	142.6165	25.1184	173.7	16.36	5
kisz–42a	Kamchatka-Kuril-Japan-Izu-Mariana-Yap	142.7641	23.8947	143.5	21.54	18.4
kisz–42b	Kamchatka-Kuril-Japan-Izu-Mariana-Yap	143.1321	24.1432	143.5	15.54	5
kisz–43a	Kamchatka-Kuril-Japan-Izu-Mariana-Yap	143.5281	23.0423	129.2	23.02	18.77
kisz–43b	Kamchatka-Kuril-Japan-Izu-Mariana-Yap	143.8128	23.3626	129.2	15.99	5

Continued on next page

Table B.4 – continued

Segment	Description	Longitude(°E)	Latitude(°N)	Strike(°)	Dip(°)	Depth (km)
kisz–44a	Kamchatka-Kuril-Japan-Izu-Mariana-Yap	144.2230	22.5240	134.6	28.24	18.56
kisz–44b	Kamchatka-Kuril-Japan-Izu-Mariana-Yap	144.5246	22.8056	134.6	15.74	5
kisz–45a	Kamchatka-Kuril-Japan-Izu-Mariana-Yap	145.0895	21.8866	125.8	36.73	22.79
kisz–45b	Kamchatka-Kuril-Japan-Izu-Mariana-Yap	145.3171	22.1785	125.8	20.84	5
kisz–46a	Kamchatka-Kuril-Japan-Izu-Mariana-Yap	145.6972	21.3783	135.9	30.75	20.63
kisz–46b	Kamchatka-Kuril-Japan-Izu-Mariana-Yap	145.9954	21.6469	135.9	18.22	5
kisz–47a	Kamchatka-Kuril-Japan-Izu-Mariana-Yap	146.0406	20.9341	160.1	29.87	19.62
kisz–47b	Kamchatka-Kuril-Japan-Izu-Mariana-Yap	146.4330	21.0669	160.1	17	5
kisz–48a	Kamchatka-Kuril-Japan-Izu-Mariana-Yap	146.3836	20.0690	158	32.75	19.68
kisz–48b	Kamchatka-Kuril-Japan-Izu-Mariana-Yap	146.7567	20.2108	158	17.07	5
kisz–49a	Kamchatka-Kuril-Japan-Izu-Mariana-Yap	146.6689	19.3123	164.5	25.07	21.41
kisz–49b	Kamchatka-Kuril-Japan-Izu-Mariana-Yap	147.0846	19.4212	164.5	19.16	5
kisz–50a	Kamchatka-Kuril-Japan-Izu-Mariana-Yap	146.9297	18.5663	172.1	22	22.1
kisz–50b	Kamchatka-Kuril-Japan-Izu-Mariana-Yap	147.3650	18.6238	172.1	20	5
kisz–51a	Kamchatka-Kuril-Japan-Izu-Mariana-Yap	146.9495	17.7148	175.1	22.06	22.04
kisz–51b	Kamchatka-Kuril-Japan-Izu-Mariana-Yap	147.3850	17.7503	175.1	19.93	5
kisz–52a	Kamchatka-Kuril-Japan-Izu-Mariana-Yap	146.9447	16.8869	180	25.51	18.61
kisz–52b	Kamchatka-Kuril-Japan-Izu-Mariana-Yap	147.3683	16.8869	180	15.79	5
kisz–53a	Kamchatka-Kuril-Japan-Izu-Mariana-Yap	146.8626	16.0669	185.2	27.39	18.41
kisz–53b	Kamchatka-Kuril-Japan-Izu-Mariana-Yap	147.2758	16.0309	185.2	15.56	5
kisz–54a	Kamchatka-Kuril-Japan-Izu-Mariana-Yap	146.7068	15.3883	199.1	28.12	20.91
kisz–54b	Kamchatka-Kuril-Japan-Izu-Mariana-Yap	147.0949	15.2590	199.1	18.56	5
kisz–55a	Kamchatka-Kuril-Japan-Izu-Mariana-Yap	146.4717	14.6025	204.3	29.6	26.27
kisz–55b	Kamchatka-Kuril-Japan-Izu-Mariana-Yap	146.8391	14.4415	204.3	25.18	5
kisz–56a	Kamchatka-Kuril-Japan-Izu-Mariana-Yap	146.1678	13.9485	217.4	32.04	26.79
kisz–56b	Kamchatka-Kuril-Japan-Izu-Mariana-Yap	146.4789	13.7170	217.4	25.84	5
kisz–57a	Kamchatka-Kuril-Japan-Izu-Mariana-Yap	145.6515	13.5576	235.8	37	24.54
kisz–57b	Kamchatka-Kuril-Japan-Izu-Mariana-Yap	145.8586	13.2609	235.8	23	5
kisz–58a	Kamchatka-Kuril-Japan-Izu-Mariana-Yap	144.9648	12.9990	237.8	37.72	24.54
kisz–58b	Kamchatka-Kuril-Japan-Izu-Mariana-Yap	145.1589	12.6984	237.8	23	5
kisz–59a	Kamchatka-Kuril-Japan-Izu-Mariana-Yap	144.1799	12.6914	242.9	34.33	22.31
kisz–59b	Kamchatka-Kuril-Japan-Izu-Mariana-Yap	144.3531	12.3613	242.9	20.25	5
kisz–60a	Kamchatka-Kuril-Japan-Izu-Mariana-Yap	143.3687	12.3280	244.9	30.9	20.62
kisz–60b	Kamchatka-Kuril-Japan-Izu-Mariana-Yap	143.5355	11.9788	244.9	18.2	5
kisz–61a	Kamchatka-Kuril-Japan-Izu-Mariana-Yap	142.7051	12.1507	261.8	35.41	25.51
kisz–61b	Kamchatka-Kuril-Japan-Izu-Mariana-Yap	142.7582	11.7883	261.8	24.22	5
kisz–62a	Kamchatka-Kuril-Japan-Izu-Mariana-Yap	141.6301	11.8447	245.7	39.86	34.35
kisz–62b	Kamchatka-Kuril-Japan-Izu-Mariana-Yap	141.7750	11.5305	245.7	35.94	5
kisz–63a	Kamchatka-Kuril-Japan-Izu-Mariana-Yap	140.8923	11.5740	256.2	42	38.46
kisz–63b	Kamchatka-Kuril-Japan-Izu-Mariana-Yap	140.9735	11.2498	256.2	42	5
kisz–64a	Kamchatka-Kuril-Japan-Izu-Mariana-Yap	140.1387	11.6028	269.6	42.48	38.77
kisz–64b	Kamchatka-Kuril-Japan-Izu-Mariana-Yap	140.1410	11.2716	269.6	42.48	5
kisz–65a	Kamchatka-Kuril-Japan-Izu-Mariana-Yap	139.4595	11.5883	288.7	44.16	39.83
kisz–65b	Kamchatka-Kuril-Japan-Izu-Mariana-Yap	139.3541	11.2831	288.7	44.16	5
kisz–66a	Kamchatka-Kuril-Japan-Izu-Mariana-Yap	138.1823	11.2648	193.1	45	40.36
kisz–66b	Kamchatka-Kuril-Japan-Izu-Mariana-Yap	138.4977	11.1929	193.1	45	5
kisz–67a	Kamchatka-Kuril-Japan-Izu-Mariana-Yap	137.9923	10.3398	189.8	45	40.36
kisz–67b	Kamchatka-Kuril-Japan-Izu-Mariana-Yap	138.3104	10.2856	189.8	45	5
kisz–68a	Kamchatka-Kuril-Japan-Izu-Mariana-Yap	137.7607	9.6136	201.7	45	40.36
kisz–68b	Kamchatka-Kuril-Japan-Izu-Mariana-Yap	138.0599	9.4963	201.7	45	5
kisz–69a	Kamchatka-Kuril-Japan-Izu-Mariana-Yap	137.4537	8.8996	213.5	45	40.36
kisz–69b	Kamchatka-Kuril-Japan-Izu-Mariana-Yap	137.7215	8.7241	213.5	45	5
kisz–70a	Kamchatka-Kuril-Japan-Izu-Mariana-Yap	137.0191	8.2872	226.5	45	40.36
kisz–70b	Kamchatka-Kuril-Japan-Izu-Mariana-Yap	137.2400	8.0569	226.5	45	5
kisz–71a	Kamchatka-Kuril-Japan-Izu-Mariana-Yap	136.3863	7.9078	263.9	45	40.36

Continued on next page

Table B.4 – continued

Segment	Description	Longitude(°E)	Latitude(°N)	Strike(°)	Dip(°)	Depth (km)
kisz–71b	Kamchatka-Kuril-Japan-Izu-Mariana-Yap	136.4202	7.5920	263.9	45	5
kisz–72a	Kamchatka-Kuril-Japan-Izu-Mariana-Yap	135.6310	7.9130	276.9	45	40.36
kisz–72b	Kamchatka-Kuril-Japan-Izu-Mariana-Yap	135.5926	7.5977	276.9	45	5
kisz–73a	Kamchatka-Kuril-Japan-Izu-Mariana-Yap	134.3296	7.4541	224	45	40.36
kisz–73b	Kamchatka-Kuril-Japan-Izu-Mariana-Yap	134.5600	7.2335	224	45	5
kisz–74a	Kamchatka-Kuril-Japan-Izu-Mariana-Yap	133.7125	6.8621	228.1	45	40.36
kisz–74b	Kamchatka-Kuril-Japan-Izu-Mariana-Yap	133.9263	6.6258	228.1	45	5
kisz–75a	Kamchatka-Kuril-Japan-Izu-Mariana-Yap	133.0224	6.1221	217.7	45	40.36
kisz–75b	Kamchatka-Kuril-Japan-Izu-Mariana-Yap	133.2751	5.9280	217.7	45	5

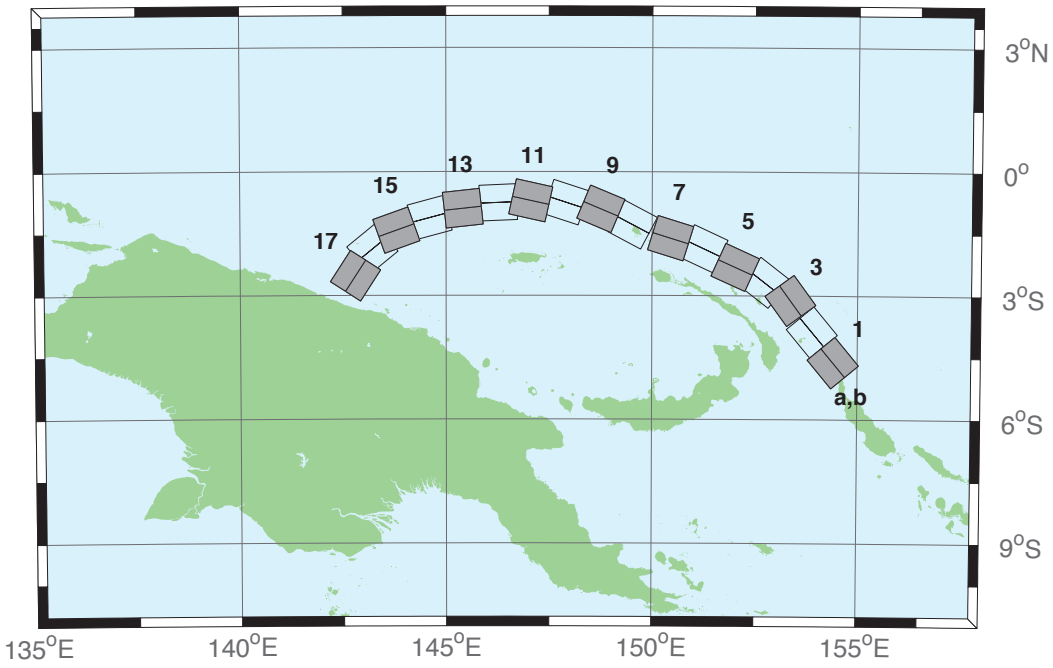

Figure B.5: Manus–Oceanic Convergent Boundary Subduction Zone unit sources.

Table B.5: Earthquake parameters for Manus–Oceanic Convergent Boundary Subduction Zone unit sources.

Segment	Description	Longitude(°E)	Latitude(°N)	Strike(°)	Dip(°)	Depth (km)
mosz–1a	Manus	154.0737	-4.8960	140.2	15	15.88
mosz–1b	Manus	154.4082	-4.6185	140.2	15	2.94
mosz–2a	Manus	153.5589	-4.1575	140.2	15	15.91
mosz–2b	Manus	153.8931	-3.8800	140.2	15	2.97
mosz–3a	Manus	153.0151	-3.3716	143.9	15	16.64
mosz–3b	Manus	153.3662	-3.1160	143.9	15	3.7
mosz–4a	Manus	152.4667	-3.0241	127.7	15	17.32
mosz–4b	Manus	152.7321	-2.6806	127.7	15	4.38
mosz–5a	Manus	151.8447	-2.7066	114.3	15	17.57
mosz–5b	Manus	152.0235	-2.3112	114.3	15	4.63
mosz–6a	Manus	151.0679	-2.2550	115	15	17.66
mosz–6b	Manus	151.2513	-1.8618	115	15	4.72
mosz–7a	Manus	150.3210	-2.0236	107.2	15	17.73
mosz–7b	Manus	150.4493	-1.6092	107.2	15	4.79
mosz–8a	Manus	149.3226	-1.6666	117.8	15	17.83
mosz–8b	Manus	149.5251	-1.2829	117.8	15	4.89
mosz–9a	Manus	148.5865	-1.3017	112.7	15	17.84
mosz–9b	Manus	148.7540	-0.9015	112.7	15	4.9
mosz–10a	Manus	147.7760	-1.1560	108	15	17.78
mosz–10b	Manus	147.9102	-0.7434	108	15	4.84
mosz–11a	Manus	146.9596	-1.1226	102.5	15	17.54
mosz–11b	Manus	147.0531	-0.6990	102.5	15	4.6
mosz–12a	Manus	146.2858	-1.1820	87.48	15	17.29
mosz–12b	Manus	146.2667	-0.7486	87.48	15	4.35
mosz–13a	Manus	145.4540	-1.3214	83.75	15	17.34
mosz–13b	Manus	145.4068	-0.8901	83.75	15	4.4
mosz–14a	Manus	144.7151	-1.5346	75.09	15	17.21
mosz–14b	Manus	144.6035	-1.1154	75.09	15	4.27
mosz–15a	Manus	143.9394	-1.8278	70.43	15	16.52
mosz–15b	Manus	143.7940	-1.4190	70.43	15	3.58
mosz–16a	Manus	143.4850	-2.2118	50.79	15	15.86
mosz–16b	Manus	143.2106	-1.8756	50.79	15	2.92
mosz–17a	Manus	143.1655	-2.7580	33	15	16.64
mosz–17b	Manus	142.8013	-2.5217	33	15	3.7

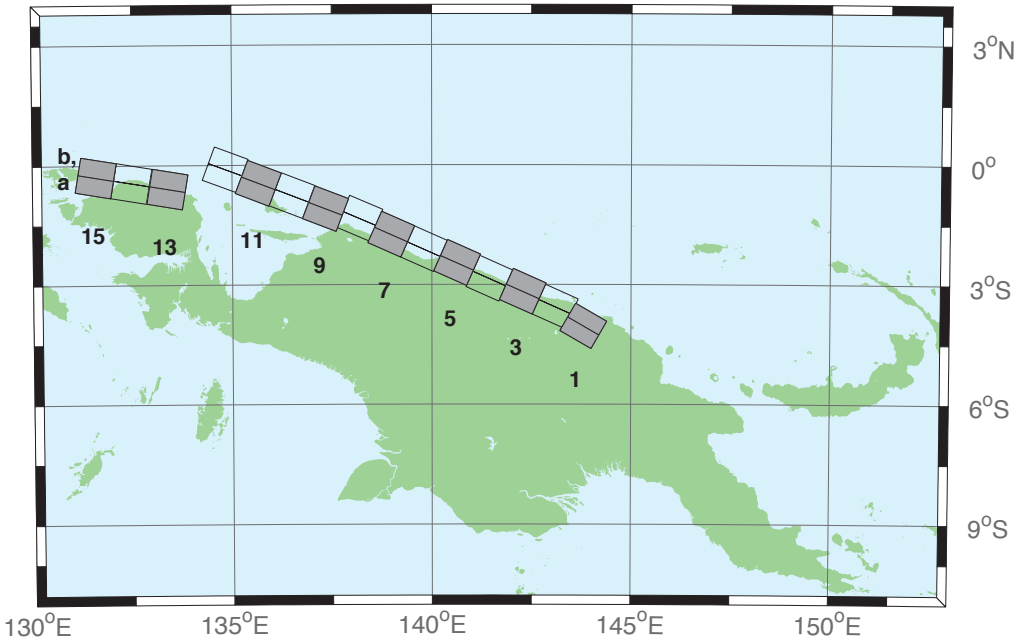

Figure B.6: New Guinea Subduction Zone unit sources.

Table B.6: Earthquake parameters for New Guinea Subduction Zone unit sources.

Segment	Description	Longitude(°E)	Latitude(°N)	Strike(°)	Dip(°)	Depth (km)
ngsz–1a	New Guinea	143.6063	-4.3804	120	29	25.64
ngsz–1b	New Guinea	143.8032	-4.0402	120	29	1.4
ngsz–2a	New Guinea	142.9310	-3.9263	114	27.63	20.1
ngsz–2b	New Guinea	143.0932	-3.5628	114	21.72	1.6
ngsz–3a	New Guinea	142.1076	-3.5632	114	20.06	18.73
ngsz–3b	New Guinea	142.2795	-3.1778	114	15.94	5
ngsz–4a	New Guinea	141.2681	-3.2376	114	21	17.76
ngsz–4b	New Guinea	141.4389	-2.8545	114	14.79	5
ngsz–5a	New Guinea	140.4592	-2.8429	114	21.26	16.14
ngsz–5b	New Guinea	140.6296	-2.4605	114	12.87	5
ngsz–6a	New Guinea	139.6288	-2.4960	114	22.72	15.4
ngsz–6b	New Guinea	139.7974	-2.1175	114	12	5
ngsz–7a	New Guinea	138.8074	-2.1312	114	21.39	15.4
ngsz–7b	New Guinea	138.9776	-1.7491	114	12	5
ngsz–8a	New Guinea	138.0185	-1.7353	113.1	18.79	15.14
ngsz–8b	New Guinea	138.1853	-1.3441	113.1	11.7	5
ngsz–9a	New Guinea	137.1805	-1.5037	111	15.24	13.23
ngsz–9b	New Guinea	137.3358	-1.0991	111	9.47	5
ngsz–10a	New Guinea	136.3418	-1.1774	111	13.51	11.09
ngsz–10b	New Guinea	136.4983	-0.7697	111	7	5
ngsz–11a	New Guinea	135.4984	-0.8641	111	11.38	12.49
ngsz–11b	New Guinea	135.6562	-0.4530	111	8.62	5
ngsz–12a	New Guinea	134.6759	-0.5216	110.5	10	13.68
ngsz–12b	New Guinea	134.8307	-0.1072	110.5	10	5
ngsz–13a	New Guinea	133.3065	-1.0298	99.5	10	13.68
ngsz–13b	New Guinea	133.3795	-0.5935	99.5	10	5
ngsz–14a	New Guinea	132.4048	-0.8816	99.5	10	13.68
ngsz–14b	New Guinea	132.4778	-0.4453	99.5	10	5
ngsz–15a	New Guinea	131.5141	-0.7353	99.5	10	13.68
ngsz–15b	New Guinea	131.5871	-0.2990	99.5	10	5

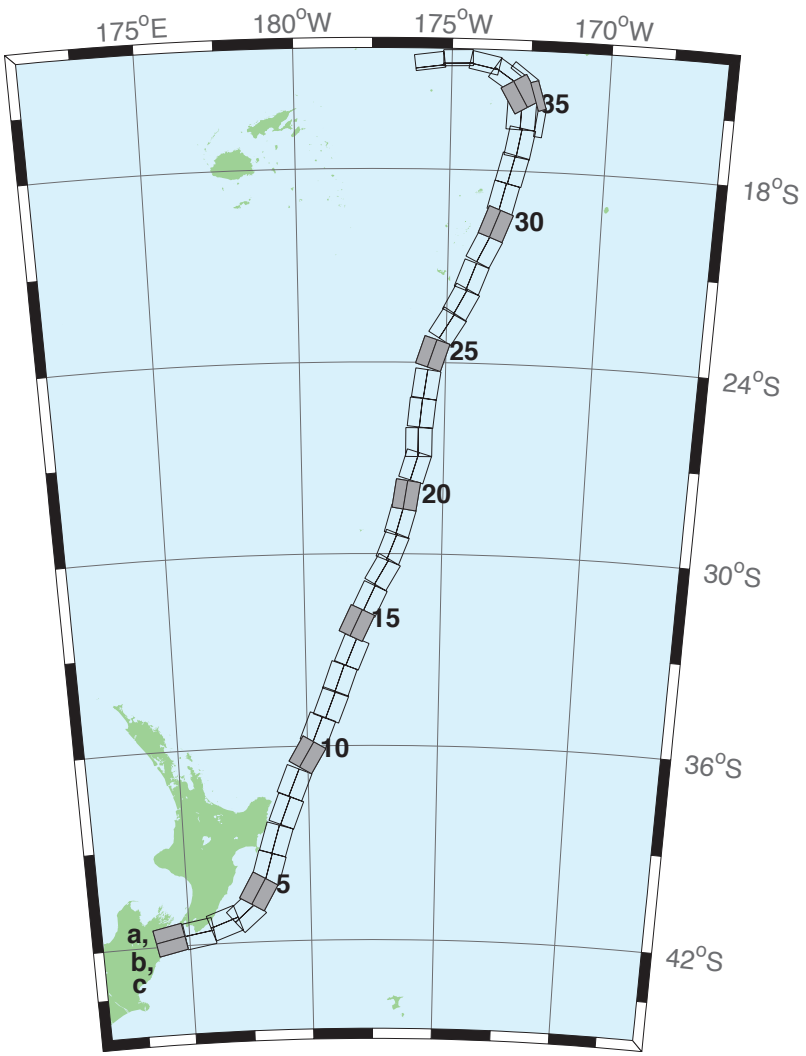

Figure B.7: New Zealand–Kermadec–Tonga Subduction Zone unit sources.

Table B.7: Earthquake parameters for New Zealand–Kermadec–Tonga Subduction Zone unit sources.

Segment	Description	Longitude(°E)	Latitude(°N)	Strike(°)	Dip(°)	Depth (km)
ntsz–1a	New Zealand–Tonga	174.0985	-41.3951	258.6	24	25.34
ntsz–1b	New Zealand–Tonga	174.2076	-41.7973	258.6	24	5
ntsz–2a	New Zealand–Tonga	175.3289	-41.2592	260.6	29.38	23.17
ntsz–2b	New Zealand–Tonga	175.4142	-41.6454	260.6	21.31	5
ntsz–3a	New Zealand–Tonga	176.2855	-40.9950	250.7	29.54	21.74
ntsz–3b	New Zealand–Tonga	176.4580	-41.3637	250.7	19.56	5
ntsz–4a	New Zealand–Tonga	177.0023	-40.7679	229.4	24.43	18.87
ntsz–4b	New Zealand–Tonga	177.3552	-41.0785	229.4	16.1	5
ntsz–5a	New Zealand–Tonga	177.4114	-40.2396	210	18.8	19.29
ntsz–5b	New Zealand–Tonga	177.8951	-40.4525	210	16.61	5
ntsz–6a	New Zealand–Tonga	177.8036	-39.6085	196.7	18.17	15.8
ntsz–6b	New Zealand–Tonga	178.3352	-39.7310	196.7	12.48	5
ntsz–7a	New Zealand–Tonga	178.1676	-38.7480	197	28.1	17.85
ntsz–7b	New Zealand–Tonga	178.6541	-38.8640	197	14.89	5
ntsz–8a	New Zealand–Tonga	178.6263	-37.8501	201.4	31.47	18.78
ntsz–8b	New Zealand–Tonga	179.0788	-37.9899	201.4	16	5
ntsz–9a	New Zealand–Tonga	178.9833	-36.9770	202.2	29.58	20.02
ntsz–9b	New Zealand–Tonga	179.4369	-37.1245	202.2	17.48	5
ntsz–10a	New Zealand–Tonga	179.5534	-36.0655	210.6	32.1	20.72
ntsz–10b	New Zealand–Tonga	179.9595	-36.2593	210.6	18.32	5
ntsz–11a	New Zealand–Tonga	179.9267	-35.3538	201.7	25	16.09
ntsz–11b	New Zealand–Tonga	180.3915	-35.5040	201.7	12.81	5
ntsz–12a	New Zealand–Tonga	180.4433	-34.5759	201.2	25	15.46
ntsz–12b	New Zealand–Tonga	180.9051	-34.7230	201.2	12.08	5
ntsz–13a	New Zealand–Tonga	180.7990	-33.7707	199.8	25.87	19.06
ntsz–13b	New Zealand–Tonga	181.2573	-33.9073	199.8	16.33	5
ntsz–14a	New Zealand–Tonga	181.2828	-32.9288	202.4	31.28	22.73
ntsz–14b	New Zealand–Tonga	181.7063	-33.0751	202.4	20.77	5
ntsz–15a	New Zealand–Tonga	181.4918	-32.0035	205.4	32.33	22.64
ntsz–15b	New Zealand–Tonga	181.8967	-32.1665	205.4	20.66	5
ntsz–16a	New Zealand–Tonga	181.9781	-31.2535	205.5	34.29	23.59
ntsz–16b	New Zealand–Tonga	182.3706	-31.4131	205.5	21.83	5
ntsz–17a	New Zealand–Tonga	182.4819	-30.3859	210.3	37.6	25.58
ntsz–17b	New Zealand–Tonga	182.8387	-30.5655	210.3	24.3	5
ntsz–18a	New Zealand–Tonga	182.8176	-29.6545	201.6	37.65	26.13
ntsz–18b	New Zealand–Tonga	183.1985	-29.7856	201.6	25	5
ntsz–19a	New Zealand–Tonga	183.0622	-28.8739	195.7	34.41	26.13
ntsz–19b	New Zealand–Tonga	183.4700	-28.9742	195.7	25	5
ntsz–20a	New Zealand–Tonga	183.2724	-28.0967	188.8	38	26.13
ntsz–20b	New Zealand–Tonga	183.6691	-28.1508	188.8	25	5
ntsz–21a	New Zealand–Tonga	183.5747	-27.1402	197.1	32.29	24.83
ntsz–21b	New Zealand–Tonga	183.9829	-27.2518	197.1	23.37	5
ntsz–22a	New Zealand–Tonga	183.6608	-26.4975	180	29.56	18.63
ntsz–22b	New Zealand–Tonga	184.0974	-26.4975	180	15.82	5
ntsz–23a	New Zealand–Tonga	183.7599	-25.5371	185.8	32.42	20.56
ntsz–23b	New Zealand–Tonga	184.1781	-25.5752	185.8	18.13	5
ntsz–24a	New Zealand–Tonga	183.9139	-24.6201	188.2	33.31	23.73
ntsz–24b	New Zealand–Tonga	184.3228	-24.6734	188.2	22	5
ntsz–25a	New Zealand–Tonga	184.1266	-23.5922	198.5	29.34	19.64
ntsz–25b	New Zealand–Tonga	184.5322	-23.7163	198.5	17.03	5
ntsz–26a	New Zealand–Tonga	184.6613	-22.6460	211.7	30.26	19.43
ntsz–26b	New Zealand–Tonga	185.0196	-22.8497	211.7	16.78	5
ntsz–27a	New Zealand–Tonga	185.0879	-21.9139	207.9	31.73	20.67

Continued on next page

Table B.7 – continued

Segment	Description	Longitude(°E)	Latitude(°N)	Strike(°)	Dip(°)	Depth (km)
ntsz–27b	New Zealand–Tonga	185.4522	-22.0928	207.9	18.27	5
ntsz–28a	New Zealand–Tonga	185.4037	-21.1758	200.5	32.44	21.76
ntsz–28b	New Zealand–Tonga	185.7849	-21.3084	200.5	19.58	5
ntsz–29a	New Zealand–Tonga	185.8087	-20.2629	206.4	32.47	20.4
ntsz–29b	New Zealand–Tonga	186.1710	-20.4312	206.4	17.94	5
ntsz–30a	New Zealand–Tonga	186.1499	-19.5087	200.9	32.98	22.46
ntsz–30b	New Zealand–Tonga	186.5236	-19.6432	200.9	20.44	5
ntsz–31a	New Zealand–Tonga	186.3538	-18.7332	193.9	34.41	21.19
ntsz–31b	New Zealand–Tonga	186.7339	-18.8221	193.9	18.89	5
ntsz–32a	New Zealand–Tonga	186.5949	-17.8587	194.1	30	19.12
ntsz–32b	New Zealand–Tonga	186.9914	-17.9536	194.1	16.4	5
ntsz–33a	New Zealand–Tonga	186.8172	-17.0581	190	33.15	23.34
ntsz–33b	New Zealand–Tonga	187.2047	-17.1237	190	21.52	5
ntsz–34a	New Zealand–Tonga	186.7814	-16.2598	182.1	15	13.41
ntsz–34b	New Zealand–Tonga	187.2330	-16.2759	182.1	9.68	5
ntsz–34c	New Zealand–Tonga	187.9697	-16.4956	7.62	57.06	6.571
ntsz–35a	New Zealand–Tonga	186.8000	-15.8563	149.8	15	12.17
ntsz–35b	New Zealand–Tonga	187.1896	-15.6384	149.8	8.24	5
ntsz–35c	New Zealand–Tonga	187.8776	-15.6325	342.4	57.06	6.571
ntsz–36a	New Zealand–Tonga	186.5406	-15.3862	123.9	40.44	36.72
ntsz–36b	New Zealand–Tonga	186.7381	-15.1025	123.9	39.38	5
ntsz–36c	New Zealand–Tonga	187.3791	-14.9234	307	57.06	6.571
ntsz–37a	New Zealand–Tonga	185.9883	-14.9861	102	68.94	30.99
ntsz–37b	New Zealand–Tonga	186.0229	-14.8282	102	31.32	5
ntsz–38a	New Zealand–Tonga	185.2067	-14.8259	88.4	80	26.13
ntsz–38b	New Zealand–Tonga	185.2044	-14.7479	88.4	25	5
ntsz–39a	New Zealand–Tonga	184.3412	-14.9409	82.55	80	26.13
ntsz–39b	New Zealand–Tonga	184.3307	-14.8636	82.55	25	5

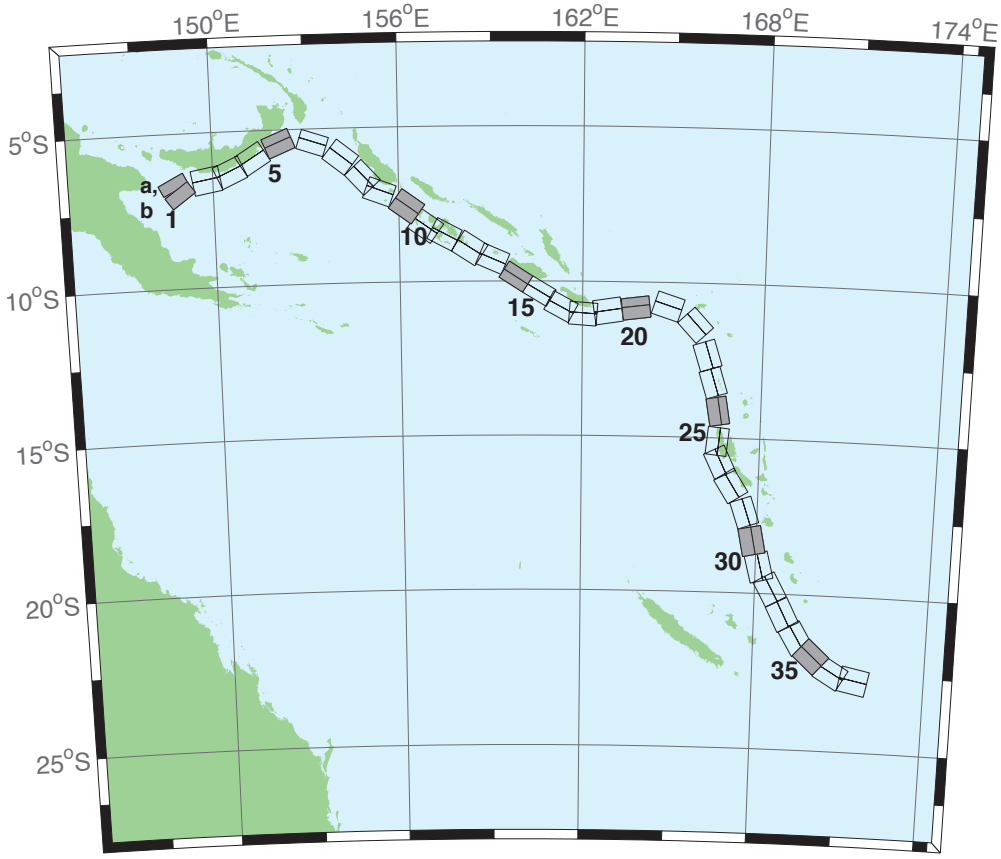

Figure B.8: New Britain–Solomons–Vanuatu Zone unit sources.

Table B.8: Earthquake parameters for New Britain–Solomons–Vanuatu Subduction Zone unit sources.

Segment	Description	Longitude(°E)	Latitude(°N)	Strike(°)	Dip(°)	Depth (km)
nvsz–1a	New Britain–Vanuatu	148.6217	-6.4616	243.2	32.34	15.69
nvsz–1b	New Britain–Vanuatu	148.7943	-6.8002	234.2	12.34	5
nvsz–2a	New Britain–Vanuatu	149.7218	-6.1459	260.1	35.1	16.36
nvsz–2b	New Britain–Vanuatu	149.7856	-6.5079	260.1	13.13	5
nvsz–3a	New Britain–Vanuatu	150.4075	-5.9659	245.7	42.35	18.59
nvsz–3b	New Britain–Vanuatu	150.5450	-6.2684	245.7	15.77	5
nvsz–4a	New Britain–Vanuatu	151.1095	-5.5820	238.2	42.41	23.63
nvsz–4b	New Britain–Vanuatu	151.2851	-5.8639	238.2	21.88	5
nvsz–5a	New Britain–Vanuatu	152.0205	-5.1305	247.7	49.22	32.39
nvsz–5b	New Britain–Vanuatu	152.1322	-5.4020	247.7	33.22	5
nvsz–6a	New Britain–Vanuatu	153.3450	-5.1558	288.6	53.53	33.59
nvsz–6b	New Britain–Vanuatu	153.2595	-5.4089	288.6	34.87	5
nvsz–7a	New Britain–Vanuatu	154.3814	-5.6308	308.3	39.72	19.18
nvsz–7b	New Britain–Vanuatu	154.1658	-5.9017	308.3	16.48	5
nvsz–8a	New Britain–Vanuatu	155.1097	-6.3511	317.2	45.33	22.92
nvsz–8b	New Britain–Vanuatu	154.8764	-6.5656	317.2	21	5
nvsz–9a	New Britain–Vanuatu	155.5027	-6.7430	290.5	48.75	22.92
nvsz–9b	New Britain–Vanuatu	155.3981	-7.0204	290.5	21	5
nvsz–10a	New Britain–Vanuatu	156.4742	-7.2515	305.9	36.88	27.62
nvsz–10b	New Britain–Vanuatu	156.2619	-7.5427	305.9	26.9	5
nvsz–11a	New Britain–Vanuatu	157.0830	-7.8830	305.4	32.97	29.72
nvsz–11b	New Britain–Vanuatu	156.8627	-8.1903	305.4	29.63	5
nvsz–12a	New Britain–Vanuatu	157.6537	-8.1483	297.9	37.53	28.57
nvsz–12b	New Britain–Vanuatu	157.4850	-8.4630	297.9	28.13	5
nvsz–13a	New Britain–Vanuatu	158.5089	-8.5953	302.7	33.62	23.02
nvsz–13b	New Britain–Vanuatu	158.3042	-8.9099	302.7	21.12	5
nvsz–14a	New Britain–Vanuatu	159.1872	-8.9516	293.3	38.44	34.06
nvsz–14b	New Britain–Vanuatu	159.0461	-9.2747	293.3	35.54	5
nvsz–15a	New Britain–Vanuatu	159.9736	-9.5993	302.8	46.69	41.38
nvsz–15b	New Britain–Vanuatu	159.8044	-9.8584	302.8	46.69	5
nvsz–16a	New Britain–Vanuatu	160.7343	-10.0574	301	46.05	41
nvsz–16b	New Britain–Vanuatu	160.5712	-10.3246	301	46.05	5
nvsz–17a	New Britain–Vanuatu	161.4562	-10.5241	298.4	40.12	37.22
nvsz–17b	New Britain–Vanuatu	161.2900	-10.8263	298.4	40.12	5
nvsz–18a	New Britain–Vanuatu	162.0467	-10.6823	274.1	40.33	29.03
nvsz–18b	New Britain–Vanuatu	162.0219	-11.0238	274.1	28.72	5
nvsz–19a	New Britain–Vanuatu	162.7818	-10.5645	261.3	34.25	24.14
nvsz–19b	New Britain–Vanuatu	162.8392	-10.9315	261.3	22.51	5
nvsz–20a	New Britain–Vanuatu	163.7222	-10.5014	262.9	50.35	26.3
nvsz–20b	New Britain–Vanuatu	163.7581	-10.7858	262.9	25.22	5
nvsz–21a	New Britain–Vanuatu	164.9445	-10.4183	287.9	40.31	23.3
nvsz–21b	New Britain–Vanuatu	164.8374	-10.7442	287.9	21.47	5
nvsz–22a	New Britain–Vanuatu	166.0261	-11.1069	317.1	42.39	20.78
nvsz–22b	New Britain–Vanuatu	165.7783	-11.3328	317.1	18.4	5
nvsz–23a	New Britain–Vanuatu	166.5179	-12.2260	342.4	47.95	22.43
nvsz–23b	New Britain–Vanuatu	166.2244	-12.3171	342.4	20.4	5
nvsz–24a	New Britain–Vanuatu	166.7236	-13.1065	342.6	47.13	28.52
nvsz–24b	New Britain–Vanuatu	166.4241	-13.1979	342.6	28.06	5
nvsz–25a	New Britain–Vanuatu	166.8914	-14.0785	350.3	54.1	31.16
nvsz–25b	New Britain–Vanuatu	166.6237	-14.1230	350.3	31.55	5
nvsz–26a	New Britain–Vanuatu	166.9200	-15.1450	365.6	50.46	29.05
nvsz–26b	New Britain–Vanuatu	166.6252	-15.1170	365.6	28.75	5
nvsz–27a	New Britain–Vanuatu	167.0053	-15.6308	334.2	44.74	25.46

Continued on next page

Table B.8 – continued

Segment	Description	Longitude(°E)	Latitude(°N)	Strike(°)	Dip(°)	Depth (km)
nvsz–27b	New Britain–Vanuatu	166.7068	-15.7695	334.2	24.15	5
nvsz–28a	New Britain–Vanuatu	167.4074	-16.3455	327.5	41.53	22.44
nvsz–28b	New Britain–Vanuatu	167.1117	-16.5264	327.5	20.42	5
nvsz–29a	New Britain–Vanuatu	167.9145	-17.2807	341.2	49.1	24.12
nvsz–29b	New Britain–Vanuatu	167.6229	-17.3757	341.2	22.48	5
nvsz–30a	New Britain–Vanuatu	168.2220	-18.2353	348.6	44.19	23.99
nvsz–30b	New Britain–Vanuatu	167.8895	-18.2991	348.6	22.32	5
nvsz–31a	New Britain–Vanuatu	168.5022	-19.0510	345.6	42.2	22.26
nvsz–31b	New Britain–Vanuatu	168.1611	-19.1338	345.6	20.2	5
nvsz–32a	New Britain–Vanuatu	168.8775	-19.6724	331.1	42.03	21.68
nvsz–32b	New Britain–Vanuatu	168.5671	-19.8338	331.1	19.49	5
nvsz–33a	New Britain–Vanuatu	169.3422	-20.4892	332.9	40.25	22.4
nvsz–33b	New Britain–Vanuatu	169.0161	-20.6453	332.9	20.37	5
nvsz–34a	New Britain–Vanuatu	169.8304	-21.2121	329.1	39	22.73
nvsz–34b	New Britain–Vanuatu	169.5086	-21.3911	329.1	20.77	5
nvsz–35a	New Britain–Vanuatu	170.3119	-21.6945	311.9	39	22.13
nvsz–35b	New Britain–Vanuatu	170.0606	-21.9543	311.9	20.03	5
nvsz–36a	New Britain–Vanuatu	170.9487	-22.1585	300.4	39.42	23.5
nvsz–36b	New Britain–Vanuatu	170.7585	-22.4577	300.4	21.71	5
nvsz–37a	New Britain–Vanuatu	171.6335	-22.3087	281.3	30	22.1
nvsz–37b	New Britain–Vanuatu	171.5512	-22.6902	281.3	20	5

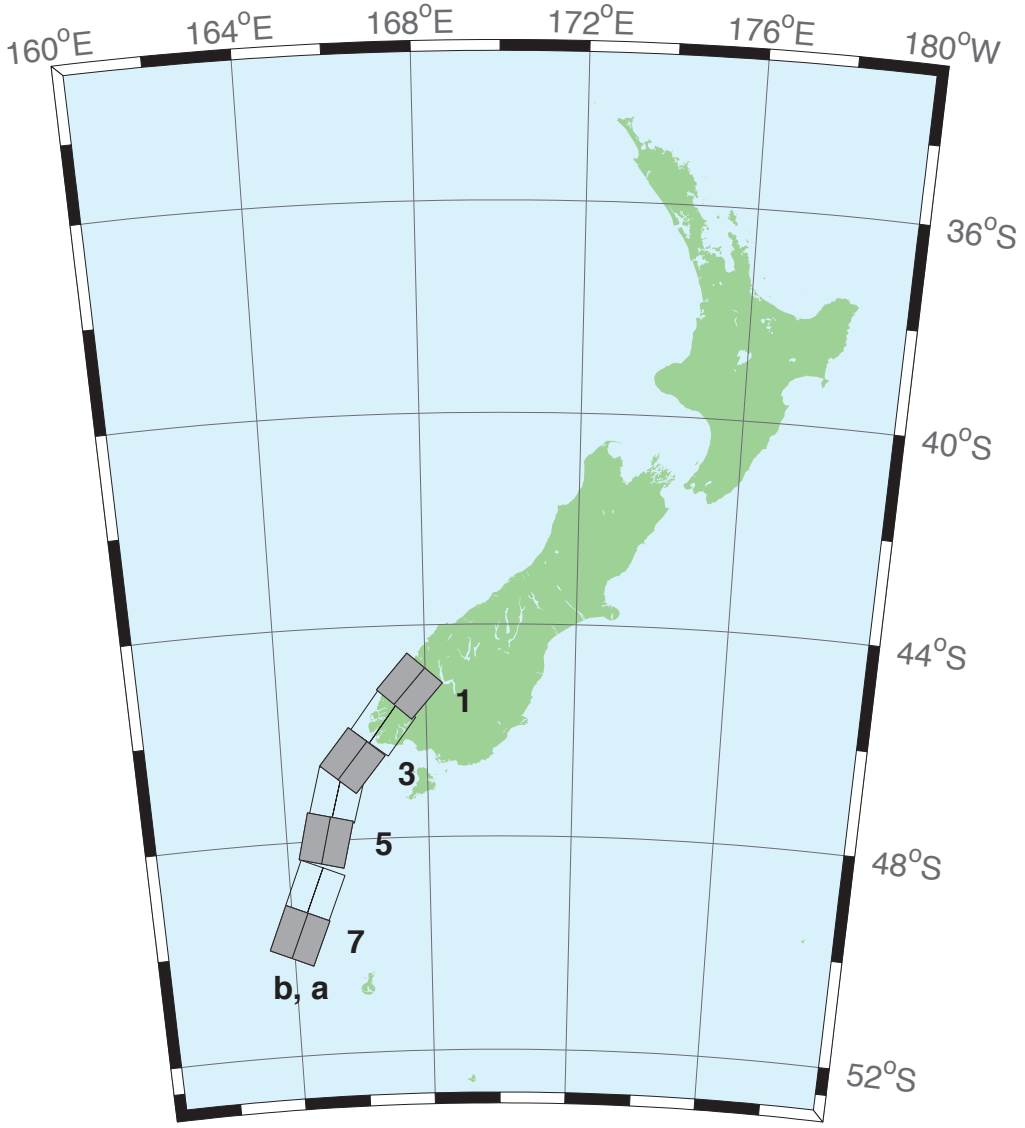

Figure B.9: New Zealand–Puysegur Zone unit sources.

Table B.9: Earthquake parameters for New Zealand–Puysegur Subduction Zone unit sources.

Segment	Description	Longitude(°E)	Latitude(°N)	Strike(°)	Dip(°)	Depth (km)
nzsz–1a	New Zealand–Puysegur	168.0294	-45.4368	41.5	15	17.94
nzsz–1b	New Zealand–Puysegur	167.5675	-45.1493	41.5	15	5
nzsz–2a	New Zealand–Puysegur	167.3256	-46.0984	37.14	15	17.94
nzsz–2b	New Zealand–Puysegur	166.8280	-45.8365	37.14	15	5
nzsz–3a	New Zealand–Puysegur	166.4351	-46.7897	39.53	15	17.94
nzsz–3b	New Zealand–Puysegur	165.9476	-46.5136	39.53	15	5
nzsz–4a	New Zealand–Puysegur	166.0968	-47.2583	15.38	15	17.94
nzsz–4b	New Zealand–Puysegur	165.4810	-47.1432	15.38	15	5
nzsz–5a	New Zealand–Puysegur	165.7270	-48.0951	13.94	15	17.94
nzsz–5b	New Zealand–Puysegur	165.0971	-47.9906	13.94	15	5
nzsz–6a	New Zealand–Puysegur	165.3168	-49.0829	22.71	15	17.94
nzsz–6b	New Zealand–Puysegur	164.7067	-48.9154	22.71	15	5
nzsz–7a	New Zealand–Puysegur	164.8017	-49.9193	23.25	15	17.94
nzsz–7b	New Zealand–Puysegur	164.1836	-49.7480	23.25	15	5

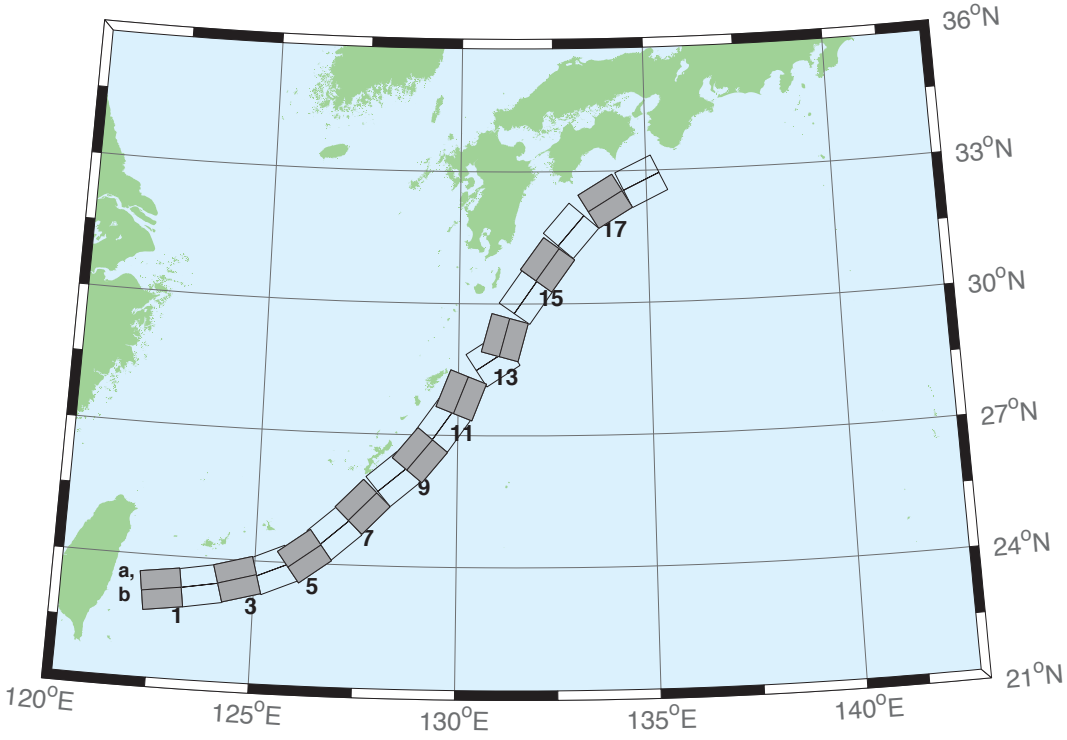

Figure B.10: Ryukyu–Kyushu–Nankai Zone unit sources.

Table B.10: Earthquake parameters for Ryukyu–Kyushu–Nankai Subduction Zone unit sources.

Segment	Description	Longitude(°E)	Latitude(°N)	Strike(°)	Dip(°)	Depth (km)
rnsz–1a	Ryukyu–Nankai	122.6672	23.6696	262	14	11.88
rnsz–1b	Ryukyu–Nankai	122.7332	23.2380	262	10	3.2
rnsz–2a	Ryukyu–Nankai	123.5939	23.7929	259.9	18.11	12.28
rnsz–2b	Ryukyu–Nankai	123.6751	23.3725	259.9	10	3.6
rnsz–3a	Ryukyu–Nankai	124.4604	23.9777	254.6	19.27	14.65
rnsz–3b	Ryukyu–Nankai	124.5830	23.5689	254.6	12.18	4.1
rnsz–4a	Ryukyu–Nankai	125.2720	24.2102	246.8	18	20.38
rnsz–4b	Ryukyu–Nankai	125.4563	23.8177	246.8	16	6.6
rnsz–5a	Ryukyu–Nankai	125.9465	24.5085	233.6	18	20.21
rnsz–5b	Ryukyu–Nankai	126.2241	24.1645	233.6	16	6.43
rnsz–6a	Ryukyu–Nankai	126.6349	25.0402	228.7	17.16	19.55
rnsz–6b	Ryukyu–Nankai	126.9465	24.7176	228.7	15.16	6.47
rnsz–7a	Ryukyu–Nankai	127.2867	25.6343	224	15.85	17.98
rnsz–7b	Ryukyu–Nankai	127.6303	25.3339	224	13.56	6.26
rnsz–8a	Ryukyu–Nankai	128.0725	26.3146	229.7	14.55	14.31
rnsz–8b	Ryukyu–Nankai	128.3854	25.9831	229.7	9.64	5.94
rnsz–9a	Ryukyu–Nankai	128.6642	26.8177	219.2	15.4	12.62
rnsz–9b	Ryukyu–Nankai	129.0391	26.5438	219.2	8	5.66
rnsz–10a	Ryukyu–Nankai	129.2286	27.4879	215.2	17	12.55
rnsz–10b	Ryukyu–Nankai	129.6233	27.2402	215.2	8.16	5.45
rnsz–11a	Ryukyu–Nankai	129.6169	28.0741	201.3	17	12.91
rnsz–11b	Ryukyu–Nankai	130.0698	27.9181	201.3	8.8	5.26
rnsz–12a	Ryukyu–Nankai	130.6175	29.0900	236.7	16.42	13.05
rnsz–12b	Ryukyu–Nankai	130.8873	28.7299	236.7	9.57	4.74
rnsz–13a	Ryukyu–Nankai	130.7223	29.3465	195.2	20.25	15.89
rnsz–13b	Ryukyu–Nankai	131.1884	29.2362	195.2	12.98	4.66
rnsz–14a	Ryukyu–Nankai	131.3467	30.3899	215.1	22.16	19.73
rnsz–14b	Ryukyu–Nankai	131.7402	30.1507	215.1	17.48	4.71
rnsz–15a	Ryukyu–Nankai	131.9149	31.1450	216	15.11	16.12
rnsz–15b	Ryukyu–Nankai	132.3235	30.8899	216	13.46	4.48
rnsz–16a	Ryukyu–Nankai	132.5628	31.9468	220.9	10.81	10.88
rnsz–16b	Ryukyu–Nankai	132.9546	31.6579	220.9	7.19	4.62
rnsz–17a	Ryukyu–Nankai	133.6125	32.6956	239	10.14	12.01
rnsz–17b	Ryukyu–Nankai	133.8823	32.3168	239	8.41	4.7
rnsz–18a	Ryukyu–Nankai	134.6416	33.1488	244.7	10.99	14.21
rnsz–18b	Ryukyu–Nankai	134.8656	32.7502	244.5	10.97	4.7
rnsz–19a	Ryukyu–Nankai	135.6450	33.5008	246.5	14.49	14.72
rnsz–19b	Ryukyu–Nankai	135.8523	33.1021	246.5	11.87	4.44
rnsz–20a	Ryukyu–Nankai	136.5962	33.8506	244.8	15	14.38
rnsz–20b	Ryukyu–Nankai	136.8179	33.4581	244.8	12	3.98
rnsz–21a	Ryukyu–Nankai	137.2252	34.3094	231.9	15	15.4
rnsz–21b	Ryukyu–Nankai	137.5480	33.9680	231.9	12	5
rnsz–22a	Ryukyu–Nankai	137.4161	34.5249	192.3	15	15.4
rnsz–22b	Ryukyu–Nankai	137.9301	34.4327	192.3	12	5

Appendix C. SIFT testing results

Authors: Jean Newman, Nazila Merati, Yong Wei, Lindsey Wright

1.0 PURPOSE

Forecast models are tested with synthetic tsunami events covering a range of tsunami source locations and magnitudes ranging from mega-events to micro-events. Testing is also done with selected historical tsunami events when available.

The purpose of forecast model testing is three-fold. The first objective is to assure that the results obtained with NOAA's tsunami forecast system, which has been released to the Tsunami Warning Centers for operational use, are identical to those obtained by the researcher during the development of the forecast model. The second objective is to test the forecast model for consistency, accuracy, time efficiency, and quality of results over a range of possible tsunami locations and magnitudes. The third objective is to identify bugs and issues in need of resolution by the researcher who developed the Forecast Model or by the forecast software development team before the next version release to NOAA's two Tsunami Warning Centers.

Local hardware and software applications, and tools familiar to the researcher(s), are used to run the Method of Splitting Tsunamis (MOST) model during the forecast model development. The test results presented in this report lend confidence that the model performs as developed and produces the same results when initiated within the forecast application in an operational setting as those produced by the researcher during the forecast model development. The test results assure those who rely on the Nikolski tsunami forecast model that consistent results are produced irrespective of system.

2.0 TESTING PROCEDURE

The general procedure for forecast model testing is to run a set of synthetic tsunami scenarios and a selected set of historical tsunami events through the forecast system application and compare the results with those obtained by the researcher during the forecast model development and presented in the Tsunami Forecast Model Report. Specific steps taken to test the model include:

1. Identification of testing scenarios, including the standard set of synthetic events, appropriate historical events, and customized synthetic scenarios that may have been used by the researcher(s) in developing the forecast model.
2. Creation of new events to represent customized synthetic scenarios used by the researcher(s) in developing the forecast model, if any.
3. Submission of test model runs with SIFTthe forecast system, and export of the results from A, B, and C grids, along with time series.
4. Recording applicable metadata, including the specific version of the forecast system used for testing.
5. Examination of SIFT forecast model results from the forecast system for instabilities in both time series and plot results.
6. Comparison of forecast model results obtained through the forecast system with those obtained during the forecast model development.
7. Summarization of results with specific mention of quality, consistency, and time efficiency.
8. Reporting of issues identified to modeler and forecast software development team.

9. Retesting the forecast models in the forecast system when reported issues have been addressed or explained.

Synthetic model runs were tested on a DELL PowerEdge R510 computer equipped with two Xeon E5670 processors at 2.93 Ghz, each with 12 MBytes of cache and 32GB memory. The processors are hex core and support hyperthreading, resulting in the computer performing as a 24 processor core machine. Additionally, the testing computer supports 10 Gigabit Ethernet for fast network connections. This computer configuration is similar or the same as the configurations of the computers installed at the Tsunami Warning Centers so the compute times should only vary slightly.

Results

The Nikolski forecast model was tested with NOAA's tsunami forecast system version 3.12, the current version installed at the NOAA Tsunami Warning Centers.

The Nikolski, Alaska forecast model was tested with twenty threefour synthetic scenarios and two one historical tsunami events. Test results from the forecast system and comparisons with the results obtained during the forecast model development are shown numerically in Table 2 and graphically in Figures 1 to 5.5 The results show that the forecast model is stable and robust, with consistent and high quality results across geographically distributed tsunami sources and mega-event tsunami magnitudes. The model run time (wall clock time) was under 262015.95 minutes for 7.9998 hours of simulation time, and under 1107.96 minutes for 4.0 hours. This run time isis underjust above the 10 minute run time for 4 hours of simulation time that and satisfies time efficiency requirements.

Four synthetic events wereas run on the Nikolski forecast model. The modeled scenarios were stable for all cases tested, with no instabilities or ringing. Results show that the largest modeled height was 186.3260.8385.1 cm and originated in in the Central and South AmericaNew Zealand-Kermadec-Tonga (ACSZ NTCSSZ 16-258930-398) source. Additionally, large (282.2-306 cm) amplitudes were recorded using the overlapping and adjacent Aleutian-Alaska-Cascadia (ACSZ 22-31 and 6-15) sources. Amplitudes greater than 100 cm were recorded for at the Kamchatka-Yap-Mariana-Izu-Bonin (KISZ 1-10), Manus OCB (MOSZ 1-10) and the New Zealand-Kermadec-Tonga (NTSZ 30-39)33 out of 4 test sources. The smallest signals of 92.10791.312.8 cm and 13.5 cm werewas recorded at the New Zealand-Kermadec-Tonga Kamchatka-Yap-Mariana-Izu-Bonin (KISZ NTSZ 1-10 and 37-462230-39-31) sources. Small scale events (Mw =7.5) and the micro events tested were also stable. Direct comparisons, of output from the forecast tool with development results of both the historical event (Kuril 2006)s and available development synthetic events, demonstrated that the wave pattern were similar identical in shape, pattern and amplitude. Maximum amplitudes for the Aleutian-Alaska-Cascadia (ACSZ 56-65) source differ by 16 cm die to different length of the model run. As the largest wave arrives late, the 20-hour model run indicates the largest wave amplitude is 126.1 cm, while the largest wave amplitude for a 10-hour run is 110.1 cm, identical to a 10-hour SIFT run.

Source Zone	Tsunami Source	α [m]	SIFT Max (cm)	Development Max (cm)	SIFT Min (cm)	Development Min (cm)
Mega-tsunami scenarios						
KISZ	A22-A31, B22-B31	25	148.3	148.3	-97.9	-97.7 (8-hour run) -104.5 (20-hour run)
ACSZ	A56-A65, B56-B65	25	110.1	110.1 (8-hour run) 126.1 (20-hour run)	-114.5	-114.5
CSSZ	A89-A98, B89-B98	25	160.8	160.8	-123.6	-123.6
NTSZ	A30-39, B30-39	25	91.3	91.3	-107.4	-107.4
Historical events						
Tohoku 2011			105.4	105.4	-72.6	-72.6

Table C1. Table of maximum and minimum amplitudes (cm) at the Nikolski, Alaska warning point for synthetic and historical events tested using SIFT 3.2 and obtained during development.

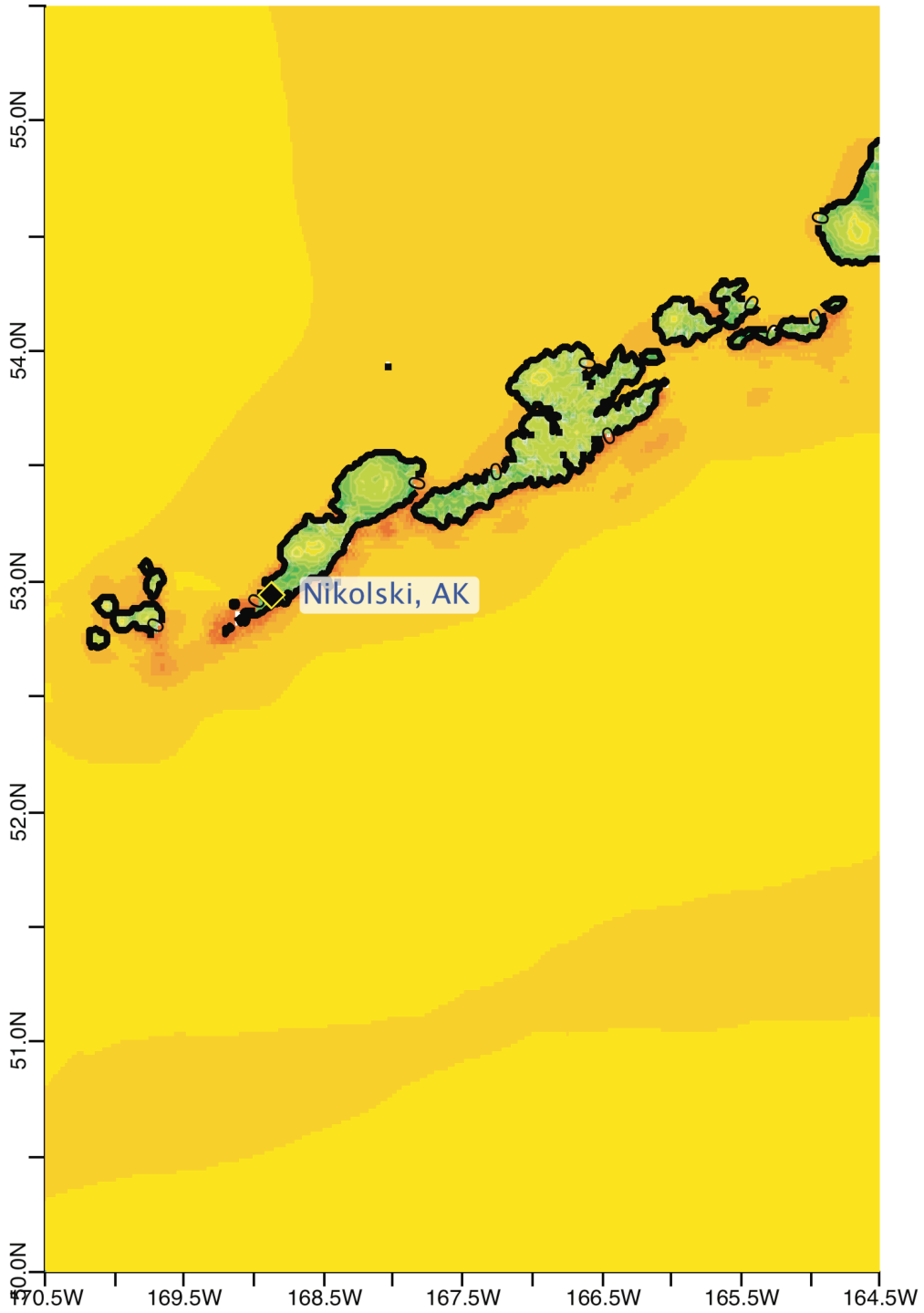

Figure C1. Max computed wave amplitude of A grid, Nikolski, Alaska, for synthetic event KISZ 22-31.

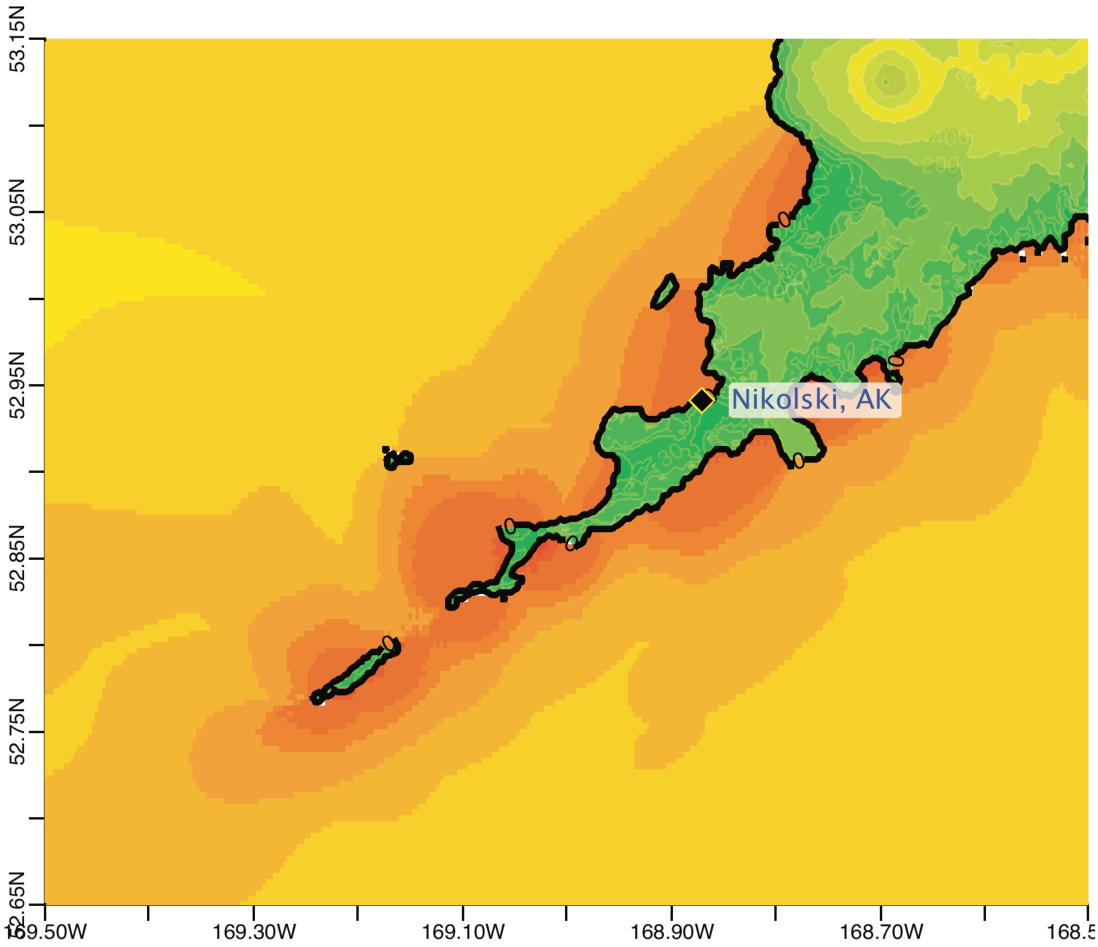

Figure C2. Max computed wave amplitude of B grid, Nikolski, Alaska, for synthetic event KISZ 22-31.

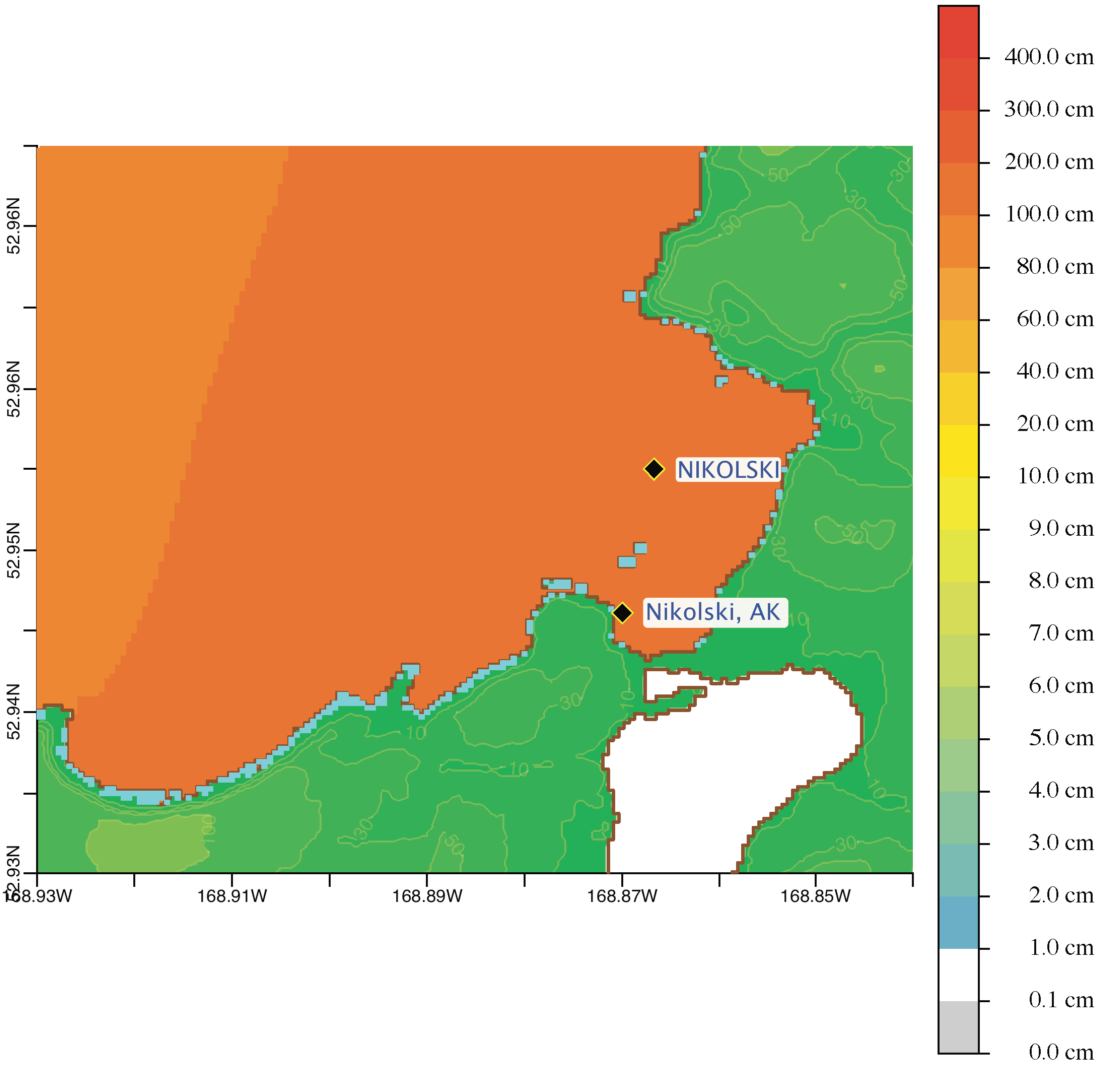

Figure C3. Max computed wave amplitude of C grid, Nikolski, Alaska, for synthetic event KISZ 22-31.

(a)

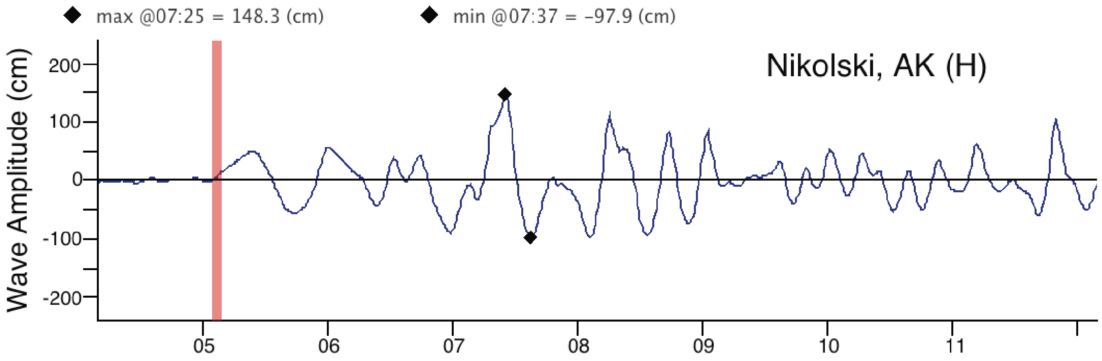

(b)

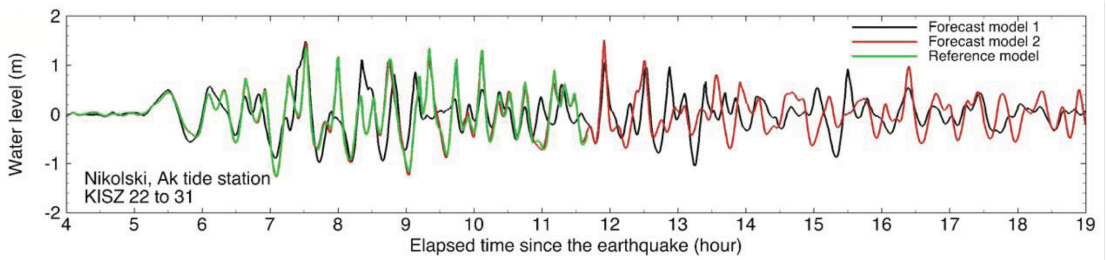

Figure C4. Computed time series at Nikolski tide gage, for synthetic event KISZ 22-31: (a) time series computed in SIFT; (b) time series shown in the forecast model report.

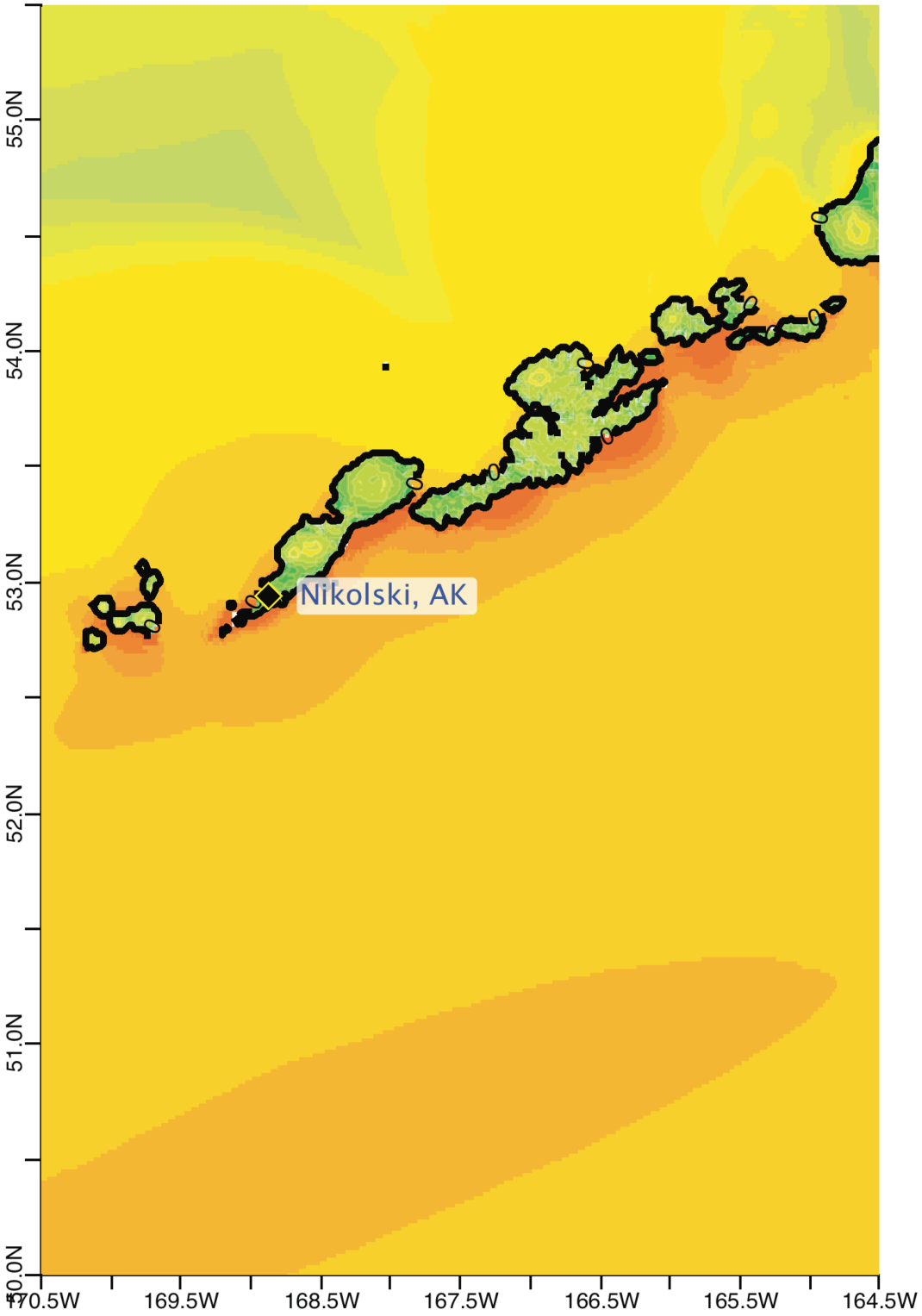

Figure C5. Max computed wave amplitude of A grid, Nikolski, Alaska, for synthetic event ACSZ 56-65.

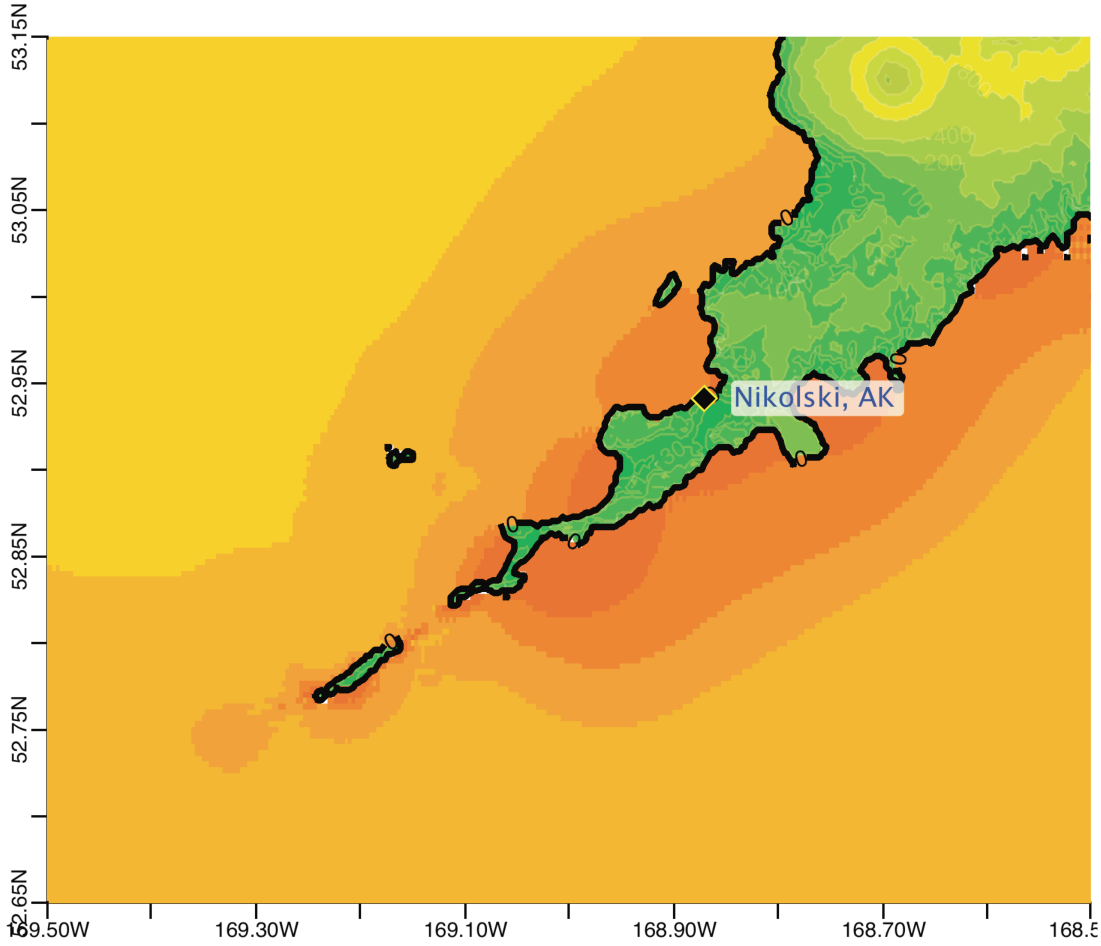

Figure C6. Max computed wave amplitude of B grid, Nikolski, Alaska, for synthetic event ACSZ 56-65.

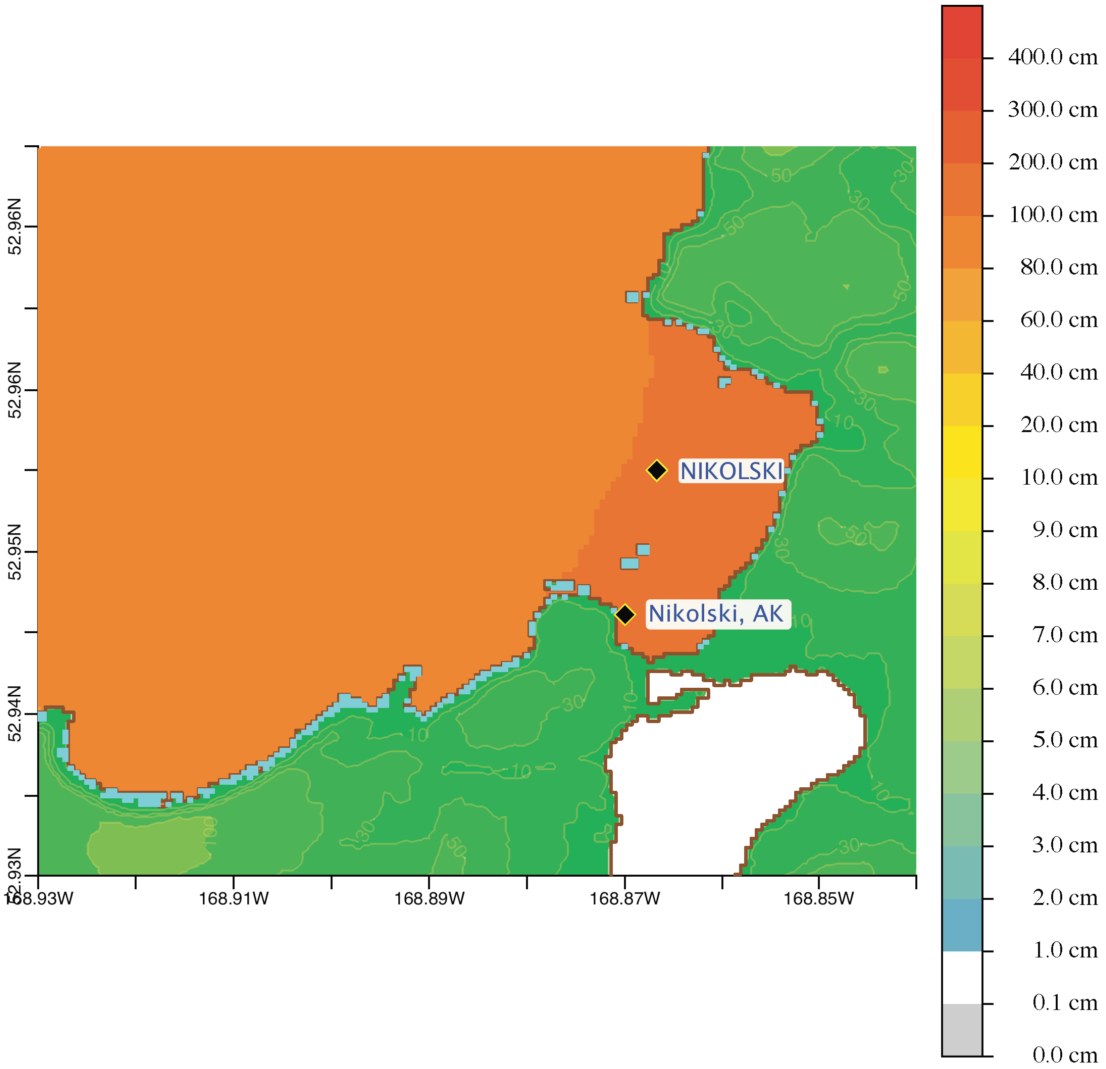

Figure C7. Max computed wave amplitude of C grid, Nikolski, Alaska, for synthetic event ACSZ 56-65.

(a)

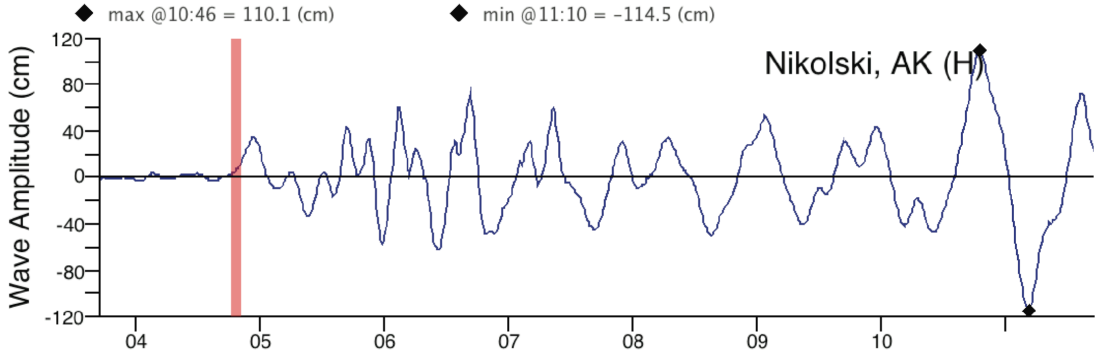

(b)

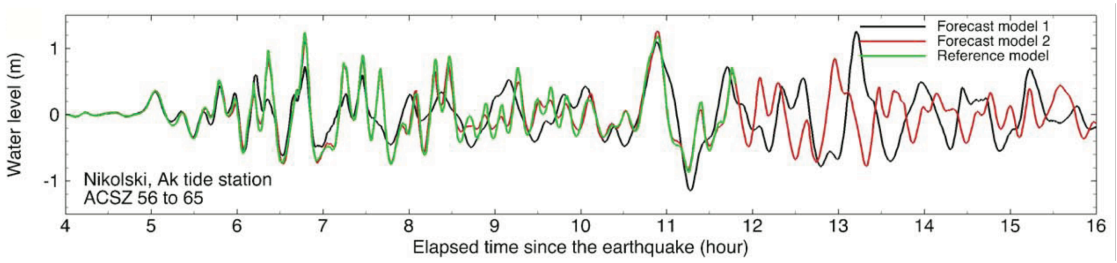

Figure C8. Computed time series at Nikolski tide gage, for synthetic event ACSZ 56-65: (a) time series computed in SIFT; (b) time series shown in the forecast model report.

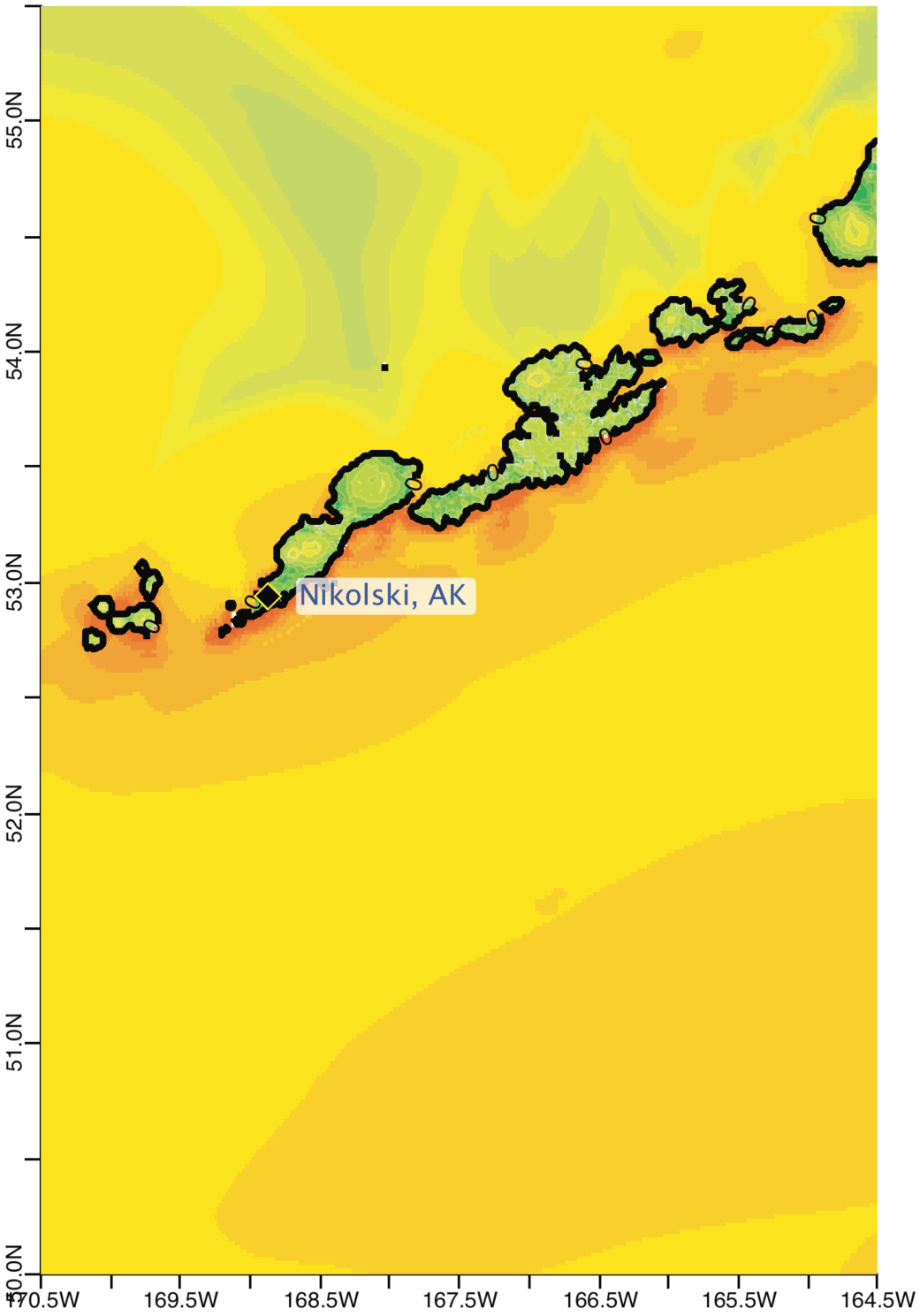

Figure C9. Max computed wave amplitude of C grid, Nikolski, Alaska, for synthetic event CSSZ 89-98.

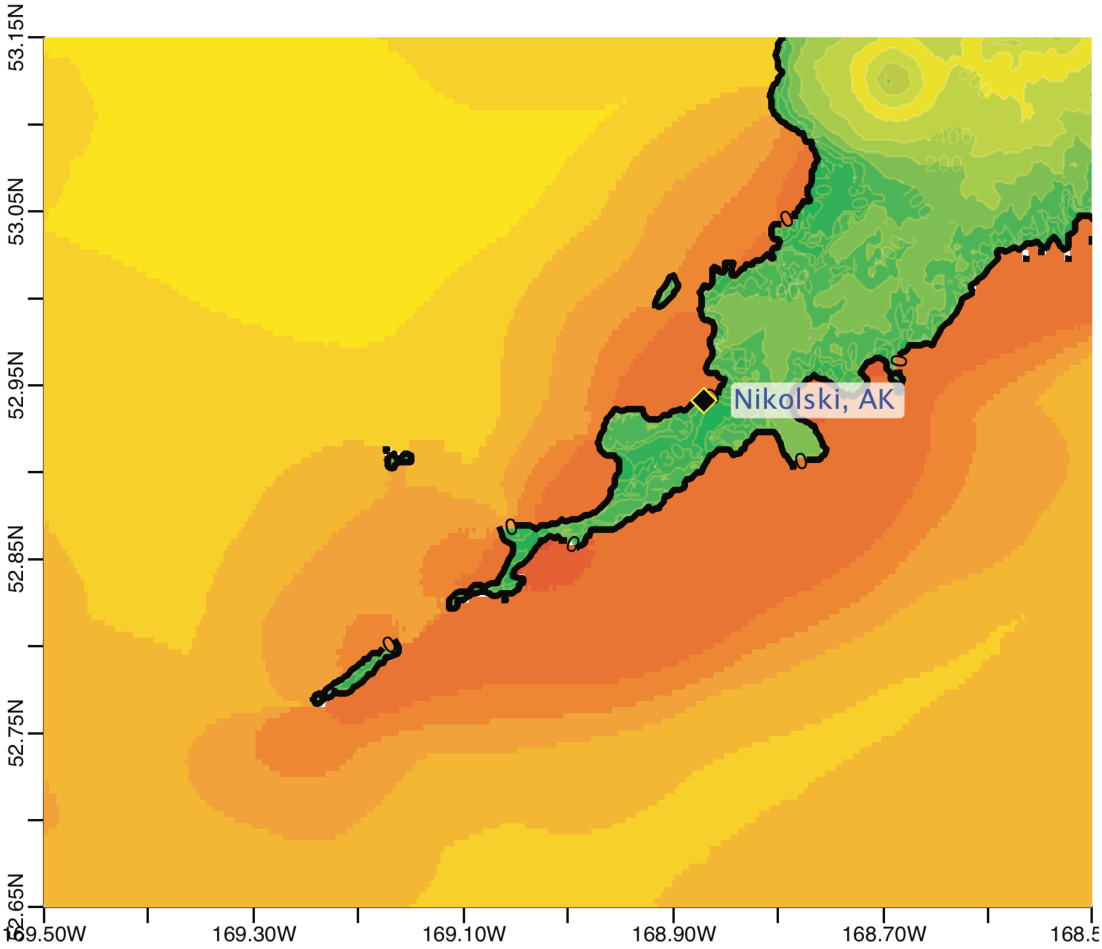

Figure C10. Max computed wave amplitude of B grid, Nikolski, Alaska, for synthetic event CSSZ 89-98.

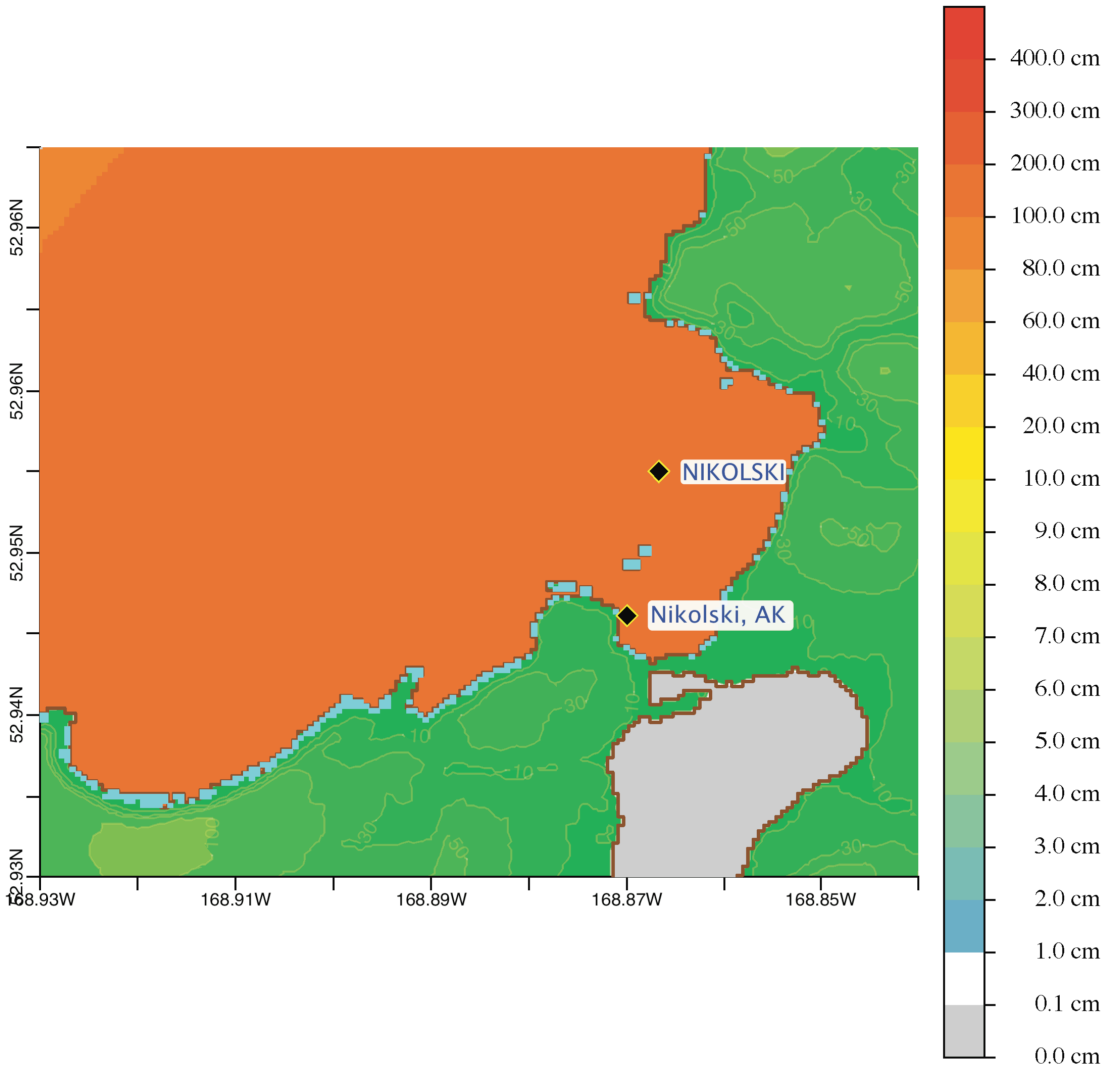

Figure C11. Max computed wave amplitude of C grid, Nikolski, Alaska, for synthetic event CSSZ 89-98.

(a)

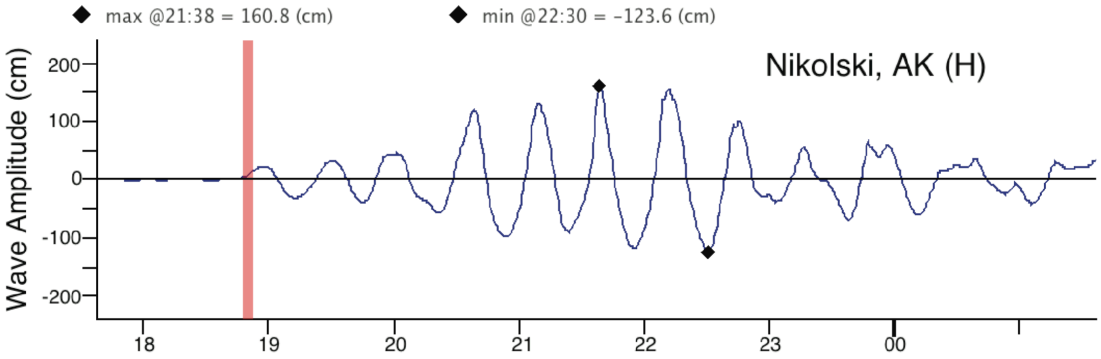

(b)

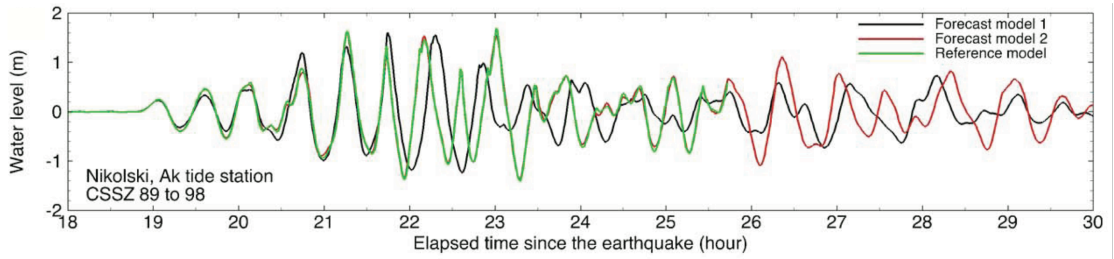

Figure C12. Computed time series at Nikolski tide gage, for synthetic event CSSZ 89-98: (a) time series computed in SIFT; (b) time series shown in the forecast model report.

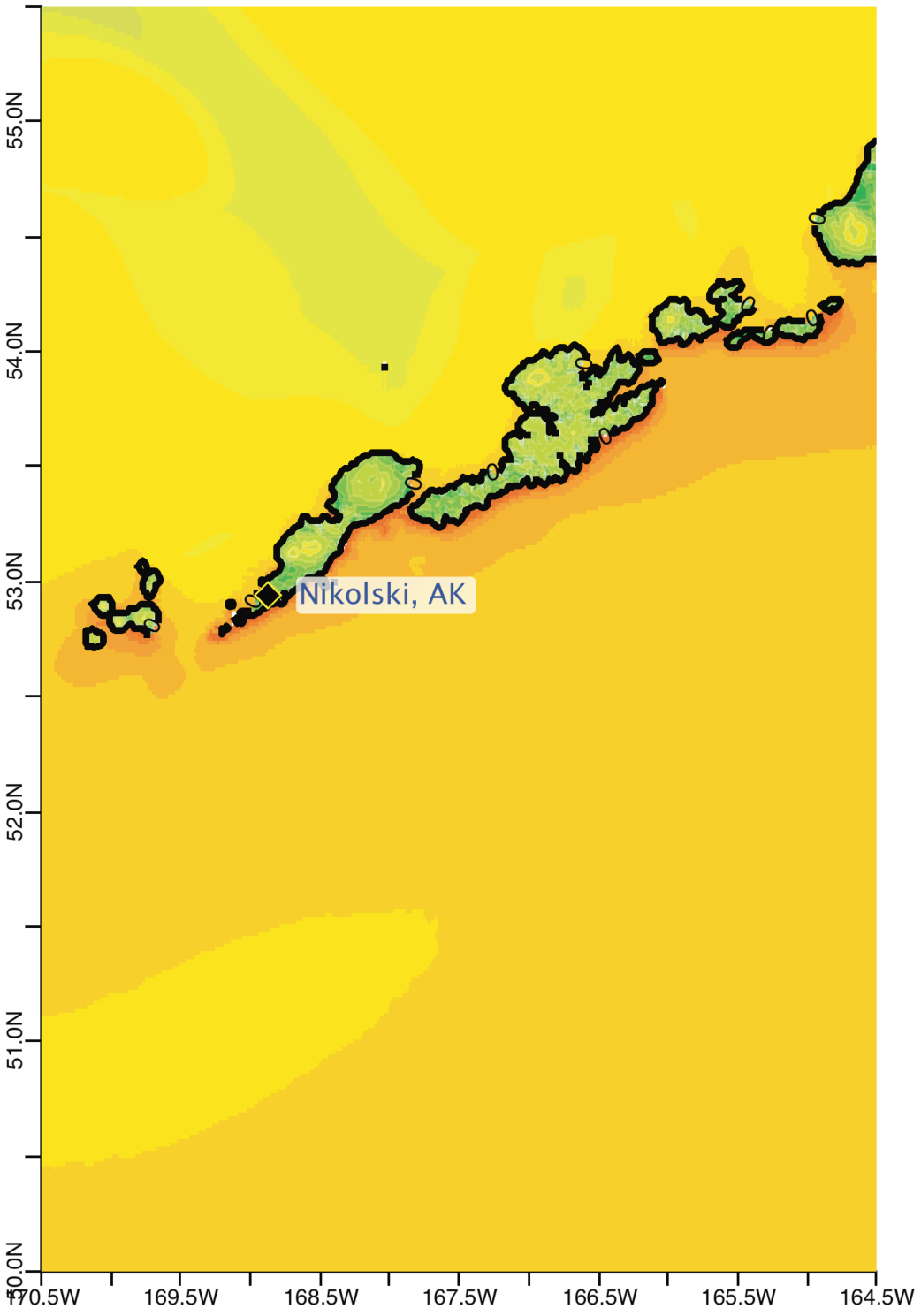

Figure C13. Max computed wave amplitude of A grid, Nikolski, Alaska, for synthetic event NTSZ 30-39.

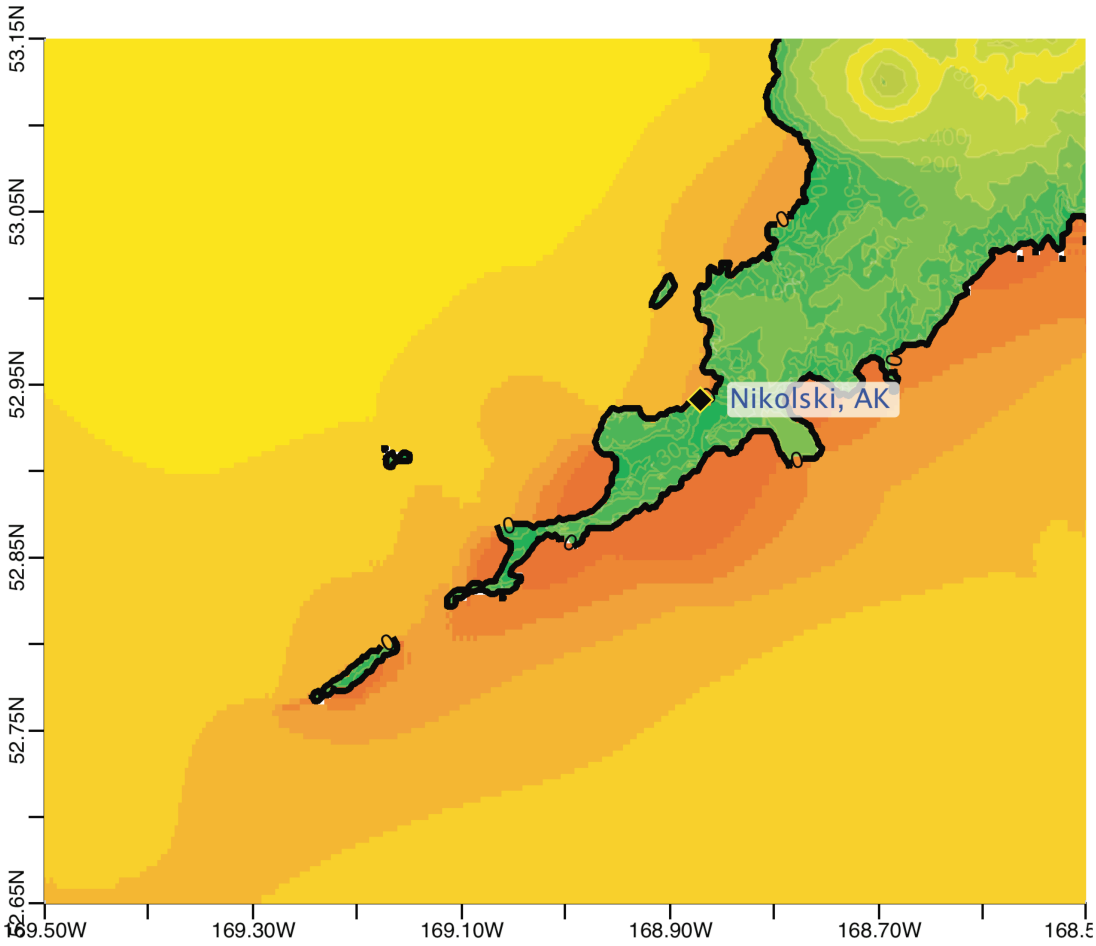

Figure C14. Max computed wave amplitude of B grid, Nikolski, Alaska, for synthetic event NTSZ 30-39.

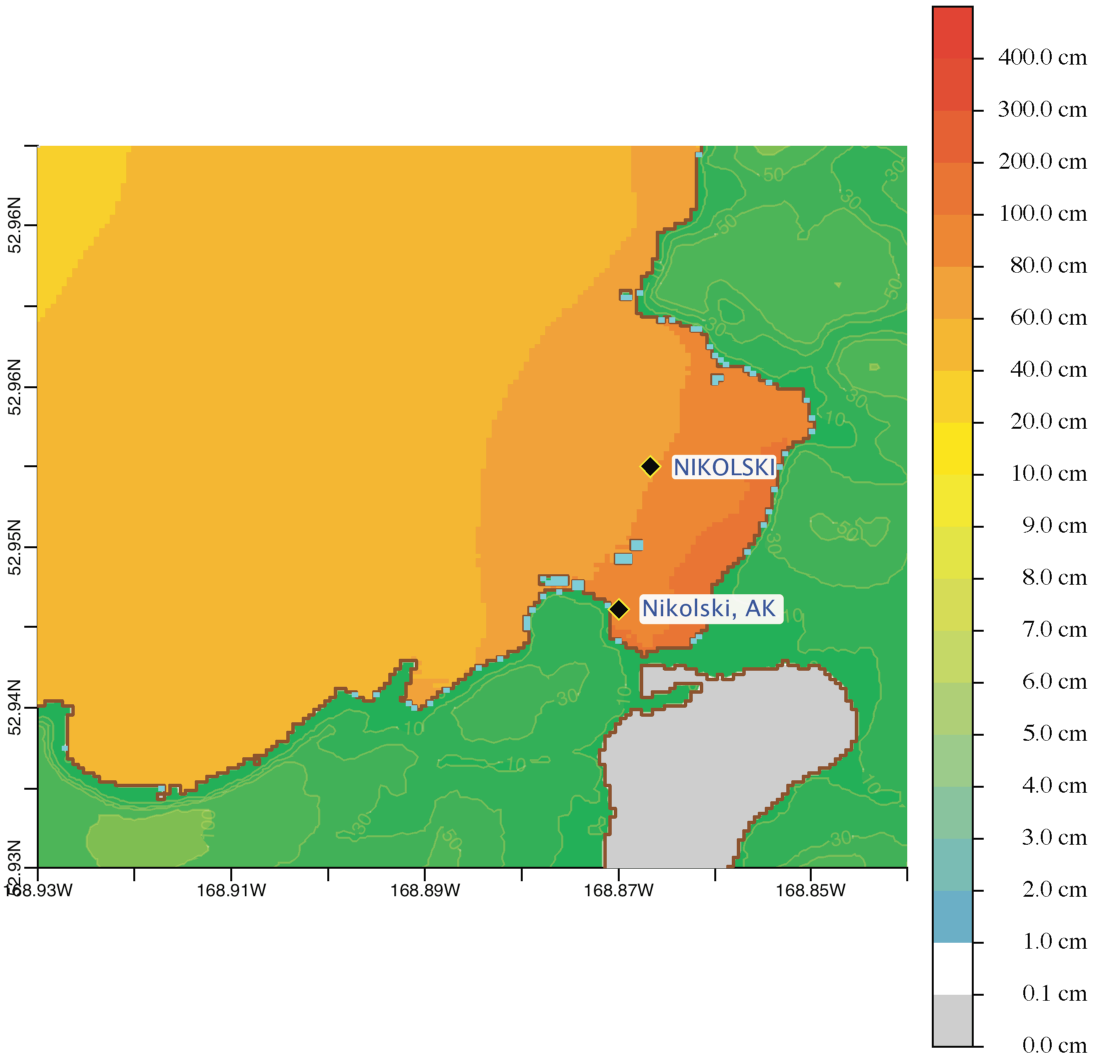

Figure C15. Max computed wave amplitude of C grid, Nikolski, Alaska, for synthetic event NTSZ 30-39.

(a)

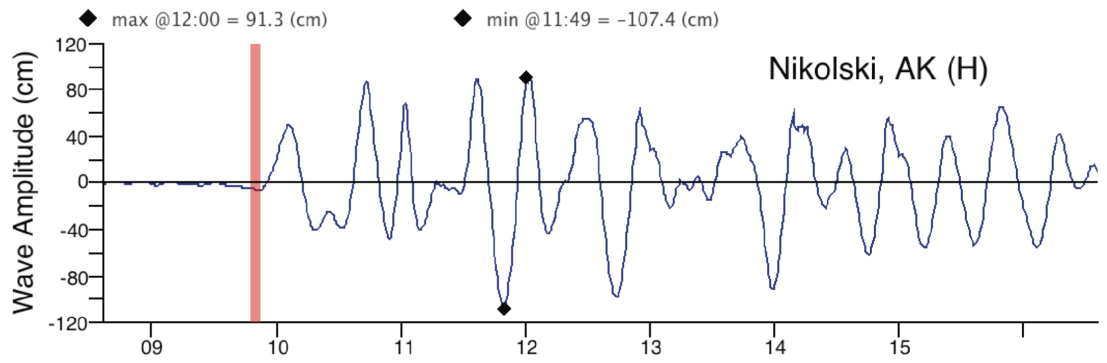

(b)

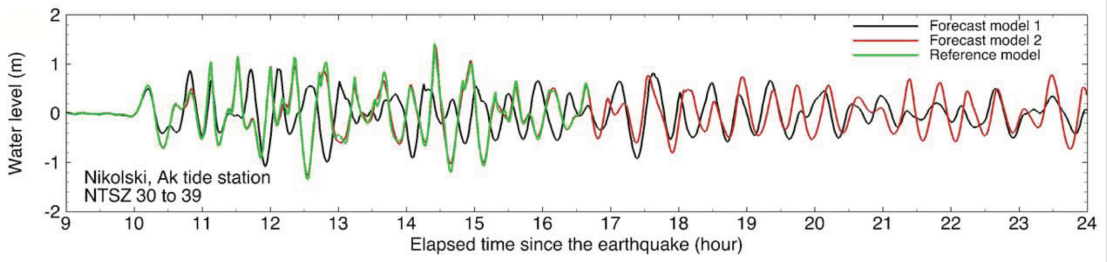

Figure C16. Computed time series at Nikolski tide gage, for synthetic event NTSZ 30-39: (a) time series computed in SIFT; (b) time series shown in the forecast model report.

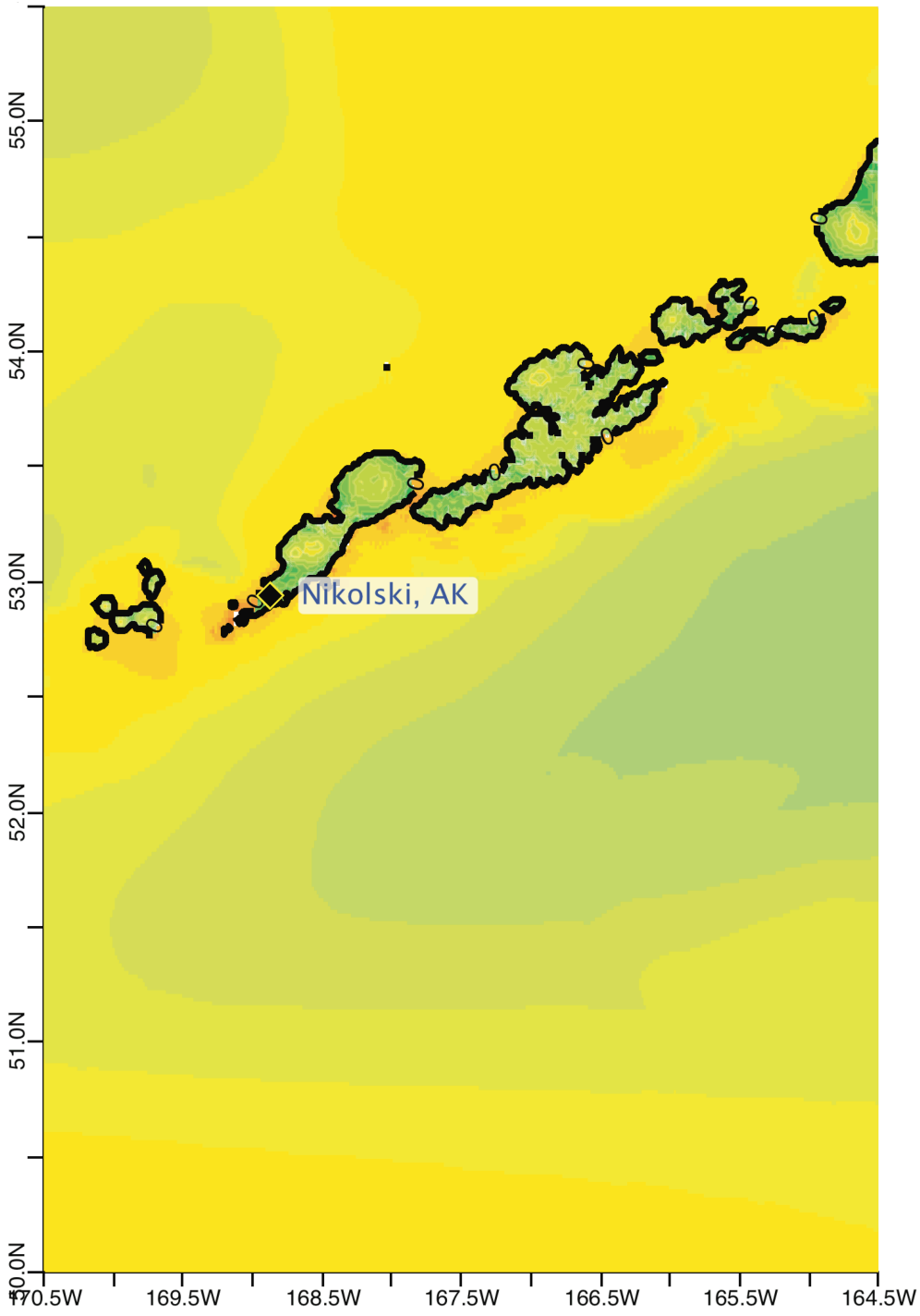

Figure C17. Max computed wave amplitude of C grid, Nikolski, Alaska, for 11 March 2011 Japan tsunami.

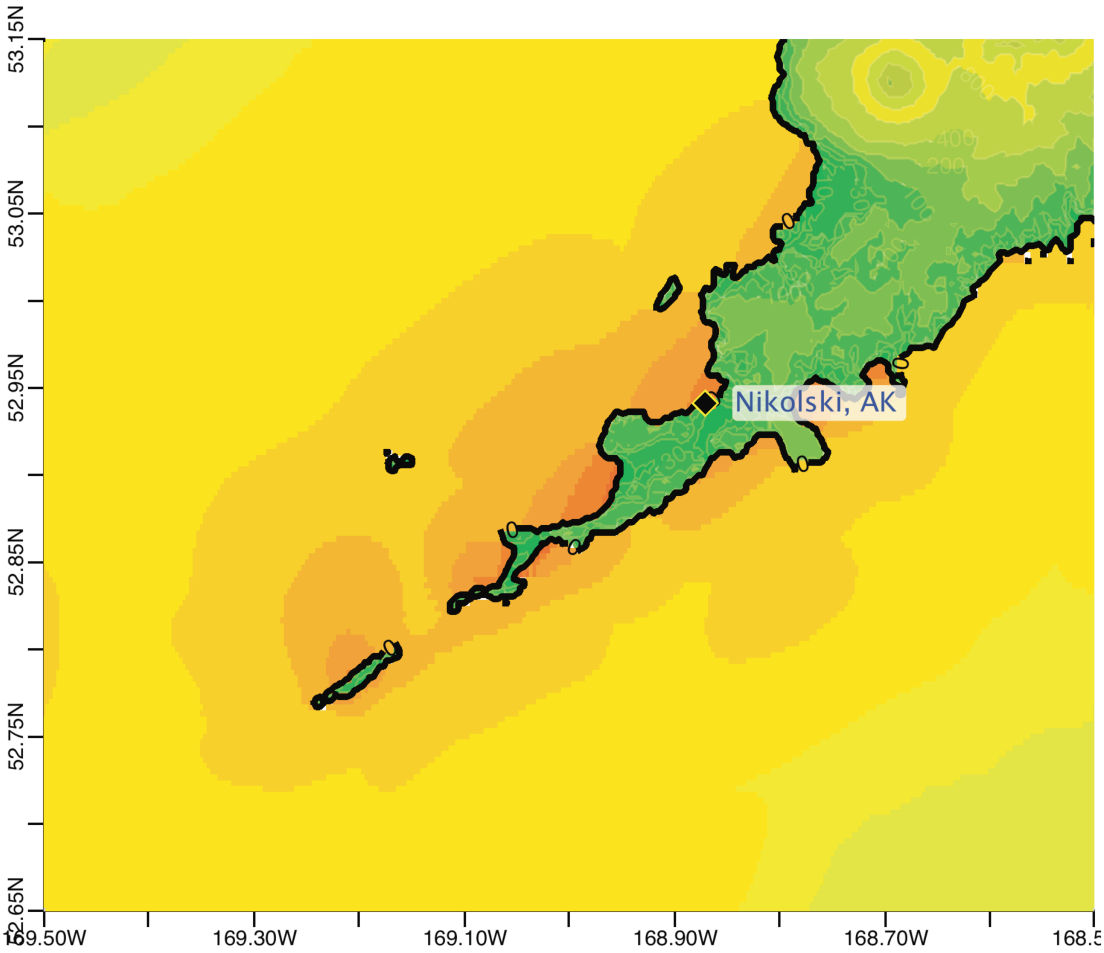

Figure C18. Max computed wave amplitude of B grid, Nikolski, Alaska, for 11 March 2011 Japan tsunami.

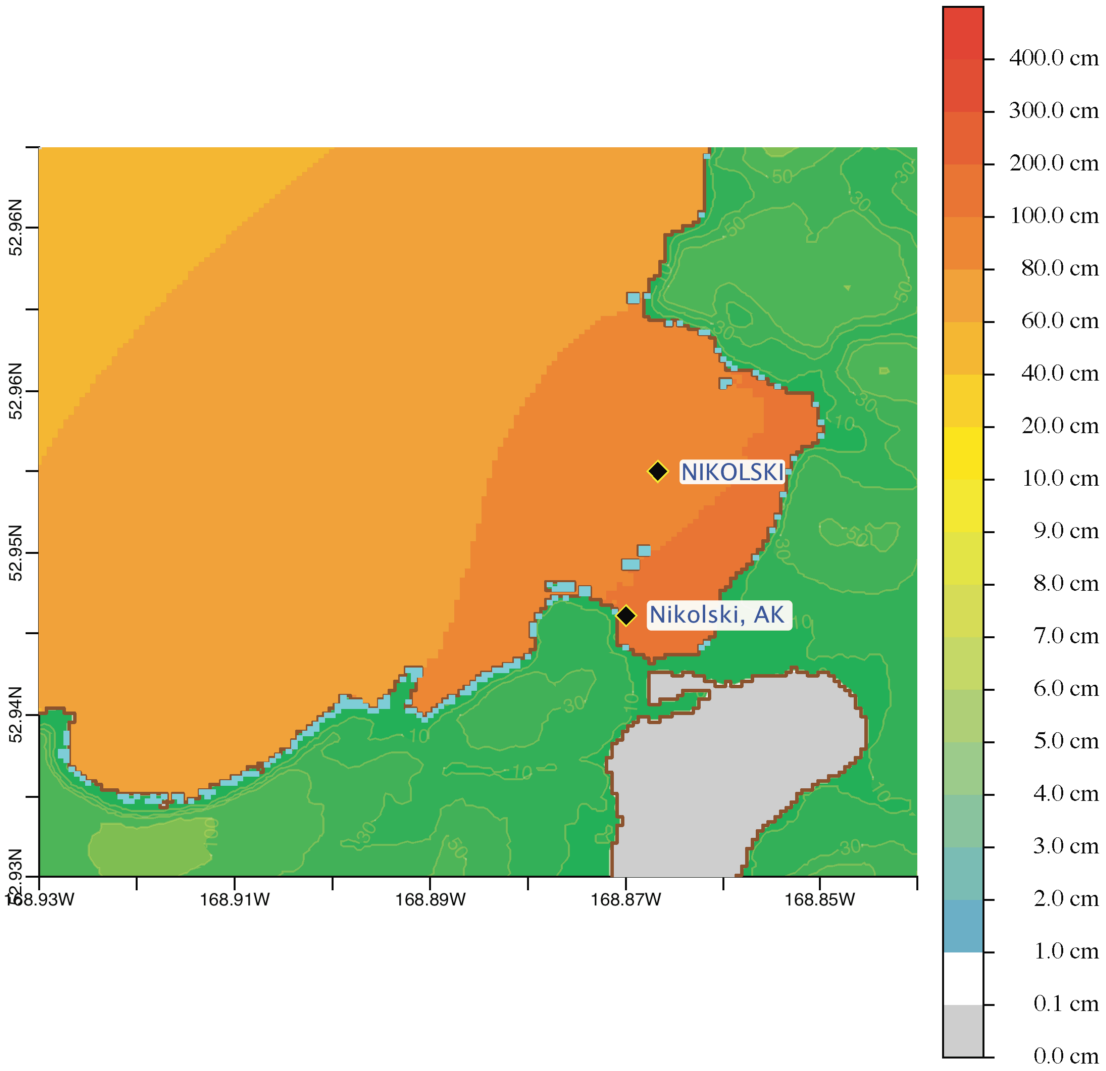

Figure C19. Max computed wave amplitude of C grid, Nikolski, Alaska, for 11 March 2011 Japan tsunami.

(a)

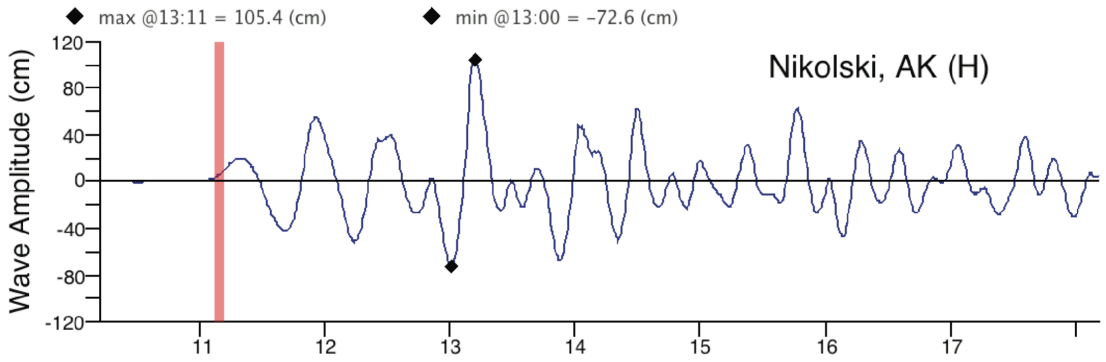

(b)

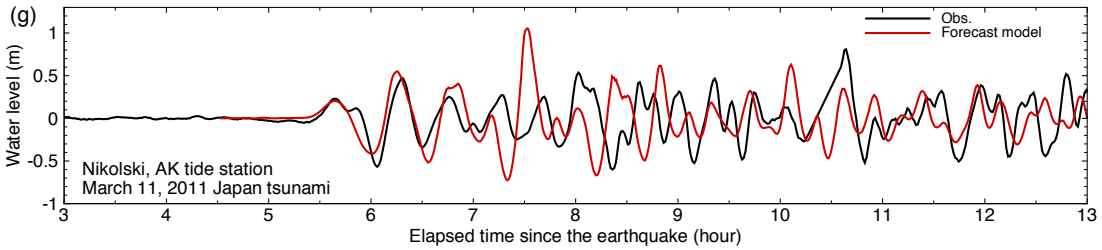

Figure C20. Computed time series at Nikolski tide gage, for11 March 2011 Japan tsunami: (a) time series computed in SIFT; (b) time series shown in the forecast model report.